

The Effects of Pre-movement on Large Building Evacuations

Lisa Carroll Ruth Farnell

A Thesis submitted to
the Faculty of Graduate Studies
in Partial Fulfillment of the Requirements
for the Degree of Master of Science

Graduate Program in Applied & Industrial Mathematics
York University
Toronto, Ontario
July 2015
© Lisa Carroll Ruth Farnell, 2015

Abstract

Evacuation times for buildings with a range of heights and occupant loads were generated by a computer simulation algorithm, assuming simultaneous start. Additional evacuation times were generated for the same buildings with pre-movement times assigned to building occupants. Pre-movement times were assigned based on uniform and gamma distributions. Building evacuation times with pre-movement were compared to those without, to determine the quantitative effects of pre-movement. Using regression analysis, equations were generated to predict the effects of pre-movement for given building heights and occupant loads. Regression equations were shown to reasonably predict the effects of pre-movement for the building cases used for the regression analysis. Additional simulations were performed with and without pre-movement for buildings with alternative heights and occupant loads. The regression function was applied to these additional simulations, and found to predict the effects of pre-movement in these building cases with some accuracy.

Table of Contents

Abstract	ii
Table of Contents	iii
List of Tables	vi
List of Figures	vi
1.0 INTRODUCTION	1
1.1 Fire Protection in Modern Buildings	1
1.2 Modelling Evacuation Times	3
1.2.1 Phases of Evacuation Time	4
1.2.2 Calculating Movement Time	5
1.2.3 Calculating Pre-Movement Time	9
2.0 METHOD FOR CALCULATING THE EFFECTS OF PRE-MOVEMENT	12
2.1 Number and Usage of Exit Routes	12
2.2 Evacuation Phasing	13
2.3 Algorithm for Modelling Evacuations	14
2.3.1 Describing Conditions within the Exit Route	14
2.3.2 Arrival Time at Exit Door.....	21
2.3.3 Identifying Possible Movements	23
2.3.4 Modelling Movement.....	25
3.0 CASE STUDIES	29
3.1 Geometry of Floor Area and Exit Route	29
3.2 Preliminary Case Studies and Model Validation	32
3.2.1 Preliminary Trial Results	32
3.2.2 Model Verification	33
3.3 Primary Case Studies	42
3.4 Pre-movement time distributions	43
3.4.1 Uniformly Distributed Pre-Movement (UPM)	43
3.4.2 Gamma Distributed Pre-Movement (GPM)	45

4.0 RESULTS	48
4.1 Effects of Uniform Pre-movement Distributions	49
4.1.1 UPM Results with Linear Regression.....	53
4.1.2 UPM Results with High Order Regression	57
4.1.3 UPM Results with High Order Regression – Extended Case Studies	65
4.2 Effects of Gamma Pre-movement Distributions (GPM)	75
4.2.1 GPM Results with Linear Regression	79
4.2.2 GPM Results with High Order Regression	82
4.2.3 GPM Results with High Order Regression – Extended Case Studies	89
5.0 CONCLUSIONS	98
6.0 FURTHER RESEARCH.....	101
7.0 REFERENCES	102
APPENDICES	103
Appendix A – UPM Primary Case Studies with Linear Regression	105
Appendix B – UPM Primary Case Studies with High Order Regression	116
Appendix C – UPM Extended Case Studies with High Order Regression – Low Occupant Loads	127
Appendix D – UPM Extended Case Studies with High Order Regression – Short Buildings	130
Appendix E – UPM Extended Case Studies with High Order Regression – Tall Buildings	132
Appendix F – GPM Primary Case Studies with Linear Regression	134
Appendix G – GPM Primary Case Studies with High Order Regression	145
Appendix H – GPM Extended Case Studies with High Order Regression – Low Occupant Loads	156

Appendix I – GPM Extended Case Studies with High Order Regression – Short Buildings	158
Appendix J – GPM Extended Case Studies with High Order Regression – Tall Buildings	161

List of Tables

Table 1.2.1 – Values of constant k for various walking surfaces [11]	6
Table 2.3.1 – Summary of Matrices	20
Table 3.2.1 – Summary of Results of Preliminary Trials	33

List of Figures

Figure 1.2.1 – Sample timeline comparison between fire development and evacuation [9]	3
Figure 1.2.2 – Specific flow as a function of density [11]	8
Figure 2.3.1 - Segments of the exit path at arbitrary floor level i	15
Figure 2.3.2 - Segments of the exit path at exit level.....	16
Figure 2.3.3 - a sample scenario during an evacuation at time t and floor i	18
Figure 2.3.4 – Where there is only room for one person from two possible streams, the algorithm randomizes which movement has priority	24
Figure 3.1.1 – Plan of exit stair at level n , with dimensions shown in mm	29
Figure 3.1.2 – Plan of exit stair at level 1, with dimensions shown in mm	30
Figure 3.1.3 – Section of St_n with tread depths and riser heights labeled in mm	30
Figure 3.2.1 – Coefficient of Variation for Preliminary Trials with No Pre-movement	33
Figure 3.2.2 - From $t=0$ to $t=10.35$, leading first floor occupant walks to final exit followed by a queue of first floor occupants	36
Figure 3.2.3 - From $t=10.35$ to $t=14.05$ a small queue forms as the leader pauses to open the door	37
Figure 3.2.4 - From $t=14.05$ to $t=20.08$ the rate of occupants arriving at the exit door is equal to the rate of occupants flowing out (queue size remains constant)	39

Figure 3.2.5 for $t > 20.08$ occupants will arrive from two different streams, and queue at the exit door will grow	40
Figure 3.4.1 – Probability Density Function for UPM with $p=6000cs$ (1 minute)	44
Figure 3.4.1 – Probability Density Function for UPM with $p=6000cs$ (1 minute)	44
Figure 3.4.3 – Self reported pre-movement times from office building evacuation [10]	45
Figure 3.4.4 – Observed pre-movement times from retail building fire evacuation [16]	46
Figure 3.4.5 – Gamma distribution probability density function	47
Figure 4.1.1 – UPM Simulation Results ($f=20$, $l=80$ to 140)	49
Figure 4.1.2 – UPM Simulation Results ($f=26$, $l=80$ to 140)	50
Figure 4.1.3 – UPM Simulation Results ($f=30$, $l=80$ to 140)	51
Figure 4.1.4 – UPM Simulation Results ($l=80$, $f=20$ to 30)	52
Figure 4.1.5 – UPM Simulation Results ($l=140$, $f=20$ to 30)	52
Figure 4.1.6 – UPM Results with Linear Regression ($f=24$, $l=110$), $R^2=0.791$	54
Figure 4.1.7 – UPM Results with Linear Regression ($f=27$, $l=90$), $R^2=0.888$	55
Figure 4.1.8 – UPM Results with Linear Regression ($f=22$, $l=120$), $R^2=0.765$	55

Figure 4.1.9 – UPM Results with Linear Regression ($f=25$, $l=140$), $R^2=0.555$	56
Figure 4.1.10 – UPM Results with Linear Regression ($f=20$, $l=80$), $R^2=0.678$	56
Figure 4.1.11 – UPM Results with Linear Regression ($f=30$, $l=140$), $R^2=0.578$	57
Figure 4.1.12 – UPM Results with High Order Regression ($f=20$, $l=80$), $R^2=0.912$	58
Figure 4.1.13 – UPM Results with High Order Regression ($f=22$, $l=90$), $R^2=0.889$	59
Figure 4.1.14 – UPM Results with High Order Regression ($f=24$, $l=100$), $R^2=0.884$	59
Figure 4.1.15 – UPM Results with High Order Regression ($f=27$, $l=90$), $R^2=0.876$	60
Figure 4.1.16 – UPM Results with High Order Regression ($f=30$, $l=140$), $R^2=0.817$	60
Figure 4.1.17 – UPM Results with High Order Regression ($f=20$, $l=80$ to 140)	61
Figure 4.1.18 – UPM Results with High Order Regression ($f=25$, $l=80$ to 140)	62
Figure 4.1.19 – UPM Results with High Order Regression ($f=30$, $l=80$ to 140)	62
Figure 4.1.20 – UPM Results with High Order Regression ($f=20$ to 30 , $l=80$)	63
Figure 4.1.21 – UPM Results with High Order Regression ($f=20$ to 30 , $l=110$)	64
Figure 4.1.22 – UPM Results with High Order Regression ($f=20$ to 30 , $l=140$)	64
Figure 4.1.23 – UPM High Order Regression Applied to Extended Case Study ($f=20$, $l=20$), $R^2=-0.675$	66

Figure 4.1.24 – UPM High Order Regression Applied to Extended Case Study (f=26, l=40), R ² =0.480	67
Figure 4.1.25 – UPM High Order Regression Applied to Extended Case Study (f=30, l=60), R ² =0.812	67
Figure 4.1.26 – UPM High Order Regression Applied to Extended Case Study (f=20, l=60), R ² =0.872	68
Figure 4.1.27 – UPM High Order Regression Applied to Extended Case Study (f=15, l=60), R ² =0.802	69
Figure 4.1.28 – UPM High Order Regression Applied to Extended Case Study (f=10, l=120), R ² =0.649	70
Figure 4.1.29 – UPM High Order Regression Applied to Extended Case Study (f=5, l=140), R ² =0.543	71
Figure 4.1.30 – UPM High Order Regression Applied to Extended Case Study (f=40, l=60), R ² =0.795	73
Figure 4.1.31 – UPM High Order Regression Applied to Extended Case Study (f=40, l=100), R ² =0.807	73
Figure 4.1.32 – UPM High Order Regression Applied to Extended Case Study (f=50, l=100), R ² =0.383	74
Figure 4.1.33 – UPM High Order Regression Applied to Extended Case Study (f=60, l=100), R ² =-4.492	75

Figure 4.2.1 – GPM Simulation Results (f=20, l= 80 to 140)	76
Figure 4.2.2 – GPM Simulation Results (f=26, l= 80 to 140)	77
Figure 4.2.3 – GPM Simulation Results (f=30, l= 80 to 140)	77
Figure 4.2.4 – GPM Simulation Results (f=20 to 30, l= 80)	78
Figure 4.2.5 – GPM Simulation Results (f=20 to 30, l= 80)	79
Figure 4.2.6 – GPM Results with Linear Regression (f=20, l=80), $R^2=0.793$	80
Figure 4.2.7 – GPM Results with Linear Regression (f=30, l=110), $R^2=0.616$	81
Figure 4.2.8 – GPM Results with Linear Regression (f=29, l=120), $R^2=0.761$	81
Figure 4.2.9 – GPM Results with High Order Regression (f=20, l=80), $R^2=0.890$	83
Figure 4.2.10 – GPM Results with High Order Regression (f=22, l=130), $R^2=0.880$	83
Figure 4.2.11 – GPM Results with High Order Regression (f=29, l=120), $R^2=0.856$	84
Figure 4.2.12 – GPM Results with High Order Regression (f=27, l=90), $R^2=0.846$	84
Figure 4.2.13 – GPM Results with High Order Regression (f=30, l=140), $R^2=0.882$	85
Figure 4.2.14 – GPM Results with High Order Regression (f=20, l=80 to 140)	86
Figure 4.2.15 – GPM Results with High Order Regression (f=25, l=80 to 140)	86
Figure 4.2.16 – GPM Results with High Order Regression (f=30, l=80 to 140)	87

Figure 4.2.17 – GPM Results with High Order Regression (f=20 to 30, l=80)	88
Figure 4.2.18 – GPM Results with High Order Regression (f=20 to 30, l=110)	88
Figure 4.2.19 – GPM Results with High Order Regression (f=20 to 30, l=140)	89
Figure 4.2.20 – GPM High Order Regression Applied to Extended Case Study (f=22, l=20), R ² =-0.131	90
Figure 4.2.21 – GPM High Order Regression Applied to Extended Case Study (f=30, l=40), R ² =0.715	91
Figure 4.2.22 – GPM High Order Regression Applied to Extended Case Study (f=20, l=60), R ² =0.883	91
Figure 4.2.23 – GPM High Order Regression Applied to Extended Case Study (f=28, l=60), R ² =0.892	92
Figure 4.2.24 – GPM High Order Regression Applied to Extended Case Study (f=15, l=80), R ² =0.813	93
Figure 4.2.25 – GPM High Order Regression Applied to Extended Case Study (f=10, l=100), R ² =0.796	94
Figure 4.2.26 – GPM High Order Regression Applied to Extended Case Study (f=5, l=140), R ² =0.556	94
Figure 4.2.27 – GPM High Order Regression Applied to Extended Case Study (f=40, l=60), R ² =0.889	96

Figure 4.2.28 – GPM High Order Regression Applied to Extended Case Study ($f=50$, $l=100$), $R^2=0.837$	96
---	----

Figure 4.2.29 – GPM High Order Regression Applied to Extended Case Study ($f=60$, $l=140$), $R^2=0.774$	97
---	----

1.0 INTRODUCTION

1.1 Fire Protection in Modern Buildings

Fire protection engineering has developed as a technical engineering discipline geared towards identifying and mitigating potential hazards in building designs, primarily with respect to life safety during a fire emergency. Today there are a variety of building and life safety codes enforced by local building and fire authorities in countries around the world [1][2][3]. These codes have been developed based on fire engineering principles, and outline building design aspects that are acceptable from a life safety perspective.

Requirements within building codes evolve over time. Amendments to existing requirements, or new requirements altogether, are generally introduced either in response to real fire disasters, or to perceived risks associated with new architecture and building trends [4]. Modern codes in particular strive to be proactive rather than reactive. As building types change, new risks can be identified and mitigated with the introduction and enforcement of new requirements [5].

A good example of the evolving nature of building codes would be the introduction of specific high building requirements within the second half of the 20th century as the construction of these became more prevalent across North America [6]. In the case of high buildings, new risks were noted to be associated with increased travel times for occupants to evacuate the building, and the inability of firefighters to combat fires on upper levels or rescue occupants trapped on upper levels from the exterior of the building with standard equipment. New code requirements to mitigate these risks included provisions for fire fighters to combat a fire from within the building, and smoke controlling measures to ensure exit routes remain tenable for the entire duration of an evacuation [7].

Until recently, code requirements have generally been prescriptive; they provided mandatory design specifications to ensure an adequate level of life safety was provided. An example of a prescriptive requirement would be: all exit stairs must be a minimum of 1100

mm in width. However, as modern technology drives building complexities to entirely new levels, these types of prescriptive building codes can limit architectural creativity in designs. Thus, in the last few decades, performance-based approaches to fire safety within buildings have been increasingly recognized as alternatives to traditional prescriptive code requirements [8]. Instead of the stair-width prescriptive requirement example given above, a performance-based approach for determining stair width would be to ensure that the stairs could allow all occupants to exit the building within a specific amount of time. Depending on the size, configuration, and use of the building, 1100 mm may, or may not, be an appropriate width to allow for a fast evacuation.

Performance-based design allows for creativity within a building's fire strategy (which includes placement of escape routes, fire detection and alarm systems, fire suppression systems, smoke management systems, and so on). Naturally, performance-based codes also allow for more architectural freedom when it comes to building designs, provided that suitable provisions for life safety can be sufficiently demonstrated.

While performance-based designs can provide more diversity in modern buildings, engineering analyses are often required to demonstrate that a design does indeed meet the required performance criteria.

A primary component of any building's fire strategy is the provision of adequate means of escape for all occupants [5]. Under prescriptive requirements, exit stair placement and sizes are dictated based on a building's size and use [1][2][3]. A performance-based solution requires analyses to demonstrate that the proposed exit routes are indeed adequate to serve the future building occupants. Egress modelling is a technique frequently used to analyze a theoretical building evacuation, and can be used to determine the efficiency of a given building's escape strategy [9][10].

1.2 Modelling Evacuation Times

Egress modelling is used to review the process of evacuation in the event of a fire. During a fire emergency, a building evacuation can be divided into several stages [9] as shown in the timeline schematic in Figure 1.2.1 below.

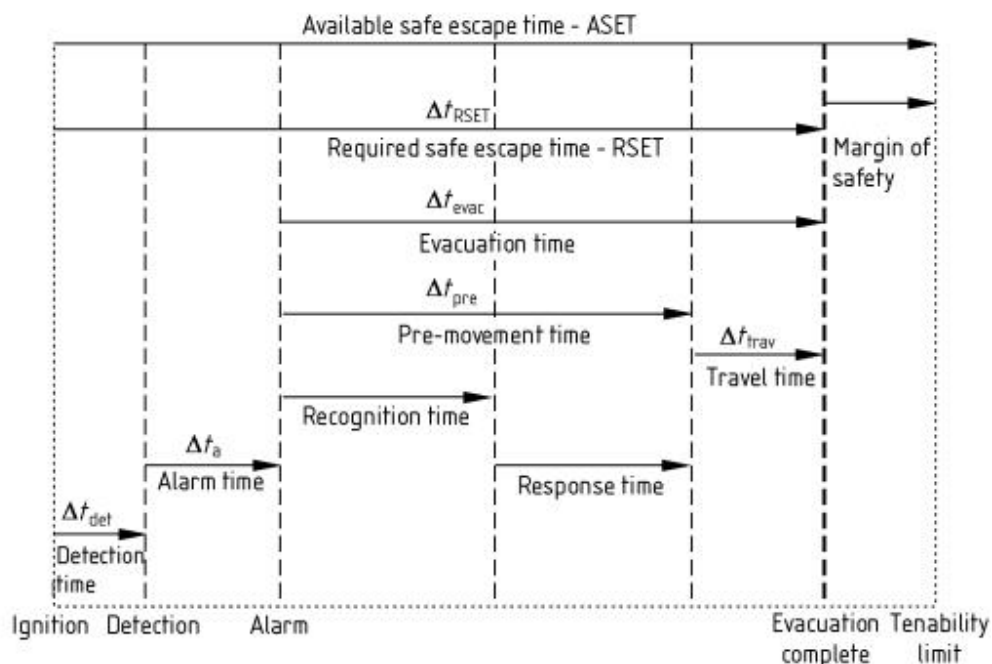


Figure 1.2.1 – Sample timeline comparison between fire development and evacuation [9]

The process of egress modelling generally requires comparing the ASET, or available safe escape time, with the RSET, or the required safe escape time [9]. The ASET is the time from fire ignition until conditions within the building (or more specifically, the escape route) become untenable, while the RSET is the time needed for all occupants to evacuate the building. In order to ensure an adequate level of life safety, it is necessary that the ASET be longer than the RSET by a sufficient factor of safety [11][10].

Calculating the ASET for a particular fire scenario requires a detailed analysis of smoke movement and fire behavior within the building over time. Consideration must be made for the building geometry, construction material, and combustible loading (i.e. the amount of combustible material, such as furniture, present in a space). This type of analysis is routinely performed by engineers who are able to use fire dynamics theory and burn test results to calculate the approximate time from the start of a fire until untenable conditions within a particular area of the building (such as an exit stair) may be reached. [11][12][13][14][15].

Determining a value for the RSET requires the calculation of the values for Δt_{det} and Δt_a (time for detection and time before alarm sounds within the building) as well as the evacuation time, which is considered to begin upon activation of the fire alarm. The values for Δt_{det} and Δt_a can be determined as part of the ASET calculation [9][11]. The calculation of the evacuation time, Δt_{evac} , requires a separate analysis, which is the primary focus of this effort.

1.2.1 Phases of Evacuation Time

The evacuation time, Δt_{evac} , for a building is often considered to have two separate phases: pre-movement time (Δt_{pre}), and travel time (Δt_{trav}). Travel time is often alternatively referred to as movement time (Δt_{mov}) [10][16][17][18].

In an evacuation scenario, the pre-movement phase is considered to be the time between when an occupant is first notified of an emergency (often when the occupant hears the building fire alarm), and when that occupant begins to proceed towards an exit. This includes both recognition time (the time for an occupant to register that there is a real emergency in the building, not just a false alarm or alarm system test), and response time (the time from the recognition of an emergency until the occupant begins to evacuate). Pre-movement time could include, for example: time to discuss the situation with colleagues or neighbors, finish the task at hand, locate companions, gather belongings, or put on a jacket [9][10][16][18].

The second component of evacuation time, the movement phase, follows the pre-movement phase, and is the length of time for an occupant to exit the building once they begin the process of evacuating [9][10][16][17][18].

Therefore, the sum of any individual's pre-movement time and movement time is the evacuation time for the individual. However, calculating the evacuation time for a group of individuals, especially large groups of people throughout a room, floor, or building is inherently more complicated, as each individual will have a different pre-movement and movement time [16].

1.2.2 Calculating Movement Time

The movement time for a group of people can be calculated through the process of egress modeling. A broad range of egress modeling tools and techniques exist, with varying benefits and drawbacks [19][5]. These can range from simplified hand calculations to sophisticated computer models [17].

Steven M. V. Gwynne and Eric R. Rosenbaum published their method of egress modeling in the 4th edition of the Society of Fire Protection Engineers' Handbook (SFPE Handbook) [11]. This method, known as the hydraulic model, is widely referenced and used in industry today [8] and has adapted fundamental traffic flow equations to describe pedestrian movements through an exit route similar to a fluid flow [11].

Walking speeds of individuals vary depending on the congestion of the environment. As crowding increases around an individual, their walking speed will slow as a result. The more impeded an occupant, the slower they are able to move. Eventually, "crush conditions" are reached, where movement forward is not possible until congestion eases [11].

The relationship between walking speed and density is defined in the hydraulic model with the following equation

$$s = k - akd \quad (1)$$

where:

s =speed along the line of travel, in m/s

d =population density described in people/m²

a = a constant, which takes the value 0.266m²/p for calculations performed in metric units

k = a constant, with unit m/s and with magnitude varying depending on the type of exit facility being used (e.g. flat surface, ramp, stairs, etc.).

Sample values of the constant k are provided in Table 1.2.1 below [11]. It is noted that case studies in this effort included horizontal walking surfaces and stairs having steps with 180 mm riser heights and 280 mm tread depths.

Table 1.2.1 – Values of constant k for various walking surfaces [11]

Escape Route Element		k (m/s)
Horizontal Surface (Corridor, Aisle, Ramp, Doorway)		1.4
Individual Step Measurements for Stairways:		
Riser Height (mm)	Tread Depth (mm)	
190	250	1
180	280	1.08
165	305	1.16
165	330	1.23

The specific flow in an evacuation route is measured as the number of people to pass an arbitrary point (a doorway, for example) within a given span of time, for a given amount of width available. The specific flow is dependent on the speed of pedestrians, s , as defined above in equation (1), and is also separately dependent on density: the denser the stream of occupants, the more people will flow past a point within the given period of time for a

particular amount of width. The hydraulic model defines the specific flow rate as per equations (2) and (3) below:

$$f_s = sd \quad (2)$$

$$f_s = (1 - ad)kd \quad (3)$$

where:

f_s = the specific flow, in people/s/m

s, a, d, k as defined above

As equation (3) is quadratic in d , there is an optimal density to maximize the specific flow. Figure 1.2.2. shows specific flow as a function of density, for k values corresponding to a variety of walking surfaces (ramps, stairs, etc.).

The specific flow, above, notes the flow of people past a point per unit width of the walking path. However, flow rate for any particular point along the exit route can be more accurately described by considering the effective width of that point. The effective width is the width of a facility (door, corridor, etc.) that is actually used by people when walking. Consider a person walking down a corridor; it would be unusual if this person were to walk with their shoulder rubbing up against wall. The space that is naturally kept between a person and whatever object they walk past is called the boundary layer, and the effective width is defined as the width of a facility reduced by the appropriate boundary layers.

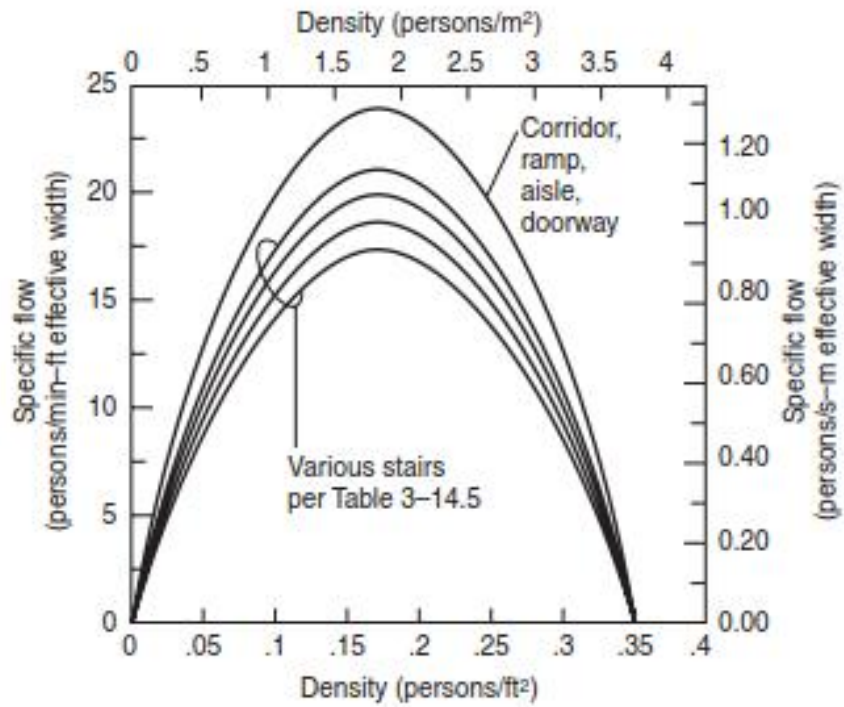


Figure 1.2.2 – Specific flow as a function of density [11]

Therefore, the flow rate for any given facility can be defined as per equations (4) and (5) below.

$$f_f = f_s w_e \quad (4)$$

$$f_f = (1 - ad) k d w_e \quad (5)$$

where:

f_f = the flow rate for the facility, in people/s

w_e = the effective width, in m

a, d, k as defined above

As people evacuate a building, density can fluctuate. This in turn can affect the flow rates throughout the exit route. Thus, an accurate egress model needs to account for varying densities and flow rates throughout the course of an evacuation.

1.2.3 Calculating Pre-Movement Time

The other portion of the evacuation time comes from the pre-movement phase. Pre-movement time, which describes the behavior of the occupants in a building, has historically been very difficult to estimate accurately, as small factors can influence the behavior of individuals in evacuation scenarios [5] [16][17] [20].

Things that are often taken into consideration include whether the occupants may be asleep (such as in an apartment building), how familiar occupants are with a building, and the types of occupants in the building [9][18].

Though some of the above aspects may be estimated for a particular evacuation event, the pre-movement time of a group is best modeled not with a single value, but with a range of values to reflect the natural variation within a group of individuals [16][17].

Despite this, pre-movement time is often simplified during an evacuation analysis [10][17]. Often, the evacuation time is estimated by simply adding a mean pre-movement time to the value calculated for movement time with simultaneous start (i.e. without considering pre-movement).

Consider an example where a fire alarm sounds within an office building. The assumption of a simultaneous start would model all employees in the building standing up in unison and walking towards their nearest exit immediately. This is unrealistic. In a real evacuation different people would begin exiting at different times, depending on their own unique mindset and some of the factors mentioned above. By ignoring pre-movement time and calculating movement time with a simultaneous start assumption, it is easy to neglect the effects that pre-movement can have on the movement phase.

Pre-movement can effect queuing and density along an evacuation route, by staggering the arrival time of individuals at an exit route. If all occupants of a building begin exiting at the same time (simultaneous start), then the density throughout the exit route is likely to spike very quickly. However, if there is a lot of variation between the start times of individuals, then the density within an exit route may not increase as quickly or as drastically. The density may even fluctuate depending on how people stagger their arrivals.

As shown in equations (1) through (5) above, flow rates are dependent on density. Therefore, fluctuating densities driven by the pre-movement phase can affect the flow rates, and consequently, the movement time. However, the relationship between the movement and pre-movement phase can be more complicated. If there are large numbers of people evacuating, queues will begin to form along the exit route, particularly at “pinch points”, such as narrow doorways.

If the queue at a pinch point is sufficiently large, then staggered additional arrivals will not impact the flow rate at that particular location. Additional arrivals will not increase the density, they will simply join the already densely packed group of people in queue.

Consider the office floor example again, but with varying pre-movement times for individuals. If it is a particularly busy office with lots of people throughout the building, one could expect a queue to form at the door to an exit stair as the stairs become full of occupants. If one occupant has an exceptionally long pre-movement time, then they will join the queue at the door and will need to wait for the queue to clear before they can continue any further. Their movement time is therefore limited by the queue, not by their pre-movement time.

Thus, queuing has the ability to “absorb” the effects of pre-movement time, particularly for occupants who have very large pre-movement times and in densely populated buildings.

So, in some cases the effects of pre-movement time can be rendered negligible if queuing is significant. But as noted earlier, pre-movement time can also affect the amount of queuing within an evacuation time.

After examining this problem, it is clear that there is a complicated relationship between pre-movement and movement phases, and that the analysis of these two aspects separately ignores the effects that one phase may have on the other.

While including a realistic range of pre-movement times into an egress model would be most accurate, this is often not feasible without sophisticated egress modeling software – which can be both expensive to obtain and time-consuming to use.

Therefore, calculating movement time assuming simultaneous start and then adding an average value of pre-movement time to generate an evacuation time is still performed in industry today. However, this type of analysis ignores the complex relationship between movement and pre-movement.

The focus of this work has been to examine the effects pre-movement can have on the overall evacuation time of a building by comparing evacuation scenarios that include various pre-movement ranges to those that assume a simultaneous start. In particular, this work focuses on evacuations of high buildings, where queuing within stairwells can be significant and the effects of pre-movement may be most evident.

Related research has been conducted regarding the effects of pre-movement and density on overall evacuations, for small rooms and two-storey buildings [17]. However scenarios reviewed as part of this previous research focused on pre-movement times that generally exceeded the movement time for the buildings being reviewed. The analysis described herein will differ on two fundamental points: it will examine effects of pre-movement on evacuations of large buildings exclusively (ranging from 5 to 60 storeys in height), and the pre-movement time ranges will typically be smaller than the movement times for the evacuation scenarios being reviewed.

2.0 METHOD FOR CALCULATING THE EFFECTS OF PRE-MOVEMENT

In order to calculate the effects of pre-movement (considered to be a range rather than a single value), comparison must be made between evacuations with varying pre-movement times to those with a simultaneous start. This can be achieved by comparing multiple evacuation trials with differing pre-movement assumptions.

In order to model numerous evacuation trials with particular input parameters, a simulation algorithm was created in MATLAB to estimate evacuation times for scenarios both with and without pre-movement times.

The simulation algorithm created for the purposes of this work is based on the principles of the hydraulic model. User inputs define the building geometry as well as the characteristics of the occupants in any given simulation.

2.1 Number and Usage of Exit Routes

The focus of this work is to examine the effects of pre-movement in high buildings. Therefore, the simulation algorithm has been designed to consider these types of buildings exclusively.

Current Canadian building codes require that each floor of a high building be served by at least two exit stairs [1]. These are often arranged within building cores, which are typically comprised of elevator, stair, and service shafts located in a cluster running vertically through the height of the building.

High buildings can be designed with additional cores or exit stairs where it is architecturally practical, but in all cases, occupants in a high building conforming to current Canadian building codes will have access to at least two distinct exit routes [1]. Thus, regardless of the number of exit stairs present, each stair will serve only a fraction of the

occupants on each floor. The time required to evacuate a building will be determined by the exit route which takes the longest to clear, or the limiting exit route.

Where multiple exit routes are geometrically similar (i.e. stairs of identical widths accessed by doors of identical width), it may not be apparent which will be the limiting route. In this case, the number of people in each route would often determine which one is limiting; the exit route used by the largest amount of people will take the longest to clear.

As part of this review, building evacuations were modeled based on the time to clear the limiting exit route. However, each evacuation could represent multiple building scenarios, depending on what percentage of occupants are assumed to be using the limiting exit route.

For example, if 100 people per floor are considered to use the limiting exit route, this could represent 50% of occupants in a building having 200 occupants per floor served by two stairs. Alternatively, it could represent 60% of occupants in a building with 166 people per floor and two stairs. Or, it could represent an even distribution in a building having 300 people per floor served by three stairs. In any case, the number of people using the limiting exit route will affect the evacuation time of the building. The percentage of occupants using the limiting exit route or any other exit is irrelevant.

Therefore, this review will consider the number of occupants using a single exit route, rather than the number of occupants that may be within an entire building.

2.2 Evacuation Phasing

If a fire is detected within a high building, occupants closest to the fire (generally those on the fire floor, and perhaps occupants on neighboring floors depending on local regulations) would be advised to evacuate immediately, while others in the building would only be told to evacuate after a delay. This practice, referred to as phased evacuation, is common in high buildings, and allows for priority to be given to those who are at the highest risk.

Phasing evacuations can certainly affect the evacuation time of a building, by directly affecting queuing and pre-movement for occupants on different floors. Indeed there is practically an infinite number of phasing scenarios that could be reviewed (which could depend on the location of a fire within a building, the type of fire alarm system used, the action of building management teams upon first detection, etc.), all of which could have a slightly different effect on the evacuation time for the building. Thus phasing could mask the more subtle effects that natural human pre-movement behaviour can have on evacuations. Therefore, in order to isolate the effects of human pre-movement (which is the primary focus of this review), phasing has been ignored within this analysis. Fire alarm systems have been modeled as single stage fire alarms, with all floors notified to evacuate at the same time. While this may not be realistic in modern high building evacuations, this has been done deliberately to investigate the effects that pre-movement time can have on building evacuations.

2.3 Algorithm for Modelling Evacuations

2.3.1 Describing Conditions within the Exit Route

In the simulation algorithm, the limiting exit route is broken into components which comprise the exit stair and corridor on each floor leading to the exit stair. Five different exit segments are identified for each typical floor, and are named as follows:

- C_i – the corridor leading to the exit door at level i
- L_i – the landing at floor level i
- St_i – the top flight of stairs, located immediately below landing L_i
- I_i – the intermediate landing between floor levels i and $i-1$
- Sb_i – the bottom flight of stairs, located below the intermediate landing I_i

Figure 2.3.1 below shows a section through the exit stair of a building at arbitrary level i , with the segments labeled. In general, every level has the five segments listed above, which are highlighted in red.

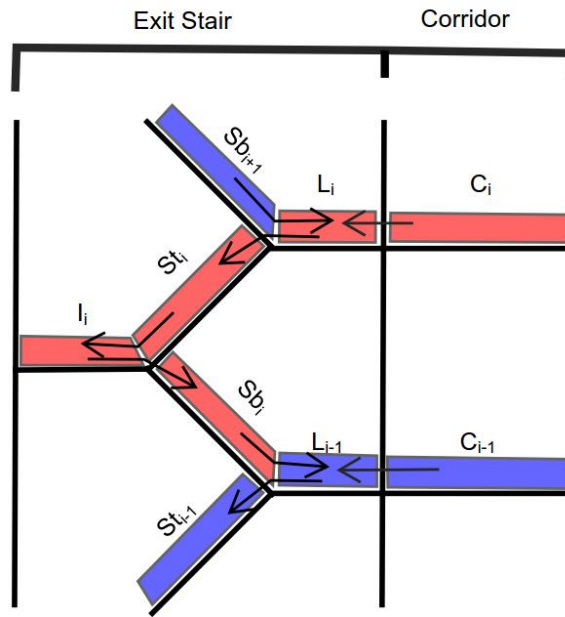


Figure 2.3.1 - Segments of the exit path at arbitrary floor level i

Figure 2.3.2 shows a similar section, but at exit discharge level, which includes the additional segment E to symbolize the exterior of the building.

Arrows in both Figures 2.3.1 and 2.3.2 show the direction of exit travel through the exit route. It is noted that for a landing L_i at any level i other than the top level, there are two entrance streams of occupants; one from above (Sb_{i+1}) and one from the corridor beyond the stair (C_i).

The algorithm simulates movement by keeping track of the number of people within each segment. The algorithm utilizes a number of matrices, whose values correspond to various properties within each segment.

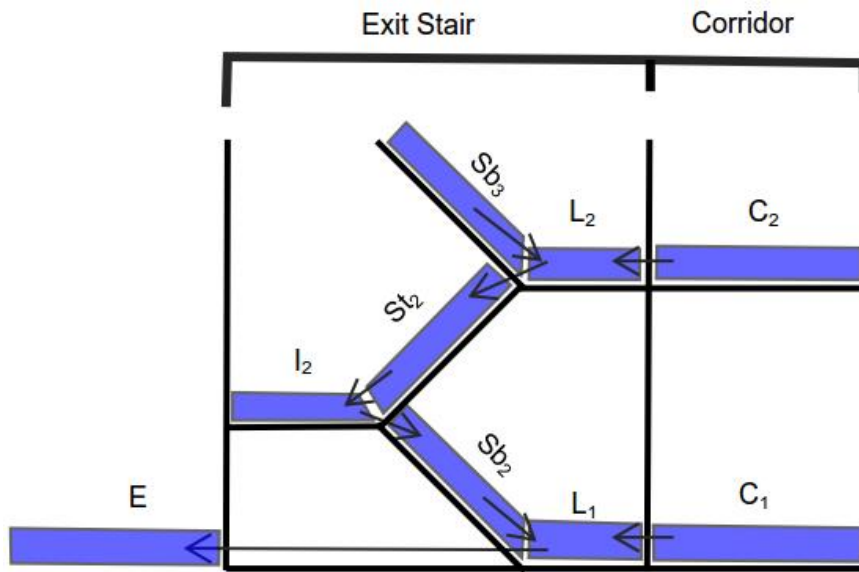


Figure 2.3.2 - Segments of the exit path at exit level

To define the matrices, a maximum time and a time interval must first be determined. It was desired to keep time steps as small as possible in order to simulate continuous movement through the modeled evacuations. The time step of $1/100^{\text{th}}$ of a second (1 cs) was chosen as this was the smallest time step which the algorithm could reasonably accommodate. This time step generally resulted in simulation run-times of between 2 seconds and 40 minutes, as described in more detail in Section 4.1. Using a smaller time step would have increased the model run time drastically, which would have made it impractical to simulate some of the larger buildings which were included in this work.

Matrices were created to include calculations for times of up to 200 minutes, or 1,200,000 cs. The maximum value of time steps within the algorithm is defined as T_n (for example, $T_n=1,200,000$).

The first sets of matrices have size $f \times T_n$, where f is the number of floors in the building and T_n is the number of discrete time steps modeled during the simulated evacuation. These matrices have the name $Xcount$, where " X " is a segment label " L ", " St ", " I ", " Sb ", or " C " as shown in Figure 2.3.1.

$$Xcount = \begin{bmatrix} Xcount(1,0) & Xcount(1,1) & \dots & Xcount(1,T_n) \\ Xcount(2,0) & Xcount(2,1) & \dots & Xcount(2,T_n) \\ \dots & \dots & \dots & \dots \\ Xcount(f,0) & Xcount(f,1) & \dots & Xcount(f,T_n) \end{bmatrix}$$

The value in the i^{th} row and t^{th} column of the matrix $Xcount$ is denoted $Xcount(i,t)$, and it is assigned a value which represents the number of people in segment X_i at time t . As an example, the value of $Xcount(2,100)$ would indicate the number of people in segment X (which could be "L", "St", "I", "Sb", or "C") on Level 2, at time step 100. All entries within this matrix are set to zero as a default at the beginning of a simulated evacuation, and the matrix is populated with values as the algorithm progresses.

The second set of matrices (also size $f \times T_n$) keep track of who is in queue to move onto the next sequential segment. These matrices are named QY , where "Y" takes on the values "L", "St", "I", "Sb", or "C" to represent occupants who are ready to move, respectively:

- to a landing from the steps above,
- to the top flight of stairs from the landing,
- to the intermediate landing from the top flight of stairs,
- to the bottom flight of stairs from the intermediate landing, and,
- to the landing from the corridor beyond the exit stair door.

$$QY = \begin{bmatrix} QY(1,0) & QY(1,1) & \dots & QY(1,T_n) \\ QY(2,0) & QY(2,1) & \dots & QY(2,T_n) \\ \dots & \dots & \dots & \dots \\ QY(f,0) & QY(f,1) & \dots & QY(f,T_n) \end{bmatrix}$$

The value in the i^{th} row and t^{th} column of these matrices is denoted $QY(i,t)$ and represents the number of people in queue to enter segment Y_i at time t .

In general Y takes the value of the destination segment. However, it is noted that there are two streams of people who will be queued to enter segment L_i , and yet only one of these

streams can be designated as QL_i . The algorithm has defined QL_i as the queue to the landing which originates from within the stair (i.e. from Segment Sb_{i+1}). The queue to a landing from the floor area has been designated QC_i to distinguish it from QL_i .

As an example, the value $QL(2,100)$ would be the number of people queued to enter the landing at Level 2 at time step 100, from the bottom flight of steps of the third floor (Sb_3). The value $QC(2,100)$ would be the number of people queued to enter the same landing at Level 2 at time step 100, but from the corridor at Level 2 (C_2).

To illustrate the use of the $Xcount$ and QY sets of matrices, Figure 2.3.3 below shows a sample scenario, with sample entries from the matrices $Lcount$, QSt , $Stcount$, and QI . These matrices are also summarized in Table 2.3.1.

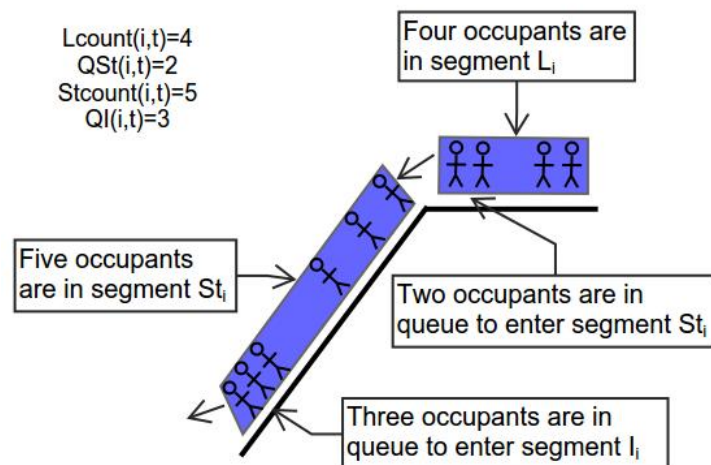


Figure 2.3.3 - a sample scenario during an evacuation at time t and floor i

It is noted that the above *count* and Q matrices track values for the entire time interval of the simulated evacuation (i.e. with entries from 1 to T_n). This was done primarily so that the algorithm could influence the values of the matrices for future time steps. For example, based on the walking speed of an occupant and distance they had to travel, the algorithm

could predict the future time step when they would enter their queue, and account for them arriving in the future.

The algorithm models the movement of occupants from one segment to the next. In particular, the speed and flow rate of occupants as they move through the exit route agree with the equations (1) and (5) given previously. In order to control the flow rate at a point when using small, finite, time steps, a delay period (i.e. some number of time steps) must be considered between the movements of two consecutive people passing the same point. A third set of matrices was introduced to track these delay periods. These matrices have names of the form $Xwait$, where " X " again is the label " L ", " St ", " I ", " Sb ", or " C ". These matrices have size $1 \times f$. Entries are denoted $Xwait(i)$, and represent the delay time required before the next person can be modeled leaving segments L_i , St_i , I_i , Sb_i , and C_i . These matrices and their functions are described in more detail in Section 2.3.4 of this report.

A fourth set of matrices of size $1 \times f$ note the density within each segment of the model, and are written as DX , for " X " as the labels " L ", " St ", " I ", " Sb ", or " C ". Entries of this matrix, noted $DX(i)$, represent the density within segment X_i , expressed as a value in people/m².

For any given segment X_i , the density at time t is calculated as follows:

$$DX(i) = \frac{Xcount(i,t)}{areaX} \quad (6)$$

where:

$DX(i)$ and $Xcount(i,t)$ are as defined above, for " X " = " L ", " St ", " I ", " Sb ", or " C "
 $areaX$ is the usable area (i.e. area available for occupants to stand) within the standard segment X , for " X " = " L ", " St ", " I ", " Sb ", or " C ". This area is predefined within the algorithm based on the physical geometry of the building being modeled.

During a simulated evacuation, the density of a particular segment is limited by the algorithm to 1.9 persons/m². As shown in Figure 1.2.2 above, this represents an optimal

density for flow rates. If density is increased beyond this cap, movement becomes rapidly impeded and crush conditions (i.e. where occupants are unable to move at all) may result. The hydraulic model of evacuation therefore proposes this limit for densities when calculating evacuation times. It is also noted that this value corresponds well with maximum densities of NFPA 101 Life Safety Code, which is widely used in industry [11][2].

One additional matrix, size $1 \times f$, keeps track of the position of the door into the exit stair on all levels from 1 to f . This matrix, Dr is filled with entries denoted $Dr(i)$, which take on discrete values as follows:

- $Dr(i)=0$: the door on floor i is closed
- $Dr(i)=1$: the door on floor i is in the process of opening, but is not fully open
- $Dr(i)=2$: the door on floor i is open.

Depending on the status of the door on level i , additional time may be added to the $Cwait(i)$ value, to account for an added delay associated with the time required for an occupant to open the door before they can walk through it.

Table 2.3.1 – Summary of Matrices

Matrix Set	Actual Matrices Used	Size	Entries	Description
$Xcount$	$Ccount, Lcount, Stcount, lcount, Sbcount$	$f \times T_n$	$Xcount(i,j)$	Notes the number of occupants in segment X_i at time j
QY	QC, QL, QSt, QI, QSb	$f \times T_n$	$QY(i,j)$	Notes the number of occupants queued to enter segment Y_i at time j ¹
$Xwait$	$Lwait, Stwait, lwait, Sbwait, Cwait$	$1 \times f$	$Xwait(i)$	Notes the delay period in cs before the next movement can occur from segment X_i
DX	DL, DSt, DI, DSb, DC	$1 \times f$	$DX(i)$	Notes the density within segment X_i , and is updated each time movement occurs on that segment
Dr	Dr	$1 \times f$	$Dr(i)$	Takes discrete values to indicate the position of the door to the exit stair on level i

Note ¹: QL describes queues from above, whereas QC describe queues from the corridor.

The matrices used by the algorithm are summarized in Table 2.3.1.

2.3.2 Arrival Time at Exit Door

For each simulation, the user must input two key variables to define the initial conditions. These are:

- the number of floors in the building, f , and
- the number of people per floor using the exit route, or “loading” l .

Thus the number of people within the building, N , can be expressed as

$$N = f \times l \quad (7)$$

At the start of a simulation, the algorithm creates two random $f \times l$ matrices, D and S . The value d_{ij} , the entry of D in the i th row and j th column, corresponds to the starting position for the j th occupant on floor i . Its value represents the walking distance, in meters, between the occupant and the nearest exit stair door.

Similarly, the entries of S are populated with walking speeds for the occupants within the building. For a simulation assuming a normal, able-bodied population, these walking speeds are selected randomly based on a truncated normal distribution, and having mean 1.25 m/s, standard deviation of 0.32 m/s. Values are truncated at 2.21 m/s and 0.29 m/s (i.e. the mean plus or minus 3 times the standard deviation). These are based on walking speeds noted in the hydraulic model [11].

A third $f \times l$ matrix, P , is generated as part of the algorithm, and accounts for individuals' pre-movement times. Based on a user-defined distribution and a pre-movement time cap, p , the entries of P are randomly generated from 0 to p , with the value p_{ij} being the pre-movement time for the j th individual on floor i .

The matrices D , S and P are used to create the matrix A , which notes the arrival time at the nearest exit for each individual. An intermediate matrix W with entries w_{ij} is generated as follows from entries d_{ij} and s_{ij} :

$$w_{i,j} = \frac{d_{i,j}}{s_{i,j}}$$

W represents the walking time for each individual to reach their nearest exit. The final matrix A of arrival times at the exit stair door is taken as the sum of an individual's walking time, plus pre-movement time, with entries a_{ij} calculated as follows:

$$a_{i,j} = w_{i,j} + p_{i,j}$$

Once A has been calculated, the algorithm then creates a second matrix, called AD , of size $f \times T_n$, to denote the time of arrival at the door for all occupants on a particular floor. The entry in the i^{th} row and t^{th} column of AD is denoted $AD(i,t)$, and it has a value corresponding to the number of occupants who arrive at the stair door on level i at time t .

The matrix AD is initially populated with all zeros. Using iterative loops, the algorithm checks every entry within matrix A . For each value $A(i,j)$, which represents the arrival time at the door for the j^{th} occupant on floor i , the algorithm adds 1 to the value of $AD(i,A(i,j))$. Once the algorithm has looped through all values of A , the matrix AD is fully populated. Entries of $AD(i,t)$ show the number of occupants to arrive at the stair door on level i at time t .

It is necessary that the sum of entries in any row i of AD will be the total number of occupants on floor i , as each occupant's arrival time is noted exactly once, in the column corresponding to the arrival time step. Therefore, when using small time steps to model large amounts of time, many entries with the matrix AD will remain zero.

Once the matrix AD has been populated, the algorithm begins its set of iterative calculations, which repeat for each consecutive time step.

2.3.3 Identifying Possible Movements

For each time step, the algorithm loops through all floors, from 1 to f . At each level, i , it performs the checks and calculations described below.

First, the values from previous time steps are carried forward to the current time step. (All matrix values are set to zero by default at the beginning of each simulation.) The algorithm executes the following command for " X " = " L ", " St ", " I ", " Sb ", and " C ":

$$Xcount(i,t) = Xcount(i,t-1) \quad (8)$$

Next, the algorithm adds any newly arrived occupants to the count of occupants in queue in the corridor. This number is both the number of people within the corridor, and also the number of people in queue to enter the stair. Thus, $Ccount(i,t)$ and $QC(i,t)$ take the same value:

$$QC(i,t) = Ccount(i,t) = Ccount(i,t) + AD(i,t) \quad (9)$$

Then, the algorithm checks each segment to see if movement can occur from any given origin segment X_i to the next consecutive destination segment Y_j (where $i=j$ in all cases except where $X_i = Sb_i$ and $Y_j = L_{i-1}$), it checks the following conditions:

- (1) Is there someone in queue ready to move from segment X_i to segment Y_j ? (i.e. Is $QY(j,t)$ nonzero?)
- (2) Has a sufficient delay time elapsed since the last movement in this location occurred? (i.e. is $Xwait(i)=0$?)

For the case where X_i is corridor C_i and Y_j is landing L_i , a third condition is also checked:

- (3) Is the door to the stair open? (i.e. is $Dr(i)=2$?)

Provided the applicable two or three conditions are met, the algorithm notes the location (origin segment name and floor number) where movement is possible. The algorithm then goes on to check all other locations in the building. As the algorithm performs these checks, it keeps an internal list of all movements that are possible for this time step.

Once the algorithm finishes checking though all segments for possible movements, it proceeds to model these movements in random order. It randomizes the list created during the checking phase, and models the movements one at a time in this random order.

Randomizing the order of movement is done to avoid bias for particular floors. In particular, when modeling movement onto an arbitrary landing, L_i , movement may be possible from two separate streams at the same time; Sb_{i+1} and C_i . However, if there is only room for one person before peak density is reached, movement would only be permitted from one of these streams. As the algorithm checks for possible movement iteratively through floors 1 to f , the algorithm would register the possible movement from level i (i.e. from C_i) before it recognized that movement was also possible from level $i+1$ (i.e. from Sb_{i+1}). Thus, if movements were performed in the order they were found, this would create bias towards movements from C_i over those from Sb_{i+1} in every instance. By first checking for possible movements, and then modeling those movements in a randomized order, this bias is removed. This concept is illustrated in Figure 2.3.4 below.

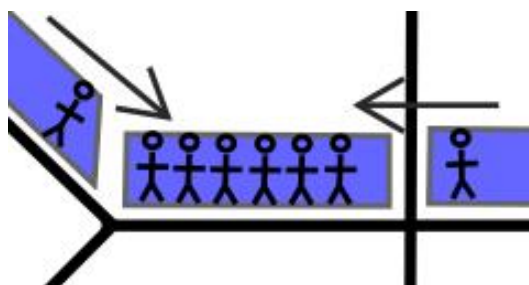


Figure 2.3.4 – Where there is only room for one person from two possible streams, the algorithm randomizes which movement has priority

The algorithm proceeds to model movements in the randomized order. However, before movement occurs, an additional condition is checked:

(3 or 4) Is there room on the destination segment for one more person? (i.e. is $DY(j) + (1/areaY) \leq Dmax$, where $Dmax$ is the predefined maximum density in which people will voluntarily stand?)

Provided this last condition is met, movement is modeled by the algorithm, as described below.

2.3.4 Modelling Movement

Movement is modeled through updating values of the matrices described in Section 2.3.2. First, the occupant is moved from the origin segment X_i to the destination segment Y_j as follows:

$$\begin{aligned} Xcount(i,t) &= Xcount(i,t) - 1 \\ QY(j,t) &= QY(j,t) - 1 \\ Ycount(j,t) &= Ycount(j,t) + 1 \end{aligned}$$

In the case of movement near the ground floor, the algorithm uses slightly different syntax and variables, modeling the counts as follows:

$$\begin{aligned} Lcount(1,t) &= Lcount(1,t) - 1 \\ QE(t) &= QE(t) - 1 \\ exitcount &= exitcount + 1 \end{aligned}$$

Next, a delay time must be established so that the next person from segment X_i cannot follow this movement too quickly. This is based on equations (1) and (5) for speed and flow rate through a specific exit route facility, and is modeled by the algorithm as:

$$V = \begin{cases} V_{max}(Y) & \text{if } DY(j) \leq D_{min} \\ k - 0.266 \times k \times DY(j) & \text{if } D_{min} < DY(j) < D_{max} \\ V_{min}(Y) & \text{if } DY(j) \geq D_{max} \end{cases}$$

$$F = V \times DY(j) \times We(Y, j)$$

$$X_{wait}(i) = \frac{1}{F}$$

where:

$V_{max}(Y)$ is the maximum walking speed expected on segment type Y, when density is sufficiently low that a person can walk unimpeded

D_{min} is the density up to which walking is considered unimpeded

$V_{min}(Y)$ is the minimum walking speed on segment type Y once density reaches its peak value

D_{max} is the density cap predetermined within the model.

$We(Y, j)$ is the effective width of segment Y_j , as predefined in the algorithm based on the geometry of the building being modeled

The delay time to exit is modeled similarly as above, but with slightly different syntax:

$$V = V_{max}(E)$$

$$F = V \times DL(1) \times WeE$$

$$E_{wait} = \frac{1}{F}$$

In both cases, E_{wait} or $X_{wait}(i)$ are rounded to the nearest integer value.

Here, it is noted that space beyond the exit door (i.e. the outdoors) is assumed to be unrestricted, and the velocity through the exit door is assumed to be unimpeded, $V_{max}(E)$. The wait time through the exit door, E_{wait} , is noted to be a function of the walking speed,

the density of the crowd at the bottom of the stairs, $DL(1)$, and the effective width of the final exit door, WeE .

Lastly, as part of the movement calculations, the algorithm determines when the occupant will reach the end of the destination segment Y_j , and reach the queue to enter the next segment, Z_k (where $k = j$, except in the case where $Y_j = Sb_j$ and $Z_k = L_{j-1}$).

This is done by first determining the new density of the destination, $DY(j)$ as described previously, using the updated $Ycount(j,t)$ value and the predefined area of the segment Y_j .

Then, the walking speed across the segment (V) is calculated once again based on the updated density.

The time to reach the next segment is computed by taking the travel distance length of the segment (YTD) and dividing it by the walking speed V , and stored in the variable $next$:

$$next = \frac{YTD}{V}$$

where:

YTD is the travel distance across segment Y , as predefined within the algorithm based on the geometry of the building being modeled

$next$ is a variable used by the algorithm to store the travel time to reach the queue to the next segment

Lastly, the queue of people at the end of segment Y_j , who are ready to enter segment Z_k , will increase by one at the future time step $t+next$.

$$QZ(k, t + next) = QZ(k, t + next) + 1$$

Once these three aspects of movement have been performed by the algorithm (updating the count of people in the origin and destination segments, calculating the delay time for future movements, and determining when the occupant will reach the end of the destination segment) the simulation of movement is complete, and the algorithm moves on to model the next movement in the predetermined randomized order.

Once all possible movements have been performed for the time step t , the algorithm advances to the next time step, $t+1$, and begins the process of checking for possible movements again. At the beginning of the new iteration, the algorithm subtracts one from all wait times:

$$Xwait(i) = Xwait(i) - 1$$

for " X " = " L ", " St ", " I ", " Sb ", and " C ".

Movement can only occur once the wait time has become zero. As noted above, this is the second condition that the algorithm checks before it considers movement to be possible.

The algorithm continues to loop through all time steps iteratively, until the value of $exitcount = N$, signifying that all N occupants in the building have successfully exited. The value of t when this occurs is considered the building evacuation time.

3.0 CASE STUDIES

As the purpose of this effort has been to review the effects of pre-movement times within evacuations of tall buildings, this type of building has been considered exclusively.

Sample buildings have been designed to comply with current National Building Code of Canada (NBC) guidelines [1], with regard to stair, landing, and door dimensions. These aspects are kept constant for all buildings reviewed, though aspects such as the number of floors (f) and the occupant loading per floor using the exit route (l) will vary depending on the simulation. These parameters can be entered by the user independently for each simulation, while the exit route dimensions remain fixed.

3.1 Geometry of Floor Area and Exit Route

The geometry of stairs and doorways that have been modeled are shown in Figures 3.1.1 and 3.1.2 below. It is noted that, in compliance with the hydraulic model, boundary layers have been considered along the edges of landings and stairways, and are also shown in these figures.

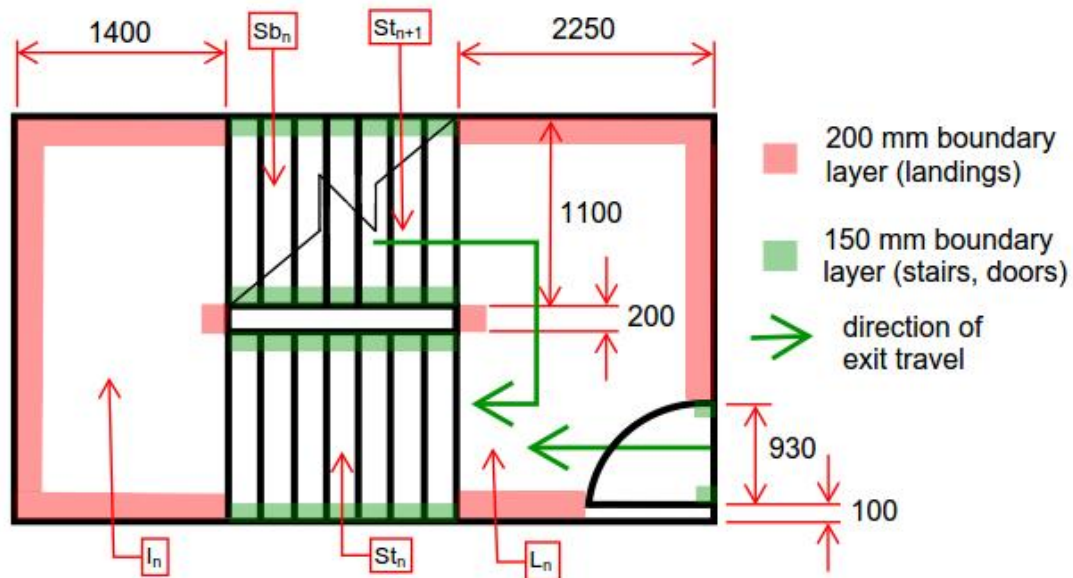


Figure 3.1.1 – Plan of exit stair at level n , with dimensions shown in mm

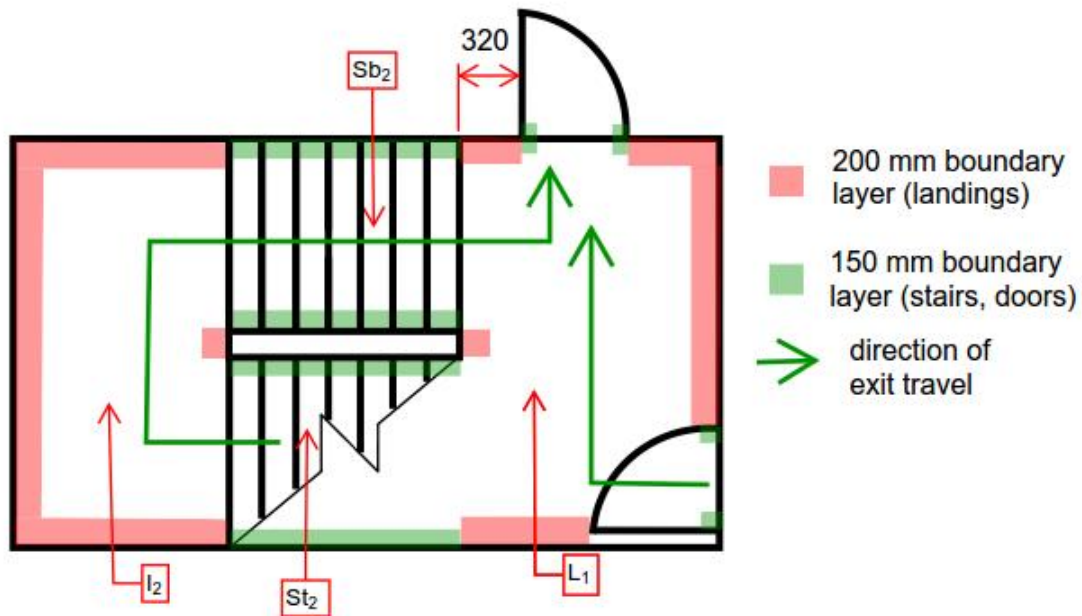


Figure 3.1.2 – Plan of exit stair at level 1, with dimensions shown in mm

Figure 3.1.3 below shows the typical stair flight in section, with the riser heights of 180 mm and tread depths of 280 mm labeled.

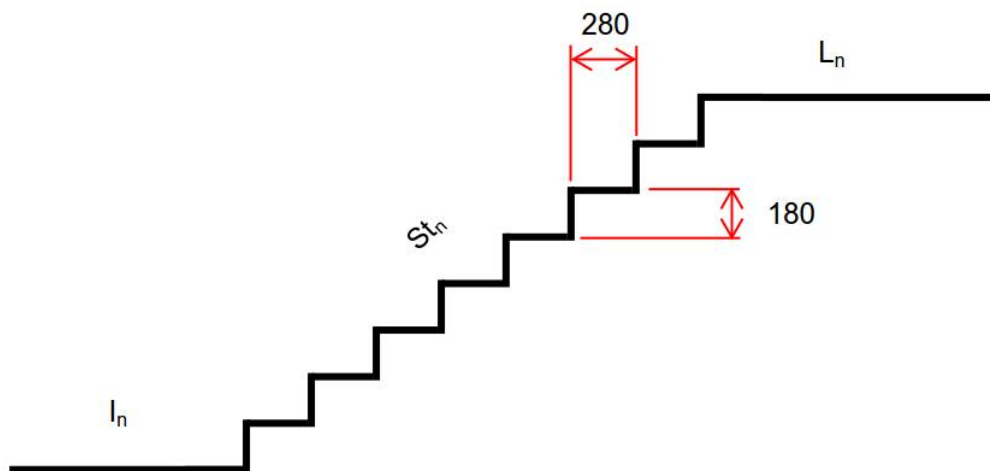


Figure 3.1.3 – Section of St_n with tread depths and riser heights labeled in mm

The physical layout of the floor areas (i.e. the areas beyond the exit stairs which would normally be occupied) was not written into the algorithm with the same level of detail. For

horizontal walking, the equations of the hydraulic model are based on distance traveled, without considering direction or path. Therefore, the travel distance for occupants to reach an exit is the relevant piece of information, and the physical layout of the path within floor is irrelevant to the calculations.

Consequently, rather than requiring elaborate floor area plans, the algorithm can simply generate travel distances for the occupants situated on a particular floor. Travel distances to reach the exit stair were randomly generated, based on uniform distribution, with values from 5 to 45m. This is in compliance with NBC travel distance requirements for tall, sprinklered buildings.

As the floor area layout was not modeled, no parameters have been included to describe the layout of the corridor leading directly to the exit stair door. The model assumes a corridor is present in nomenclature only (i.e. with use of the label “C” to describe the area immediately beyond the exit stair door) the shape of this area is irrelevant to the calculations. Whether there is a narrow corridor leading to the exit stair or not, the shape of the queue is unimportant. The only aspect of the queue relevant to the algorithm is its density.

Unless the queue has only a single person, the queue density has been assumed to be $1.9p/m^2$. This is noted within the SFPE hydraulic model as a reasonable maximum density to assume [11], is consistent with standing room densities noted within building codes such as the NBC [1]. As the algorithm makes no assumption regarding the layout of the floor area beyond the exit stair (e.g. whether there is a narrow corridor leading to the stair, or a wide open floor area, etc.), a manual calculation of the density outside the stair is not feasible based on number of individuals and space available. Therefore, the density of $1.9p/m^2$ has been applied to the queuing scenario (i.e. when occupants are bunched closely together in queue waiting to enter the stair), as this represents the density cap used by the algorithm. When only one person is in queue, the density is assumed to be D_{min} , and the walking speed is unimpeded.

3.2 Preliminary Case Studies and Model Validation

Once the building core geometry was defined, simulations of preliminary case studies were conducted to review how various building sizes and occupant loads behaved during simulated evacuations.

With the format of the algorithm, each simulation includes three randomized elements which affect the final outcome. These are:

- the starting position of each occupant (i.e. travel distance to exit door),
- the walking speed of each occupant as they approach the exit door, and
- the priority of events occurring during the simulation.

All of these randomizations will affect the final exit time for a particular simulation. However, as the purpose of this effort is to review the effects of pre-movement time on high buildings, it was desired to choose case studies where the effects of the above noted factors would be minimal. Therefore, a series of preliminary simulations were performed without pre-movement time to determine the magnitude of the effects the above factors could have on the overall outcome.

3.2.1 Preliminary Trial Results

Trials were run without pre-movement times for the parameter values as follows:

- occupant loading into the exit route per floor, $l = 20, 70, 120$
- number of floors in the building, $f = 5, 10, 20, 30$

Each combination of l and f values is considered a single case. A total of 10 simulations were performed for each case.

For each case, the mean evacuation time (in cs), variance, standard deviation, and coefficient of variation (CV, defined as the standard deviation divided by the mean) were

estimated. These values are shown in Table 3.2.1 below. The CV for all trials has also been shown in Figure 3.2.1 as a scatter plot, for easy visual comparison.

Table 3.2.1 – Summary of Results of Preliminary Trials

Number of Floors, f	Loading, l	Mean Evacuation Time, t_0 (cs)	Variance	Standard Deviation	Coefficient of Variation
5	20	13194	27986.60	167.29	0.0126794
	70	43271.6	8849.44	94.07	0.0021740
	120	73490.3	2122.01	46.07	0.0006268
10	20	25291.6	28454.04	168.68	0.0066695
	70	85656.5	3055.05	55.27	0.0006453
	120	146110.6	5726.24	75.67	0.0005179
20	20	49517.1	37212.89	192.91	0.0038958
	70	170313.8	4439.96	66.63	0.0003912
	120	291301.8	1100.76	33.18	0.0001139
30	20	73788.7	24159.01	155.43	0.0021064
	70	255008.6	7943.04	89.12	0.0003495
	120	436483.4	5328.04	72.99	0.0001672

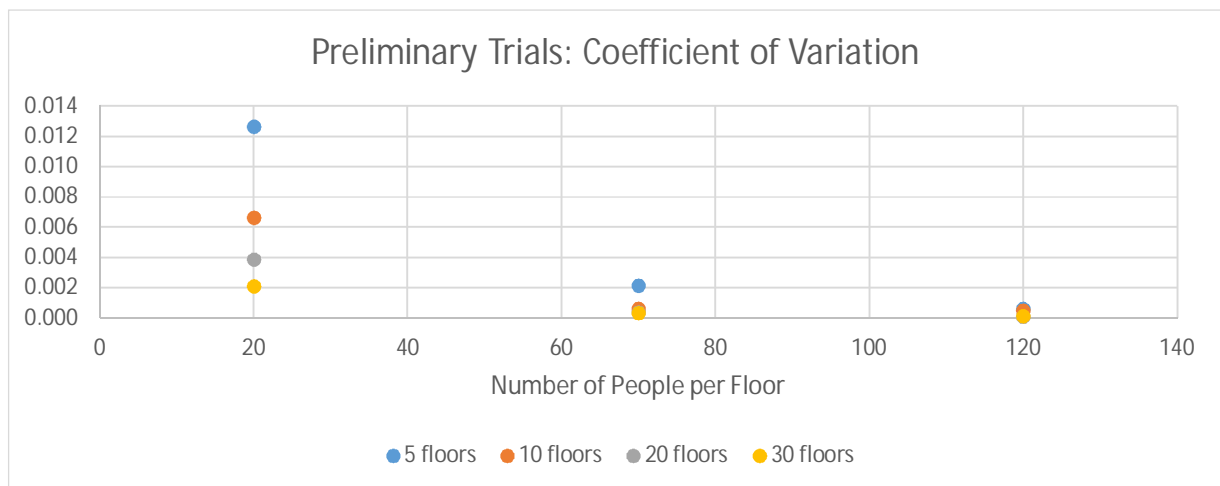


Figure 3.2.1 – Coefficient of Variation for Preliminary Trials with No Pre-movement

For all trials, it is noted that the CV of the output decreases as either the number of floors, f , increases, or if the loading, l , increases. The CV for a 5 storey building with loading of 20

people per floor is larger than for a building with the same number of floors and a loading of 70 people per floor. Similarly, a 5 storey building with a loading of 70 people per floor has a larger CV than a 30 storey building with the same loading.

The amount of queuing in an exit route depends on the total number of people using an exit route. This will increase if either the number of floors is increased or the number of people per floor using an exit route is increased. The results of these preliminary simulations indicate that increased queuing within the stairs minimizes the effect of minor variations such as walking speed, starting position, and order of movements occurring within the exit stair.

3.2.2 Model Verification

The SFPE hydraulic model is generally used to calculate exit times assuming simultaneous start (i.e. no pre-movement) and constant density at optimal values of 1.9 p/m^2 . As the equations of the simulation algorithm are based on the SFPE hydraulic model, and the density values are capped at the same optimal value of 1.9 p/m^2 the algorithm should agree with the SFPE hydraulic model when there is no pre-movement.

In order to verify that the algorithm is performing as it should, an analysis of a 20 storey building having 70 people per floor has been calculated below using the hydraulic model.

The same starting locations have been assumed as were used in the simulation algorithm; specifically, occupants are located between 5 m and 45 m from the exit door at the start of evacuation. Stair geometry below is also the same as used by the algorithm.

It is noted that, while people are indeed discrete items, the equations of the hydraulic model simulate movement of a crowd similar to a fluid flow. The calculations, therefore, will yield values that will appear to be partial values of people at certain points within the evacuation. These can be considered as a person in motion at a given point in time, in the act of joining a queue or walking through a door, for example.

The first person to exit the building is assumed to be located closest to the exit on the first floor (i.e. 5 m from the exit stair door). Since all occupants evacuate simultaneously, other occupants will follow closely behind this “leader”.

With a walking speed of 1.25 m/s, the leader will walk unimpeded for 5 m to reach the exit stair door on the first floor. Travel time for this occupant to reach the exit stair (t_{trav1}) is calculated as follows:

$$t_{trav1} = \frac{5m}{1.25m/s}$$

$$= 4 \text{ s}$$

Upon reaching the exit stair door, the occupant must spend 3.7 seconds to open the exit door, t_{door} .

$$t_{door} = 3.7 \text{ seconds}$$

Based on the stair geometry of Figure 3.1.2 for the first floor, the leading occupant must then travel 3.315 m to reach the final exit door.

$$t_{trav2} = \frac{3.315m}{1.25m/s}$$

$$= 2.65 \text{ seconds}$$

Therefore the leading occupant from the first floor reaches the exit door within 10.35 seconds (i.e. 4+3.7+2.65). If evacuation starts at time $t=0$, then the occupant reaches the exit door at time $t=10.35$. This is depicted in Figure 3.2.2 below.

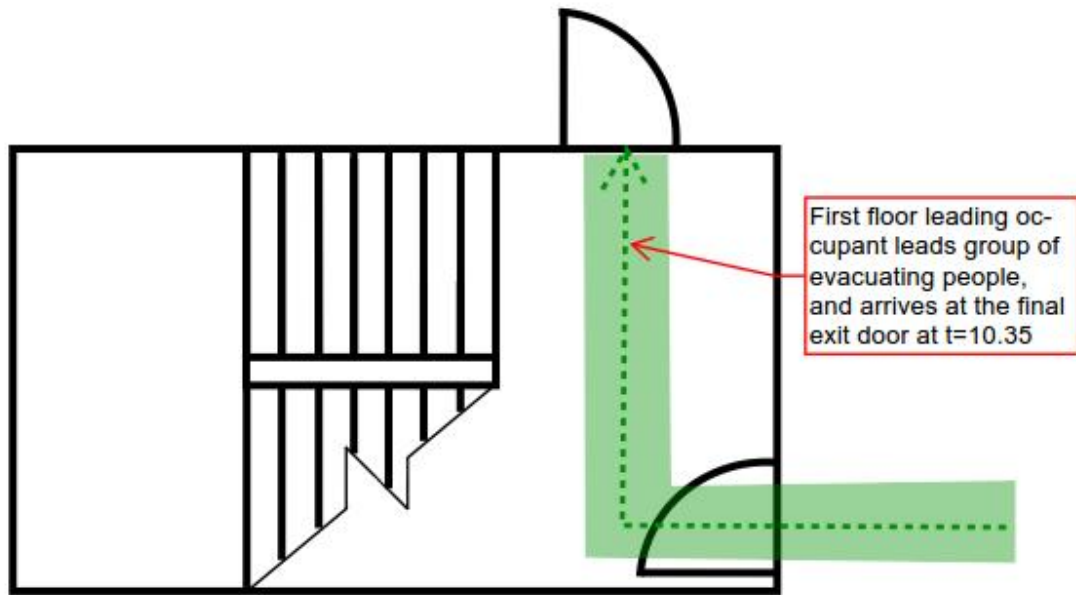


Figure 3.2.2 - From $t=0$ to $t=10.35$, leading first floor occupant walks to final exit followed by a queue of first floor occupants

As all occupants on the first floor are assumed to evacuate simultaneously, other occupants will follow the leader. The flow rate of these occupants will be limited by the width of the door into the exit stair. It is assumed that peak queue density is reached immediately (1.9 p/m^2) as everyone evacuates at the same time and immediately forms a queue. The limiting flow rate of these occupants is therefore:

$$\begin{aligned}
 f_f &= (1 - ad)kdw_e \\
 &= (1 - 0.266(1.9))(1.4)(1.9)(0.930 - 0.150 - 0.150) \\
 &= 0.8296 \text{ p/s}
 \end{aligned}$$

So, after $t=10.35$, people will follow the leader and arrive at the final exit at a rate of 0.8296 p/s . (Prior to $t=10.35$, the arrival rate of people at the final exit door is zero.)

The leading occupant must open the exit door before he can evacuate. Thus, a delay of 3.7 seconds is considered.

The flow out of the exit door is 0 while the leader has paused to open the door. However, while they open the door, the flow of occupants arriving behind continues at the rate of 0.8296p/s. Therefore, during this delay, a queue forms at the net rate of 0.8296p/s.

During the 3.7 seconds between $t=10.35$ and $t=14.05$, a queue of 3.07 people is considered to form (i.e. 0.8296p/s for 3.7 seconds).

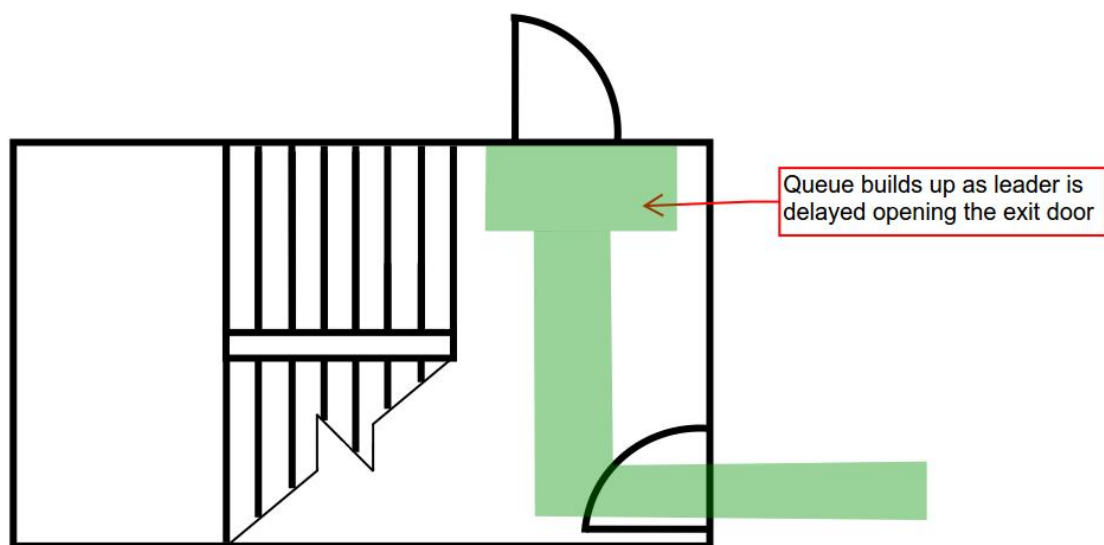


Figure 3.2.3 - From $t=10.35$ to $t=14.05$ a small queue forms as the leader pauses to open the door

Once the exit door is opened, occupants will begin to flow out of the building. The flow rate out will be limited by the exit door to 0.8296p/s, as the final exit door has the same effective width as the door into the stair.

In consideration that there is a large number of people yet to exit, after $t=14.05$, the flow rate out the exit door is equal to the flow rate arriving at the exit door (since the door width of the final exit is identical to the exit stair door, and the density is assumed to remain constant at 1.9 p/m²). Therefore, the queue size stays the same for a period of time, as occupants exit and arrive at the same rate.

Meanwhile, occupants from upper floors have also started to evacuate. Occupants from the second floor have a longer travel distance to reach the exit door on level 1. Because each floor in the building is assumed to have the same layout, and the travel distances are assumed to be the same on all levels, the time for the leading second floor occupant to reach the exit stair on Level 2 and the delay to open the stair door will be the same as for the leading occupant on Level 1 (i.e. 4 seconds to walk to the door, and 3.7 seconds to open the door). Beyond the stair door, additional travel distances must be considered, as follows:

- 2.25 m across the landing L_2
- 2.66 m down stair flight St_2
- 2.3 m across intermediate landing I_2
- 2.66 m down stair flight Sb_2
- 1.43 m travel across L_1 to the final exit door

The total travel time for the leader on the second floor to reach the final exit door is equal to the sum of the horizontal travel time and the stair travel time. Mean unimpeded speed for horizontal travel is 1.25m/s as previously noted, while the mean unimpeded speed for stair travel is given as 0.70 m/s in the SFPE handbook. Therefore, total travel for the leader from the second floor (t_{trav2}) can be calculated as:

$$t_{trav3} = 4s + 3.7s + \frac{2.25m + 2.3m + 1.43m}{1.25m/s} + \frac{2.66m + 2.66m}{0.7m/s}$$

$$= 20.08 \text{ seconds}$$

Therefore, between $t=14.05$ and $t=20.08$, only occupants from the first floor will be arriving at the final exit door (at the constant rate of 0.8296p/s). After $t=20.08$, the arrival rate will increase due to the additional flow of occupants from above.

During this interval, occupants will continue flowing out of the exit door. At $t=20.08$, a total of 5 people would have exited the building. The queue size inside the stair would remain unchanged at 3.07 people.

In summary, at $t=20.08$, the following would be true:

- 5 people would have exited the building. These would be from the first floor.
- 3.07 people would be in queue at the door. These people would also be from the first floor.
- The remaining 61.93 people from the first floor would be on their way to queue at the door (i.e. $70 - 5 - 3.07$).
- The leading occupant from the upper floors would be just arriving to join the queue at the exit door.

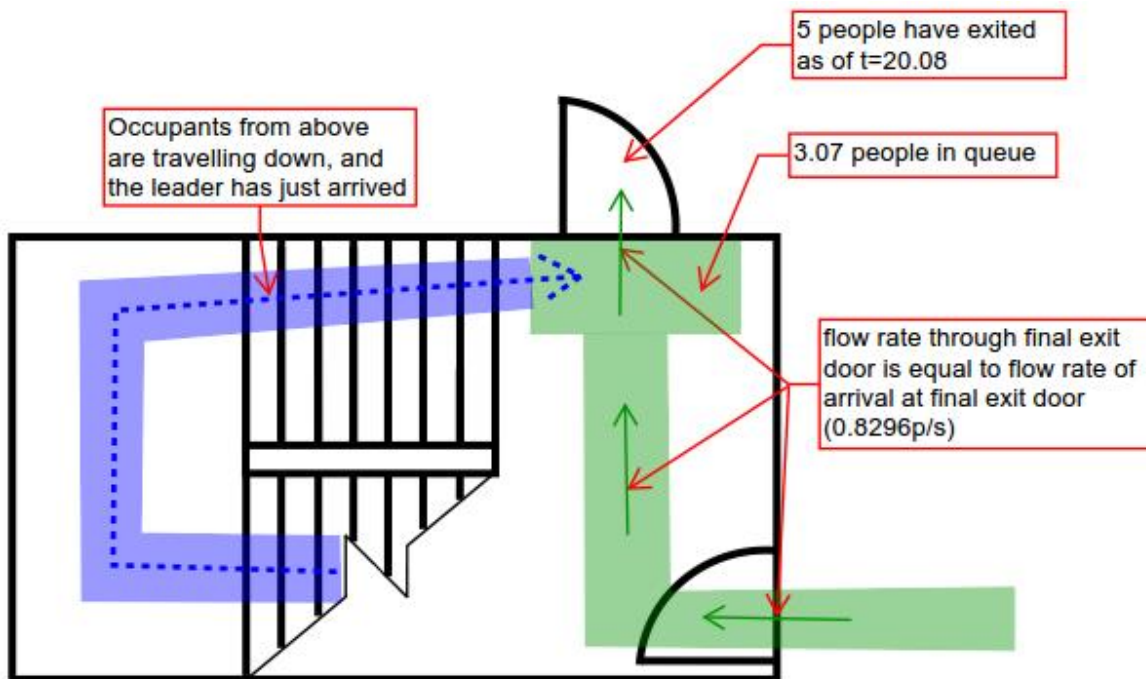


Figure 3.2.4 - From $t=14.05$ to $t=20.08$ the rate of occupants arriving at the exit door is equal to the rate of occupants flowing out (queue size remains constant)

Starting at $t=20.08$, the arrival rate at the exit door will increase, as there will be two flows of people arriving. The rate at which people arrive from the second floor (and all other floors above) will be limited by the maximum flow rate down the stairs. This is calculated to be:

$$\begin{aligned}
 f_f &= (1 - ad)kdw_e \\
 &= (1 - 0.266(1.9))(1.08)(1.9)(1.1 - 0.150 - 0.150) \\
 &= 0.812p/s
 \end{aligned}$$

So, after $t=20.08$, the flow of people arriving at the final exit door will be $1.642p/s$ (i.e. $0.8296p/s$ from the ground floor plus $0.812p/s$ from above). The flow rate of people exiting through the door will remain $0.8296p/s$. Therefore, the net rate of queue growth at the exit door will be $0.812p/s$.

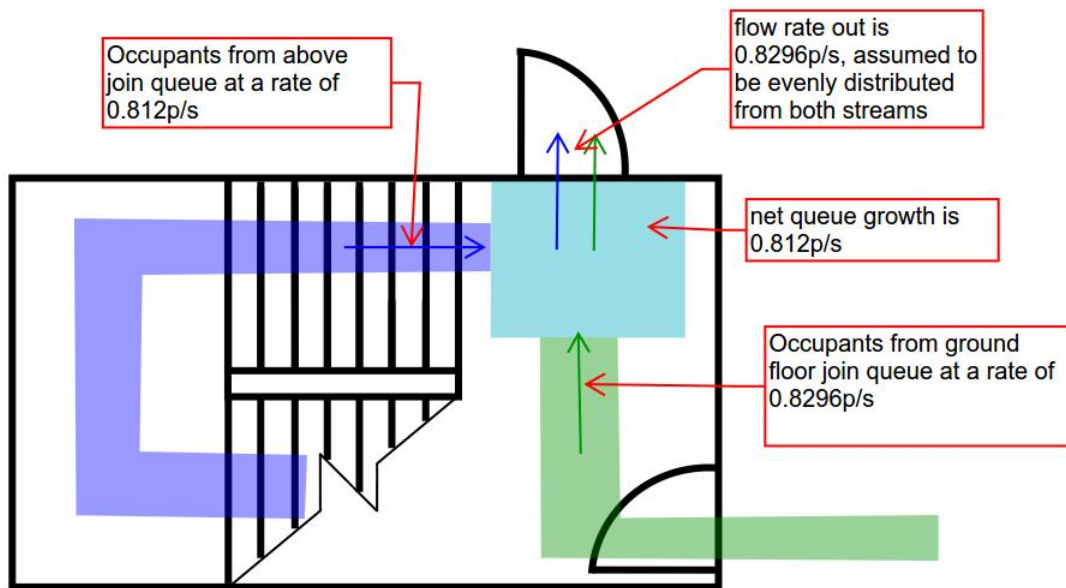


Figure 3.2.5 for $t > 20.08$ occupants will arrive from two different streams, and queue at the exit door will grow

For this analysis, it is assumed that occupants who arrive first in queue will exit first. Furthermore, as discrete items (i.e. people) are being considered, we assume that the two queues arriving at the exit door will merge equally, to account for people from each queue alternating as they walk through the exit door.

Based on these assumptions, we assume 4 occupants from the first floor (3.07 in queue, rounded to 4 in consideration that the person 7% partially in queue will be slightly ahead of occupants from above) will exit before alternating exiting will begin.

The time required for four occupants to exit is 4.82 seconds (4 people at 0.8296 p/s).

Therefore, after 24.90 seconds (i.e. 20.08 plus 4.82 seconds), 9 occupants from the first floor would have exited the building. An additional 61 first floor occupants and 1330 upper level occupants would still be in the building. At this point, it is assumed that these two groups will alternate exiting.

The next 122 people (i.e. 61 from upper levels and the last 61 from the ground floor) will evacuate within 147.06 seconds, based on the exit flow rate of 0.8296p/s. Therefore, at $t=171.96$ there will be a total of 131 people out of the building, including all of the first floor occupants.

Beyond this time, there will only be one stream of occupants arriving at the final exit door; those from upper levels. They will arrive at a slower rate (0.812p/s) than they will exit (0.8296p/s). Therefore, the queue at the door will shrink. However, between $t=20.08$ and $t=171.96$, the queue at the door would have grown at rate of 0.812p/s as noted above. Thus the queue at $t=171.96$ would be over 123 occupants. This queue would shrink at the gradual rate of 0.0806 p/s based on the difference between the arrival and the exiting flow rate. However at this slow rate, all the remaining occupants from above would reach the queue before the queue size reduced to zero. Therefore, a queue would remain until all people finish exiting, and the flow rate out the exit doors of 0.8296 would be maintained for the remainder of the evacuation.

At $t=171.96$, 61 people from upper levels would have evacuated. An additional 1269 people would remain. These occupants would require an additional 1529.65 seconds to evacuate based on the exit flow rate.

Therefore, based on the above analysis, the last person would evacuate at time $t=1701.61$ seconds (i.e. 171.96 plus 1529.65). This represents the calculated evacuation time for the building, using the manual calculation method.

In comparison, the simulation results produced by the algorithm for the evacuation of a building of the same size and loading averaged 1703.13 seconds over 10 trials, with a standard deviation of 0.66 seconds, and a 95% confidence interval of (1702.72, 1703.55). This value (1703.13s) agrees well with the manually calculated result described above (1701.61s), indicating that the algorithm performs calculations of the SFPE hydraulic model accurately. The model's slightly larger evacuation time may be the result of minor gaps within the modeled evacuating occupants, which would result in a less-than-optimal density and slower flow rates. However, with large numbers of people (i.e. 70 people per floor over 20 floors), instances of gaps within the evacuation would be infrequent. Thus, it is reasonable that the difference between the model results and the results of the hand calculations are small, but positive.

3.3 Primary Case Studies

Based on the results in section 3.2.1, it was noted that for small buildings and for buildings with small occupant loads, the algorithm produced results which varied relatively widely. Therefore, the primary case studies were chosen with loading and floor numbers large enough to ensure the results with zero pre-movement would produce consistent results. Parameters for the primary case studies were chosen as follows:

- $I=80, 90, 100, 110, 120, 140$
- $f=20, 21, 22, 23, 24, 25, 26, 27, 28, 29, 30$

Based on preliminary case studies, it was anticipated that these buildings would have sufficient loading and numbers of floors such that variation in evacuation times without pre-movement would be small. The variation of evacuation time resulting from the addition of pre-movement time could then be observed.

3.4 Pre-movement time distributions

The effects of two different distributions for pre-movement time were selected for examination: the uniform distribution, and the gamma distribution. Throughout this document, uniformly distributed pre-movement time may be abbreviated UPM, and gamma distributed pre-movement time may be abbreviated GPM. Modelled scenarios without pre-movement time will be abbreviated OPM.

3.4.1 Uniformly Distributed Pre-Movement (UPM)

The uniform distribution was chosen as this represented a simple distribution which may yield mathematically interesting results. If pre-movement time was shown to affect the evacuation time of a building, it was reasonable to assume that different sets of uniformly distributed pre-movement times may best show a pattern of effects.

In addition, the uniform distribution could be considered to represent evacuation scenarios where occupants are isolated from one another, and are therefore not influenced by the behaviour of others. Crowd behaviour during an evacuation tends to result in groups of people leaving at the same time. A uniformly distributed pre-movement time could therefore represent a case with zero crowd influence.

Figures 3.4.1 and 3.4.2 show probability density functions for two sample pre-movement distributions that were examined. Intervals for pre-movement times were defined based on the pre-movement time cap, p , and as the interval $[0,p]$. Ten pre-movement time caps were chosen for review: $p= 6,000\text{cs}$ (1 minute), $12,000\text{cs}$ (2 minutes), ... $54,000\text{cs}$ (9 minutes) and $60,000\text{cs}$ (10 minutes).

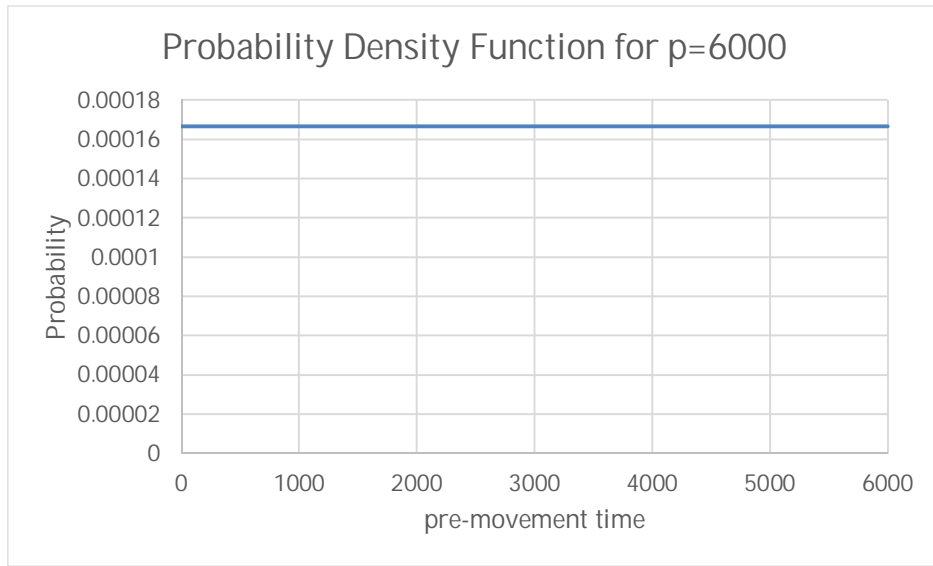


Figure 3.4.1 – Probability Density Function for UPM with p=6000cs (1 minute)

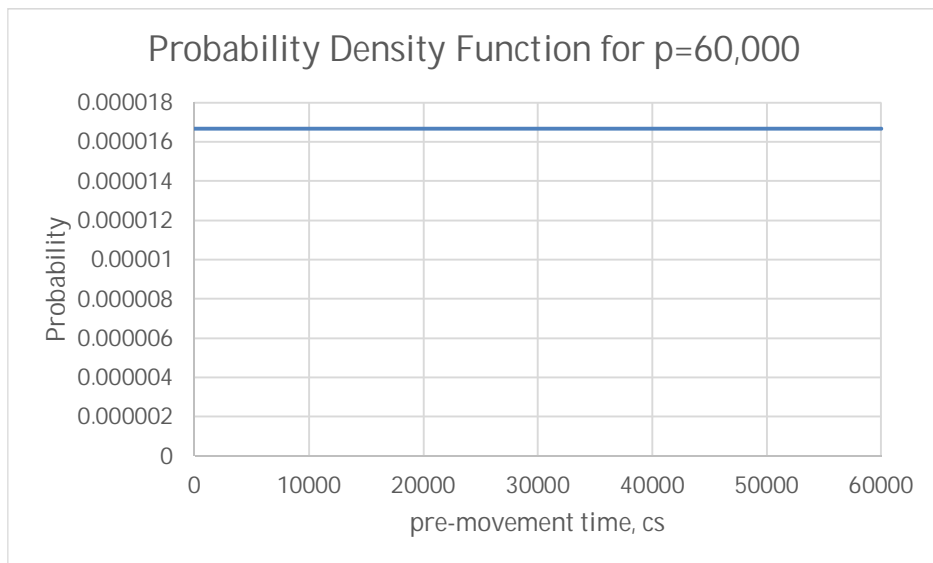


Figure 3.4.2 – Probability Density Function for UPM with p=60000cs (10 minutes)

3.4.2 Gamma Distributed Pre-Movement (GPM)

In addition to uniformly distributed pre-movement times, it was desired to examine the effects of a distribution for pre-movement time which might better reflect actual pre-movement times observed in building evacuations.

While there is no way to predict an exact distribution of pre-movement times, Figure 3.4.3 below shows pre-movement times reported by actual survivors of a fire in an office building, with a sample distribution curve. Figure 3.4.4 shows pre-movement times for a retail store evacuation, with sample distribution curve. It is noted that for both evacuations, the majority of people begin evacuating the building relatively soon after the fire alarm sounded, while a small number of people remained in the building for a longer period of time.

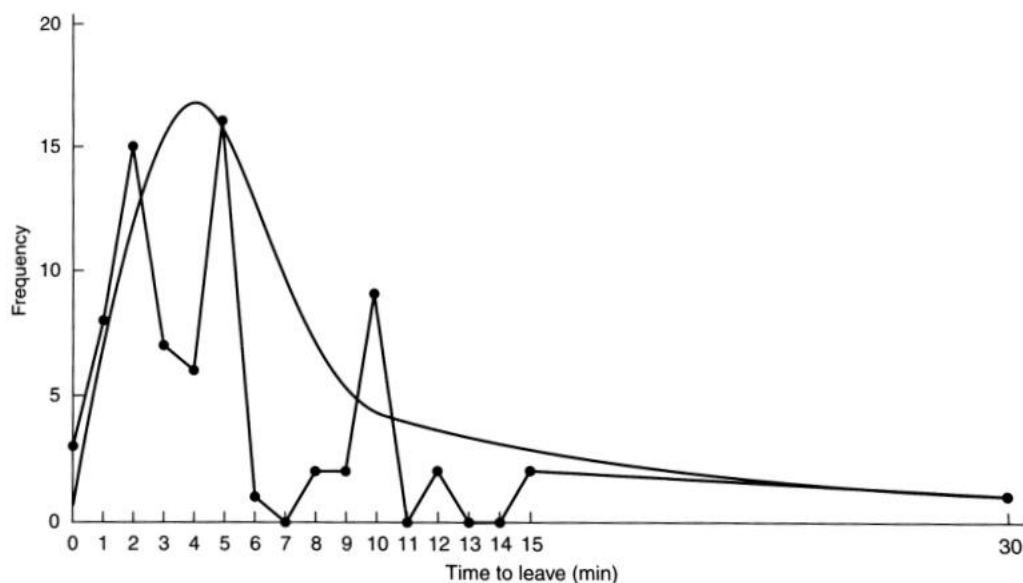


Figure 3.4.3 – Self reported pre-movement times from office building evacuation [10]

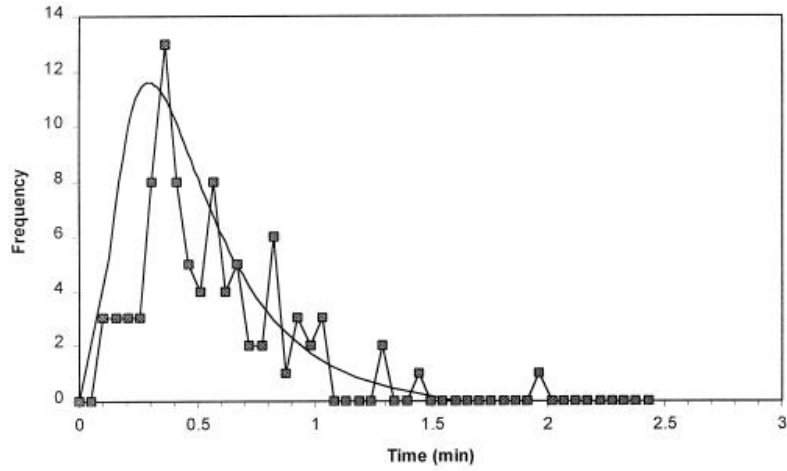


Figure 3.4.4 – Observed pre-movement times from retail building fire evacuation
[16]

Pre-movement time describes human behaviour during an emergency, and is therefore difficult to describe with complete accuracy [16] [5][20][17]. The sample pre-movement times shown in Figures 3.4.3 and 3.4.4 indicate a general trend of a proportionally high number of individuals evacuating relatively early during an emergency, with a proportionally lower number of individuals evacuating later. The gamma distribution was chosen as a pre-movement time distribution for this effort as it produces this same type of general shape and trend; representing a large number of people with relatively small pre-movement times, and a small number of “stragglers” with longer pre-movement times.

The probability density function for the gamma distribution with shape parameter a and scale parameter b is defined as:

$$f(x, a, b) = \frac{1}{\Gamma(a)b} \left(\frac{x}{b}\right)^{a-1} e^{-\frac{x}{b}} \quad (10)$$

where the gamma function, $\Gamma(a)$, is:

$$\Gamma(a) = \int_0^{\infty} x^{a-1} e^{-x} dx \quad (11)$$

The probability density function of gamma distribution for a shape parameter $a=2$ and a scale parameter $b=1$ is shown in Figure 3.4.5 below. These parameters were chosen as they produced the desired shape that may be seen in a realistic evacuation scenario.

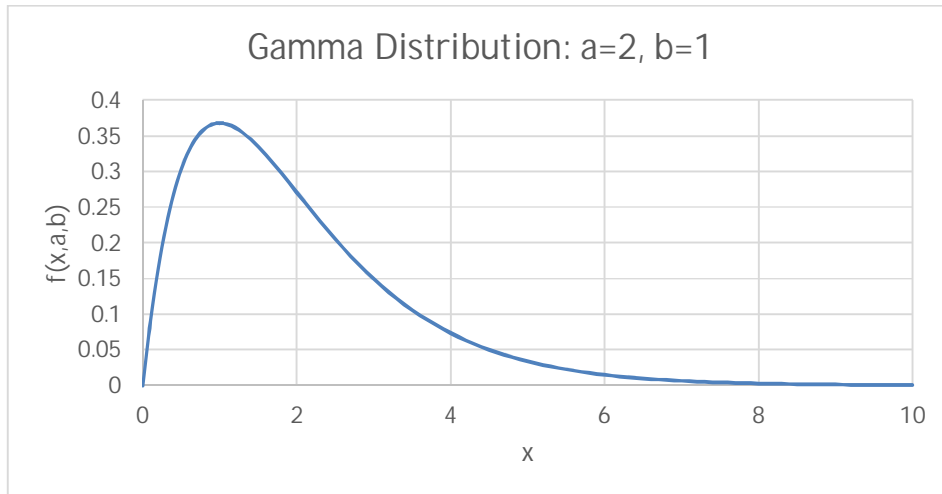


Figure 3.4.5 – Gamma distribution probability density function

This distribution was used to generate pre-movement times for occupants within the evacuation algorithm. Similar to the uniform distribution described in Section 3.4.1, ten separate intervals were selected for the gamma distribution, with each interval defined as $[0, p]$ with pre-movement time cap p taking values of 6,000cs (1 minute), 12,000cs (2 minutes), ... 54,000cs (9 minutes) and 60,000cs (10 minutes). For any given p value, the algorithm randomly generated a value x between 0 and 10 based on the distribution curve shown above. (The distribution was truncated at $x=10$, so if values greater than 10 were selected by the computer these were rounded down to 10.) This value was then scaled up to represent the corresponding pre-movement value in cs for the given interval $[0, p]$. The pre-movement time p_{ij} for an individual was computed as:

$$p_{i,j} = \frac{x}{10}p \quad (12)$$

for the randomly generated x value and the pre-movement time cap p defined for the particular simulation.

4.0 RESULTS

In all, a total of 77 primary cases were chosen for review (parameter values $l=80, 90, \dots, 140$ and $f=20, 21, \dots, 30$). For each of these cases, a set of 10 simulations were performed without pre-movement time to establish the OPM “base values”, denoted as t_0 when describing a particular case. These values were used as the basis of comparison for all UPM and GPM simulations of the same building cases.

As noted in Section 3.4 above, for both of the pre-movement time distributions, ten separate distribution intervals were examined: $[0, p]$ for $p=6000, 12000, \dots, 54,000, 60,000$. For each of these distribution intervals, 4 separate simulations were performed.

In order to evaluate results for the UPM and GPM simulations as unitless values, the effects of pre-movement (i.e. the difference between evacuation times for cases with and without pre-movement) were expressed relative to the OPM base values. Results for a particular simulation with pre-movement cap p , t_p , have been expressed as a relative difference to the base case, in the form:

$$\frac{\Delta t}{t_0} = \frac{t_p - t_0}{t_0}$$

where t_0 is the evacuation time for the OPM simulation of the same building.

These results have been examined with respect to the input value p . Results also display this value in a unitless form relative to the OPM case for a particular building. That is, the pre-movement time has been considered as:

$$\frac{p}{t_0}$$

for each pre-movement cap p and base OPM result t_0 .

Using these two unitless values, the relative effects of pre-movement times can be compared across all building cases.

A selection of simulation results are included and discussed in the subsequent sections. Full results are provided as an appendix to this thesis.

4.1 Effects of Uniform Pre-movement Distributions

Figures 4.1.1 to 4.1.3 below show results from a sample of the UPM simulations performed. Plots show the relative pre-movement time along the x axis, and the relative effect along the y axis. These figure each show a single building (defined by f , the number of floors) with various loading scenarios.

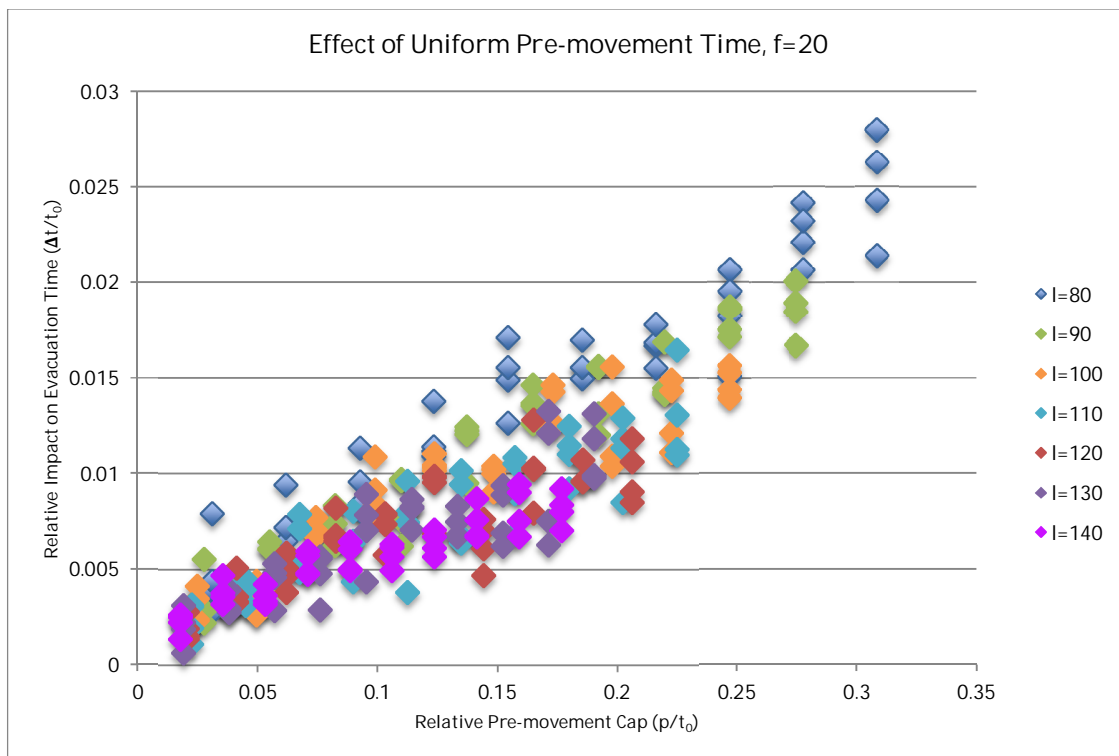


Figure 4.1.1 – UPM Simulation Results ($f=20$, $l=80$ to 140)

As shown in Figure 4.1.1 above, it was noted that pre-movement times produced smaller relative changes in evacuation times when there was increased loading, I . This can be visually seen in the slope of the data for different I values plotted together for the fixed value $f=20$. For example, the slope of the data for $I=80$ is much steeper than for the $I=140$ case, indicating that pre-movement time has a relatively larger effect on evacuation time for buildings with smaller values of I , when f is fixed. This general trend was noted for all building cases.

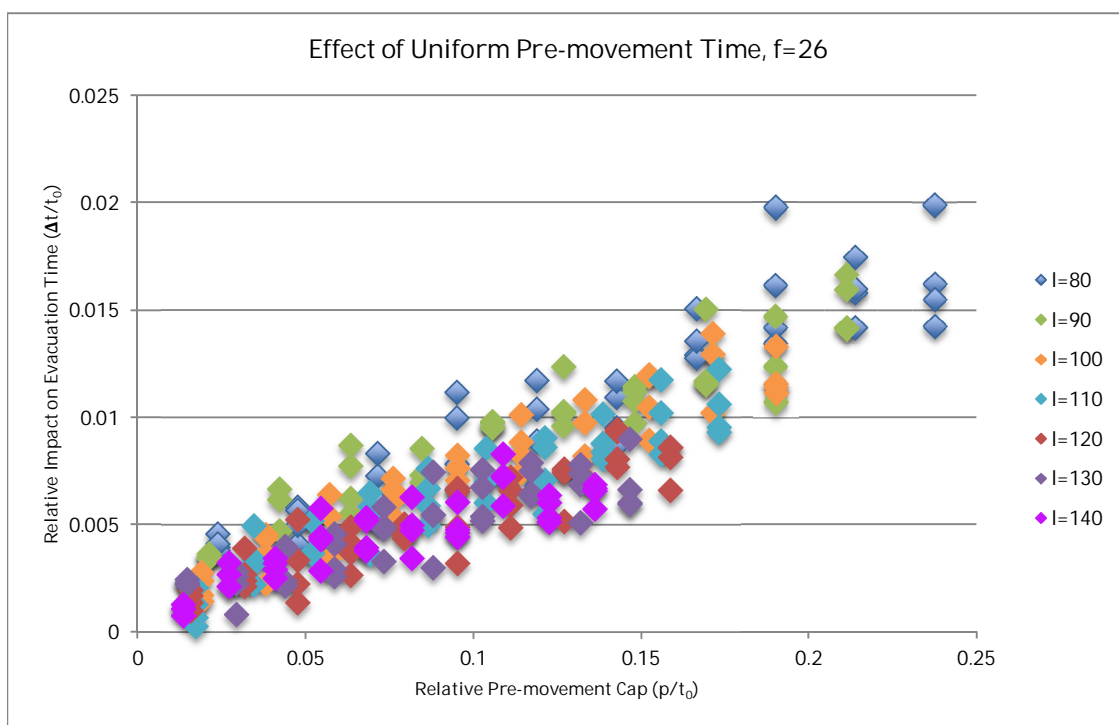


Figure 4.1.2 – UPM Simulation Results ($f=26$, $I=80$ to 140)

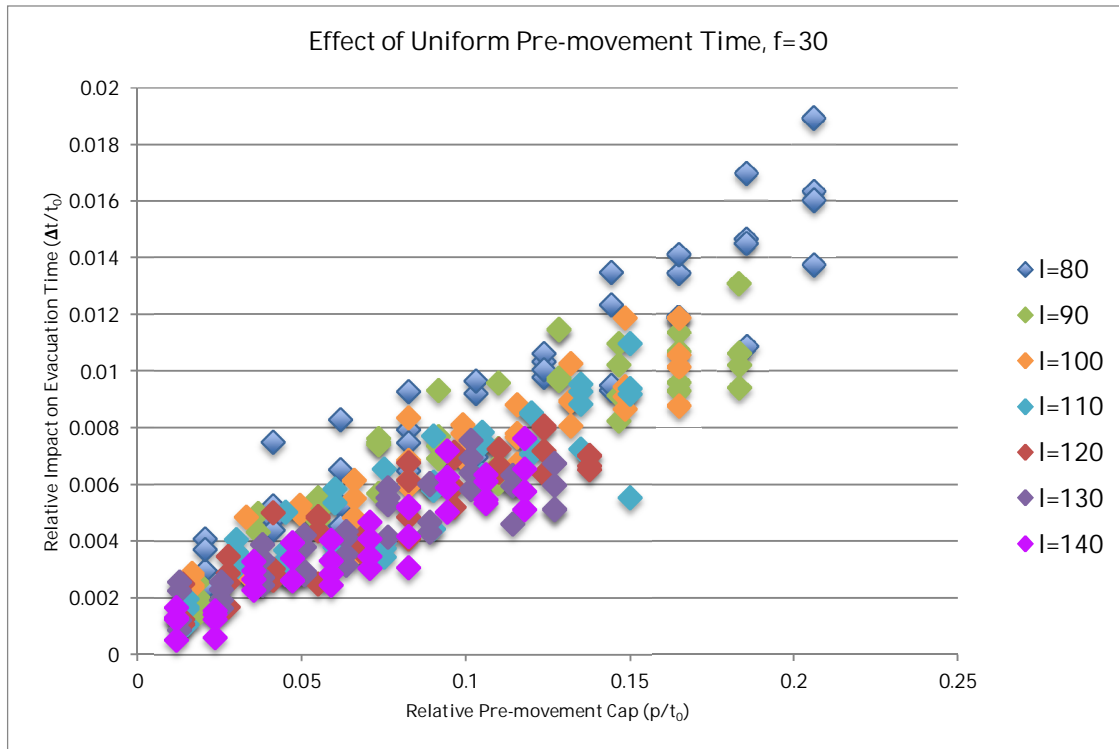


Figure 4.1.3 – UPM Simulation Results ($f=30$, $l= 80$ to 140)

Thus, it was noted that the relative effect of pre-movement time $\Delta t/t_0$ decreases as stair loading, l , increases when the number of floors, f , remains constant. However, for cases where l is held constant and f varies, no significant trends were noted, as shown in Figures 4.1.4 and 4.1.5. Visually, the different sets of data for fixed l values and varying f values appear to have the same slope, implying that relative changes in pre-movement time produce the same relative effects in evacuation time.

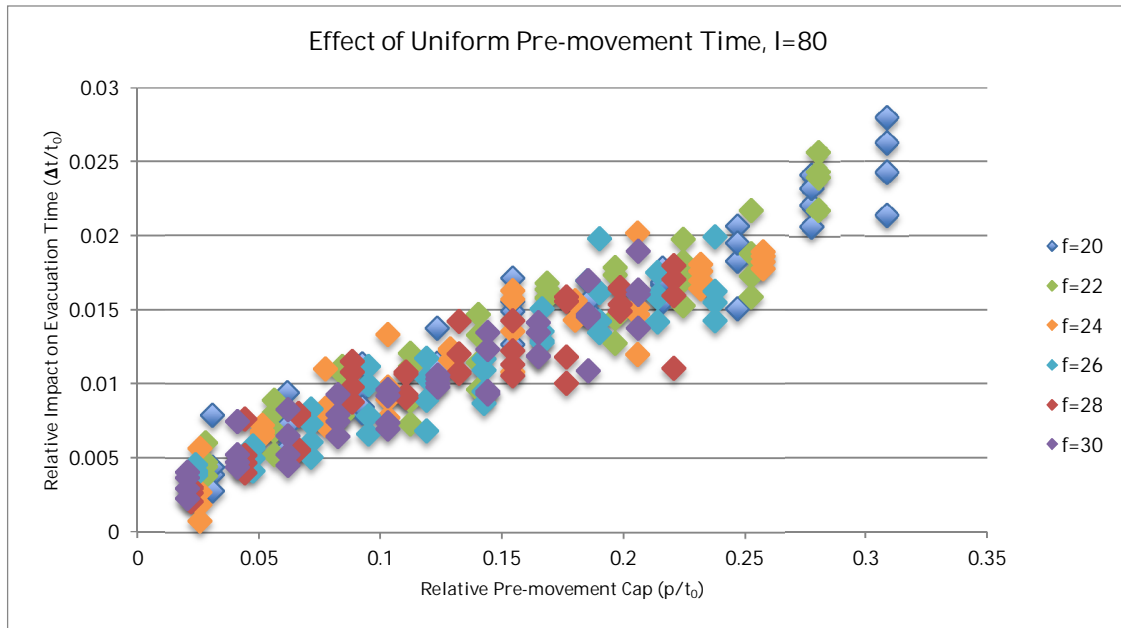


Figure 4.1.4 – UPM Simulation Results ($l=80$, $f=20$ to 30)

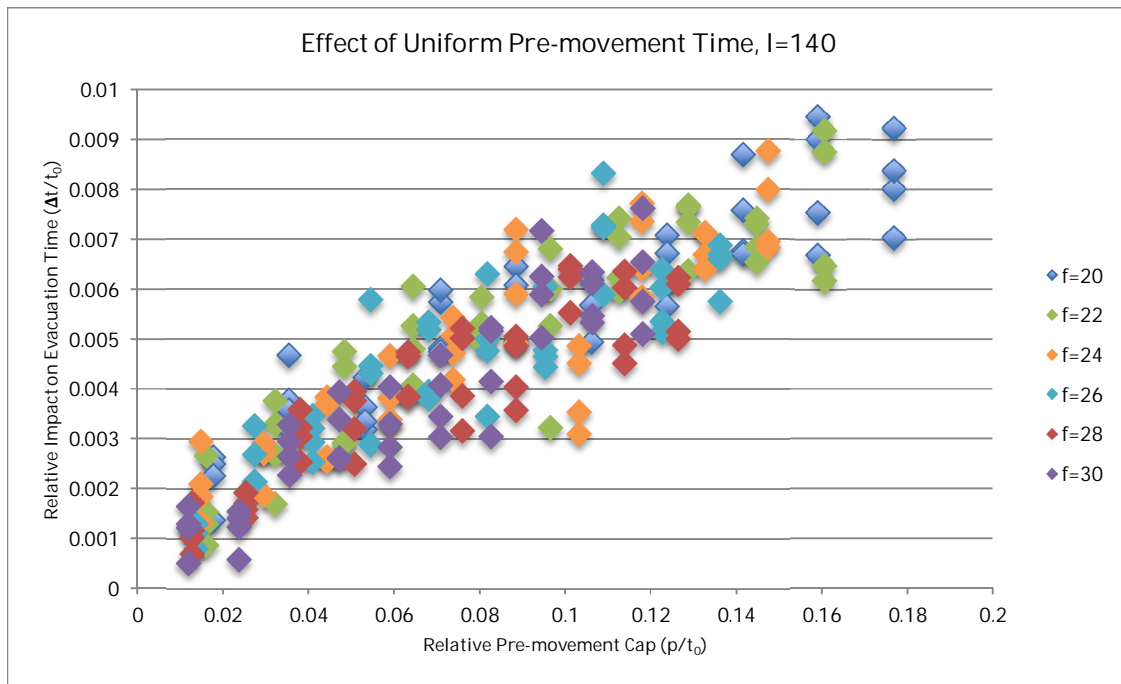


Figure 4.1.5 – UPM Simulation Results ($l=140$, $f=20$ to 30)

The trends observed in Figures 4.1.1 to 4.1.5 above indicate that for cases with fixed f , the effect of pre-movement decrease for increasing values of l , whereas for cases with fixed l , the effects of pre-movement remain relatively constant for increasing values of f . This is an

important result, and this trend was noted for all cases reviewed (full results are appended).

When the value of l increases and f is held constant, the density throughout the building would increase in general (as this represents more people occupying the same size building). As density within the evacuation route has a finite cap during evacuation, it follows that increasing l would increase the likelihood that the peak density is reached, which increases likelihood of queuing. As queues have the tendency to “absorb” the effects of pre-movement time, as discussed in Section 1.2.3, it makes sense that there is a diminished effect of pre-movement time when l increases for a fixed f .

However, when the number of floors, f , is increased with fixed loading, l , the building size increases, and therefore the density of the building would not necessarily increase. Therefore, there is not the same obvious diminishing effects of pre-movement for increasing f with fixed l .

4.1.1 UPM Results with Linear Regression

A linear regression analysis was performed for the results of the UPM primary cases, to see if the effect of pre-movement time could be reasonably expressed by a linear equation of the form:

$$\frac{\Delta t}{t_0} = u_1 l + u_2 f + u_3 \frac{p}{t_0} \quad (13)$$

for some parameters u_1 , u_2 , and u_3 .

Using MATLAB to perform the regression analysis, the following parameters were generated:

$$u_1 = -3.12782\text{E-}05$$

$$u_2 = 0.000163884$$

$$u_3 = 0.063558263$$

The resulting linear equation was plotted for each building case along with the values generated by the algorithm. Sample results are shown in Figure 4.1.6 to 4.1.11. It is noted that these figures (and other figures showing regression functions) show the algorithm results in blue, with the regression line show in red. Red points on the regression line correspond to the p values used for the simulated trials.

For some cases, the regression shows a reasonable fit, as noted in Figures 4.1.6 and 4.1.7

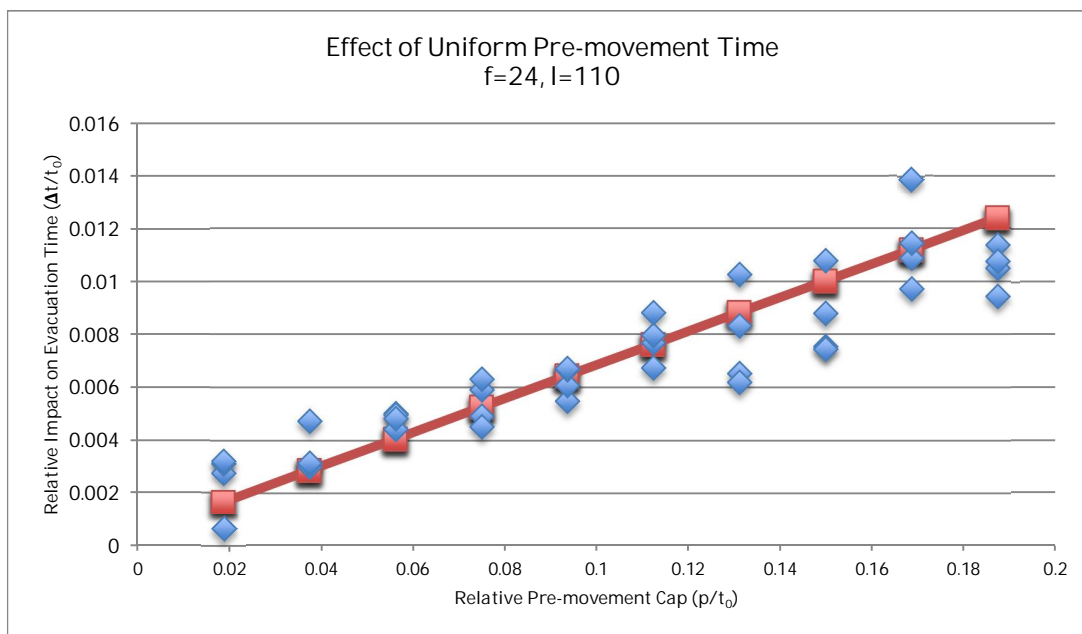


Figure 4.1.6 – UPM Results with Linear Regression ($f=24, l=110$), $R^2=0.791$

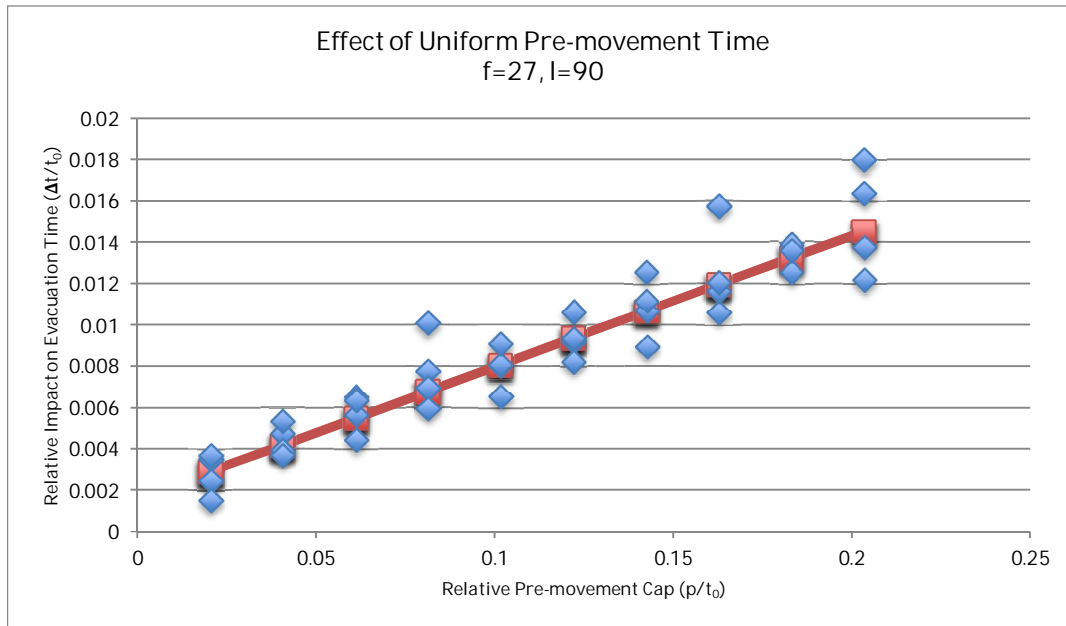


Figure 4.1.7 – UPM Results with Linear Regression (f=27, l=90), $R^2=0.888$

However, the linear expression (13) showed a trend of overestimating the effect of larger pre-movement times, and underestimating the effects of smaller pre-movement time caps, as shown in the cases of Figures 4.1.8 and 4.1.9.

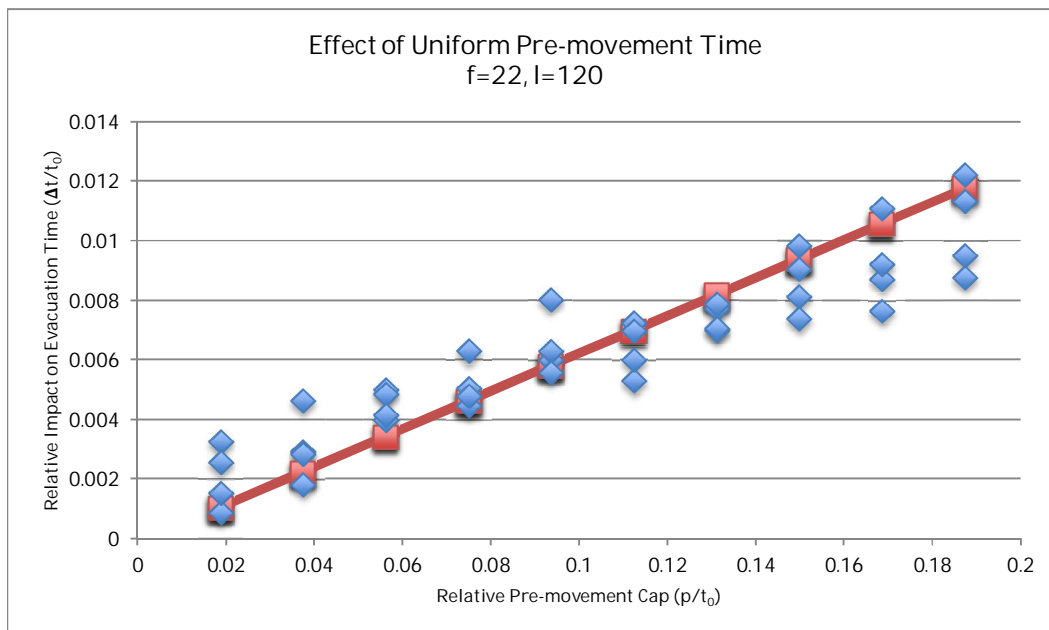


Figure 4.1.8 – UPM Results with Linear Regression (f=22, l=120), $R^2=0.765$

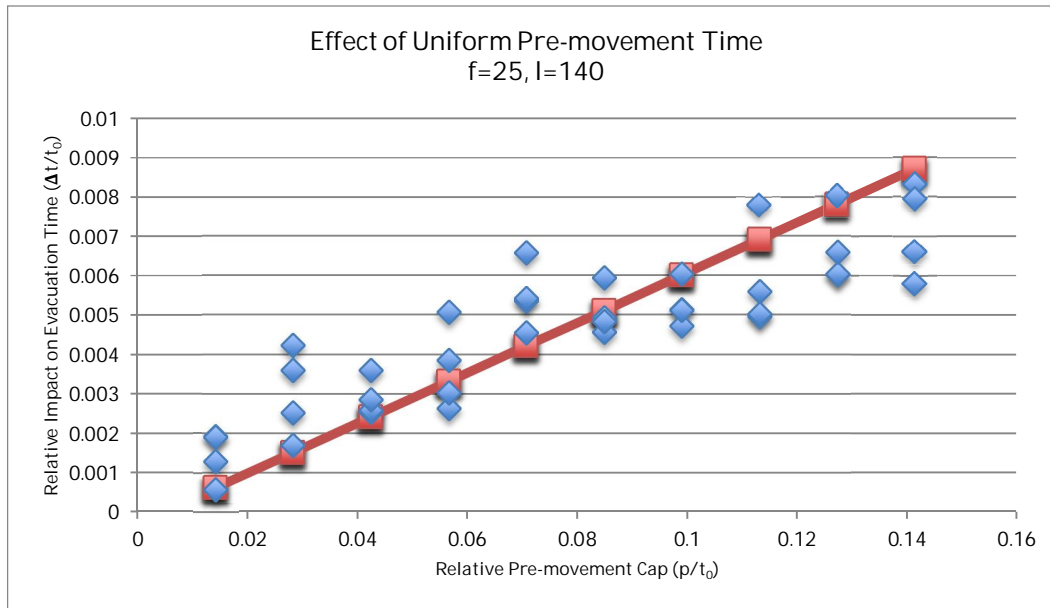


Figure 4.1.9 – UPM Results with Linear Regression (f=25, l=140), $R^2=0.555$

Also in general the regression model underestimated the effects of smaller, less populated buildings, as per Figure 4.1.10, and overestimate the effects in larger buildings, as per Figure 4.1.11.

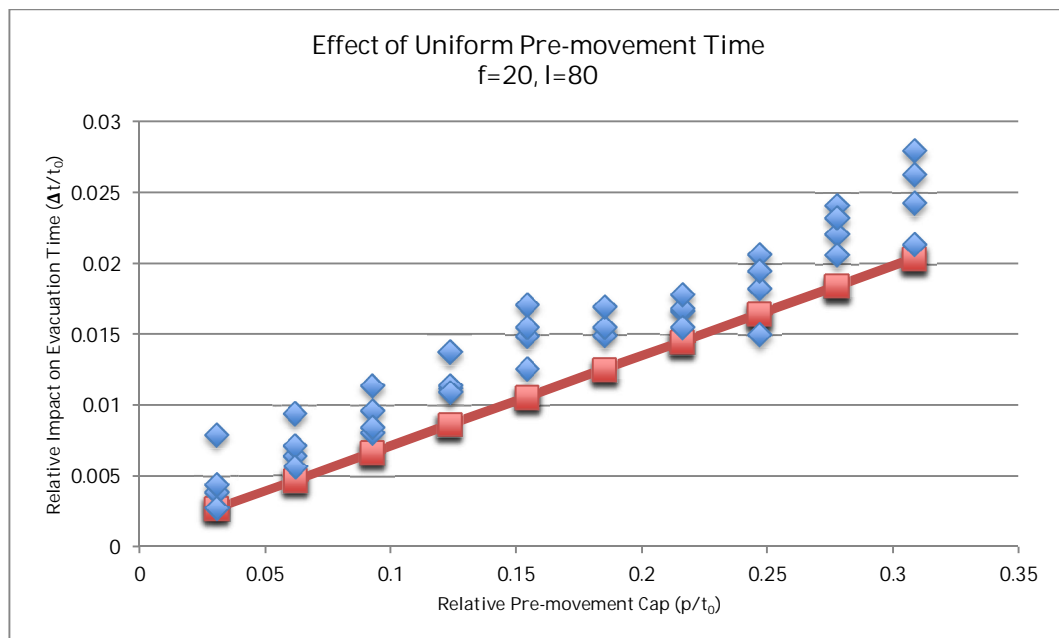


Figure 4.1.10 – UPM Results with Linear Regression (f=20, l=80), $R^2=0.678$

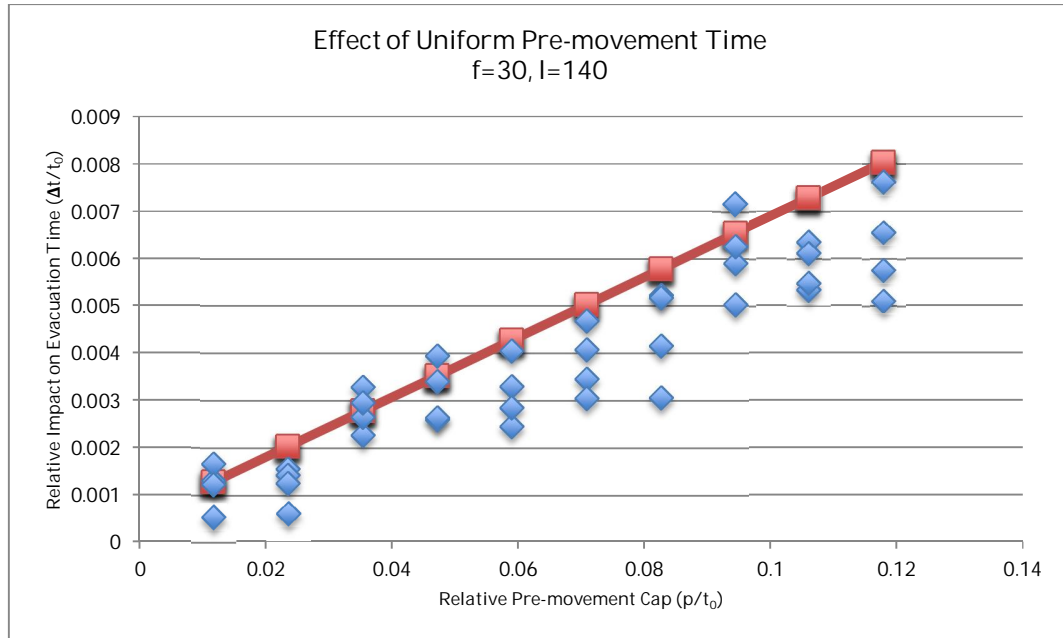


Figure 4.1.11 – UPM Results with Linear Regression ($f=30, l=140$), $R^2=0.578$

The linear expression determined by the regression analysis ultimately was not a good fit for all primary case studies reviewed.

4.1.2 UPM Results with High Order Regression

It was clear that the linear expression (13) could not describe the curvature in the results with the increase in p/t_0 . In particular, the linear expression seemed to over-estimate the effect of higher relative pre-movements. With p/t_0 plotted along the x- axis, the results seemed to curve similarly to the function $y=x^{1/2}$. Thus, in order to account for this curvature, the equation (14) below was considered. This includes the linear terms of equation (13), with the added terms for l , f , and (p/t_0) raised to the power of $1/2$, along with their products.

$$\begin{aligned} \frac{\Delta t}{t_0} = & u_1 l + u_2 l^{\frac{1}{2}} + u_3 f + u_4 f^{\frac{1}{2}} + u_5 \frac{p}{t_0} + u_6 \frac{p^{\frac{1}{2}}}{t_0} + u_7 (lf)^{\frac{1}{2}} \\ & + u_8 \left(l \frac{p}{t_0} \right)^{\frac{1}{2}} + u_9 \left(f \frac{p}{t_0} \right)^{\frac{1}{2}} + u_{10} \left(lf \frac{p}{t_0} \right)^{\frac{1}{2}} \end{aligned} \quad (14)$$

Using MATLAB to perform the regression analysis, the following coefficients were generated:

$u_1 = 0.000257934$	$u_6 = 0.239462703$
$u_2 = -0.002046069$	$u_7 = -0.000553405$
$u_3 = 0.000317196$	$u_8 = -0.020105238$
$u_4 = 0.002693285$	$u_9 = -0.031882975$
$u_5 = 0.026077581$	$u_{10} = 0.002793998$

This regression expression was plotted again with the UPM simulation results. Results are shown in Figures 4.1.12 to 4.1.16 below.

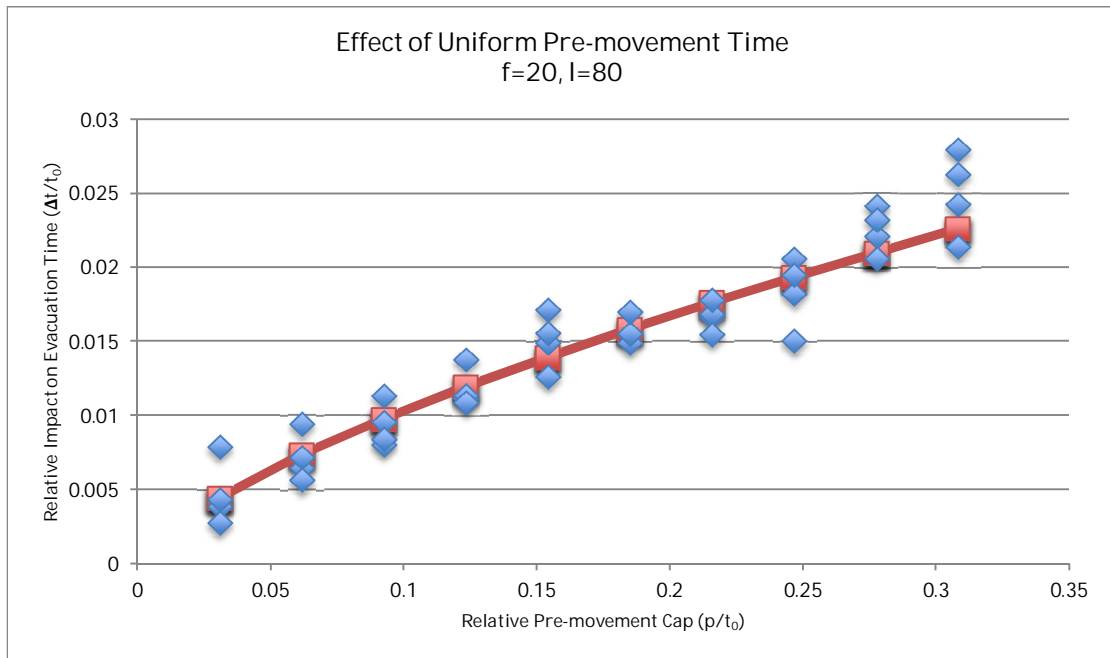


Figure 4.1.12 – UPM Results with High Order Regression (f=20, l=80),
R²=0.912

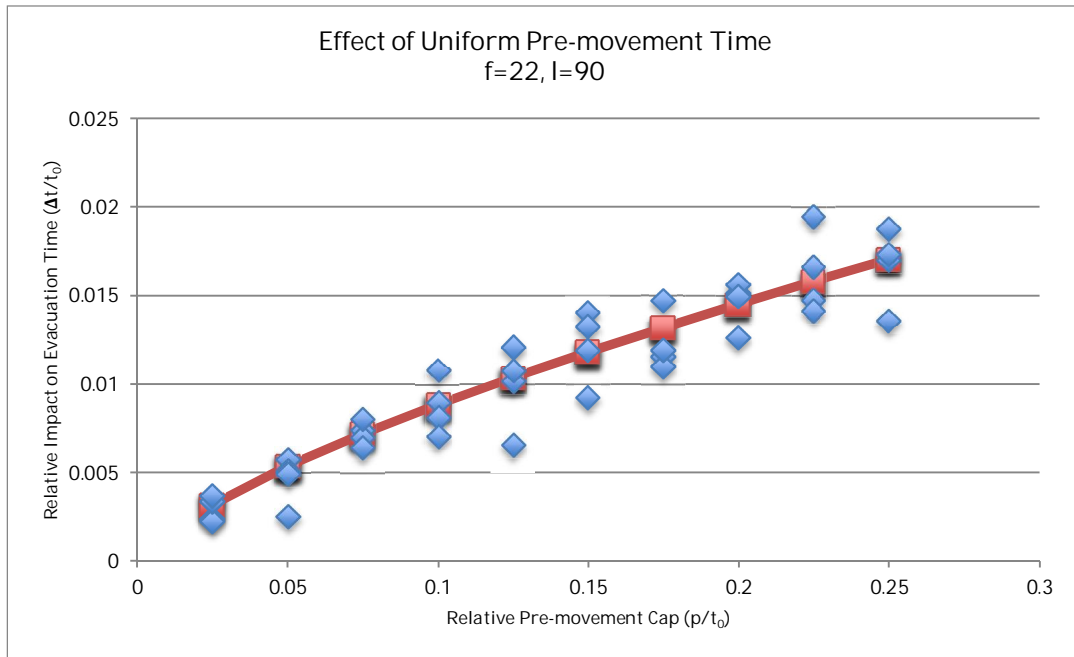


Figure 4.1.13 - UPM Results with High Order Regression ($f=22, l=90$),
 $R^2=0.889$

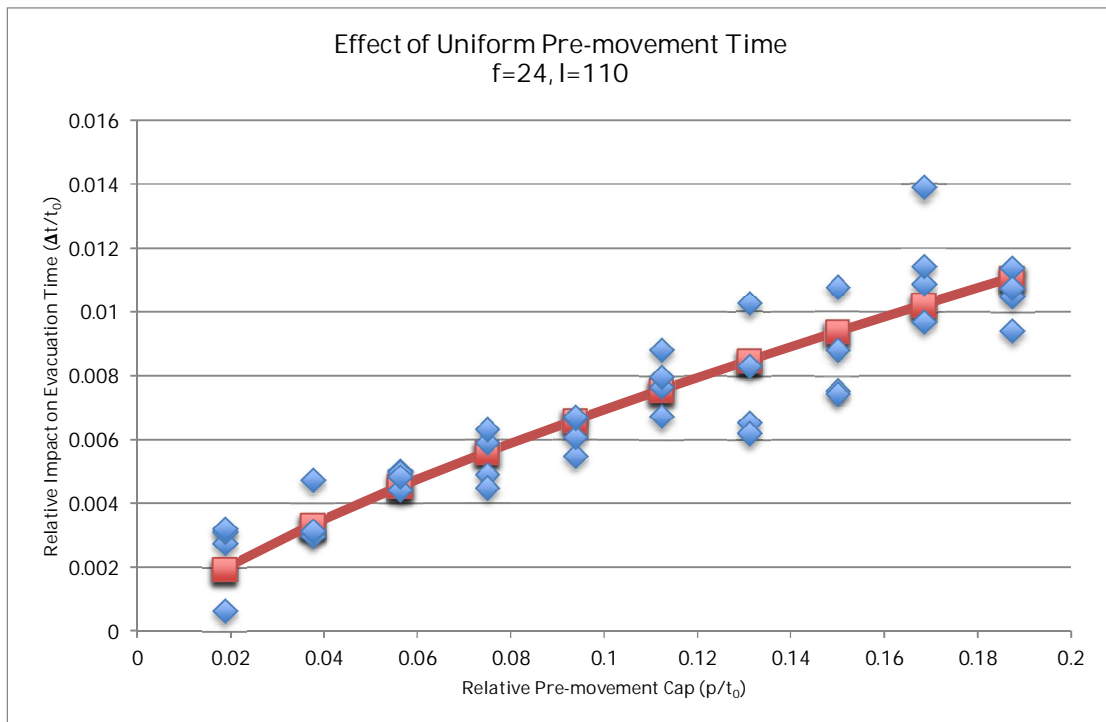


Figure 4.1.14 - UPM Results with High Order Regression ($f=24, l=100$),
 $R^2=0.884$

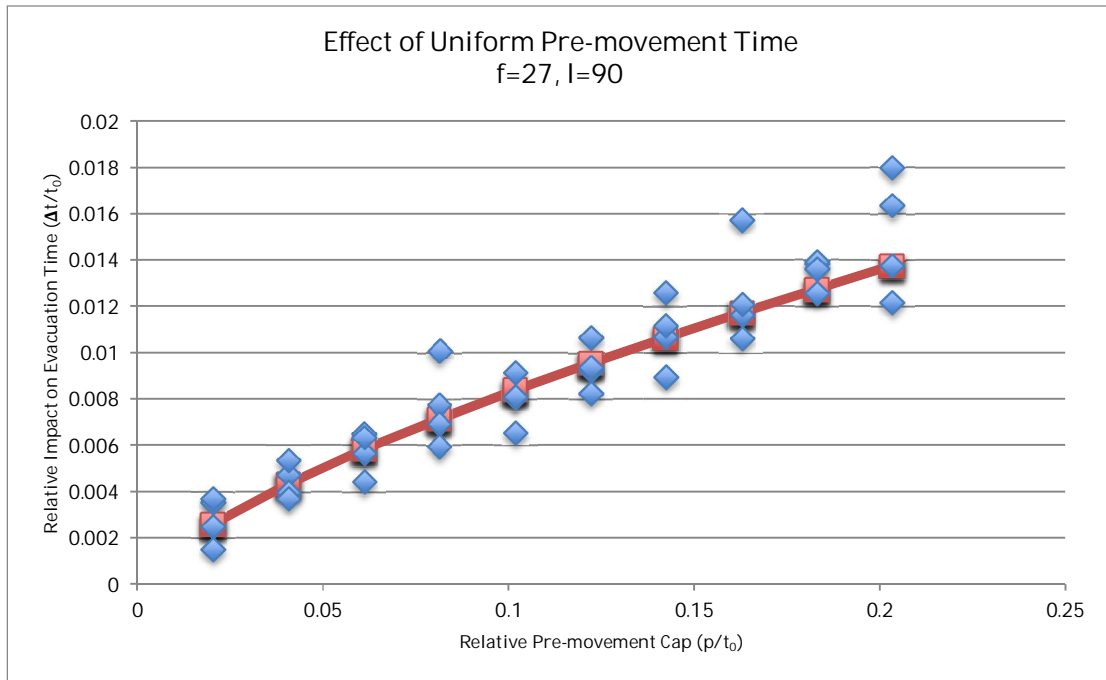


Figure 4.1.15 - UPM Results with High Order Regression ($f=27, l=90$),
 $R^2=0.876$

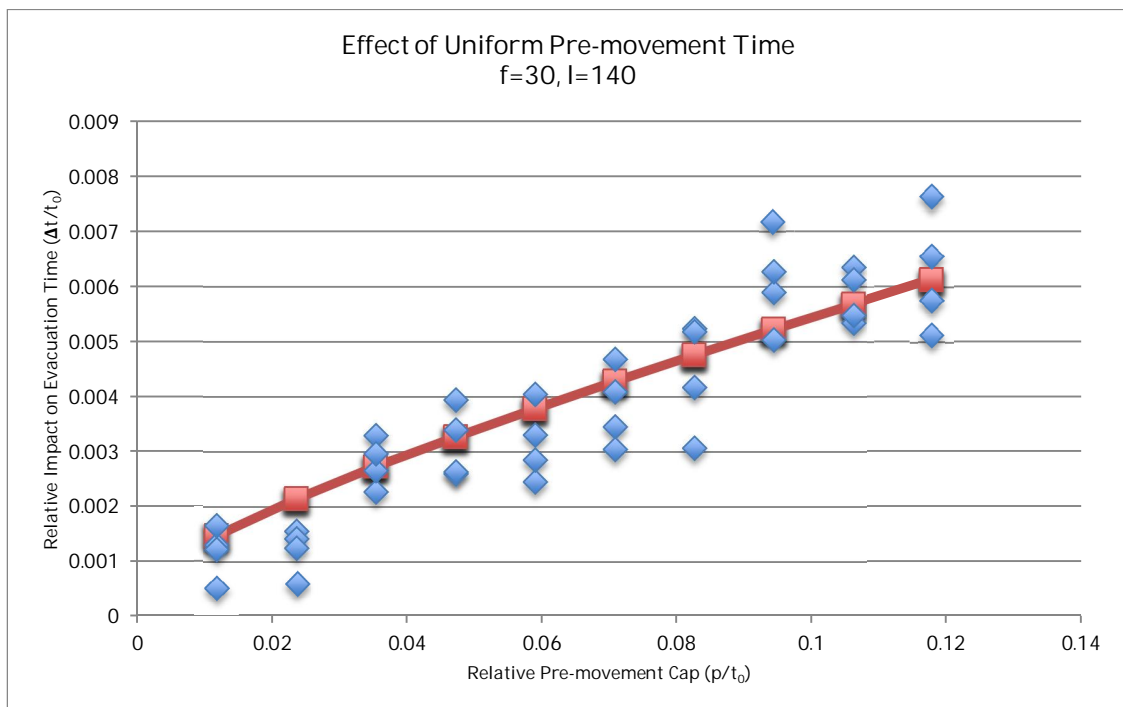


Figure 4.1.16 - UPM Results with High Order Regression ($f=30, l=140$),
 $R^2=0.817$

Generally, equation (14) generated by the regression analysis was a good fit for all primary case data.

When several building cases were plotted together, the expression (14) showed the general trends that the relative effect of pre-movement time diminishes as loading increases for a constant f , as shown in Figures 4.1.17 through 4.1.19 below.

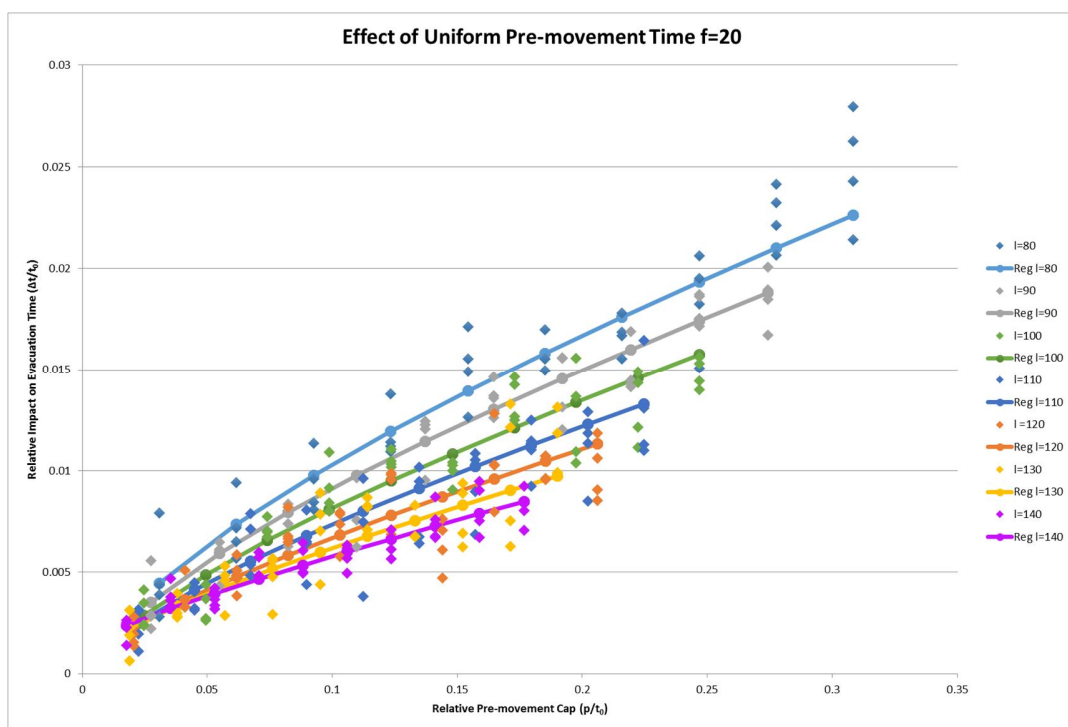


Figure 4.1.17 – UPM Results with High Order Regression (f=20, l=80 to 140)

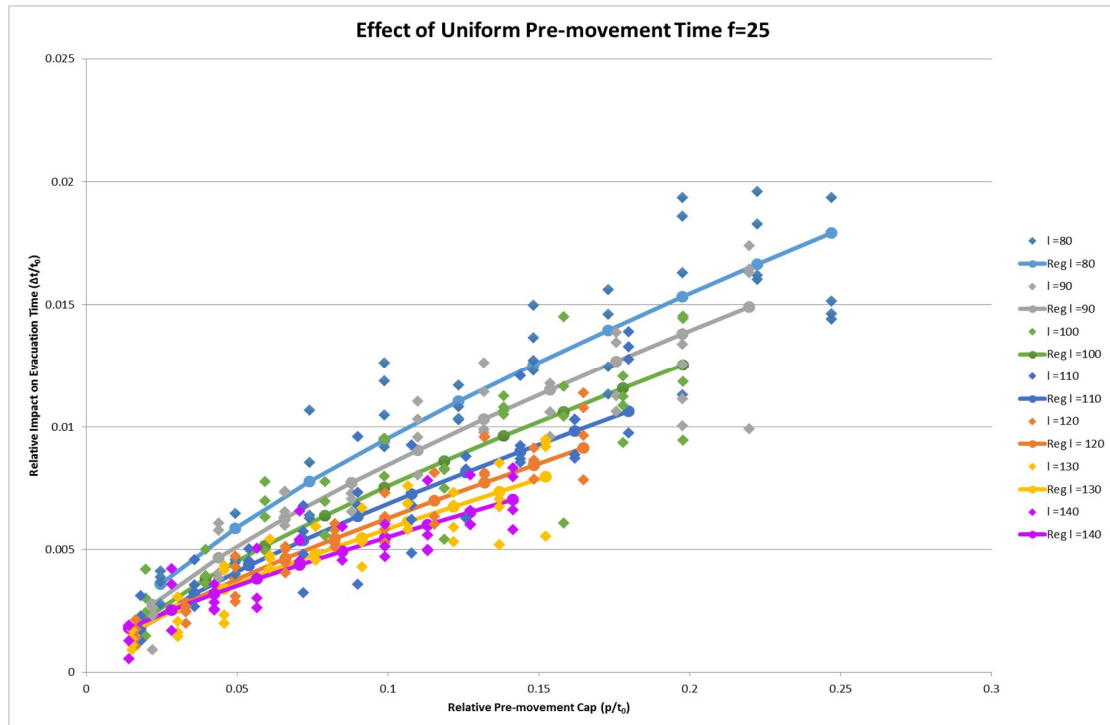


Figure 4.1.18 – UPM Results with High Order Regression (f=25, l=80 to 140)

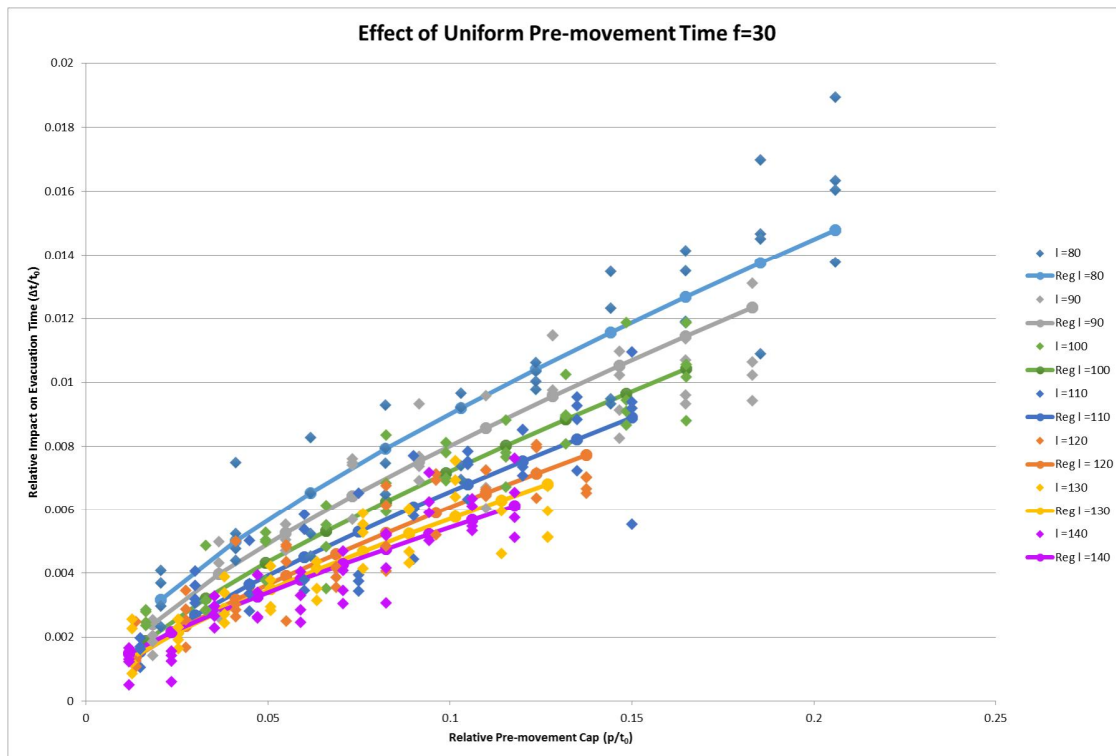


Figure 4.1.19 – UPM Results with High Order Regression (f=30, l=80 to 140)

When l is kept constant and f varies, the expression (14) reveals a slight tendency for the effects of pre-movement time to diminish as the building size (i.e. number of floors) increases. This is shown in Figures 4.1.20 to 4.1.22 below.

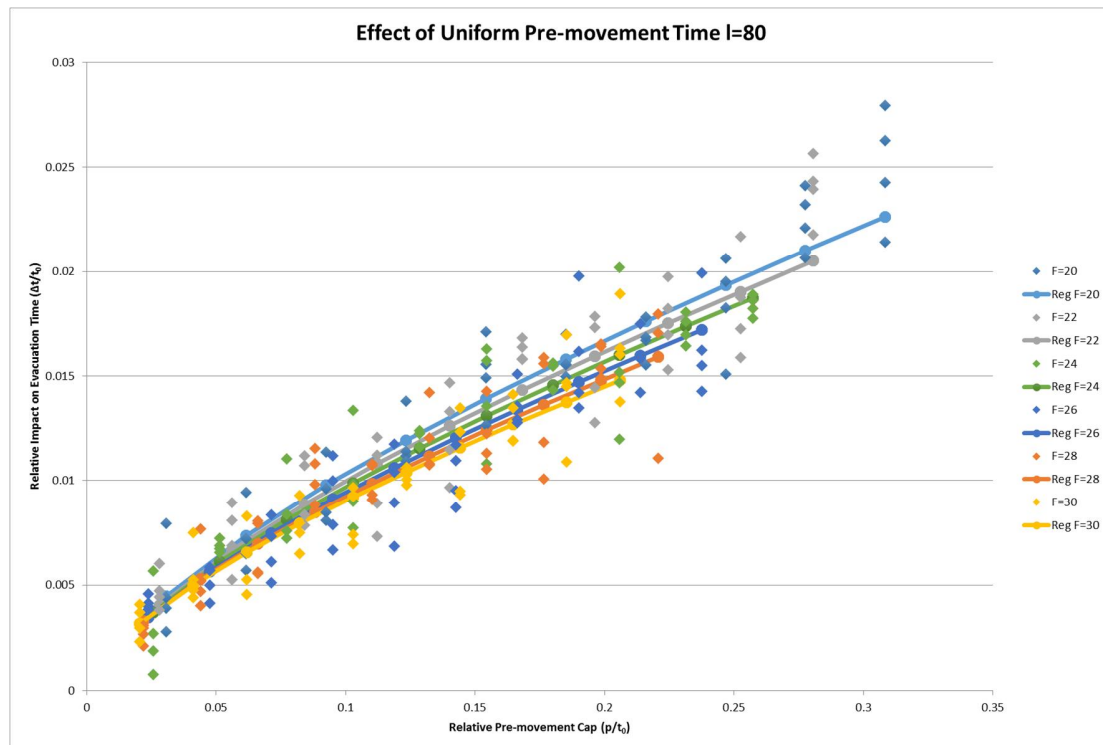


Figure 4.1.20 – UPM Results with High Order Regression ($f=20$ to 30 , $l=80$)

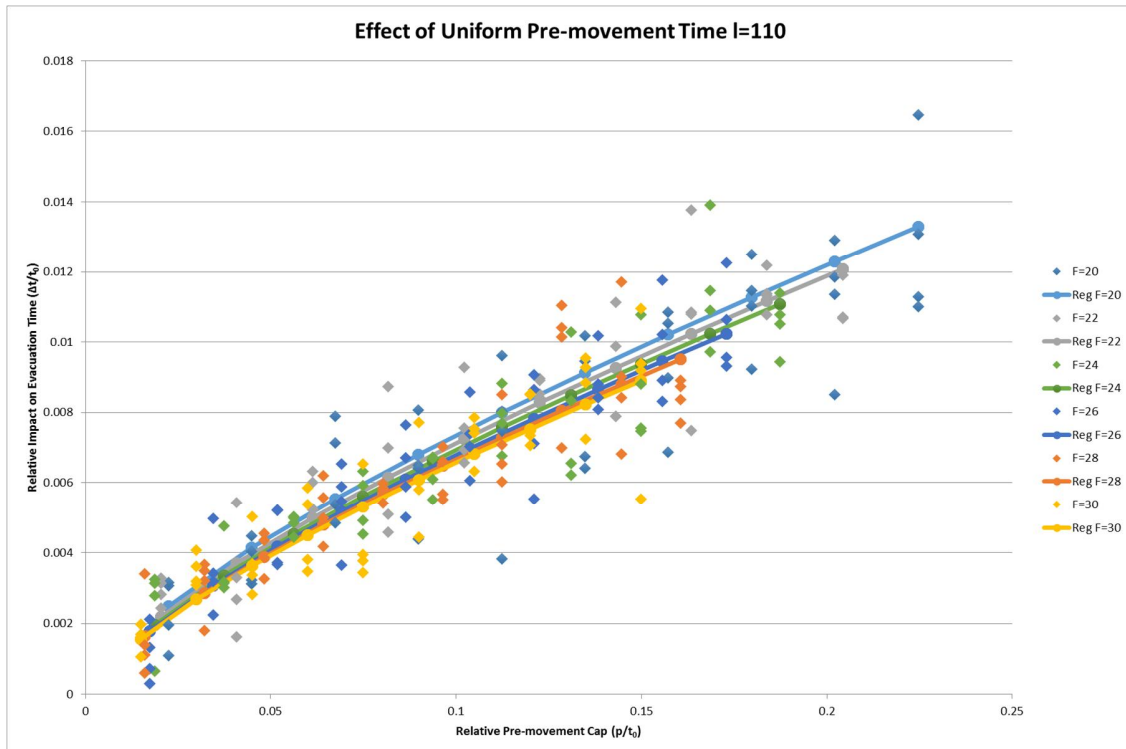


Figure 4.1.21 – UPM Results with High Order Regression ($f=20$ to 30 , $l=110$)

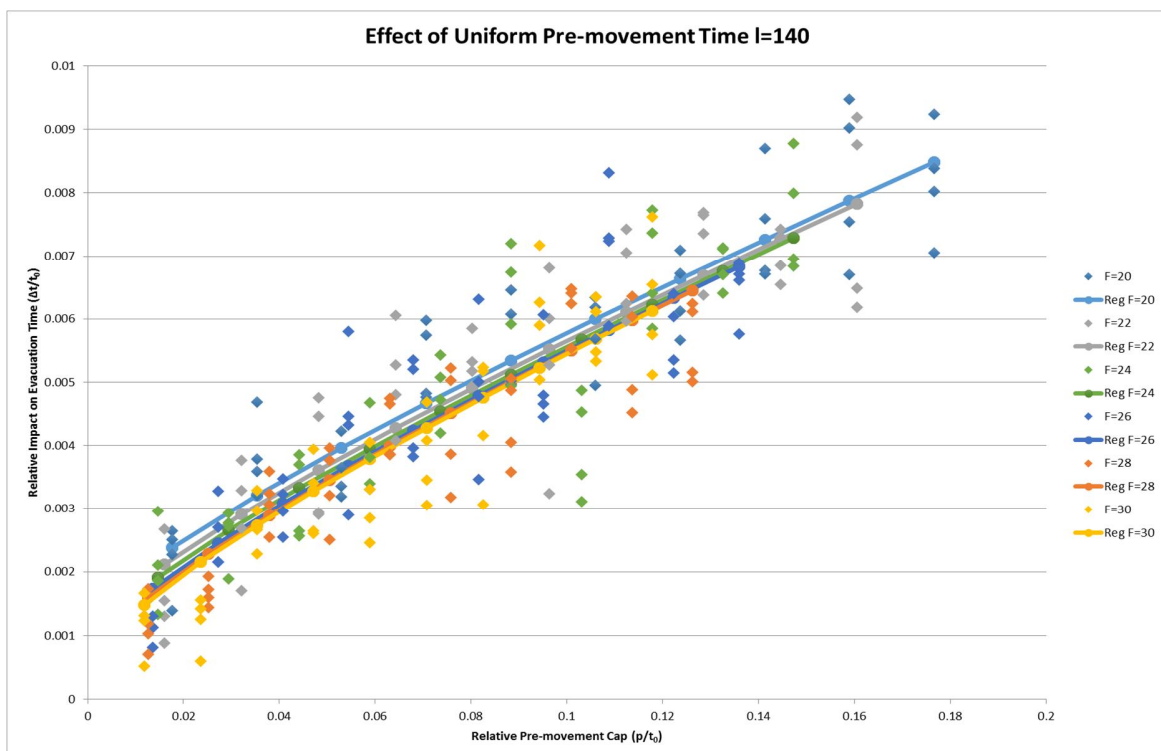


Figure 4.1.22 – UPM Results with High Order Regression ($f=20$ to 30 , $l=140$)

4.1.3 UPM Results with High Order Regression – Extended Case Studies

The results of section 4.1.2 show that the expression (14) describes the effect of pre-movement time as a relationship between loading, number of floors, and pre-movement time with relatively good accuracy, with R^2 values in Figures 4.1.12 to 4.1.16 ranging between 0.817 and 0.912.

In order to determine if this relationship exists beyond the primary case studies used for the basis of the regression analysis, additional simulations were performed with l and f parameter values outside of those used for the primary case studies. The regression equation (14) was then applied to the parameter values of the extended case studies, to determine if it could be extended with reasonable accuracy.

Low Loading

A group of extended case studies was reviewed with loading, l , at values less than the 80 people per floor. Extended cases were simulated for parameter values as follows:

- $l=20, 40, 60$
- $f=20, 22, 24, 26, 28, 30$

A sample of results is shown in Figures 4.1.23 to 4.1.26 below.

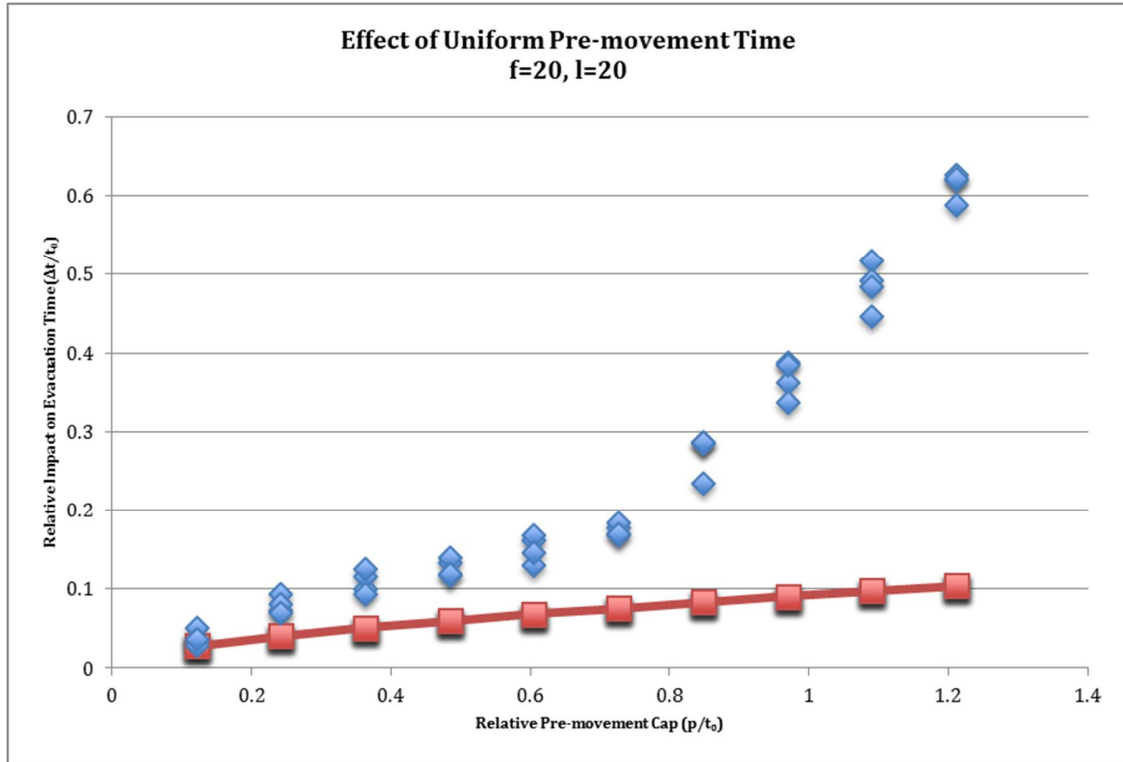


Figure 4.1.23 – UPM High Order Regression Applied to Extended Case Study
(f=20, l=20), $R^2=-0.675$

For particularly low occupant loads ($l=20$), there are some obvious cases of poor fit with the expression (14). For cases where the t_0 values are of a similar magnitude as p , it is obvious that occupants with pre-movement time p will cause relatively large delays in the evacuation. For example, for the case shown in Figure 4.1.23 where $f=20$ and $l=20$, $t_0 = 49508$, or approximately 8.5 minutes. It is obvious that when considering pre-movement times of up to 10 minutes, there will be a large proportional effect on the overall exit time. This is evident in many instances where p/t_0 approaches or exceeds 1.

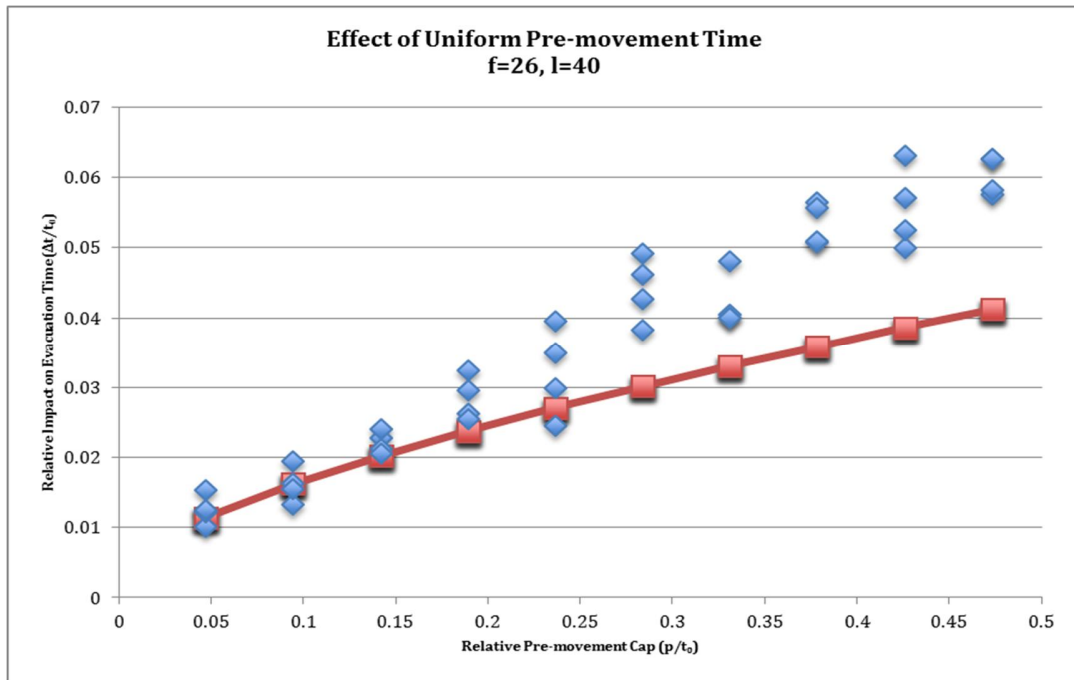


Figure 4.1.24 – UPM High Order Regression Applied to Extended Case Study
(f=26, l=40), $R^2=0.480$

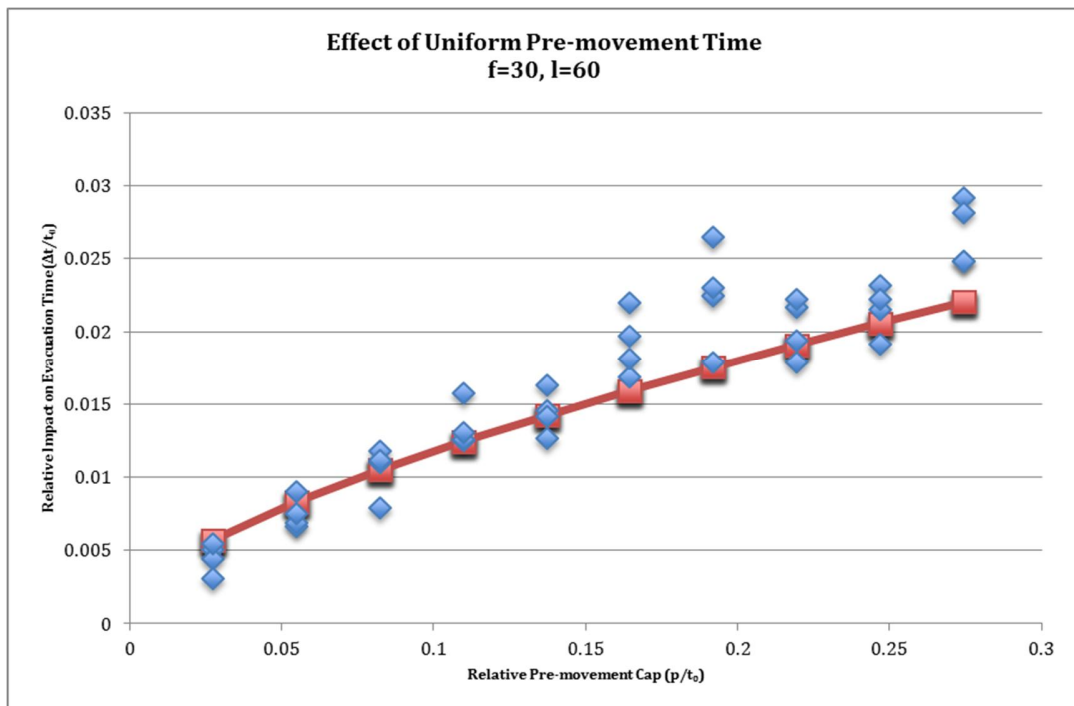


Figure 4.1.25 – UPM High Order Regression Applied to Extended Case Study
(f=30, l=60), $R^2=0.812$

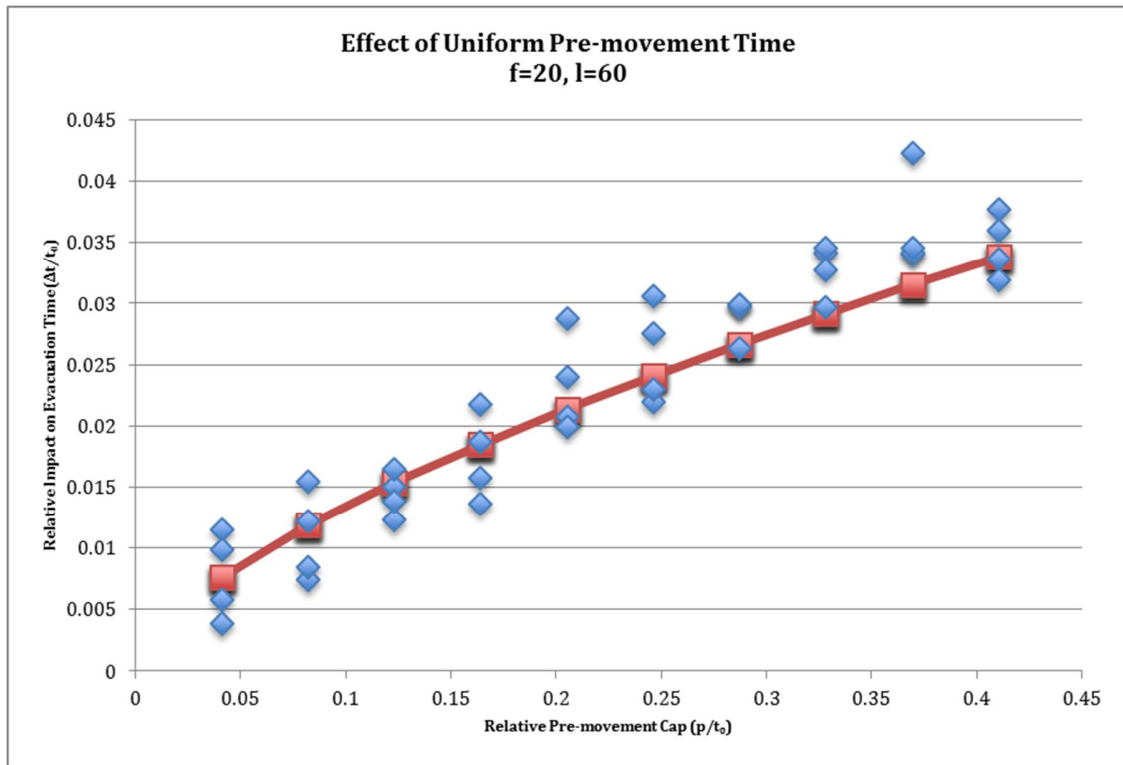


Figure 4.1.26 – UPM High Order Regression Applied to Extended Case Study ($f=20$, $l=60$), $R^2=0.872$

However, with loading values that approach the values used for the primary case studies, the expression (14) fits the data of the extended case studies very well. In particular, the fit seems better for smaller values of p/t_0 . Figure 4.1.25 and 4.1.26 show expression (14) with a reasonable fit for low occupant loading case studies (R^2 values of 0.812 and 0.872).

Short Buildings

The equation (14) was also extended to a group of case studies representing shorter buildings than the primary case studies. For these extended cases, simulations were performed for parameter values as follows:

- $l=20, 40, 60, 80, 100, 120, 140$
- $f=5, 10, 15,$

For these cases, low loading was also included, to account for building which could be not only shorter but also less populated than the primary cases. It was noted that the values of t_0 for the short buildings were in some cases significantly smaller than for some of the primary case studies. For example, t_0 for a 5 storey building with loading of 20 people per floor was 13160cs, or about 2.2 minutes. For these cases, the range of pre-movement times reviewed were adjusted, in an attempt to generate the same amount of data, but without the inconsistent results that occur when p/t_0 approaches or exceeds 1. Pre-movement time caps for this set of extended cases were chosen to be 3000 cs (0.5 minute), 6000 cs, (1 minute), 9000 cs (1.5 minutes), ... 30,000cs (5 minutes).

Results are shown in Figures 4.1.27 to 4.1.29.

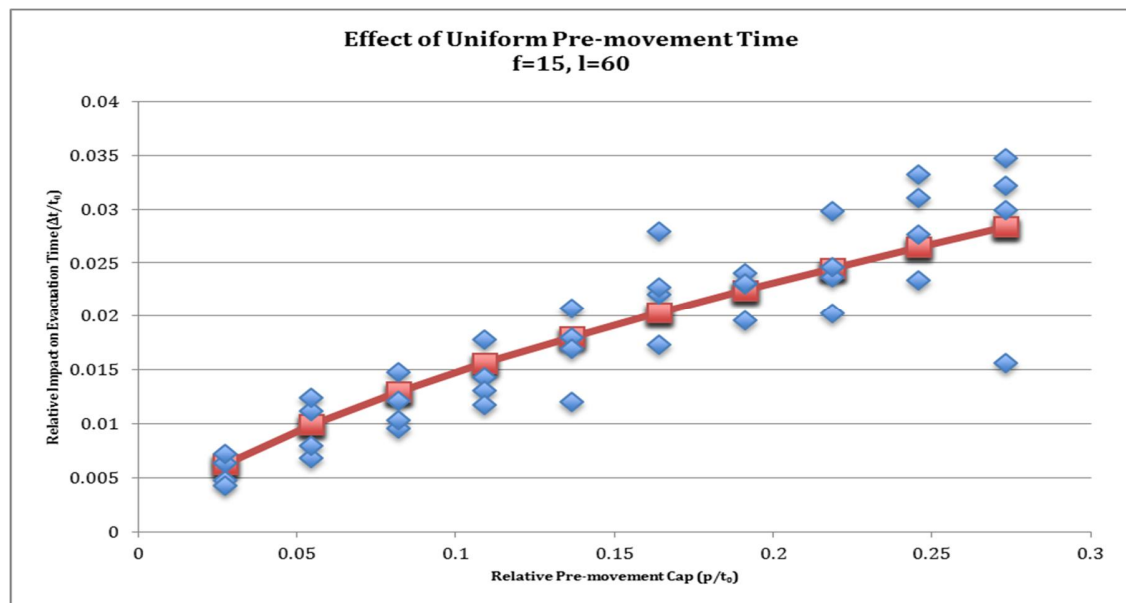


Figure 4.1.27 – UPM High Order Regression Applied to Extended Case Study
($f=15$, $l=60$), $R^2=0.802$

Results were shown to be very good for these cases, with equation (14) approximating the simulation results well, aside from cases of particularly short

buildings (i.e. $f = 5$ in particular) for very low occupant loads. However for occupant loads of $l=40$ and $l=60$, the fits were reasonable. For very short buildings, such as $f=5$, a there was good fit for higher occupant loads (as per Figure 4.1.29 in particular)

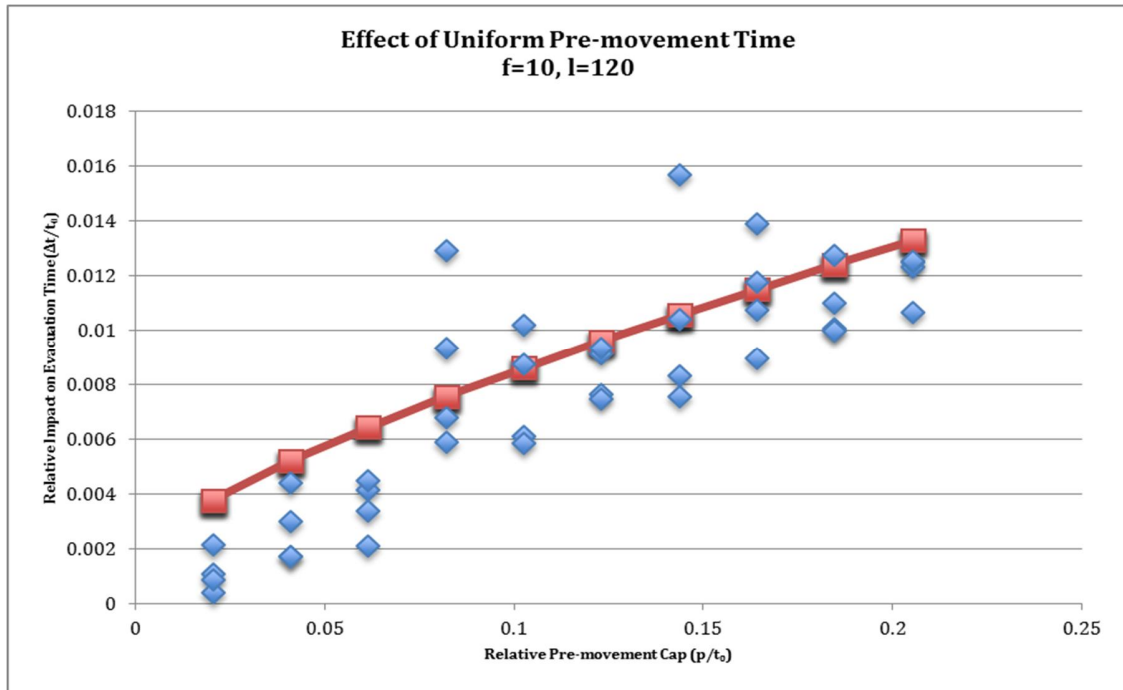


Figure 4.1.28 – UPM High Order Regression Applied to Extended Case Study
($f=10, l=120$), $R^2=0.649$

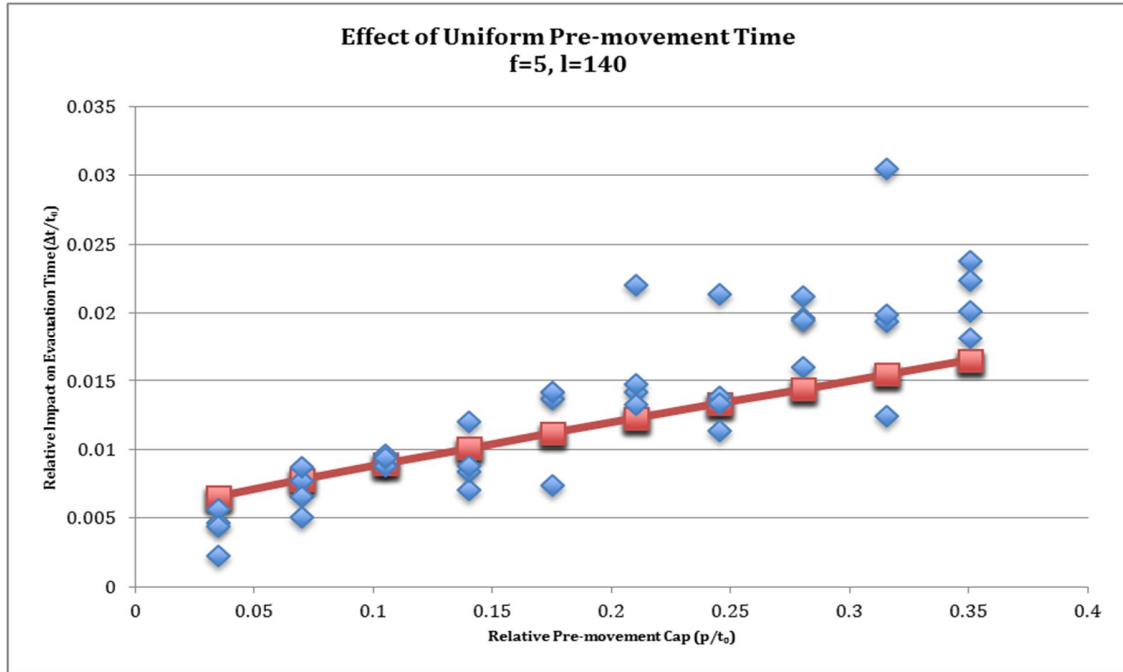


Figure 4.1.29 – UPM High Order Regression Applied to Extended Case Study
($f=5, l=140$), $R^2=0.543$

Tall Buildings

The equation (14) was also extended to a group of cases representing taller buildings than the primary case studies. For these extended cases, simulations were performed for parameter values as follows:

- $l=20, 60, 100, 140$
- $f=40, 50, 60$

It should be noted here that the algorithm running time was primarily dependent on the total number of occupants being modeled. For the low occupant load and short building cases, a total number of 720,000 and 784,000 occupants, respectively, were modeled for all simulations (the sum of occupants across all building cases, multiplied by 10 for the 10 different pre-movement values, then multiplied by four for the four separate simulations of each input value). Due to the large f values in the tall building cases noted above, if 10 pre-movement cases were considered, a

total of 1,920,000 occupants would need to be modeled. This would require more running time than both the other extended cases combined.

An evacuation of a very small building (5 floors, with 20 people per floor) could be simulated within 2 seconds. However large buildings (such as the case proposed above, with 60 floors and 140 people per floor) required approximately 41 minutes for a single simulation.

The algorithm was written so that a range of parameter values could be simulated with a single prompt, allowing the user to execute a large number of simulations for a defined range of l , f , and p values, with multiple simulations for each set of values. Running sets of simulations to generate all of the data used for each of the extended case studies (low occupancy, short buildings, and tall buildings) required several days of running time.

For the case of tall buildings, given the long running time for a single simulation, the total number of simulations for this data set was reduced. Only 5 sample pre-movement time intervals were simulated, for $p = 6000cs$ (1 minute), 18,000cs (3 minutes), 30,000cs (5 minutes), 42,000cs (7 minutes) and 54,000cs (9 minutes). Thus, the total of 960,000 occupants were modeled, which required a similar amount of time as the low occupancy and short building extended case studies.

Sample results are shown in Figures 4.1.30 to 4.1.33.

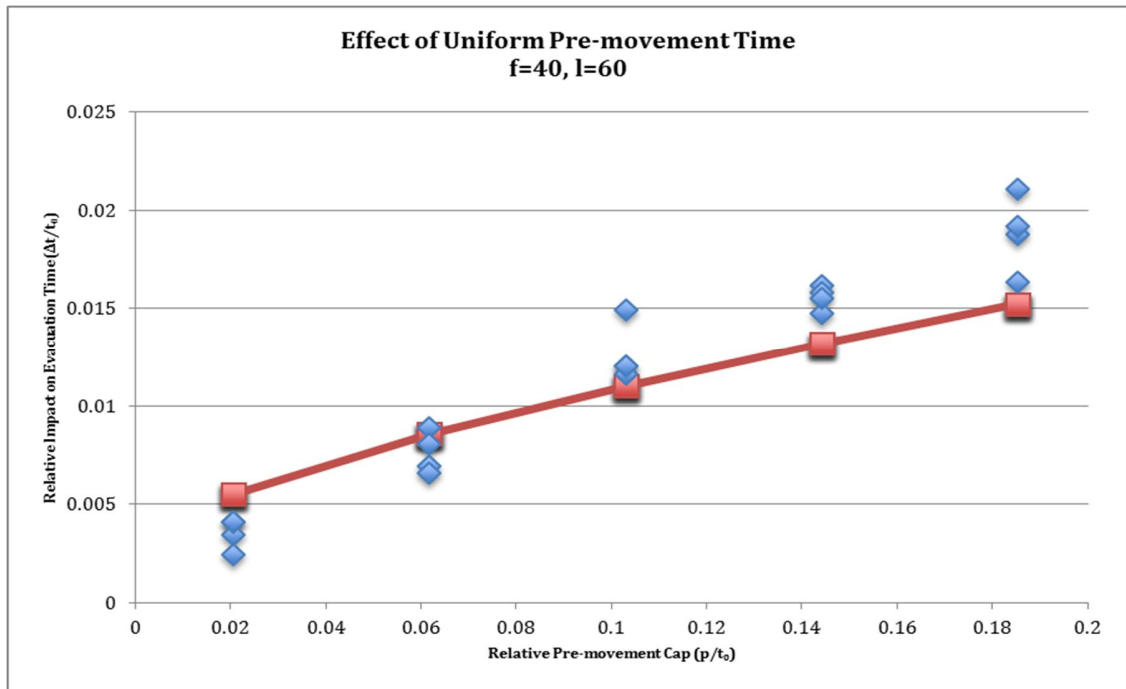


Figure 4.1.30 – UPM High Order Regression Applied to Extended Case Study
(f=40, l=60), $R^2=0.795$

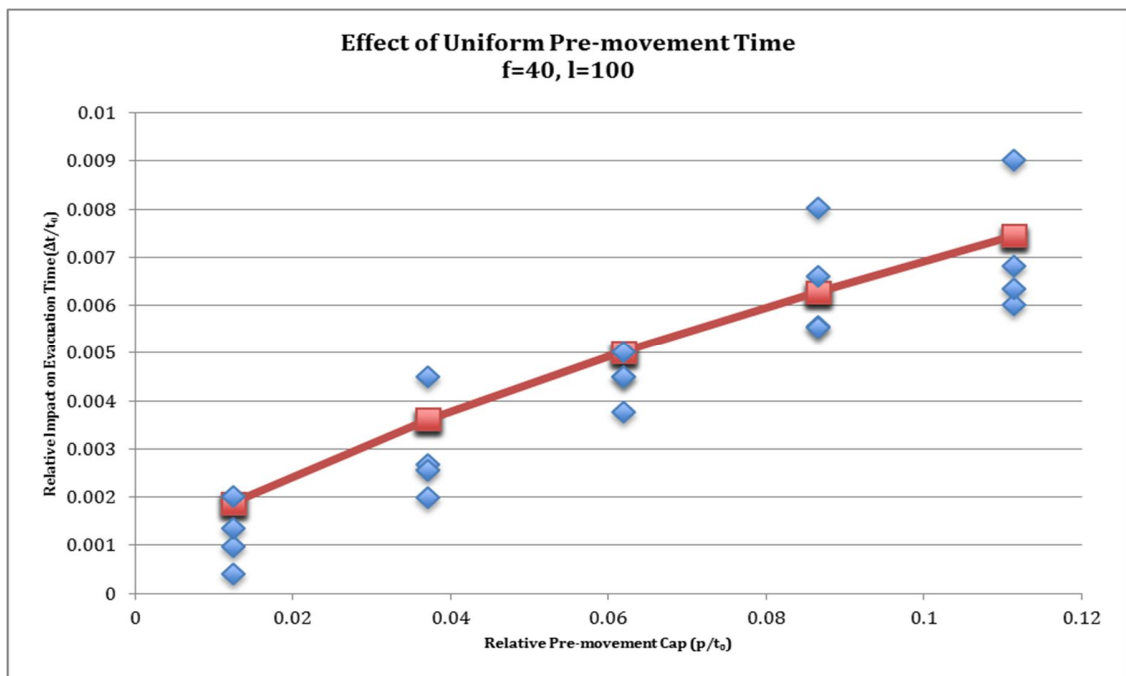


Figure 4.1.31 – UPM High Order Regression Applied to Extended Case Study
(f=40, l=100), $R^2=0.807$

In many cases, the expression (14) fits reasonably well with the simulated data, as shown in Figures 4.1.30 and 4.1.31 (R^2 values of 0.795 and 0.807). However, for tall buildings of 50 and 60 storeys in height, the expression is no longer valid, as shown in Figures 4.1.32 and 4.1.33.

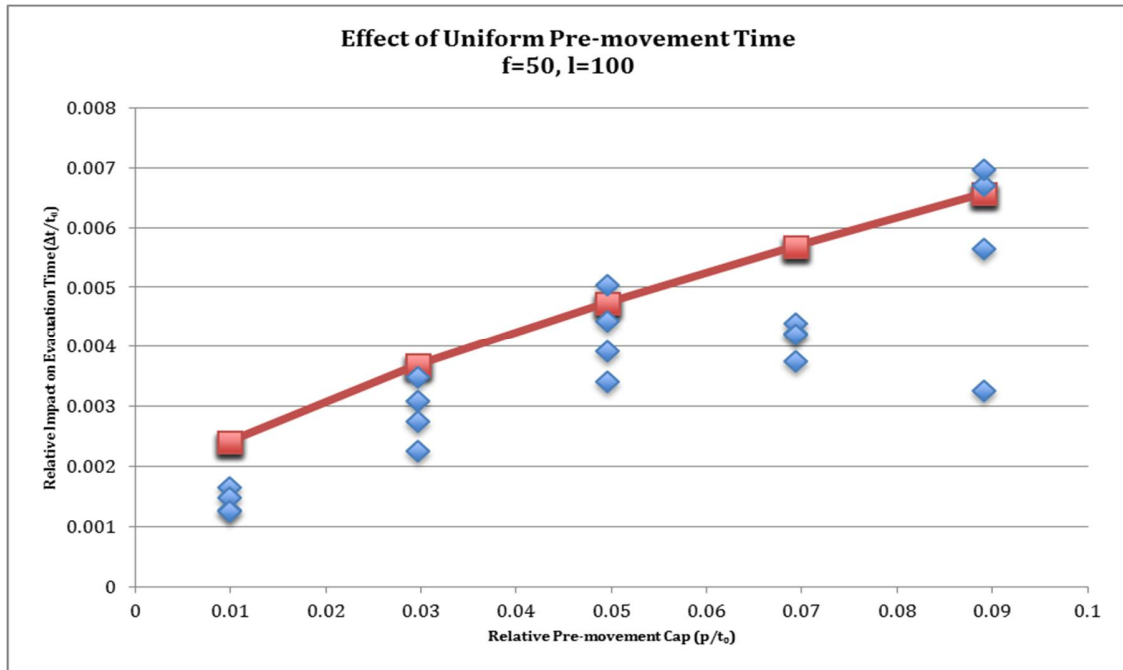


Figure 4.1.32 – UPM High Order Regression Applied to Extended Case Study
($f=50$, $l=100$), $R^2=0.383$

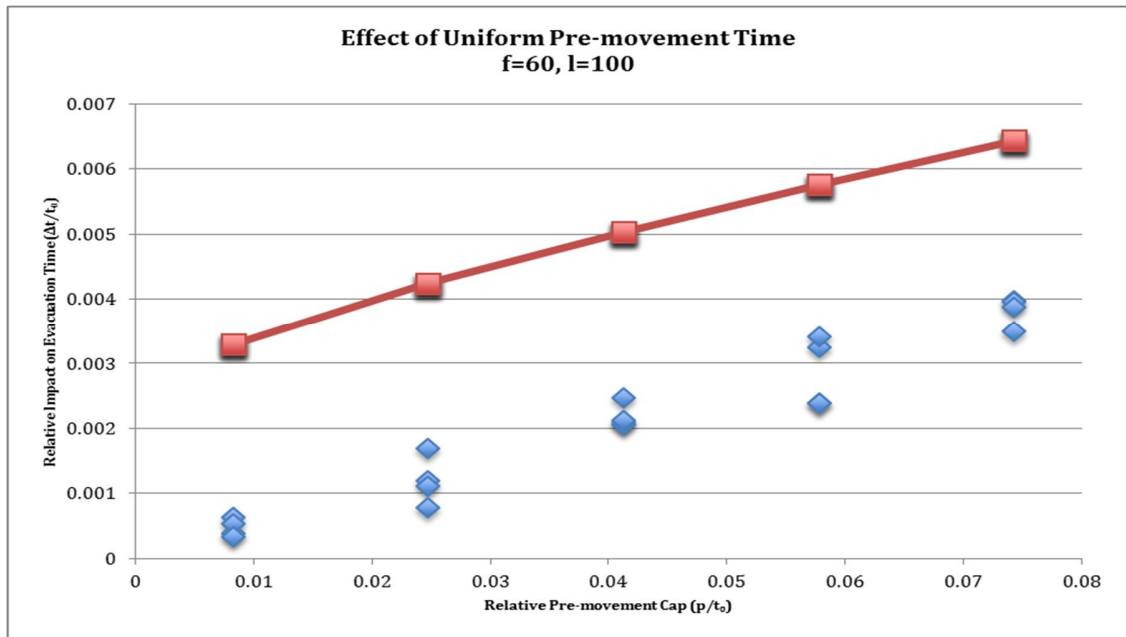


Figure 4.1.33 – UPM High Order Regression Applied to Extended Case Study
($f=60, l=100$), $R^2=-4.492$

4.2 Effects of Gamma Pre-movement Distributions (GPM)

The same primary case studies that were examined in Section 4.1. for UPM were also examined for GPM. Figures 4.2.1 to 4.2.3 below show the results. Plots show the relative pre-movement time along the x axis, and the relative effect along the y axis. Each figure represents a single building (defined by f , the number of floors) with various loading scenarios.

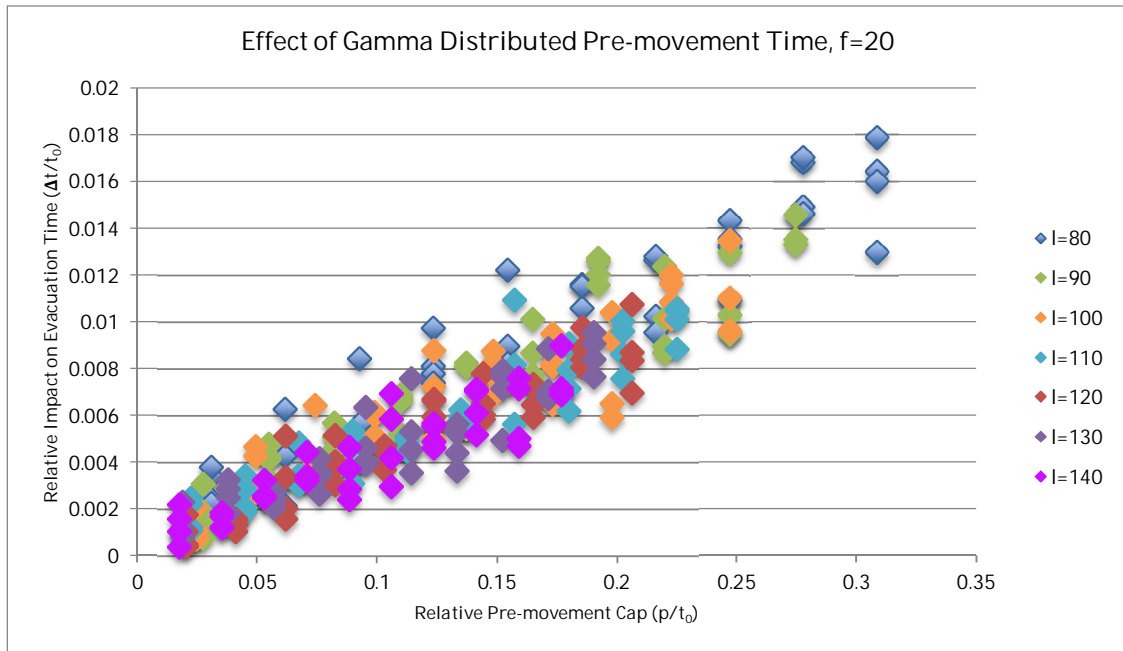


Figure 4.2.1 – GPM Simulation Results ($f=20$, $I= 80$ to 140)

It is noted that, for the same building size, the relative impact of pre-movement time decreases as the loading increases. This same trend was present in results for UPM simulations as well, and is present for GPM building simulations of all sizes

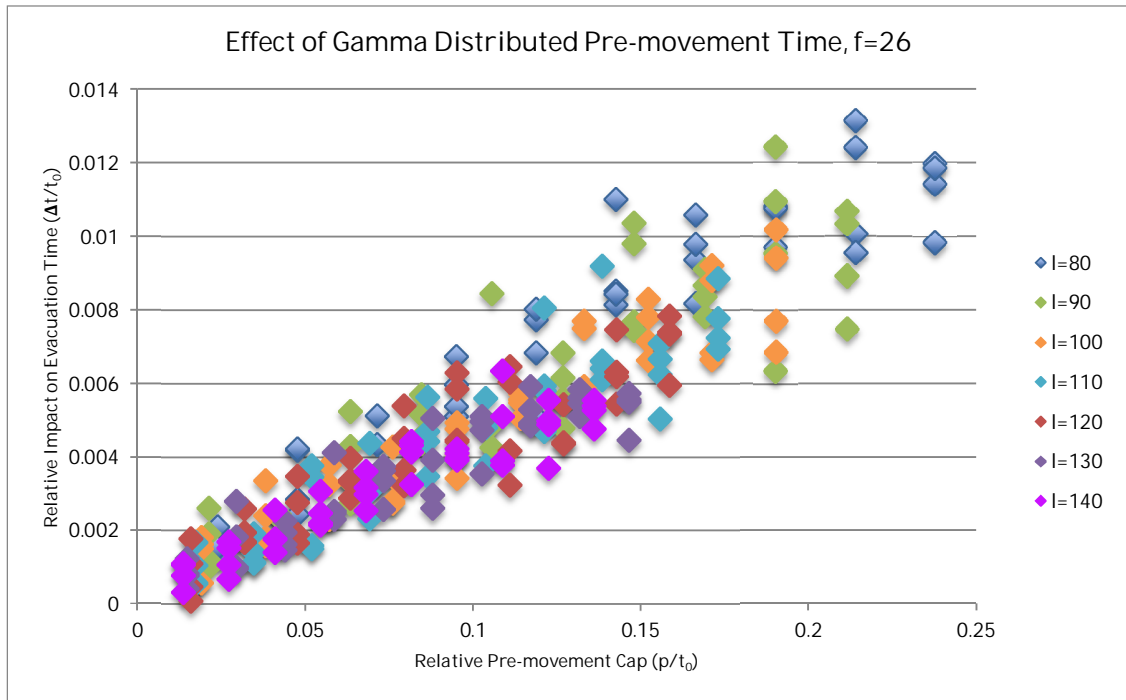


Figure 4.2.2 – GPM Simulation Results ($f=26$, $I=80$ to 140)

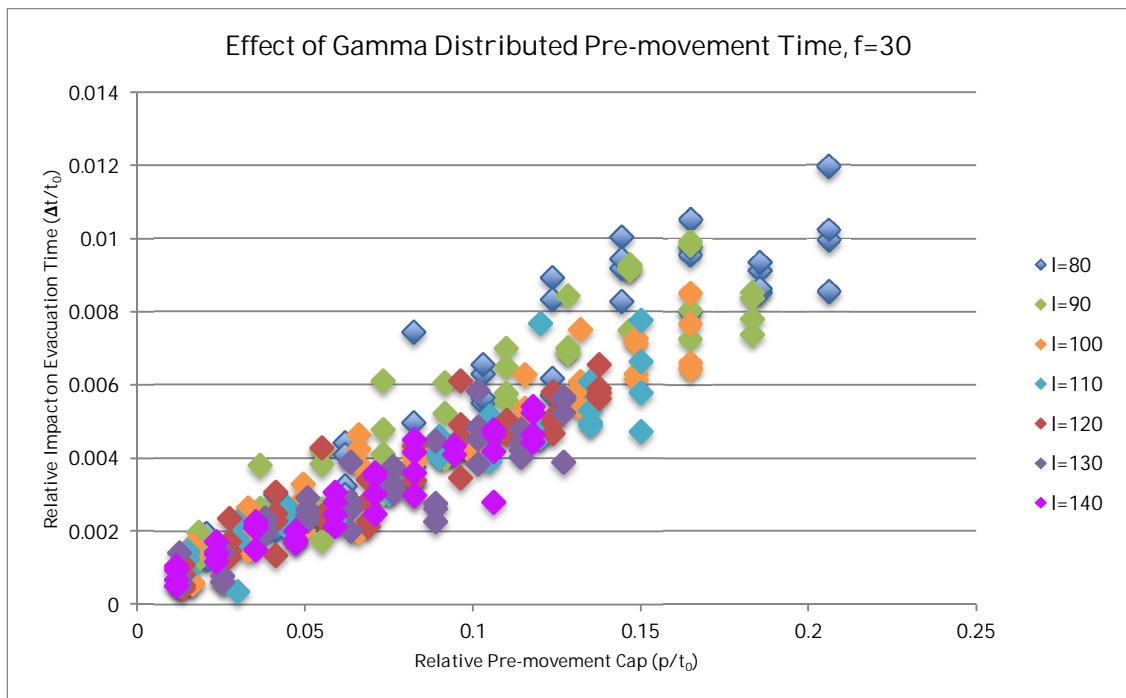


Figure 4.2.3 – GPM Simulation Results ($f=30$, $I=80$ to 140)

As was seen with the UPM results, it was noted here that the relative effect of pre-movement time $\Delta t/t_0$ also decreases as stair loading, I , increases when the number of floors, f , remains constant. However, when I was held constant and f varied, no significant trends were noticed, as shown in Figures 4.2.4 and 4.2.5.

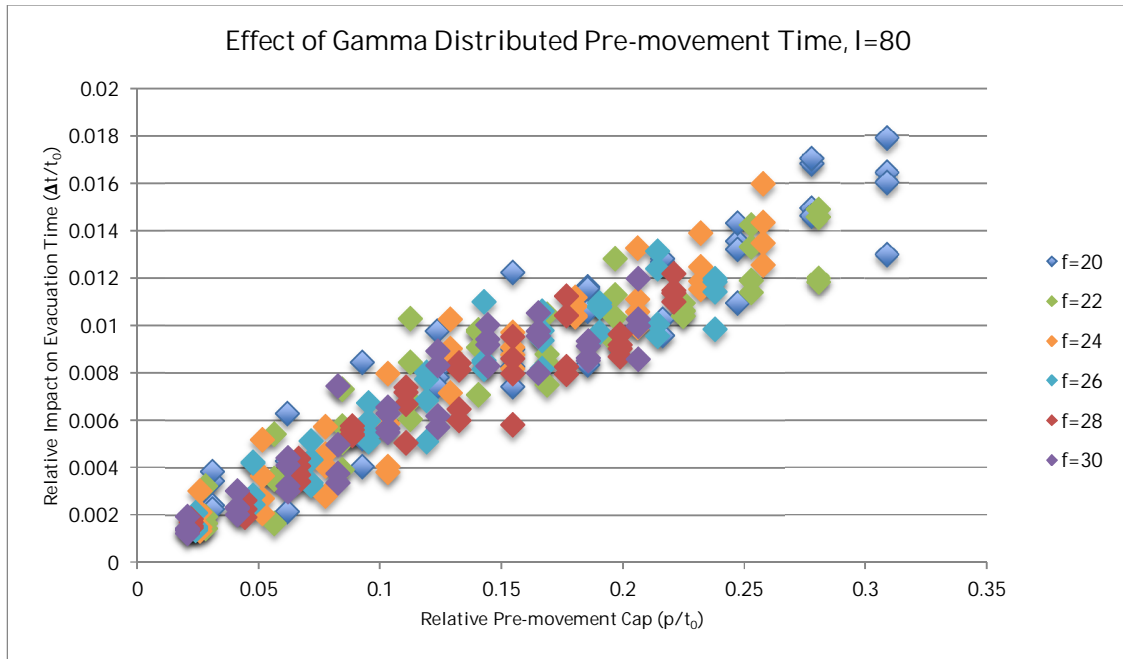


Figure 4.2.4 – GPM Simulation Results ($f=20$ to 30 , $I=80$)

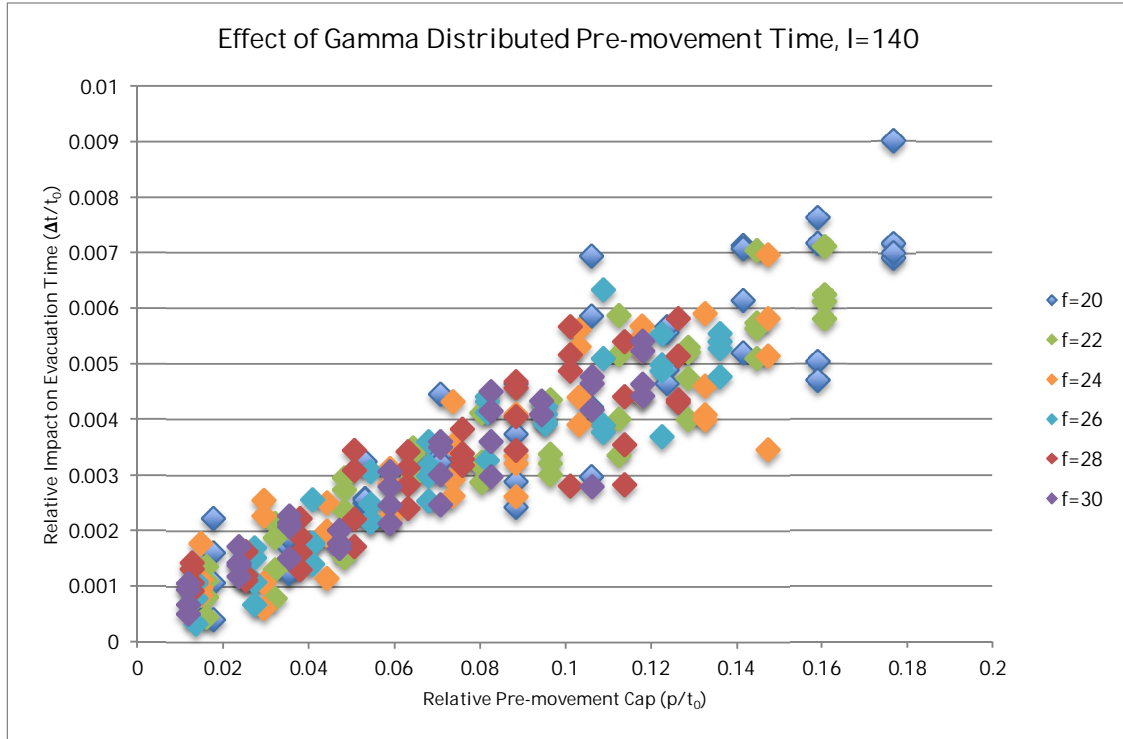


Figure 4.2.5 – GPM Simulation Results (f=20 to 30, l= 80)

4.2.1 GPM Results with Linear Regression

As was done with the UPM results, a linear regression analysis was performed for the results of the GPM primary cases, to see if the effect of pre-movement time could be reasonably expressed by a linear equation of the form:

$$\frac{\Delta t}{t_0} = g_1 l + g_2 f + g_3 \frac{p}{t_0} \quad (15)$$

for some parameters g_1 , g_2 , and g_3 .

Using MATLAB to perform the regression analysis, the following parameters were generated:

$$g_1 = -1.51673 \times 10^{-5}$$

$$g_2 = 7.51596 \times 10^{-5}$$

$$g_3 = 0.047073912$$

The resulting linear equation was plotted for each building case along with the values generated by the algorithm. Sample results are shown in Figure 4.2.6 to 4.2.9.

For some cases, the regression shows a reasonable fit, as noted in Figure 4.2.6. However, as was noted for the UPM cases, the curved nature of the data is not captured with the linear expression, and in particular, model results for higher p values are overestimated by the regression function, as shown in Figures 4.2.7 and 4.2.8. As was the case for the UPM linear regression, the curvature of the results does not appear to be modeled well by a linear expression.

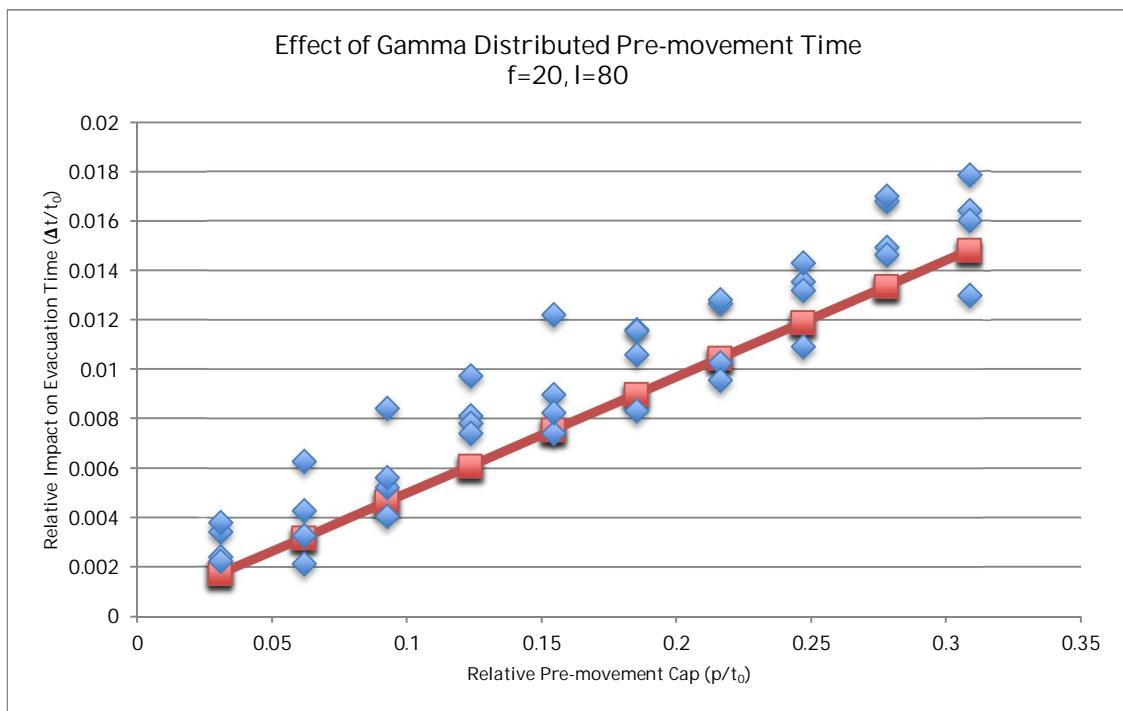


Figure 4.2.6 – GPM Results with Linear Regression ($f=20, l=80$), $R^2=0.793$

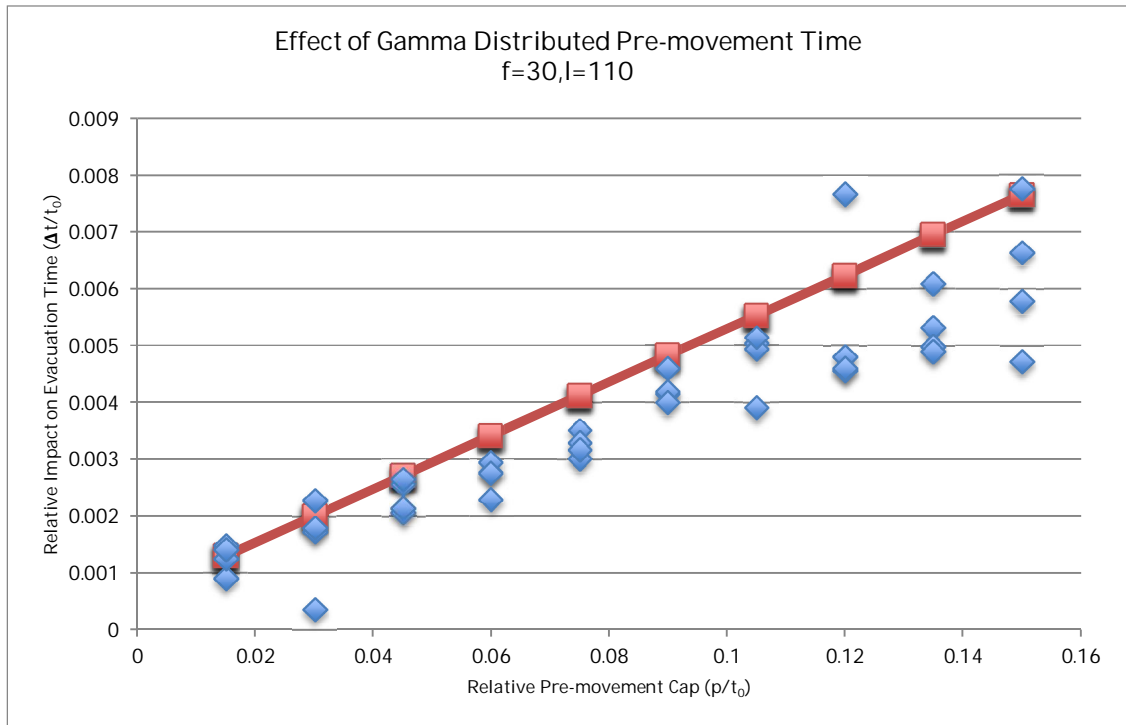


Figure 4.2.7 – GPM Results with Linear Regression ($f=30, l=110$), $R^2=0.616$

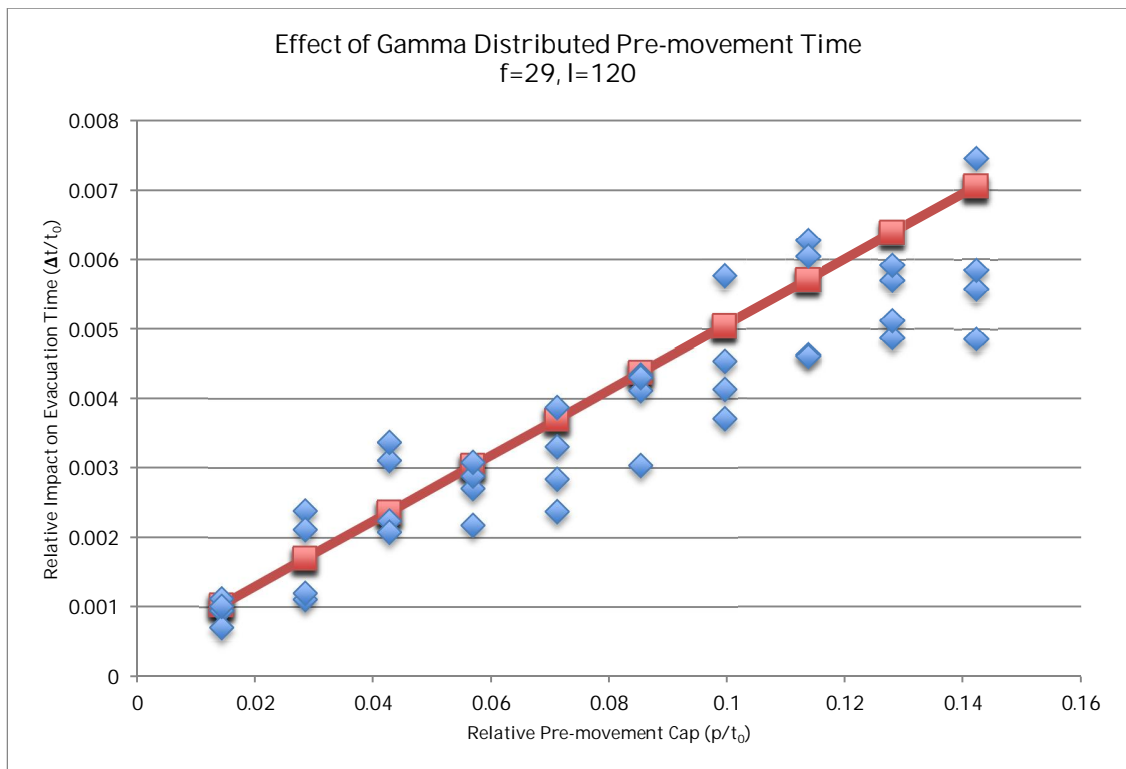


Figure 4.2.8 – GPM Results with Linear Regression ($f=29, l=120$), $R^2=0.761$

4.2.2 GPM Results with High Order Regression

As was the case for the UPM data, the linear expression generated by regression was not an ideal fit for the results observed. In order to account for the curvature of the data, a higher order regression analysis was performed in MATLAB, in order to generate an expression in the same form as (14) for UPM data, as in (16), below:

$$\begin{aligned} \frac{\Delta t}{t_0} = & g_1 l + g_2 l^{\frac{1}{2}} + g_3 f + g_4 f^{\frac{1}{2}} + g_5 \frac{p}{t_0} + g_6 \frac{p^{\frac{1}{2}}}{t_0} + g_7 (lf)^{\frac{1}{2}} + g_8 \left(l \frac{p}{t_0} \right)^{\frac{1}{2}} \\ & + g_9 \left(f \frac{p}{t_0} \right)^{\frac{1}{2}} + g_{10} \left(lf \frac{p}{t_0} \right)^{\frac{1}{2}} \end{aligned} \quad (16)$$

Using MATLAB to perform the regression analysis, the following coefficients were generated:

$g_1= 0.000113734$	$g_6=0.090211842$
$g_2= -0.001337955$	$g_7=-0.000144582$
$g_3= 1.15109\text{E-}05$	$g_8=-0.006844728$
$g_4= 0.001646692$	$g_9=-0.009907932$
$g_5= 0.027512013$	$g_{10}=0.000756612$

This regression expression was plotted again with the GPM simulation results. Results are shown in Figures 4.2.9 to 4.2.13 below.

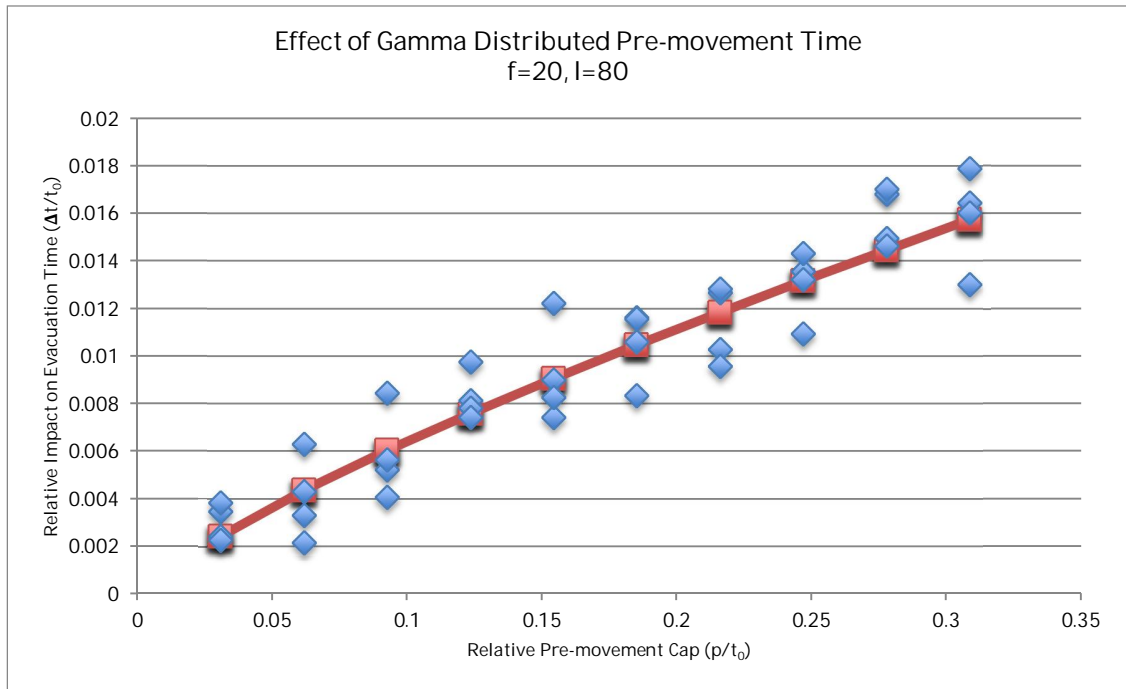


Figure 4.2.9 - GPM Results with High Order Regression (f=20, l=80), $R^2=0.890$

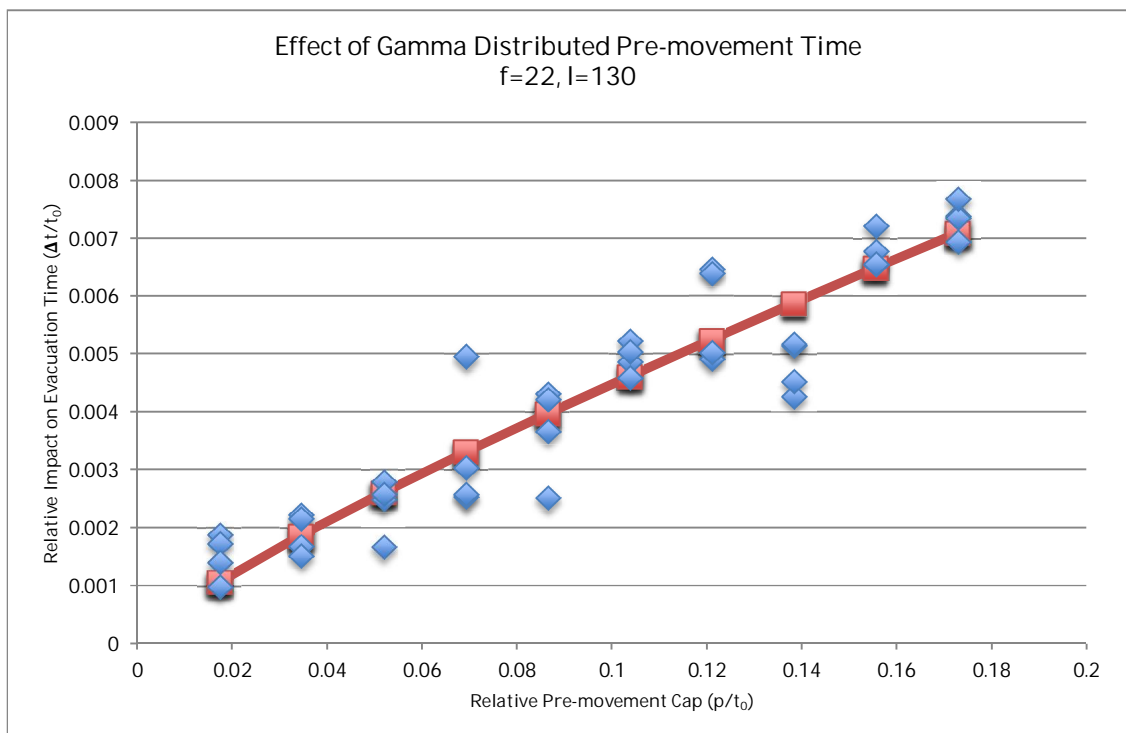


Figure 4.2.10 - GPM Results with High Order Regression (f=22, l=130),
 $R^2=0.880$

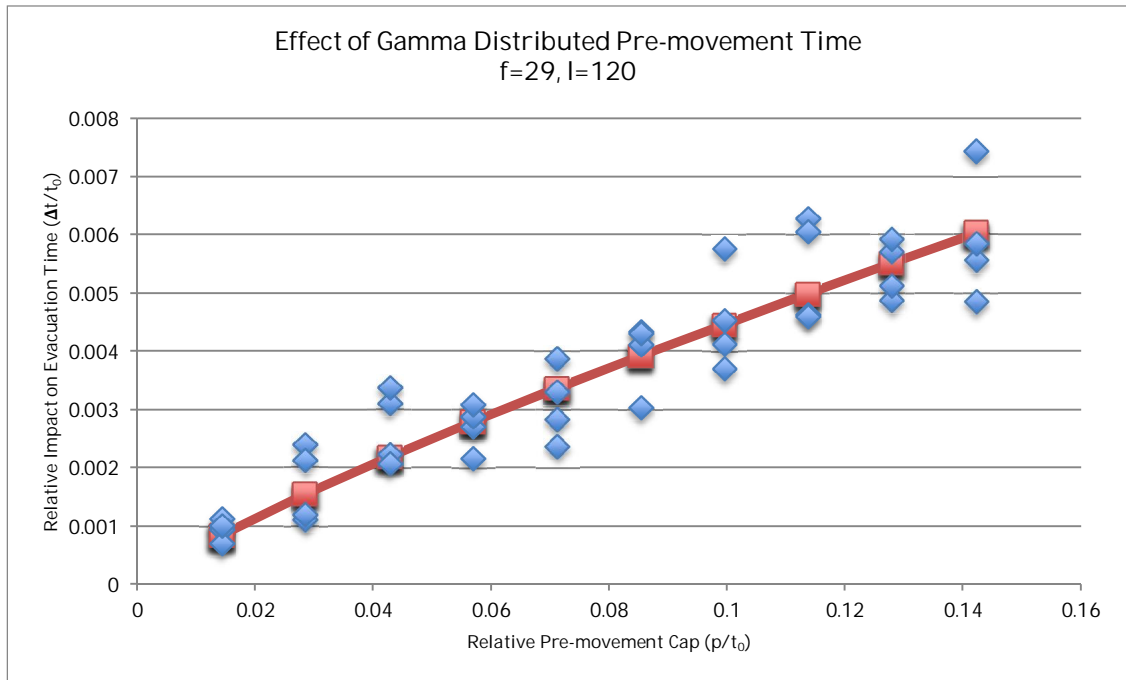


Figure 4.2.11 – GPM Results with High Order Regression ($f=29, l=120$),
 $R^2=0.856$

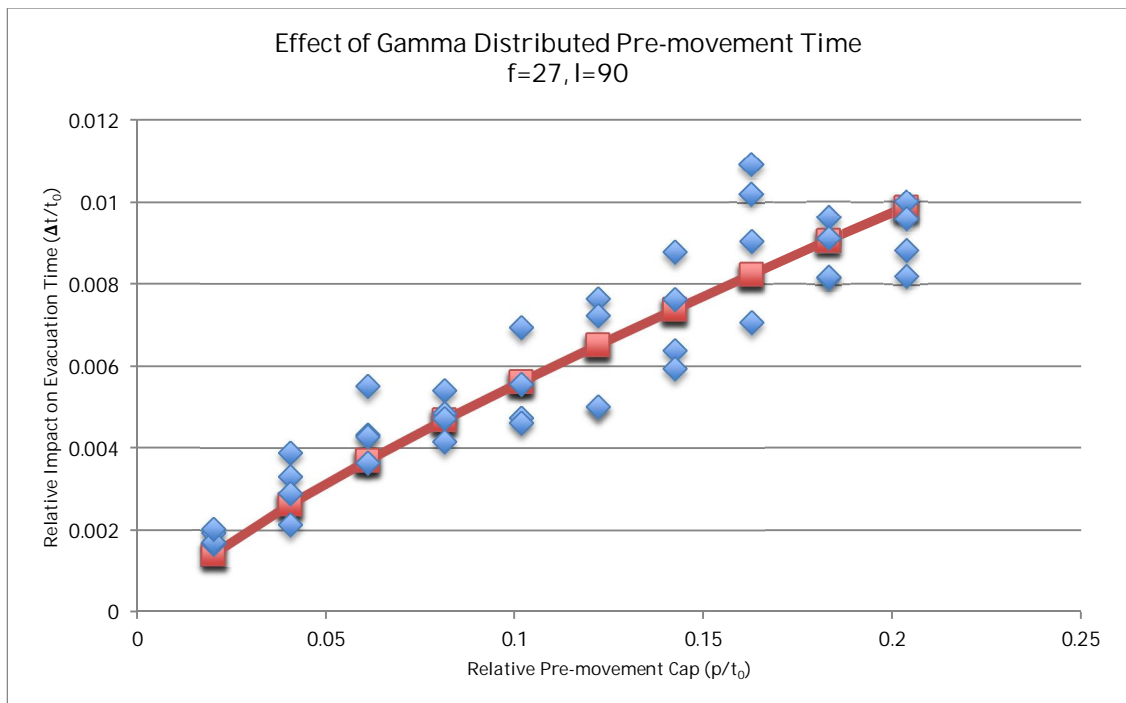


Figure 4.2.12 – GPM Results with High Order Regression ($f=27, l=90$),
 $R^2=0.846$

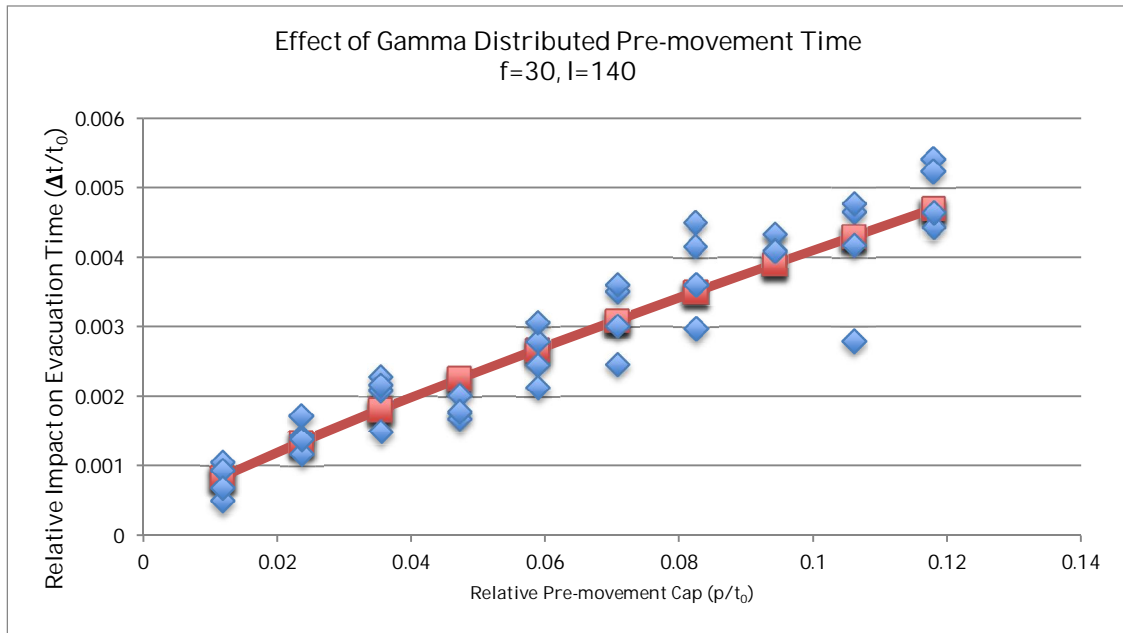


Figure 4.2.13 – GPM Results with High Order Regression (f=30, l=140),
R²=0.882

In general, for all primary cases, the regression expression (16) provides a good fit for the algorithm results.

Figures 4.2.14 through 4.2.17 show the trends of decreasing impact of pre-movement when occupant loading increases and number of floors stays constant. This same trend was present for the UPM Case studies.

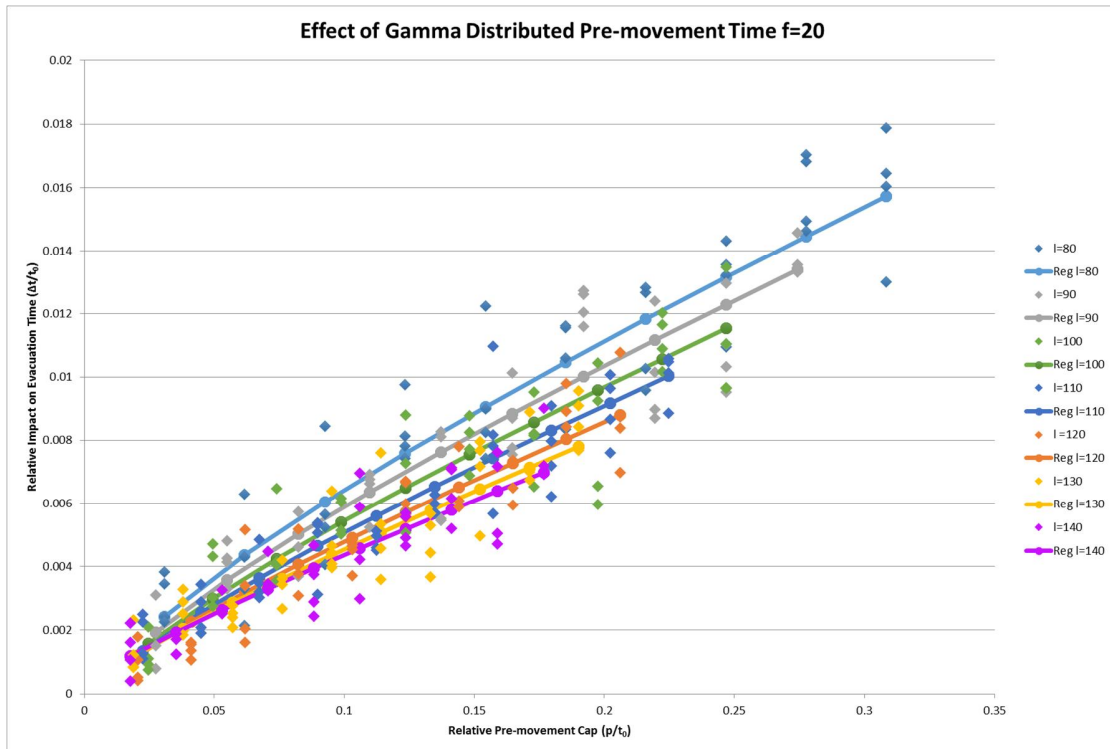


Figure 4.2.14 – GPM Results with High Order Regression ($f=20$, $l=80$ to 140)

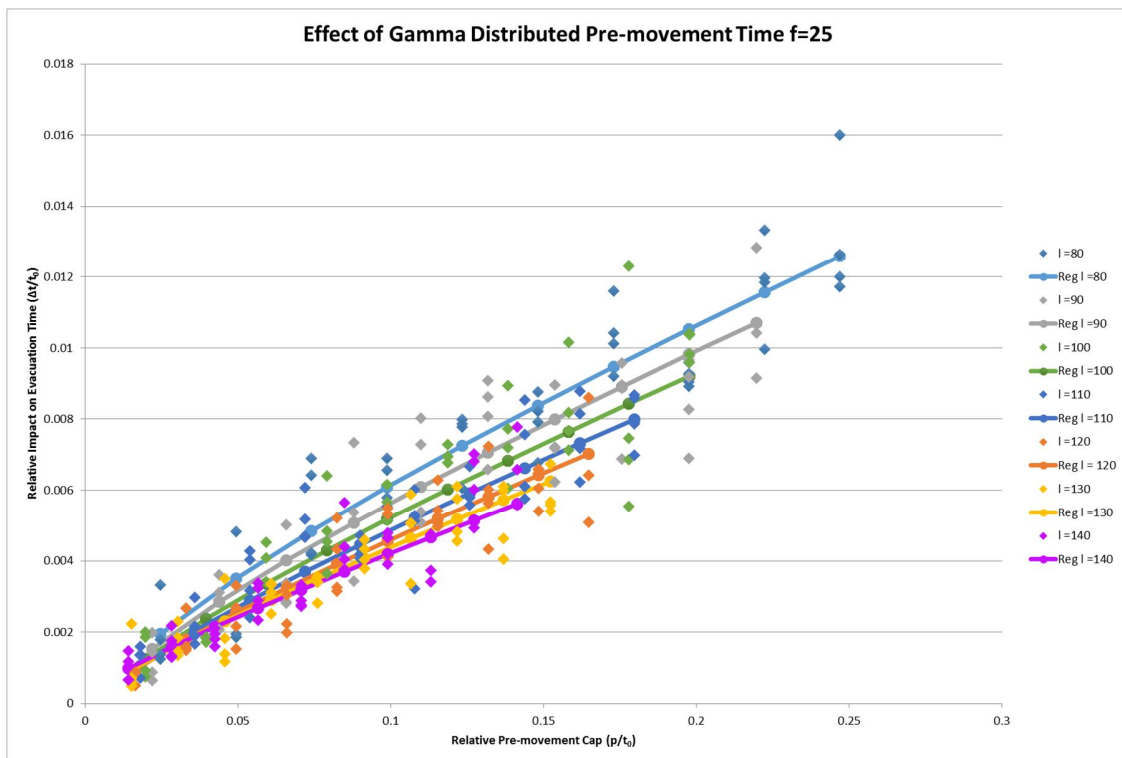


Figure 4.2.15 – GPM Results with High Order Regression ($f=25$, $l=80$ to 140)

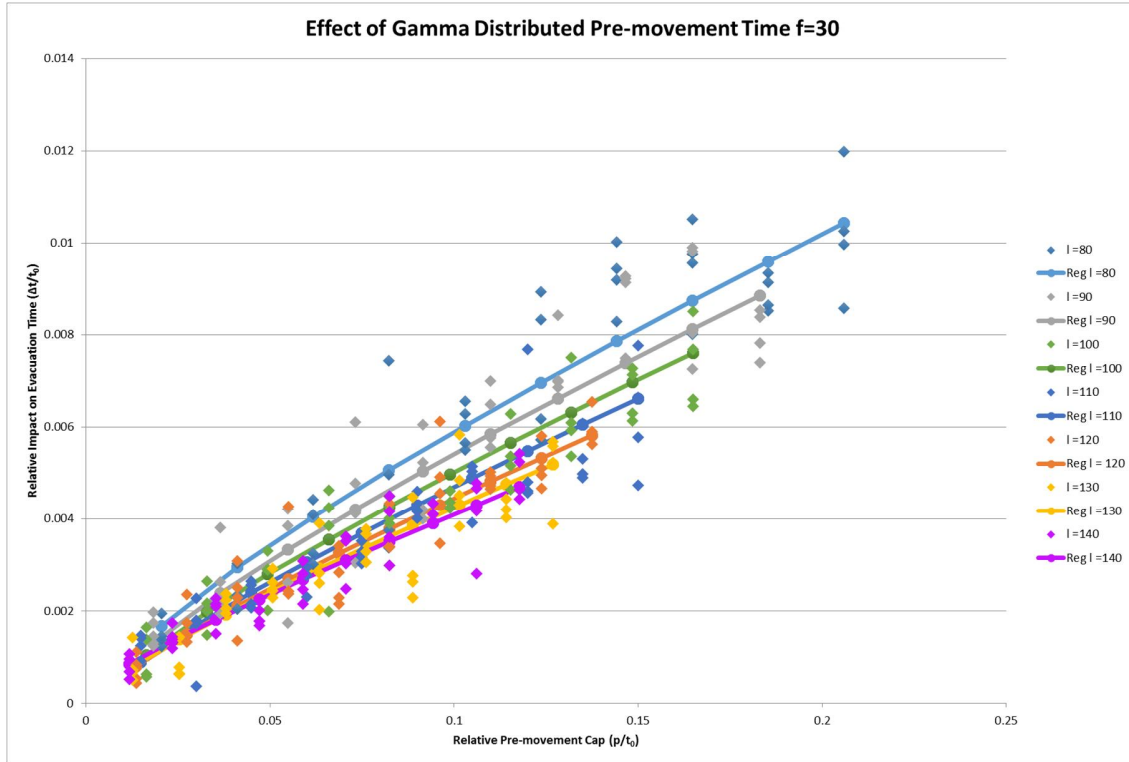


Figure 4.2.16 – GPM Results with High Order Regression ($f=30$, $l=80$ to 140)

The regression analysis indicated that there was a very small decreasing trend in effect of pre-movement when loading remains constant and the number of floors increasing. However, for all values of l reviewed, this trend was very minimal, as shown in Figures 4.2.17 through 4.2.19

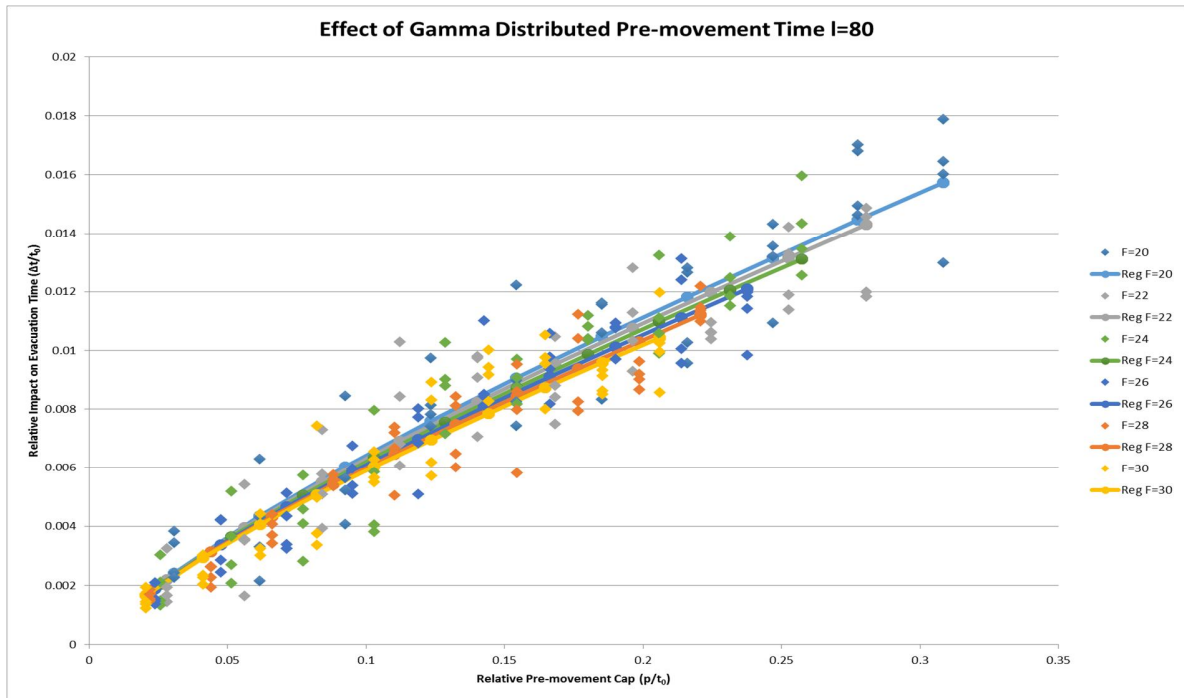


Figure 4.2.17 – GPM Results with High Order Regression ($f=20$ to 30 , $l=80$)

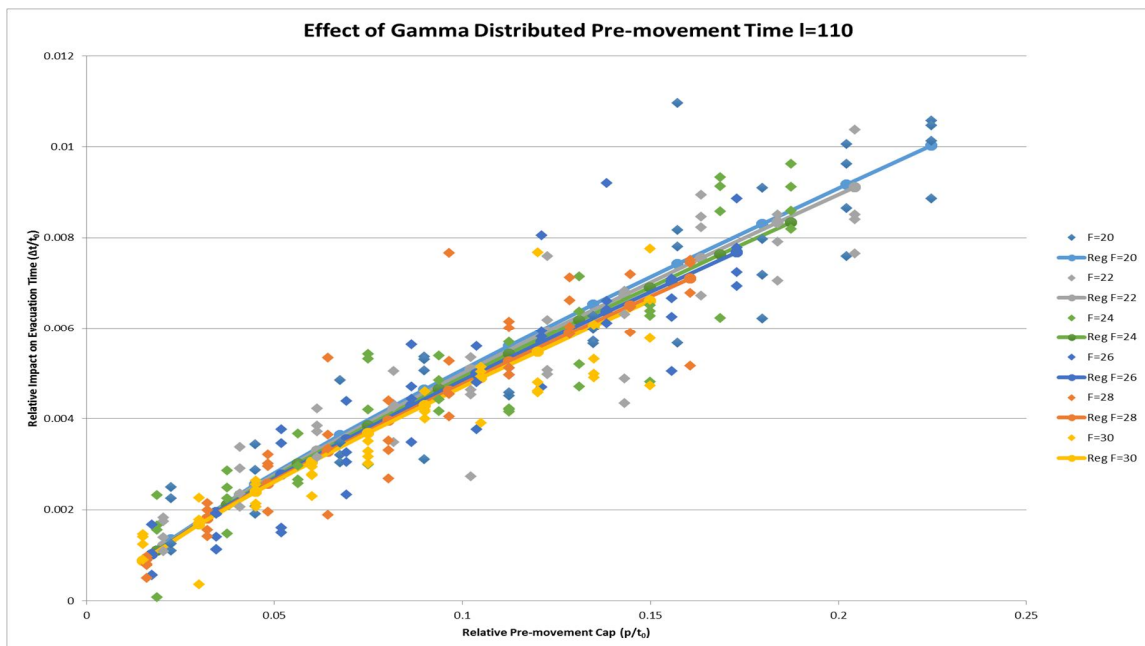


Figure 4.2.18 – GPM Results with High Order Regression ($f=20$ to 30 , $l=110$)

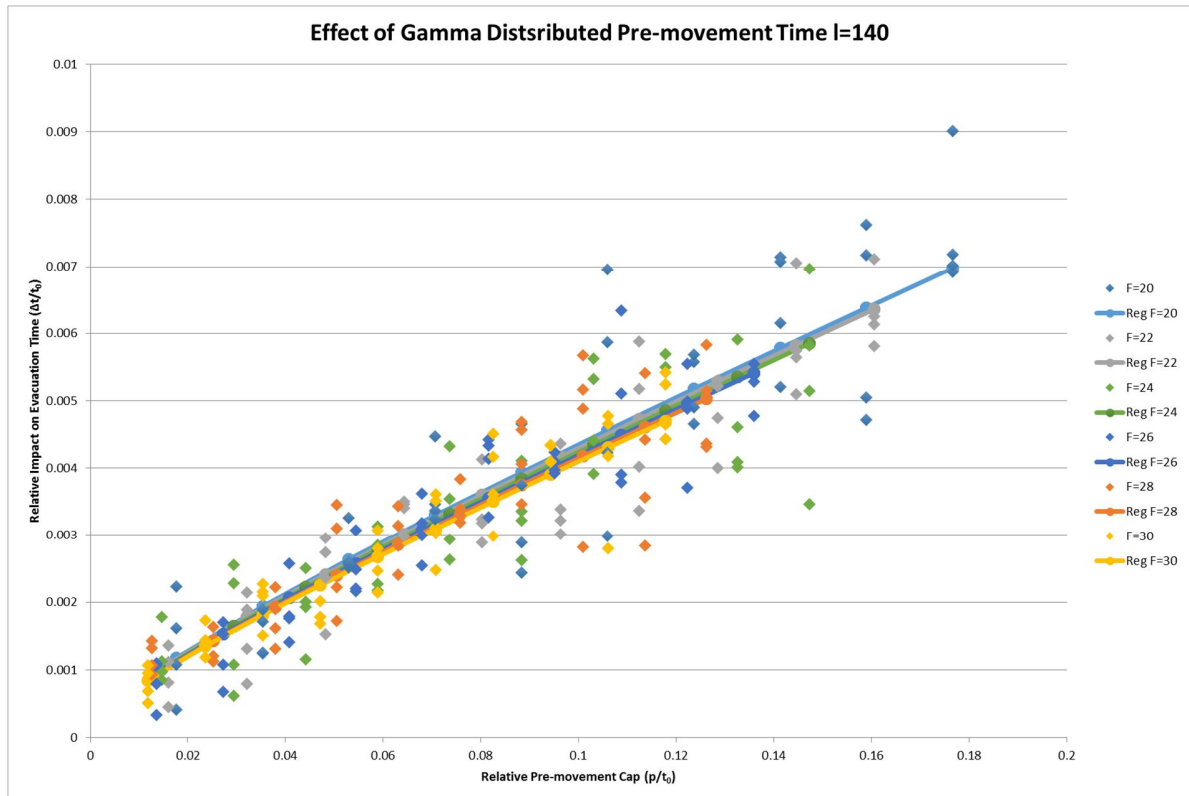


Figure 4.2.19 – GPM Results with High Order Regression ($f=20$ to 30 , $l=140$)

4.2.3 GPM Results with High Order Regression – Extended Case Studies

The results of section 4.2.2 show that the expression (16) describes the effect of pre-movement time as a relationship between loading, number of floors, and pre-movement time relatively well, with R^2 values in Figures 4.2.9 to 4.2.13 ranging from 0.846 to 0.890. In order to determine if this relationship exists beyond the primary cases, additional simulations were performed with l and f parameter values outside of those used for the primary case studies as was done for the UPM analysis.

Low Loading

As was done with the UPM review, a group of extended case studies was reviewed with loading, l , taking values less than the 80 people per floor. Extended cases were simulated for parameter values as follows:

- $l=20, 40, 60$
- $f=20, 22, 24, 26, 28, 30$

A sample of results are shown in Figures 4.2.20 to 4.2.23. As was seen for the UPM case studies, there is good correlation for many of the extended short building trials. However, where p/t_0 approaches or exceeds 1, there are some obvious results which are not well estimated by the regression equation (16).

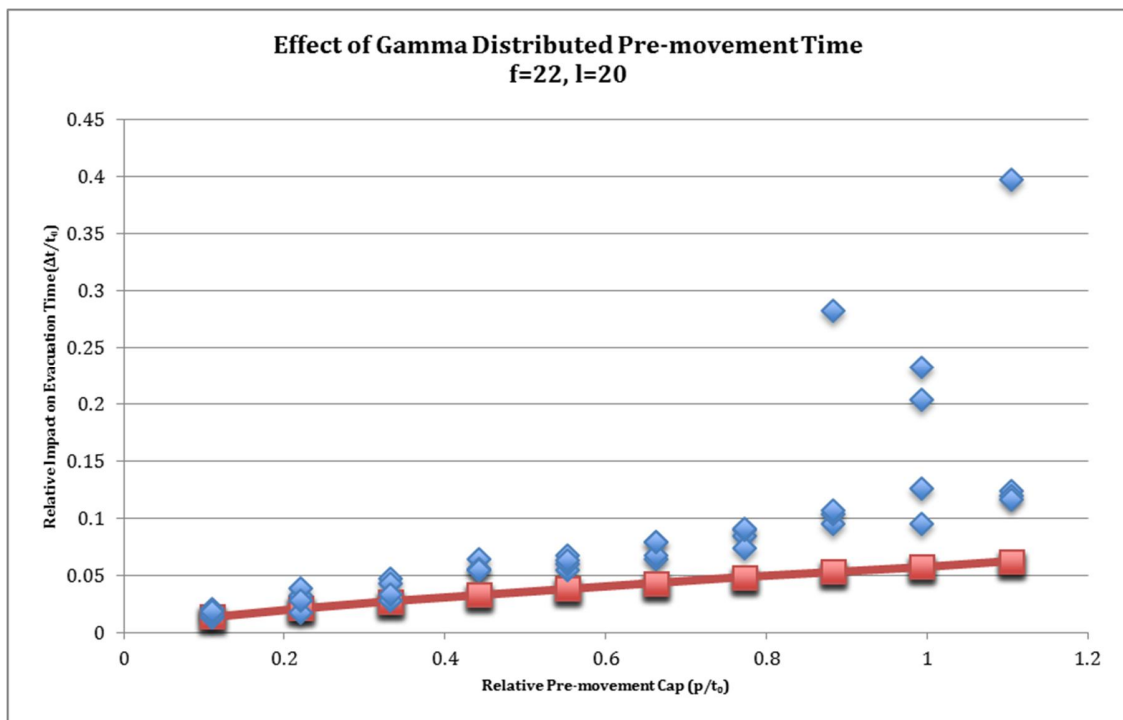


Figure 4.2.20 – GPM High Order Regression Applied to Extended Case Study
(f=22, l=20), $R^2=-0.131$

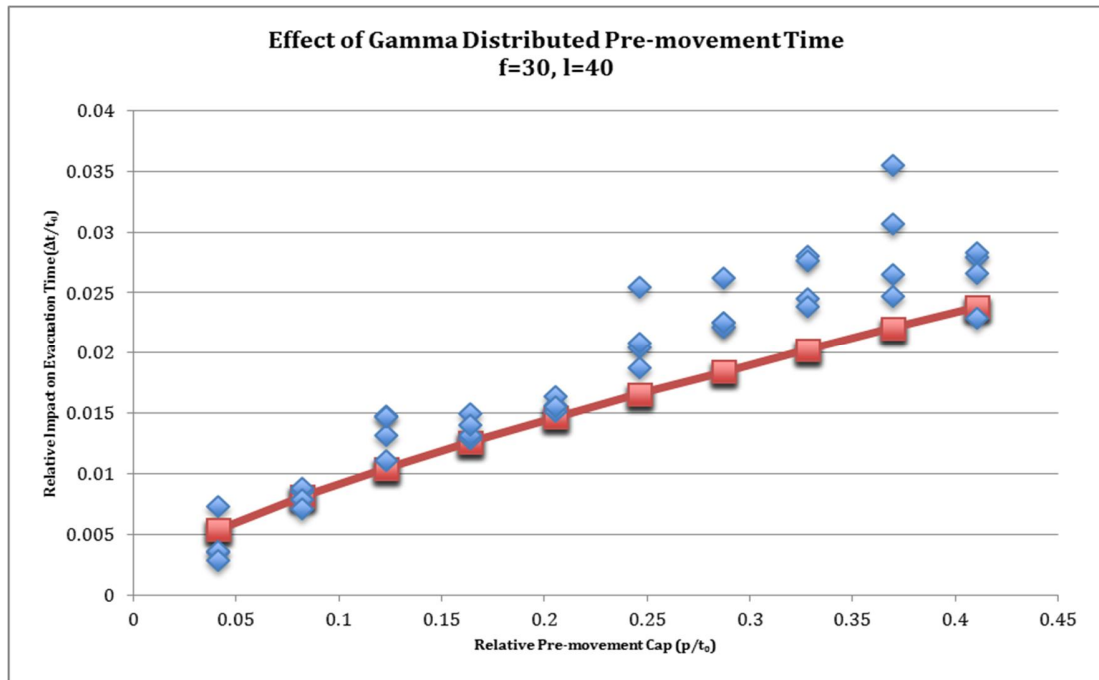


Figure 4.2.21 – GPM High Order Regression Applied to Extended Case Study
($f=30, l=40$), $R^2=0.715$

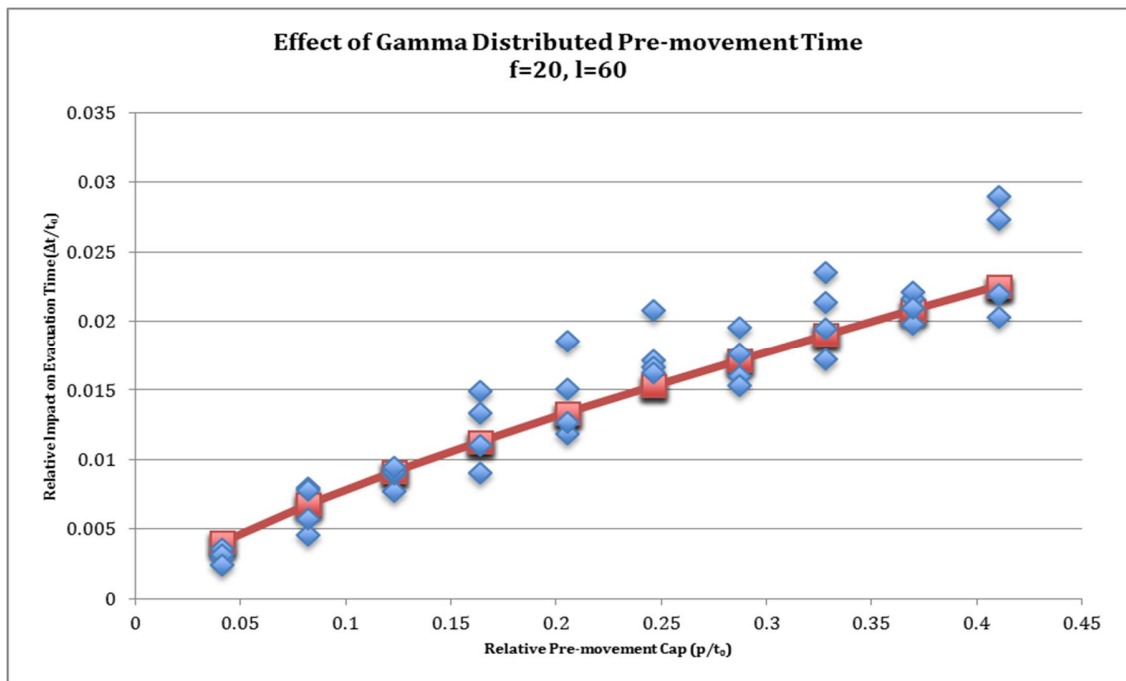


Figure 4.2.22 – GPM High Order Regression Applied to Extended Case Study
($f=20, l=60$), $R^2=0.883$

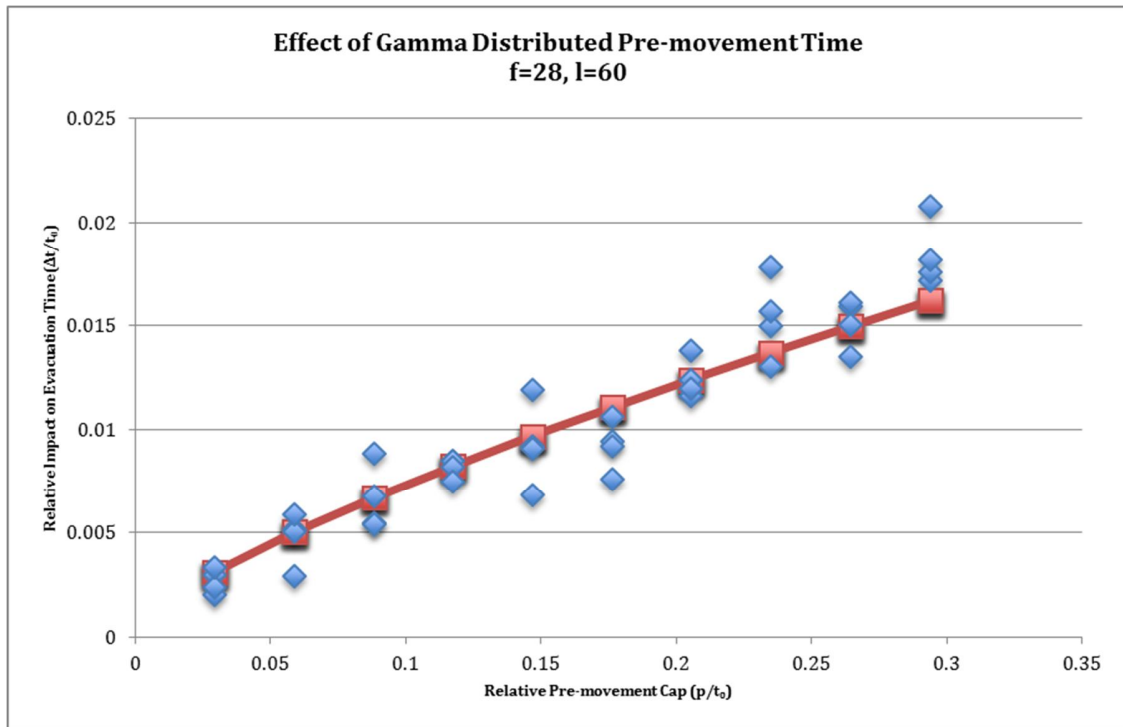


Figure 4.2.23 – GPM High Order Regression Applied to Extended Case Study
($f=28$, $l=60$), $R^2=0.892$

Short Buildings

As was done for the UPM review, the high order regression equation (16) was also extended to a group of case studies representing shorter buildings than the primary case studies. For these extended cases, simulations were performed for parameter values as follows:

- $l=20, 40, 60, 80, 100, 120, 140$
- $f=5, 10, 15,$

For these cases, low loading was also included, to account for buildings which could be not only shorter but also less populated.

As was described for the UPM results, the values of t_0 for the short buildings modeled (and particularly for short buildings with low occupant loads) were significantly smaller than results for the primary case studies. Thus, as was the case

for the UPM data, pre-movement caps for this set of simulations were reduced to be 3000 cs (0.5 minute), 6000 cs, (1 minute), 9000 cs (1.5 minutes), ... 30,000cs (5 minutes) to avoid obvious impacts of large pre-movement.

A sample of results is shown in Figures 4.2.24 to 4.1.26. In general, the expression (16) fits well with the data, except in instances of obvious large effects of pre-movement when p/t_0 approaches or exceeds 1 (not shown in the figures below).

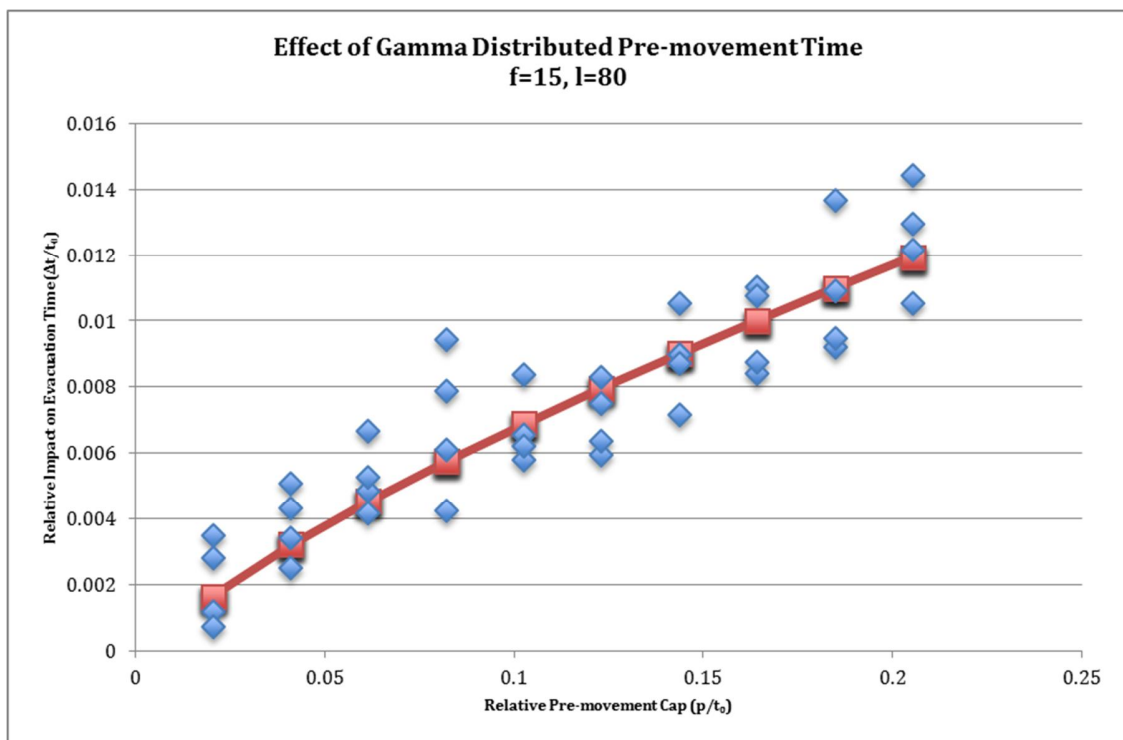


Figure 4.2.24 – GPM High Order Regression Applied to Extended Case Study
($f=15, l=80$), $R^2=0.813$

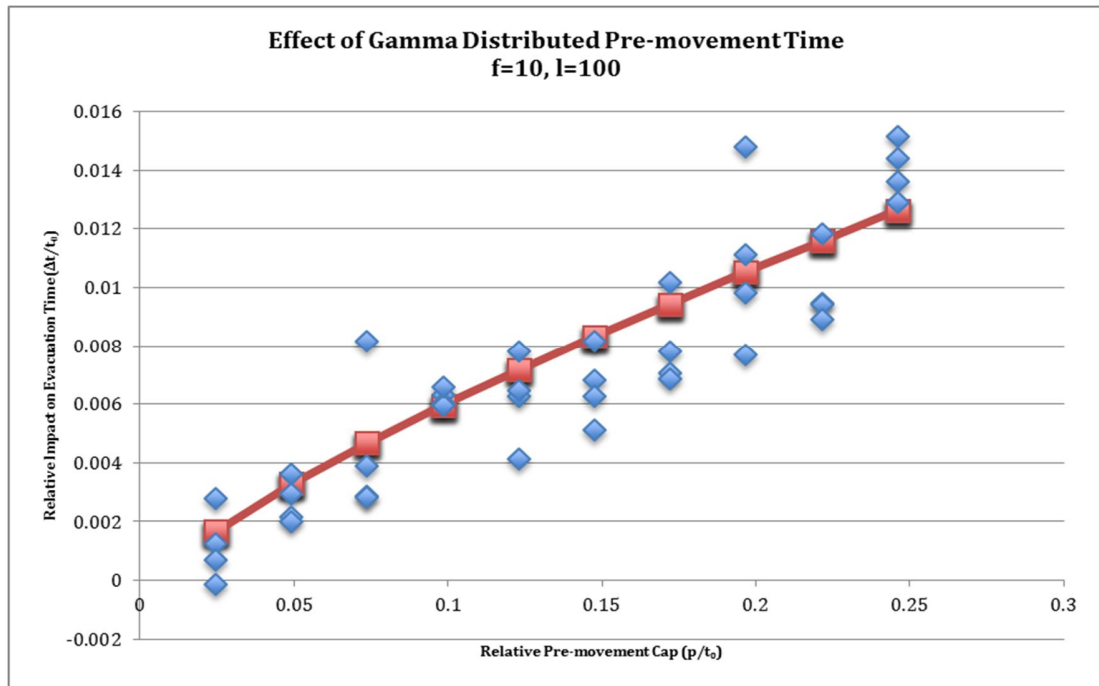


Figure 4.2.25 – GPM High Order Regression Applied to Extended Case Study
(f=10, l=100), $R^2=0.796$

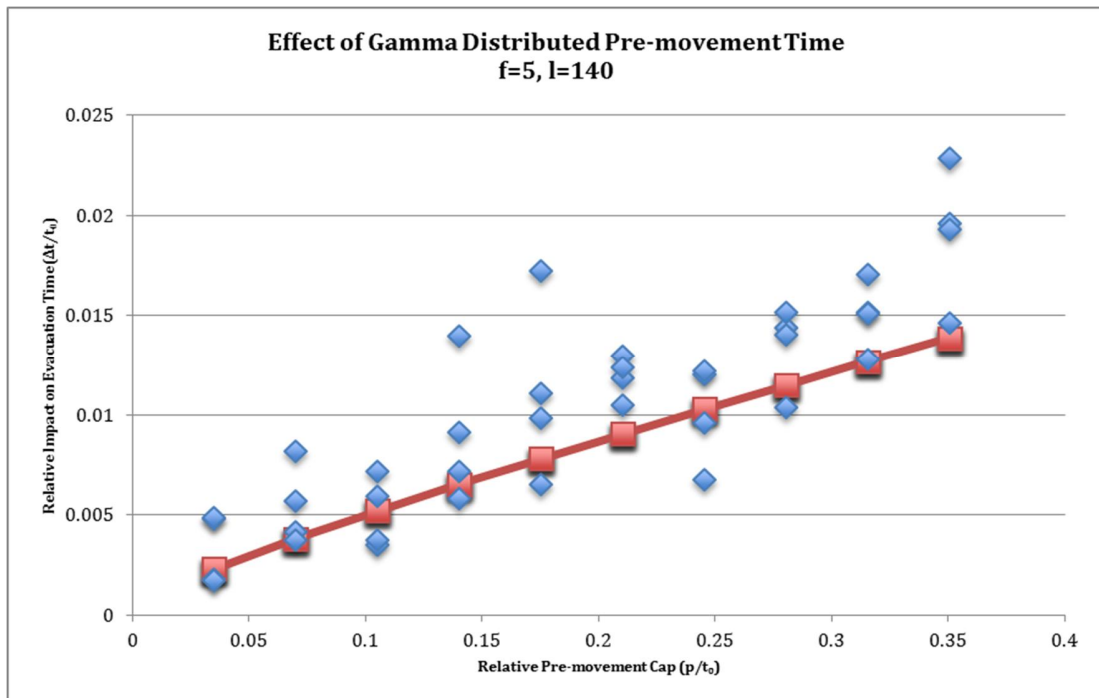


Figure 4.2.26 – GPM High Order Regression Applied to Extended Case Study
(f=5, l=140), $R^2=0.556$

Tall Buildings

The equation (16) was also extended to a group of extended case studies representing taller building than the primary case studies, as was done for the UPM cases. For these extended cases, simulations were performed for parameter values as follows:

- $l=20, 60, 100, 140$
- $f=40, 50, 60$

As was noted in Section 4.1.3, due to the extended running time of the simulation for buildings of this size, fewer evacuations of these tall building cases were simulated, with only five sample pre-movement time intervals, for $p = 6000cs$ (1 minute), 18,000cs (3 minutes), 30,000cs (5 minutes), 42,000cs (7 minutes) and 54,000cs (9 minutes).

Sample results are shown below in Figures 4.2.27 to 4.2.29. It is noted that for many of the buildings, the expression (16) provided a reasonable fit. Even for the extreme case in Figure 4.2.29 where $f=60$ and $l=140$ (the largest, most heavily occupied building that was simulated) the regression expression fits the simulated results with reasonable accuracy.

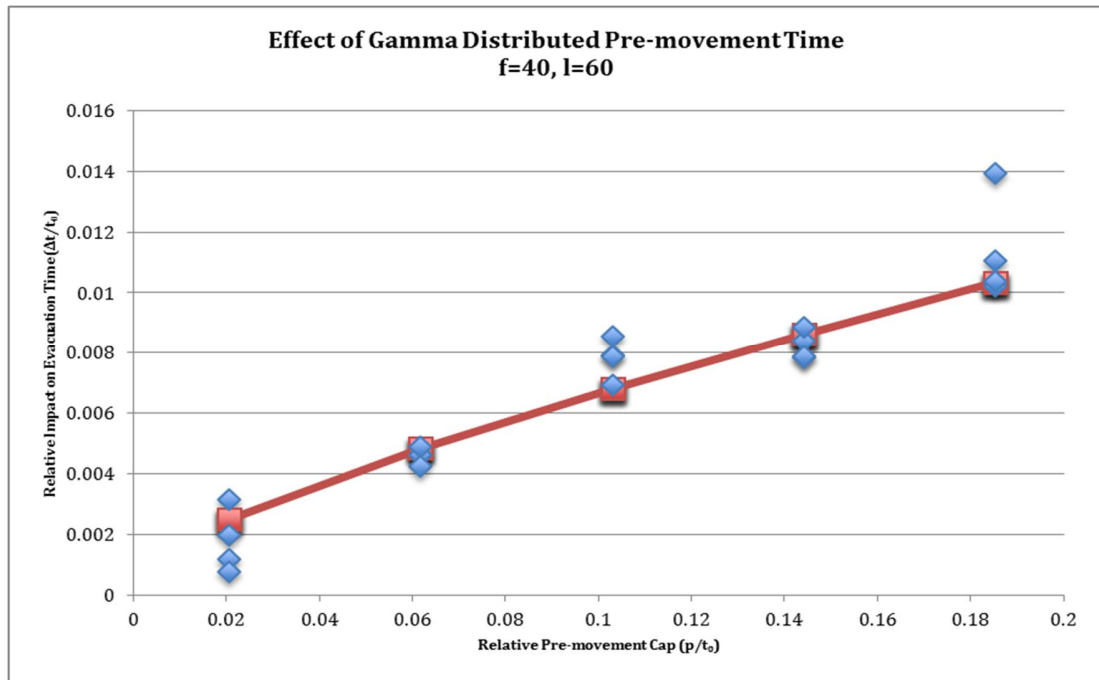


Figure 4.2.27 – GPM High Order Regression Applied to Extended Case Study
($f=40, l=60$), $R^2=0.889$

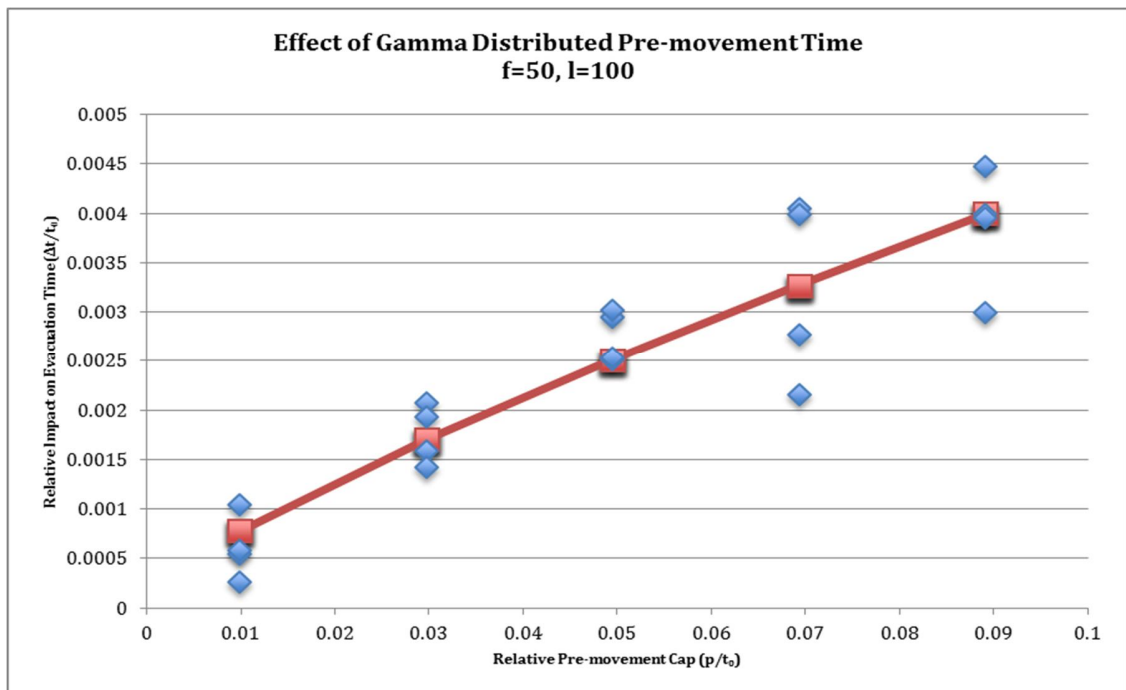


Figure 4.2.28 – GPM High Order Regression Applied to Extended Case Study
($f=50, l=100$), $R^2=0.837$

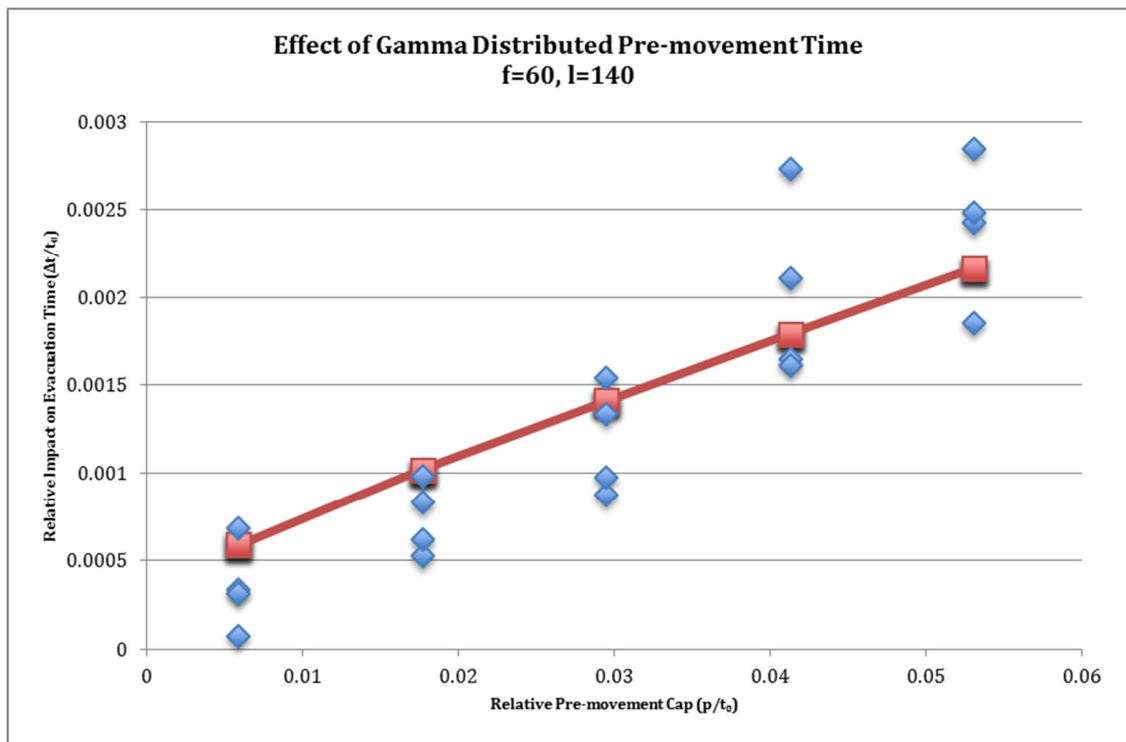


Figure 4.2.29 – GPM High Order Regression Applied to Extended Case Study
(f=60, l=140), $R^2=0.774$

5.0 CONCLUSIONS

The regression analyses noted in Section 4, and in particular the high order regression analysis of 4.1.2 and 4.2.2 indicated that there is a relationship between the relative effects of pre-movement and the values of l , f , and p . Simulation results for both UPM and GPM cases indicated that for fixed f values, the effect of pre-movement decreased for increasing values of l , whereas for cases with fixed l , the effects of pre-movement remain relatively constant for increasing values of f . This trend was shown in the high order regression equations (14) and (16).

These equations were able not only to provide a good fit for the data of the primary cases (R^2 values ranging between 0.817 and 0.912 for UPM example results shown, and between 0.846 and 0.890 for GPM example results shown), but could also be extended to other building cases (low loading, short buildings, and tall buildings) and predict the results with reasonable accuracy.

The results of this analysis indicate that it is possible to estimate the relative effect of pre-movement time for a high building evacuation when the loading, number of floors, and estimated pre-movement range are known. As shown by the extended case studies, for loading and building size conditions beyond the case studies, the expressions (14) and (16) can still yield a fairly high degree of accuracy.

The primary results of this analysis indicate that, while pre-movement time has an effect that can be measured and predicted by expressions (14) or (16), the effects of the pre-movement are often very small.

For UPM results, primary case studies for pre-movement ranges up to 10 minutes indicated that effects of pre-movement were only as much as a 2% impact on the total evacuation time. For some of the extended case studies (particularly short buildings and low loading), effects of UPM pre-movement approached as much as 7%. However, the UPM distribution was selected more for its potential to yield

mathematically interesting results than for its reflection of realistic conditions during an emergency. Therefore, while it revealed a more pronounced pattern of decreasing impact of pre-movement with increasing loading or increasing number of floors, GPM results provide a better reflection of real conditions which could be used in engineering analyses.

For GPM results, generally smaller effects were noted than for the UPM cases. Primary case studies consistently indicated that impacts of pre-movement time, even for the largest distributions with $p = 10$ minutes, the impact was less than 2% at most, and often less than 1%. Even in extended case studies, impacts of less than 5% were noted for all cases.

This information could be useful in the field of engineering, where safety factors much greater than 1%, 2% or 5% are often applied. Depending on building characteristics and the factor of safety selected for an analysis, pre-movement time may be entirely negligible. Rather than proceed with complicated calculations involving changing flow rates and densities, or relying on often time-consuming and expensive software programs to accurately account for pre-movement time, the regression expression (16) developed for this thesis can estimate the effects of pre-movement relatively well. For specific engineering analyses where comparatively large factors of safety are used, this analysis could be used to indicate that the effects of pre-movement may in fact be negligible in some cases.

Furthermore, the results of this thesis indicate that the common industry practice of adding a value of mean pre-movement time to the movement would likely overestimate the effects of pre-movement. As an example, for a 20 storey building with loading of 80 people per floor and, the effect of GPM with cap $p=10$ minutes is estimated to be 0.75 minutes based on equation (16) and the previously calculated movement time $t_0=32.42$ minutes. However, the mean pre-movement time for this distribution would be approximately 1.679 minutes, so adding 1.679 minutes to the evacuation time would more than double the estimated effect of pre-movement. As

pre-movement time has been shown to have a diminishing effect for increased loading, the error of this practice increase for cases of higher loading.

Therefore, the results of this thesis provide yet another tool that can be used with engineering judgement to quickly estimate building evacuation times to the required degree of accuracy.

6.0 FURTHER RESEARCH

There are several areas where additional research can be performed regarding the effects of pre-movement time on evacuations. In particular, this effort reviewed specifically tall buildings with relatively high occupant loads evacuating simultaneously. In reality, a building of 20 or 30 storeys in height built in accordance with NBC requirements would evacuate in phases, with occupants on the fire floor (i.e. the floor on which fire was detected) getting priority and evacuating before occupants on other floors. It is uncertain if pre-movement times would yield the same type of impact on overall evacuation time for phased evacuations. This algorithm could be easily adapted to simulate evacuations with phasing. However, additional research and consideration would be required in order to determine the best method for comparing various strategies for evacuation phasing.

Furthermore, a similar review could be conducted with pre-movement time distributions other than the two types selected for this review. As noted in Section 3.4, no distribution can perfectly predict human behavior in an emergency. Therefore, examining a range of alternative pre-movement time distributions would be useful. In particular, normal distribution of pre-movement times centered around some specific mean might yield different results from the UPM and GPM trials reviewed here.

Lastly, a similar analysis could be performed examining building geometry in addition to the l , f , and p variables reviewed here. This analysis assumed fixed stair and door dimensions for all simulations. As these dimensions often differ from building to building, it would be useful to perform a similar analysis using varied escape route geometry.

7.0 REFERENCES

- [1] National Research Council Canada (2011). *National Building Code of Canada 2010*, National Research Council Canada.
- [2] National Fire Protection Association (2011). *NFPA 101 Life Safety Code 2012 Edition*, American National Standards Institute
- [3] British Standards Institutions (2008). *Code of practice for fire safety in the design, management and use of buildings*, British Standards Institutions
- [4] Wolski, A., Dembsey, N. A., & Meacham (2000). Accommodation perceptions of risk in performance-based building fire safety code development. *Fire Safety Journal, Volume 34*, 297-309
- [5] [PD01] Kobes, M., Helsloot I., de Vries, B., & Post, J. G. (2010). *Fire Safety Journal, Volume 45*, 1-11
- [6] Galbreath, M. (1984). Canadian Experience of Fire Safety in High Buildings. *Fire Safety Journal, Volume 7*, 87-91
- [7] Miller, G. R. (1984). Building Codes and Smoke Control. *Fire Safety Journal, Volume 7*, 99-106
- [8] Tavares, R. M. (2009). Evacuation Processes Versus Evacuation Models: “Quo Vadimus”?, *Fire Technology, Volume 45*, 419-430
- [9] British Standards Institutions (2004). *Published Document 7974-6:2004 The application of fire safety engineering principles to fire safety design of buildings*, Standards Policy and Strategy Committee
- [10] Proulx, G. (2008). Evacuation Time. In DiNenno, P. J., Drysdale, D., Beyler, C. L., Walton, W. D., Custer, R. L. P., Hall, J. R. Jr., & Watts, J. M. Jr. (Eds) *SFPE Handbook of Fire Protection Engineering* (Section 3 pp 355 – 372). Bethesda, Maryland: Society of Fire Protection Engineers
- [11] Gwynne, S. M. V., & Rosenbaum, E. R. (2008). Employing the Hydraulic Model in Assessing Emergency Movement. In DiNenno, P. J., Drysdale, D., Beyler, C. L., Walton, W. D., Custer, R. L. P., Hall, J. R. Jr., & Watts, J. M. Jr. (Eds) *SFPE Handbook of Fire Protection Engineering* (Section 3 pp 373 – 396). Bethesda, Maryland: Society of Fire Protection Engineers
- [12] Ramachandran, G. (2008). Stochastic models of fire growth, In DiNenno, P. J., Drysdale, D., Beyler, C. L., Walton, W. D., Custer, R. L. P., Hall, J. R. Jr., & Watts, J. M. Jr. (Eds) *SFPE*

Handbook of Fire Protection Engineering (Section 3 pp 397-417). Bethesda, Maryland: Society of Fire Protection Engineers

[13] Jin, T. (2008). Visibility and Human Behavior in Fire Smoke, In DiNenno, P. J., Drysdale, D., Beyler, C. L., Walton, W. D., Custer, R. L. P., Hall, J. R. Jr., & Watts, J. M. Jr. (Eds) *SFPE Handbook of Fire Protection Engineering* (Section 2 pp 54-66). Bethesda, Maryland: Society of Fire Protection Engineers

[14] Gottuk, D. T., & Lattimer, B. Y. (2008). Effects of Combustion Conditions on Species Production, In DiNenno, P. J., Drysdale, D., Beyler, C. L., Walton, W. D., Custer, R. L. P., Hall, J. R. Jr., & Watts, J. M. Jr. (Eds) *SFPE Handbook of Fire Protection Engineering* (Section 2 pp 67-95). Bethesda, Maryland: Society of Fire Protection Engineers

[15] Purser, D. A. (2008). Assessment of Hazards to Occupants from Smoke, Toxic Gases, and Heat, In DiNenno, P. J., Drysdale, D., Beyler, C. L., Walton, W. D., Custer, R. L. P., Hall, J. R. Jr., & Watts, J. M. Jr. (Eds) *SFPE Handbook of Fire Protection Engineering* (Section 2 pp 96-103). Bethesda, Maryland: Society of Fire Protection Engineers

[16] Purser, D. A., & Bensilum, M. (2001). Quantification of behaviour for engineering design standards and escape time calculations. *Safety Science, Volume 38*, 157-182

[17] Guanquan C., & Jinhua, S. (2005). The Effect of Pre-movement Time and Occupant Density on Evacuation Time. *State Key Laboratory of Fire Science, University of Science and Technology of China*

[18] Graham, T. L. & Roberts, D. J. (2000). Qualitative overview of some important factors affecting the egress of people in hotel fires. *International Journal of Hospitality Management, Volume 19*, 79-87

[19] Gwynne, S., Galea, E. R., Owen, M., Lawrence, P. J., & Flippidis, L. (1999), A review of the methodologies used in the computer simulation of evacuation from the built environment.

[20] Olsson, P. A. & Regan, M. A. (2001). A comparison between actual and predicted evacuation times. *Safety Science, Volume 38*, 139-145

APPENDICES

Appendix A – UPM Primary Case Studies with Linear Regression

Appendix B – UPM Primary Case Studies with High Order Regression

Appendix C – UPM Extended Case Studies with High Order Regression – Low Occupant Loads

Appendix D – UPM Extended Case Studies with High Order Regression – Short Buildings

Appendix E – UPM Extended Case Studies with High Order Regression – Tall Buildings

Appendix F – GPM Primary Case Studies with Linear Regression

Appendix G – GPM Primary Case Studies with High Order Regression

Appendix H – GPM Extended Case Studies with High Order Regression – Low Occupant Loads

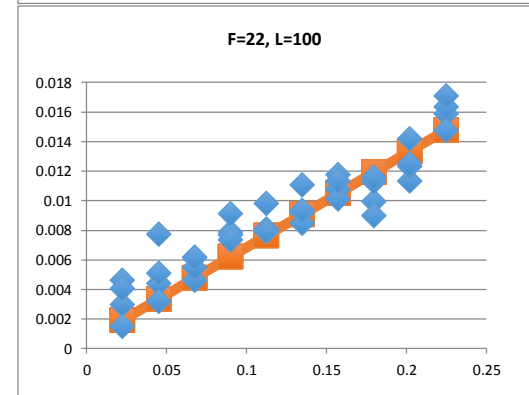
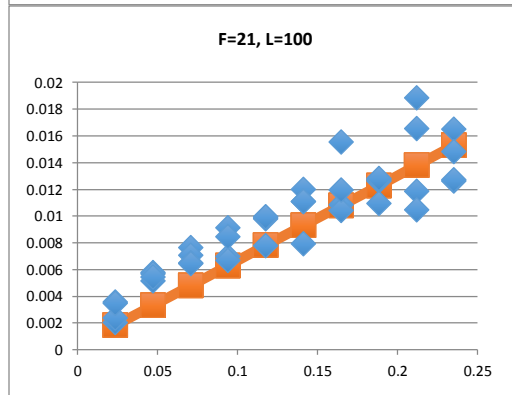
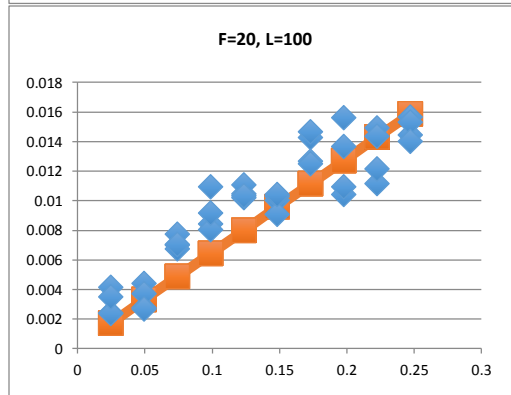
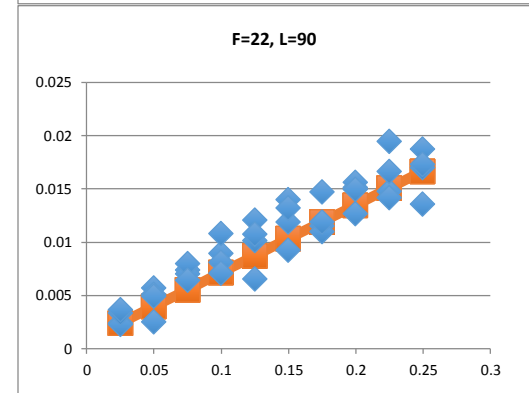
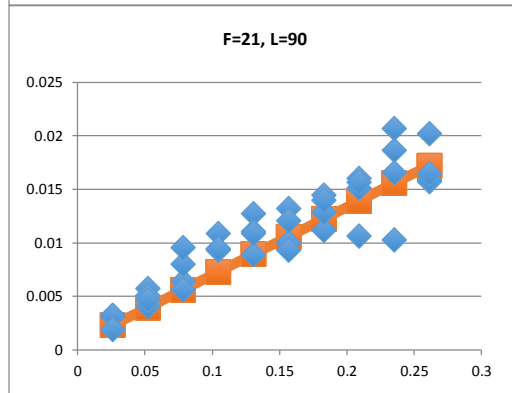
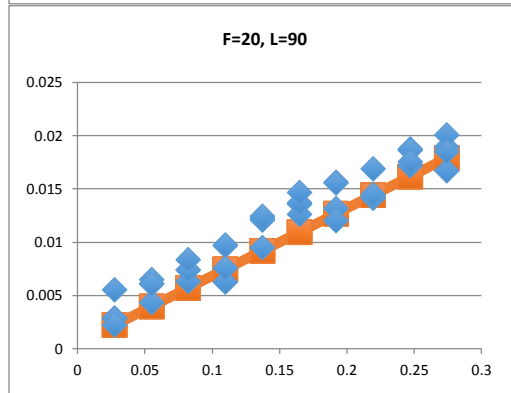
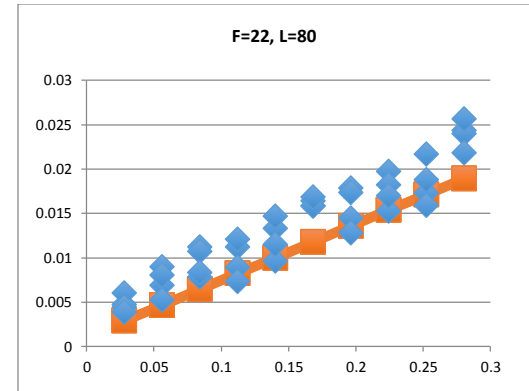
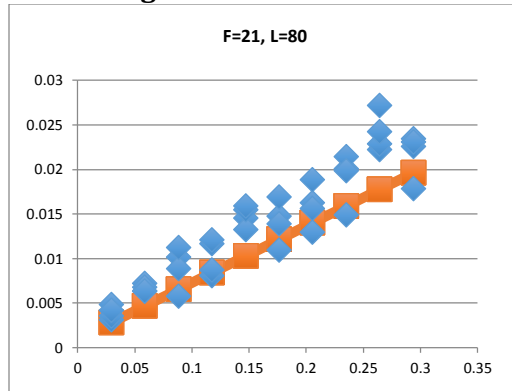
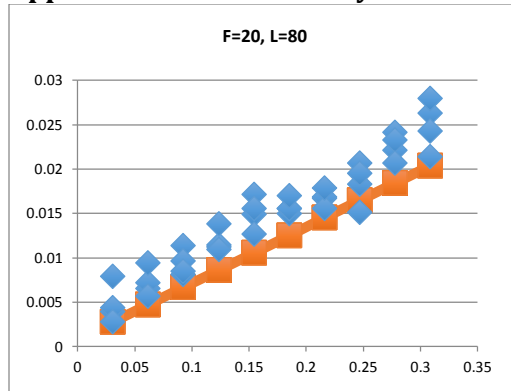
Appendix I – GPM Extended Case Studies with High Order Regression – Short Buildings

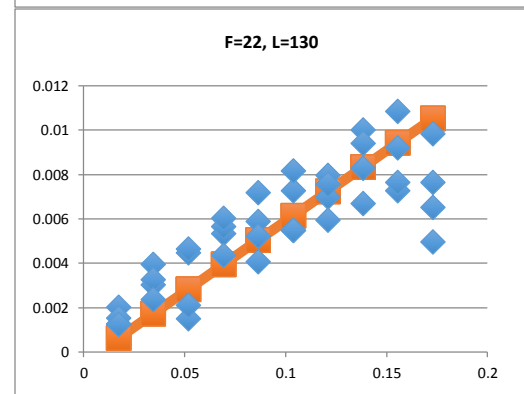
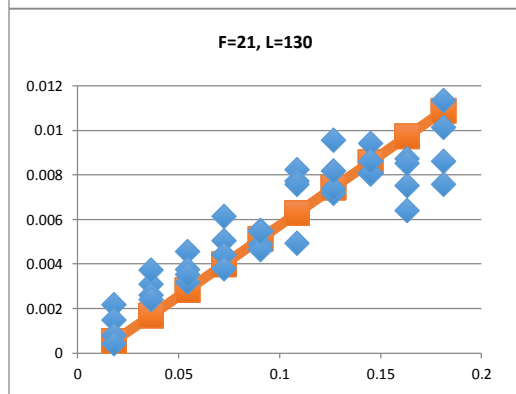
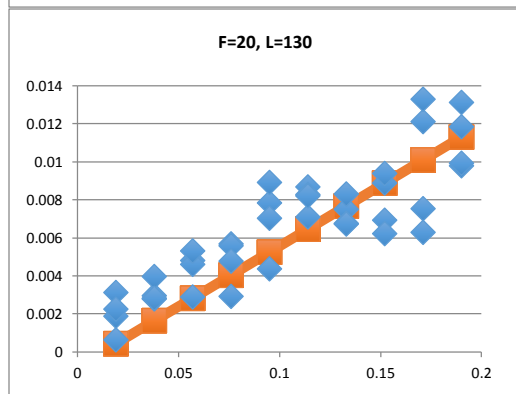
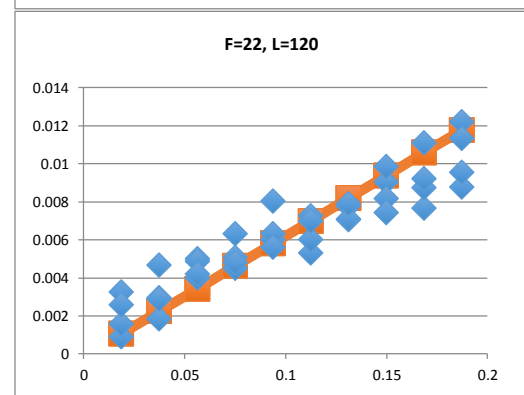
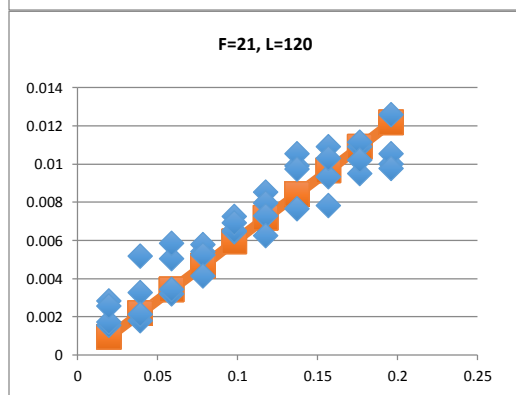
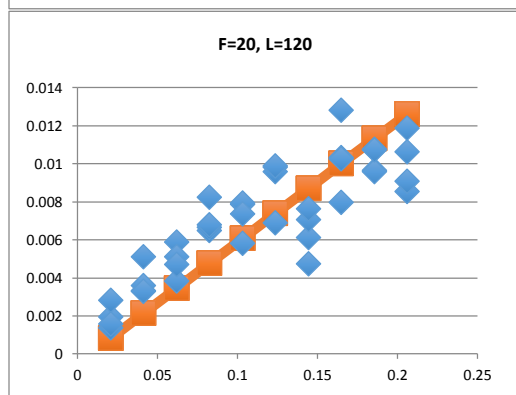
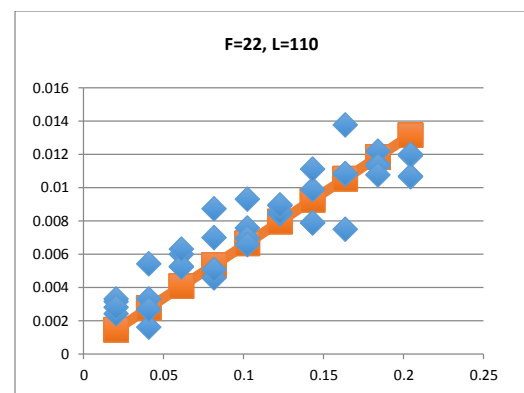
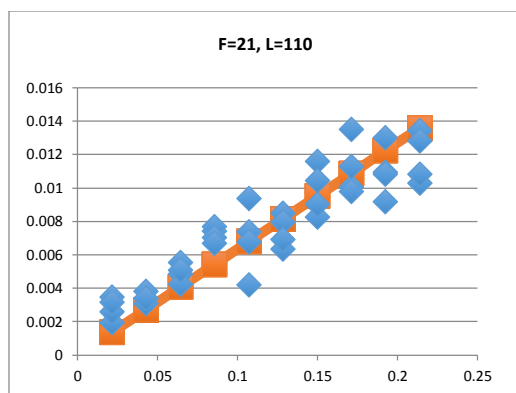
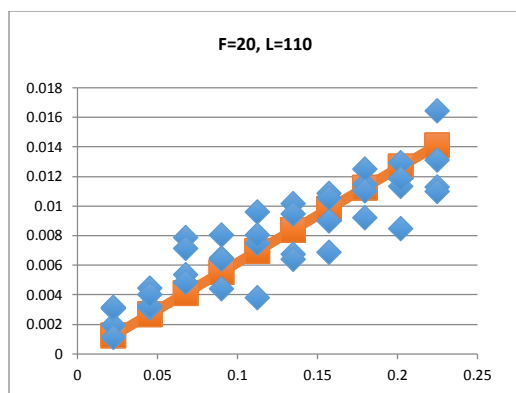
Appendix J – GPM Extended Case Studies with High Order Regression – Tall Buildings

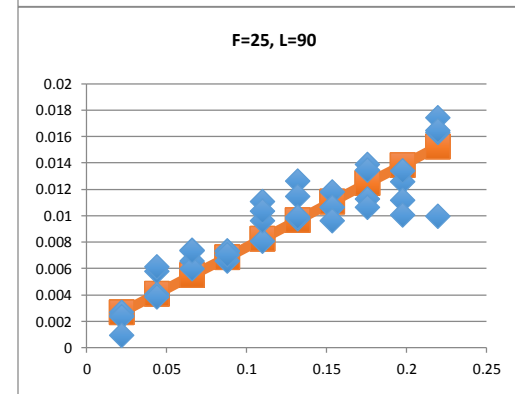
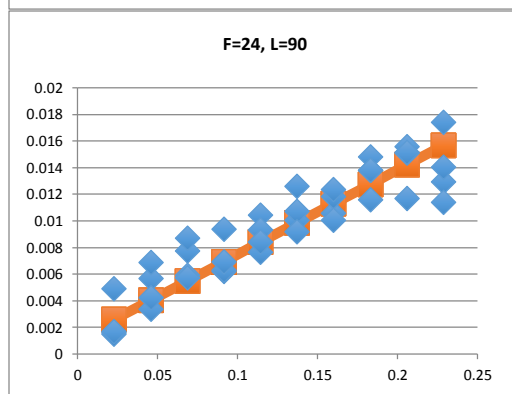
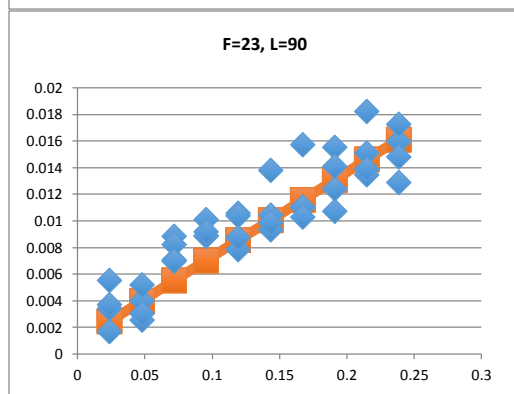
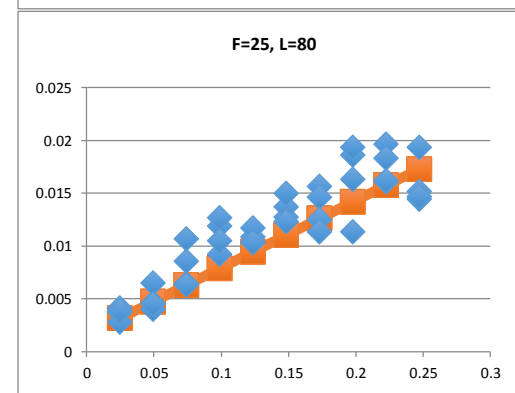
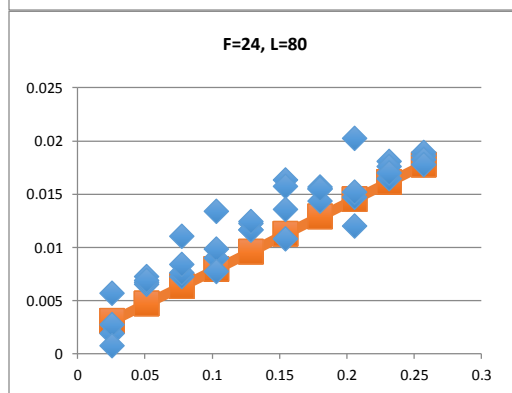
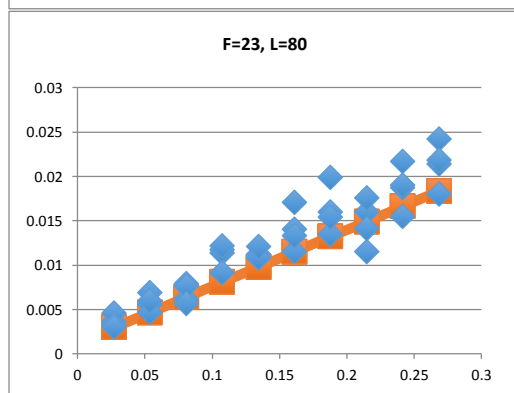
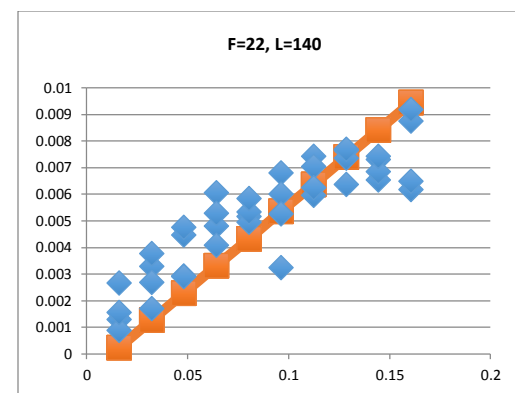
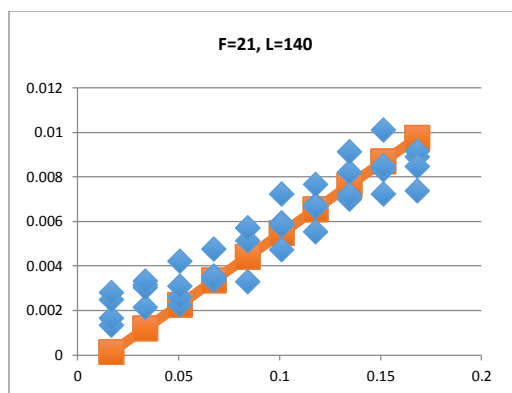
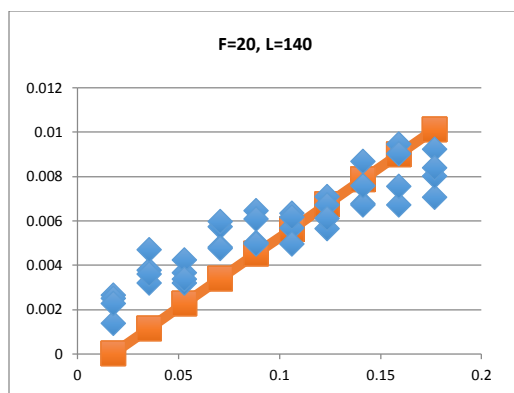
Note:

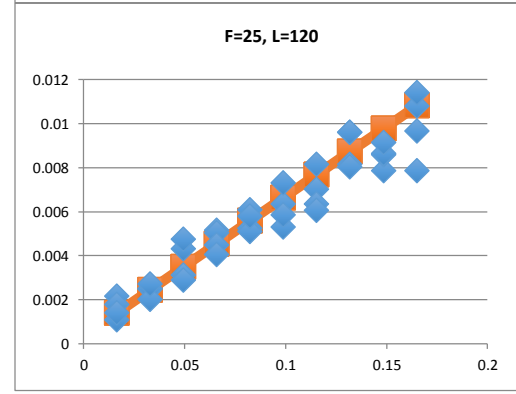
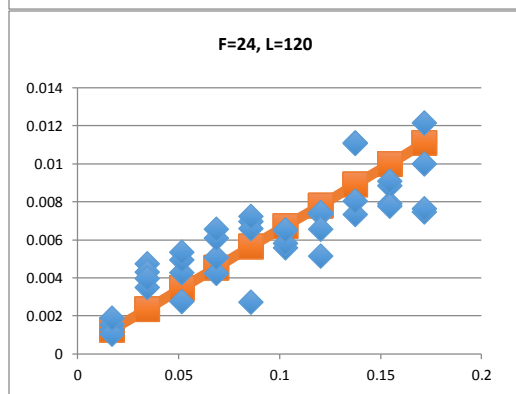
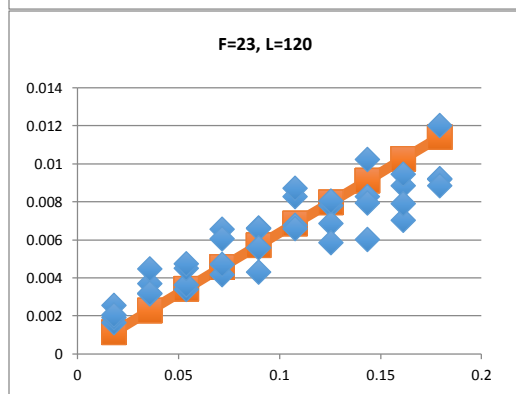
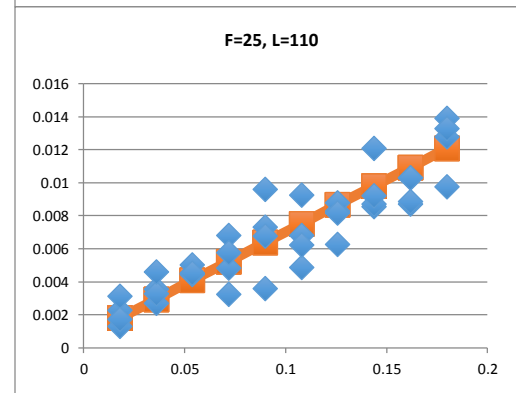
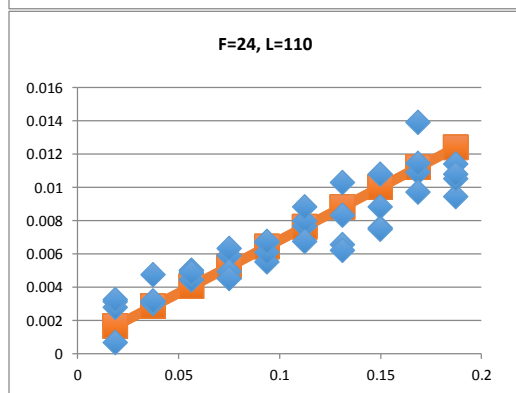
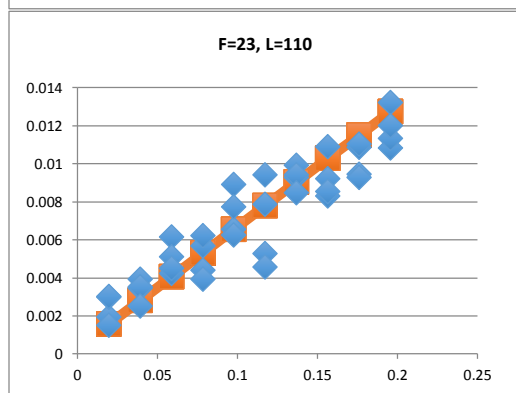
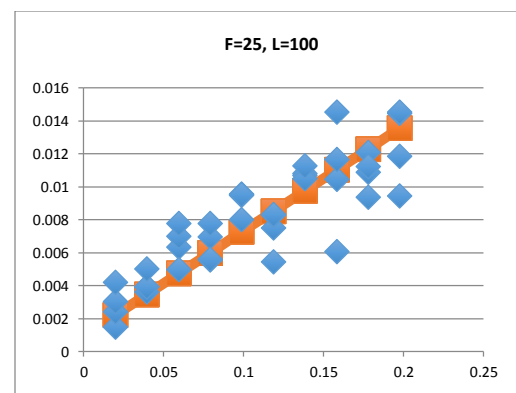
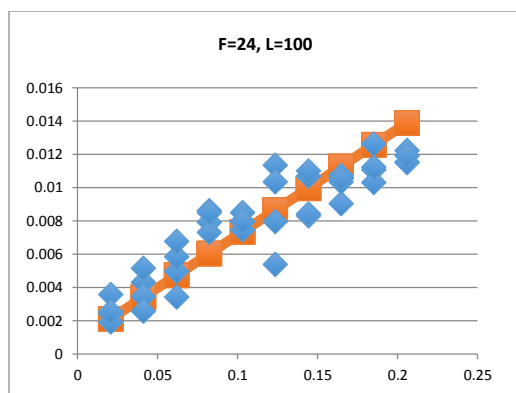
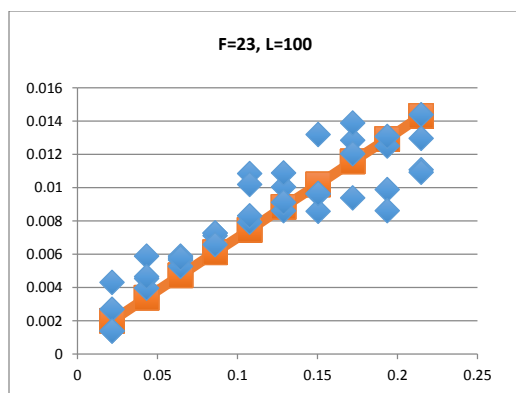
Appendix plots show simulation results with relative pre-movement time cap (p/t_0) along the horizontal axis, and relative difference of total evacuation time ($\Delta t/t_0$) along the vertical axis. Plots are labelled with the number of floors as “F” and the loading per floor level as “L”.

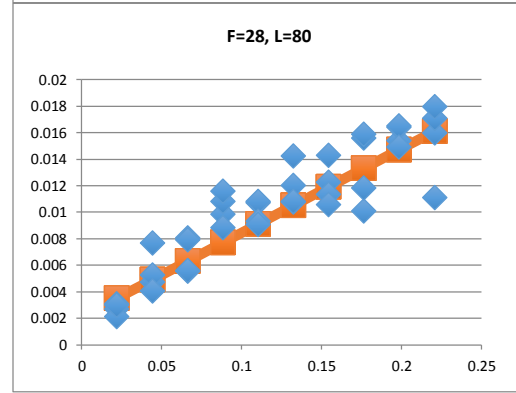
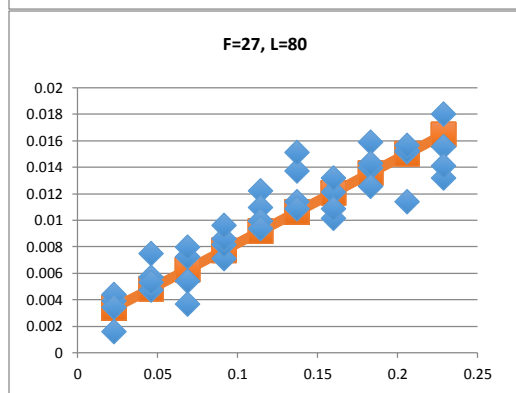
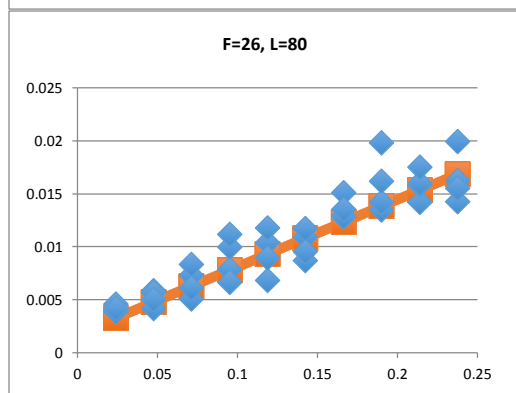
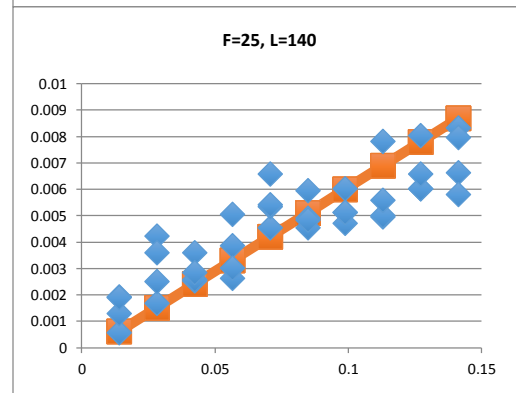
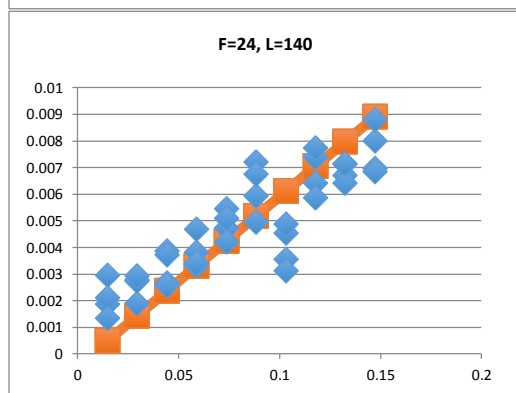
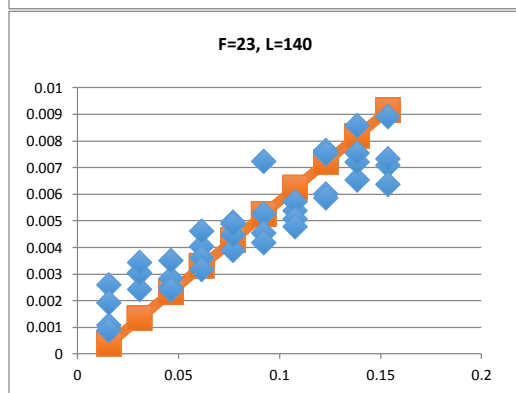
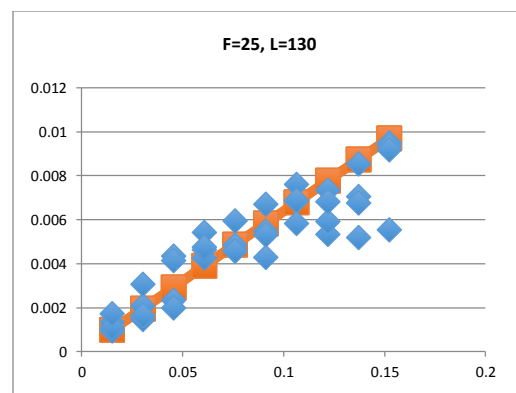
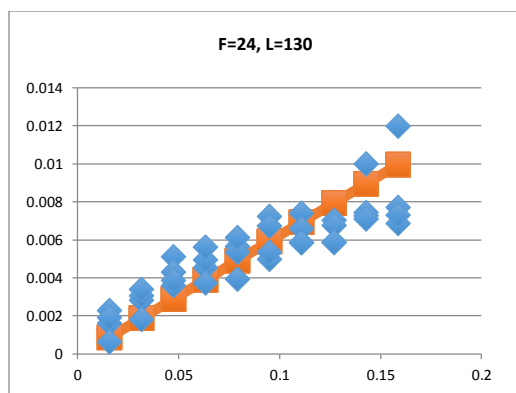
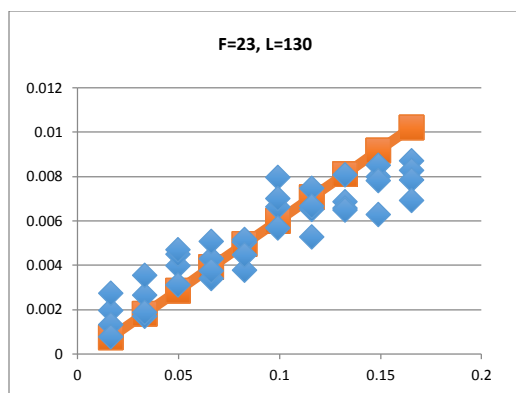
Appendix A – UPM Primary Case Studies with Linear Regression

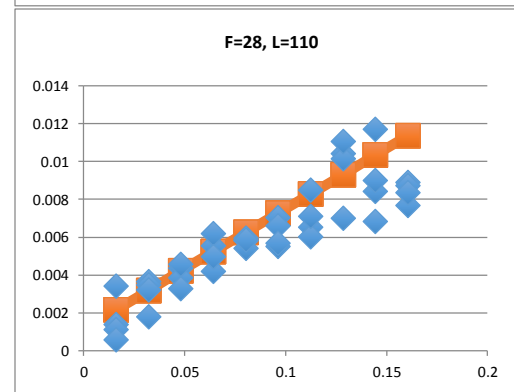
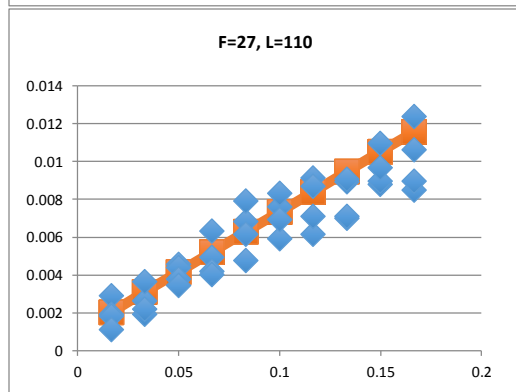
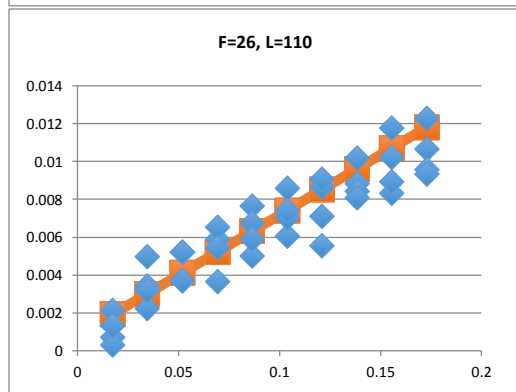
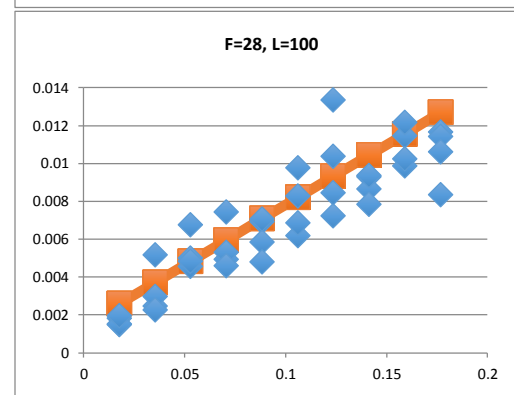
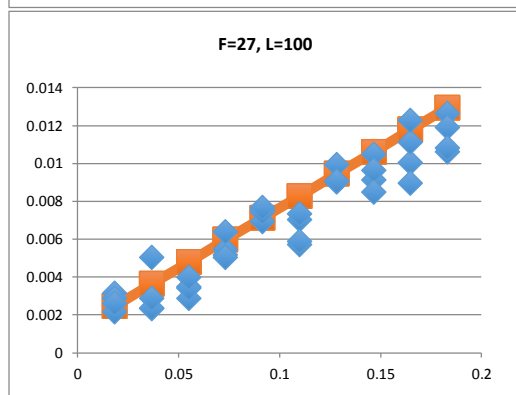
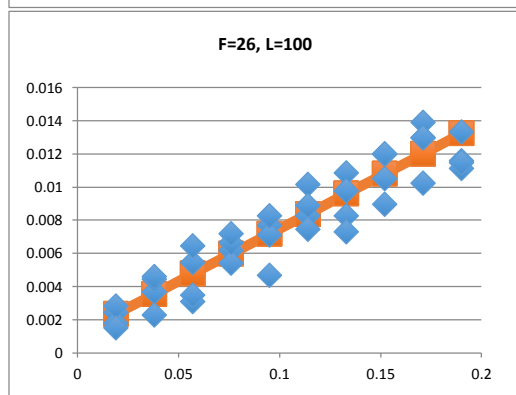
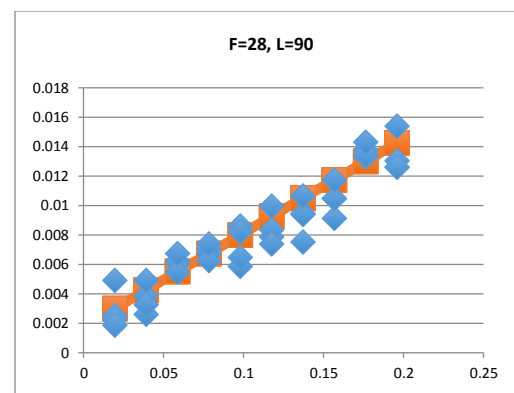
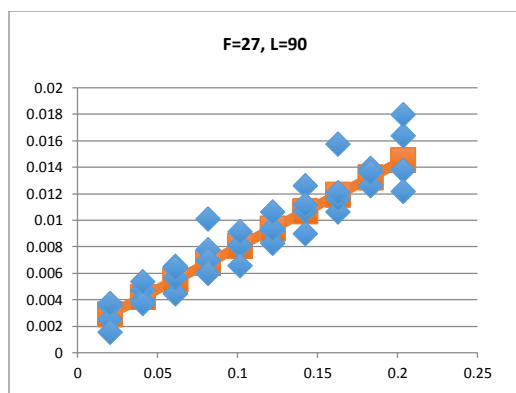
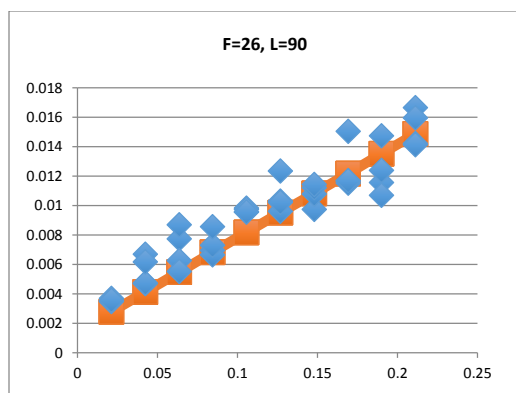


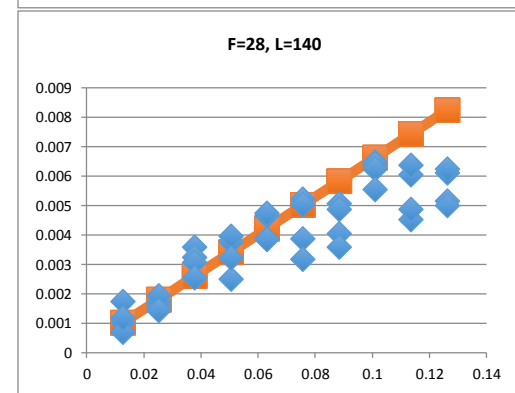
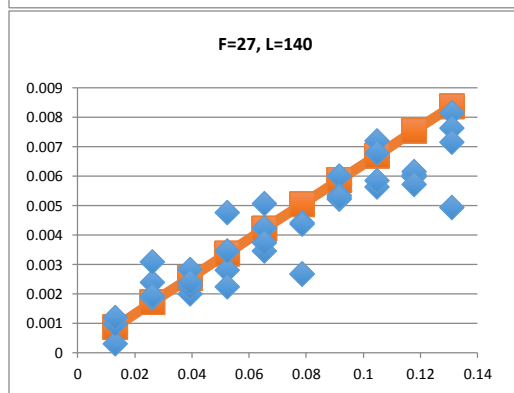
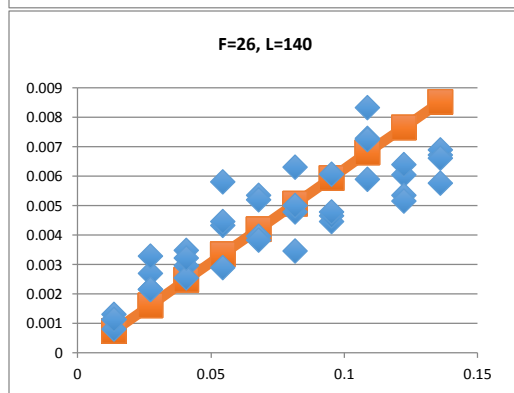
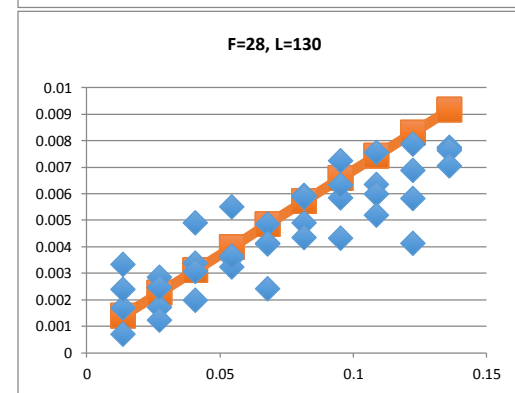
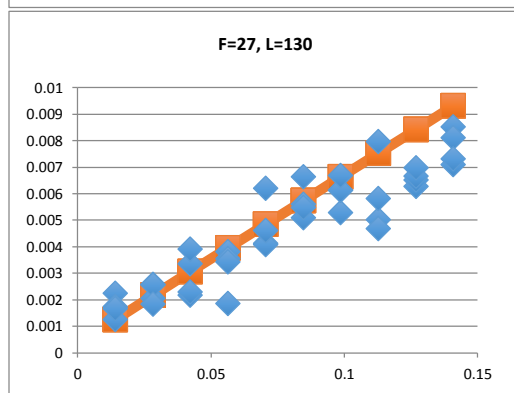
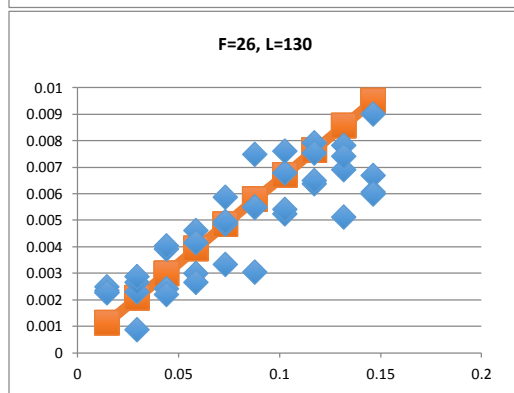
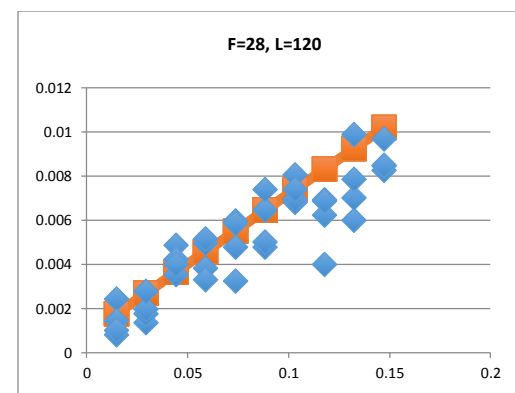
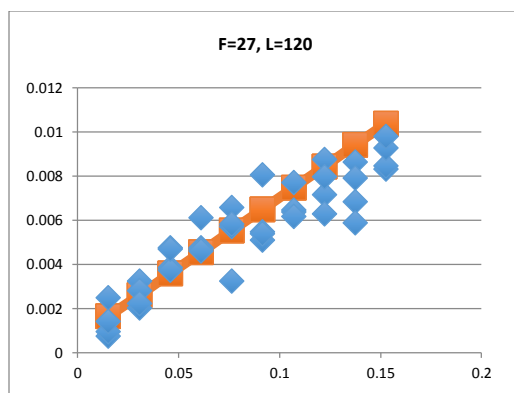
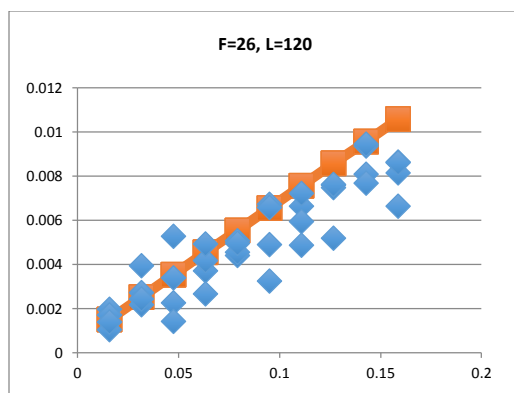


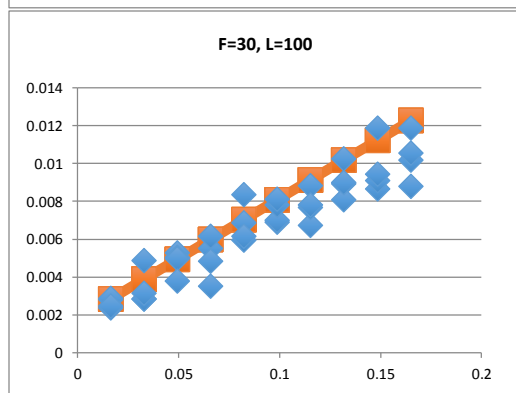
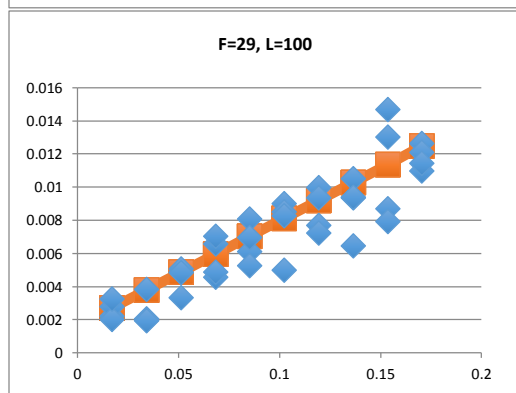
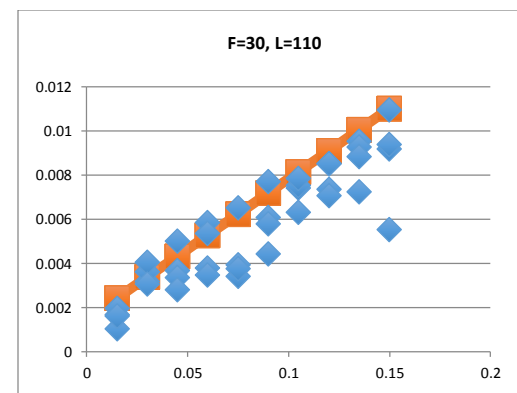
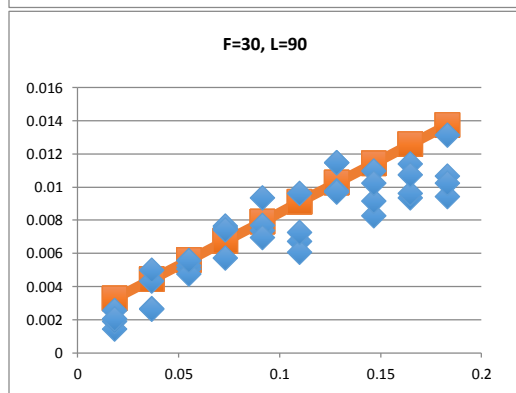
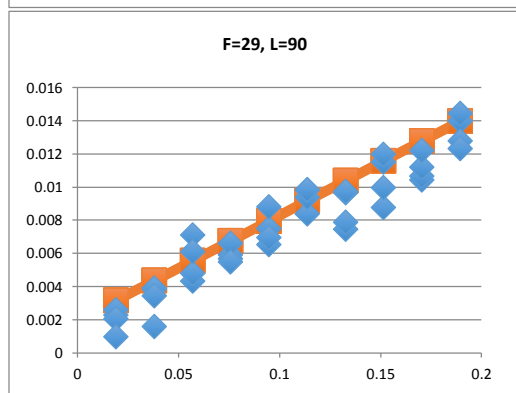
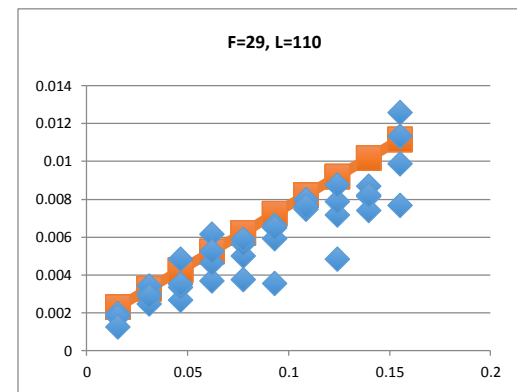
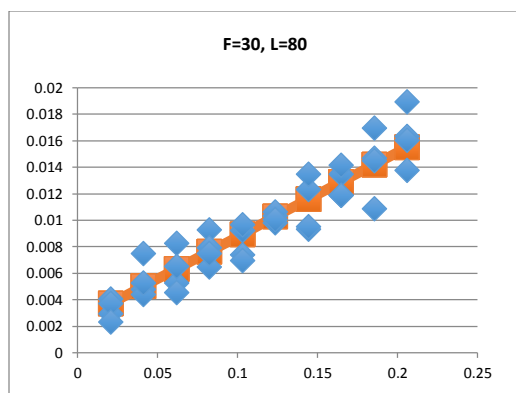
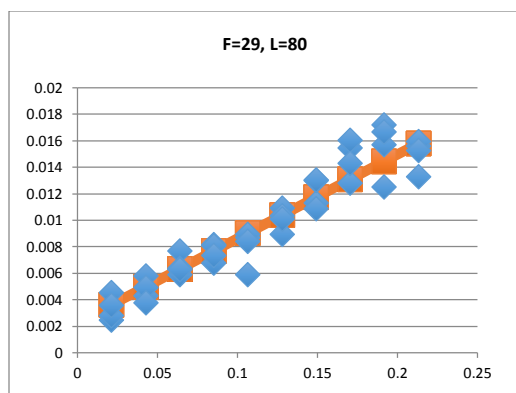


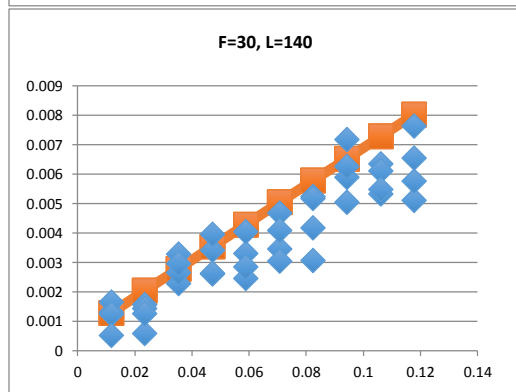
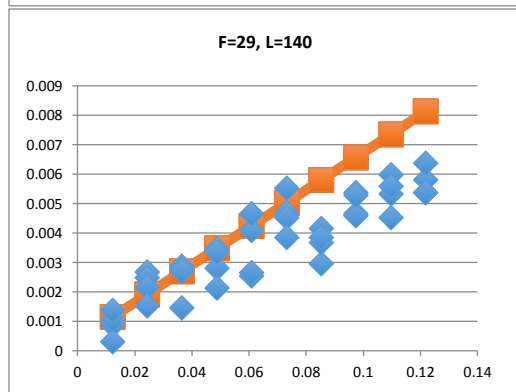
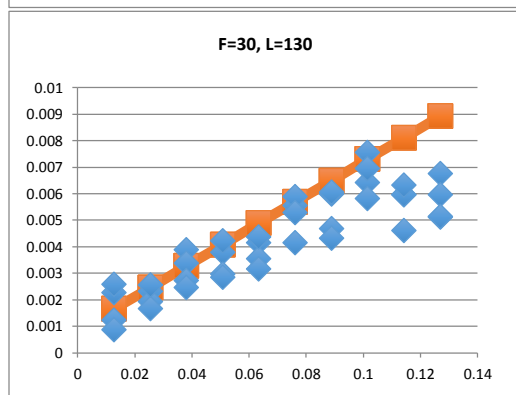
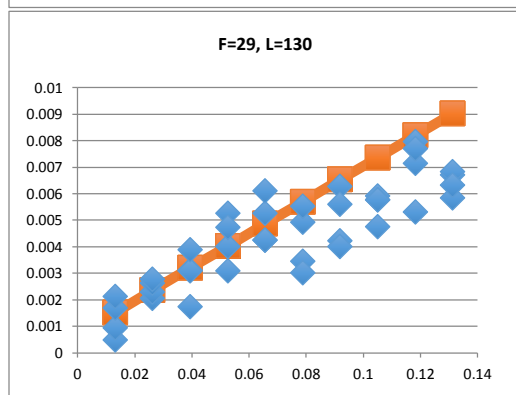
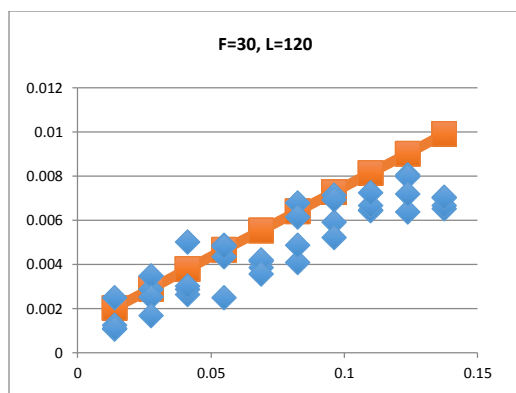
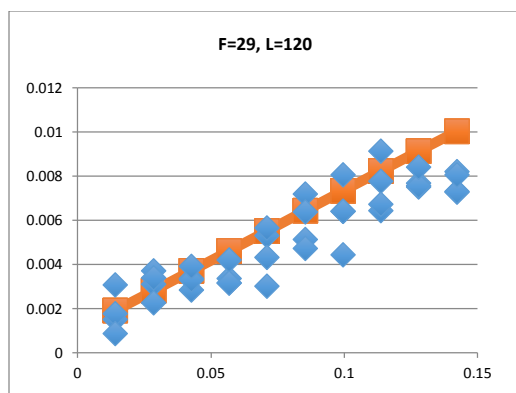


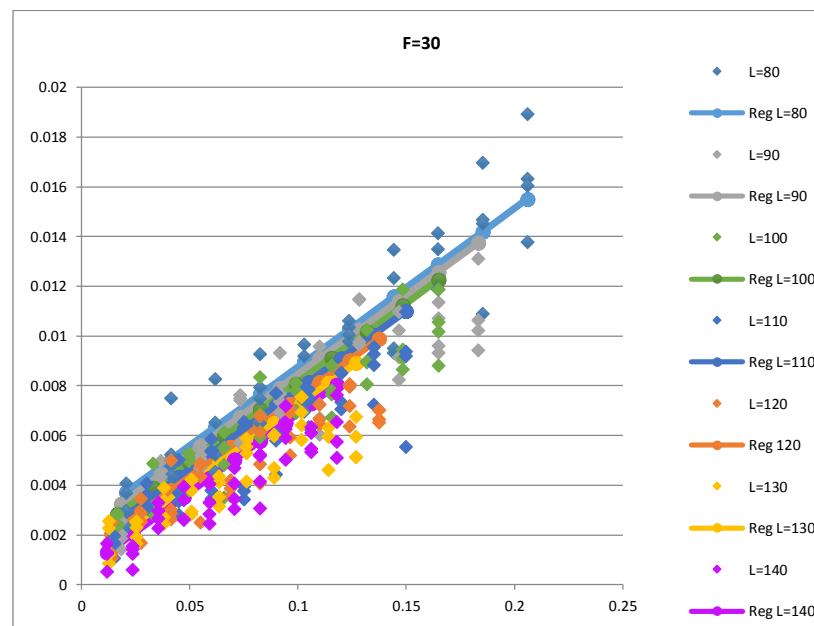
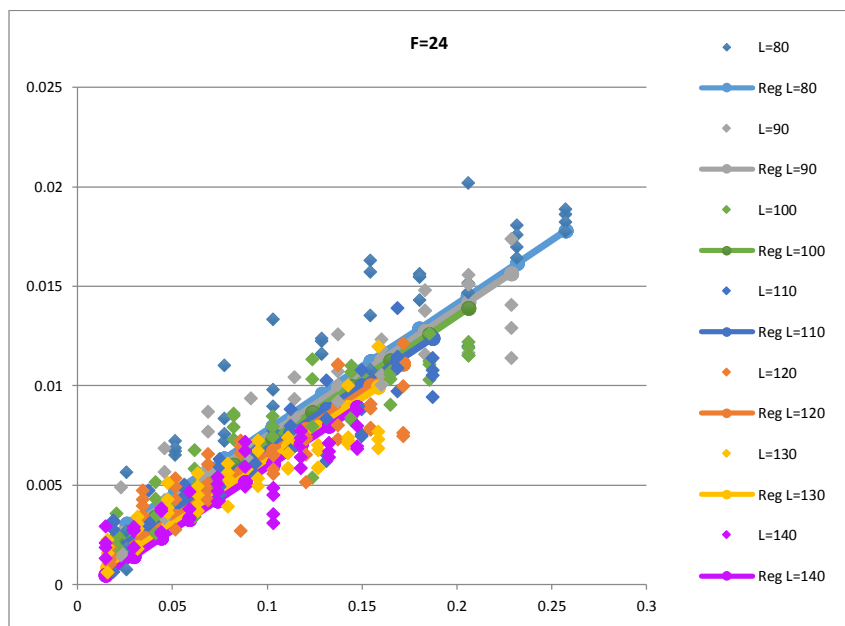
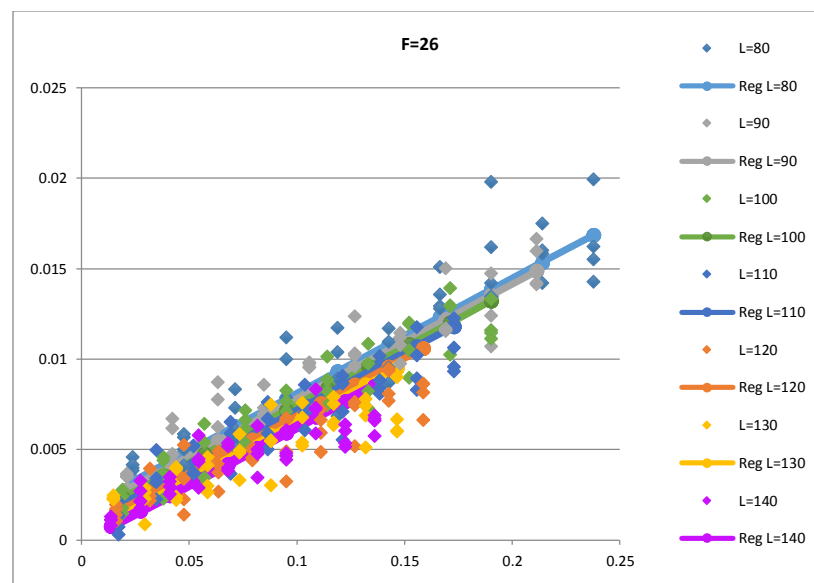
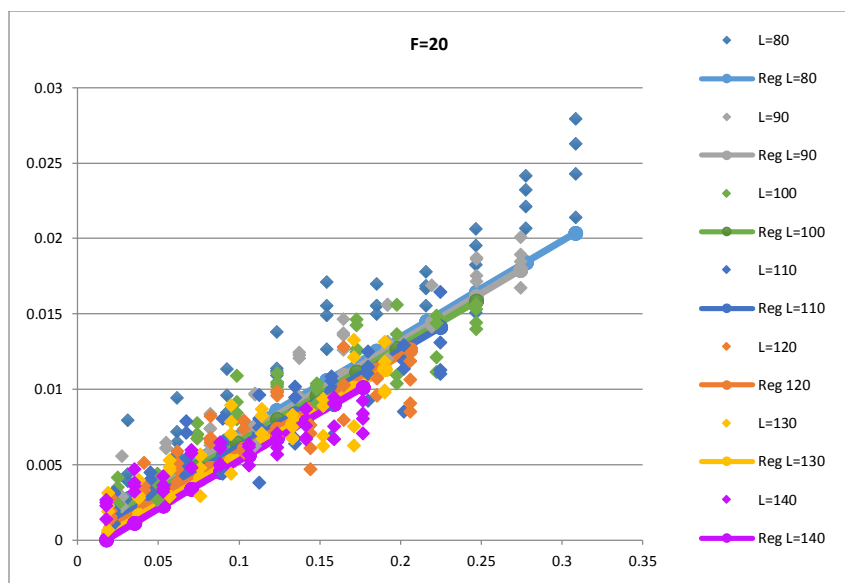


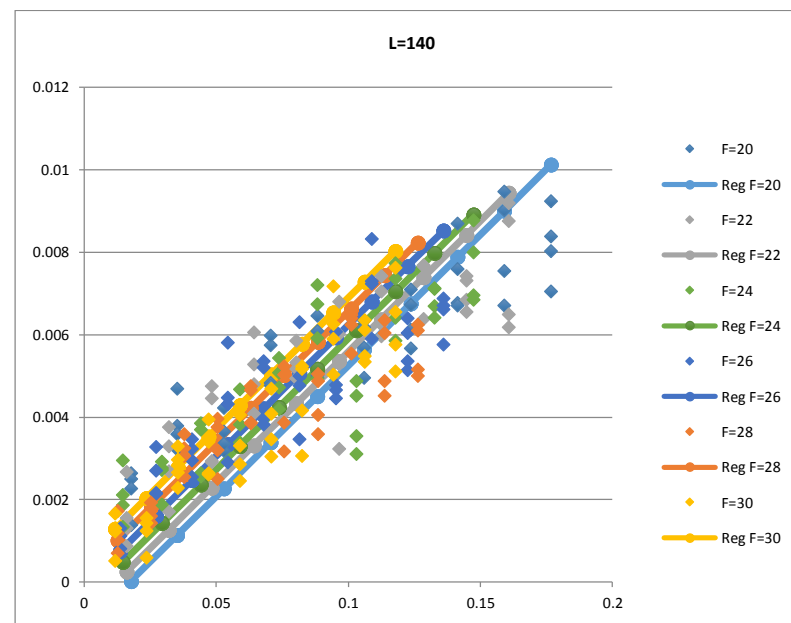
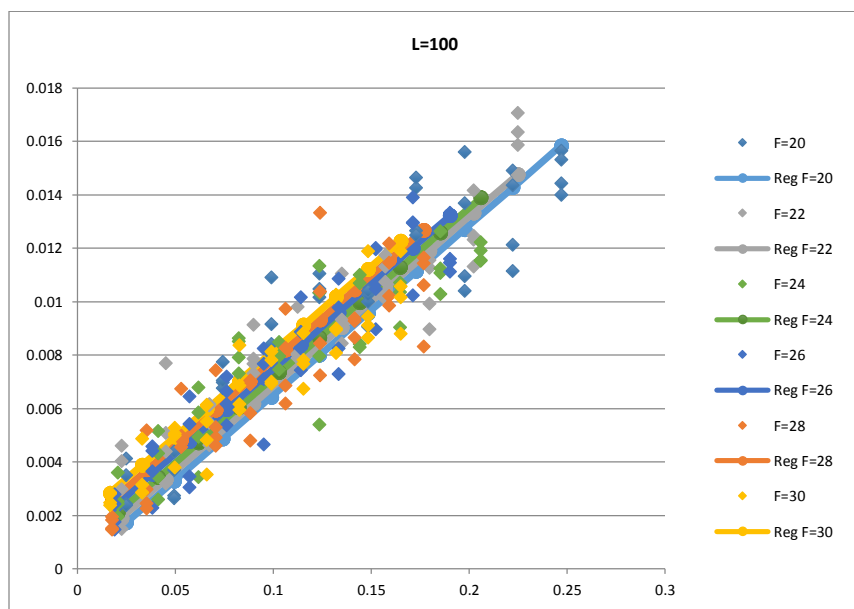
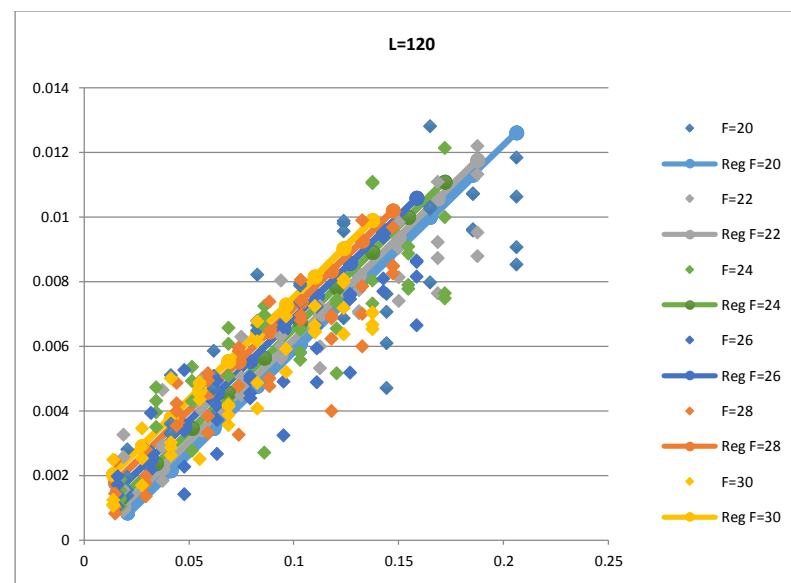
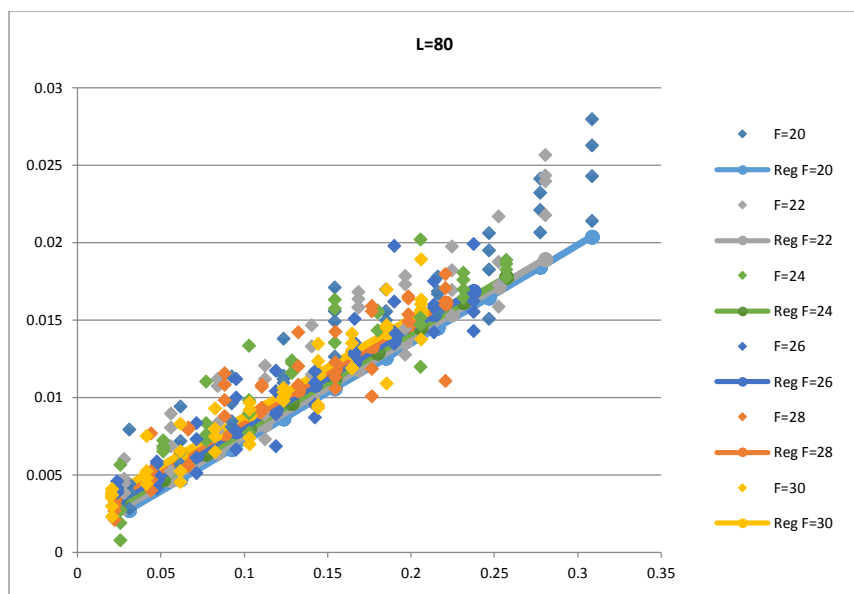




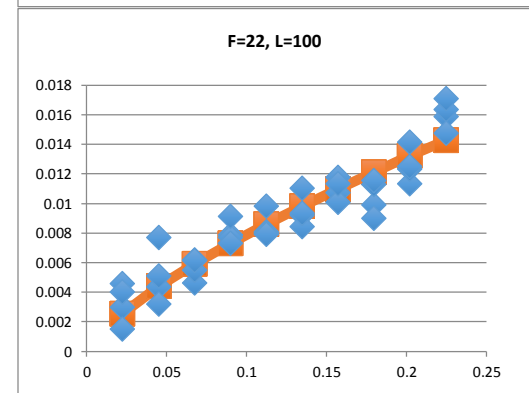
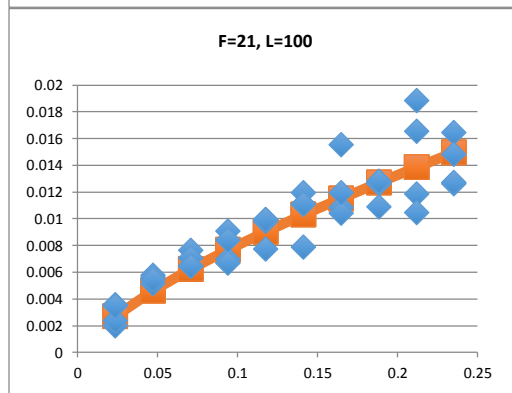
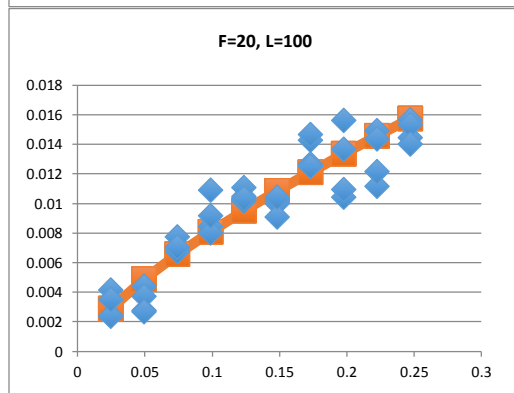
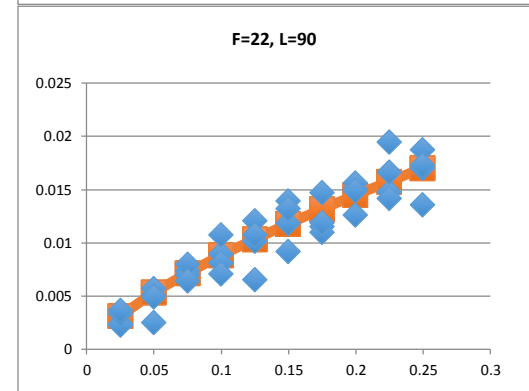
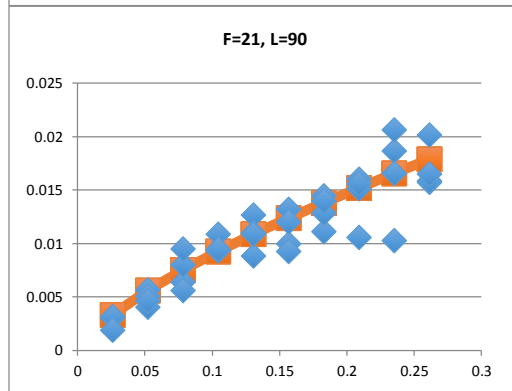
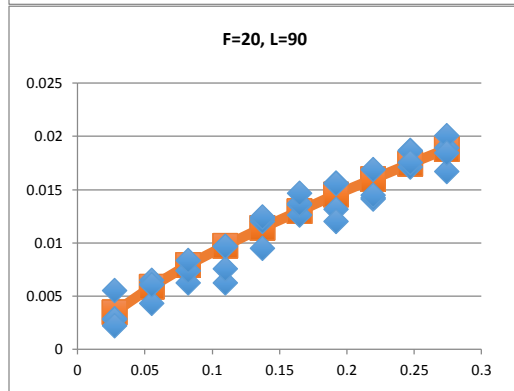
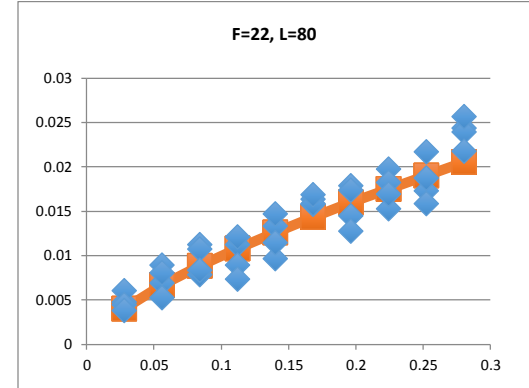
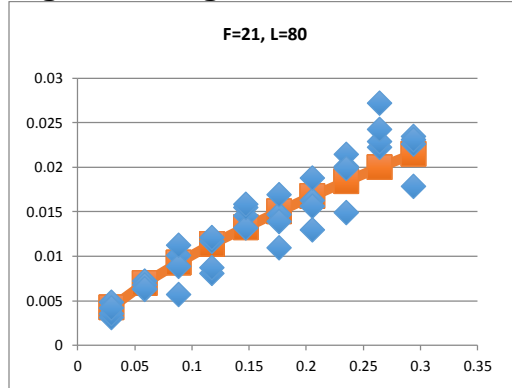
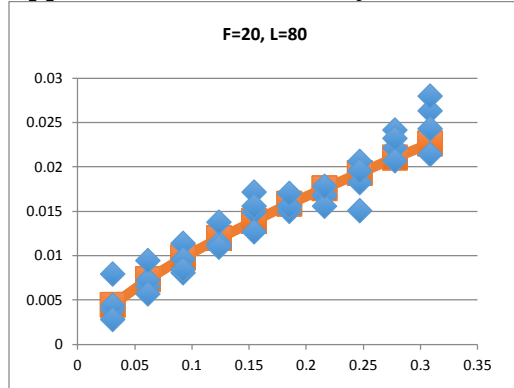


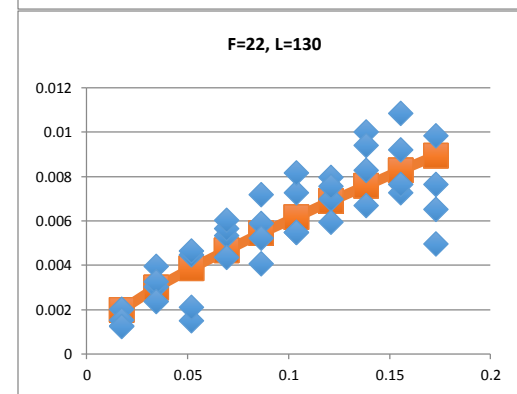
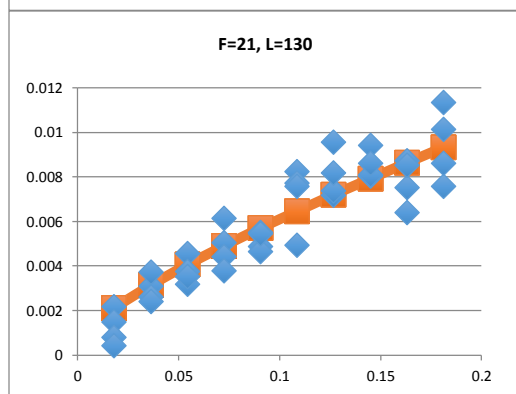
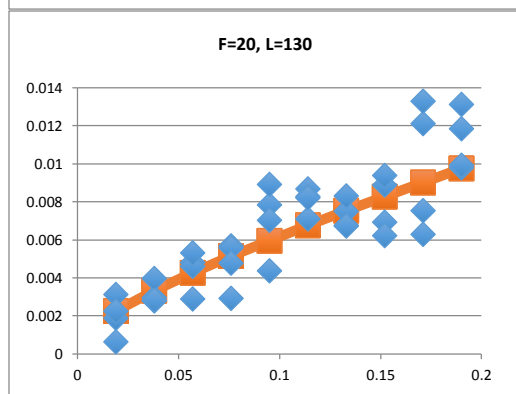
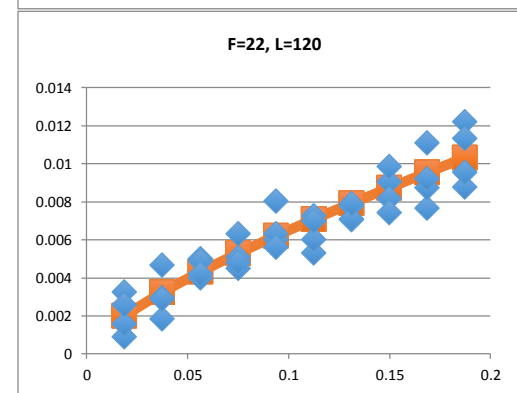
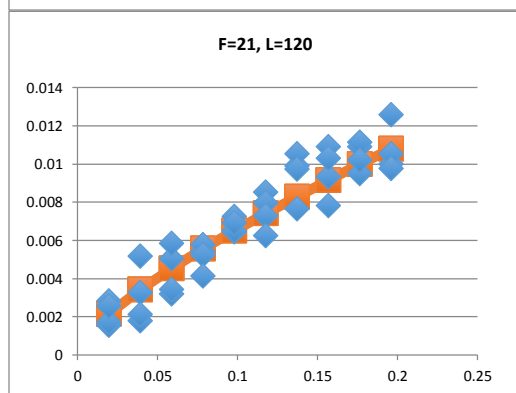
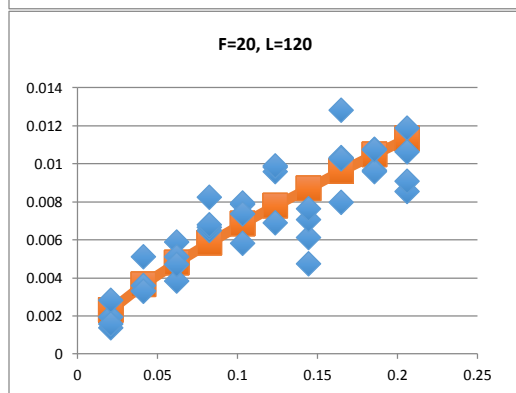
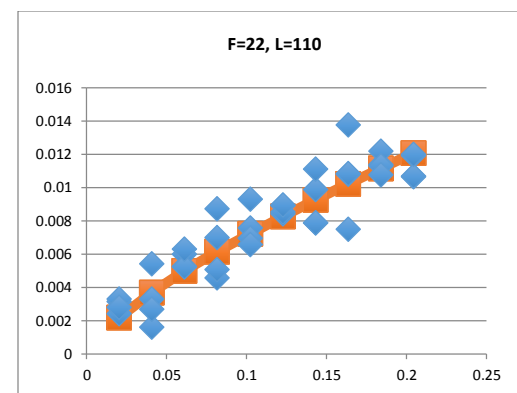
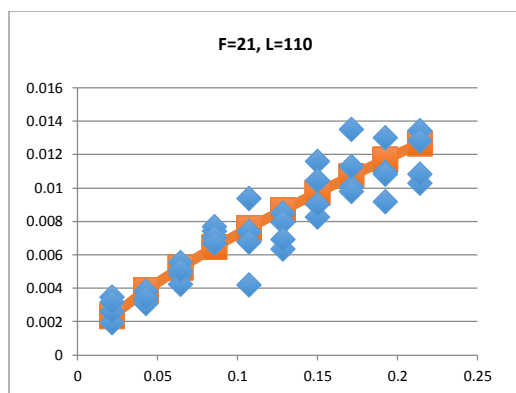
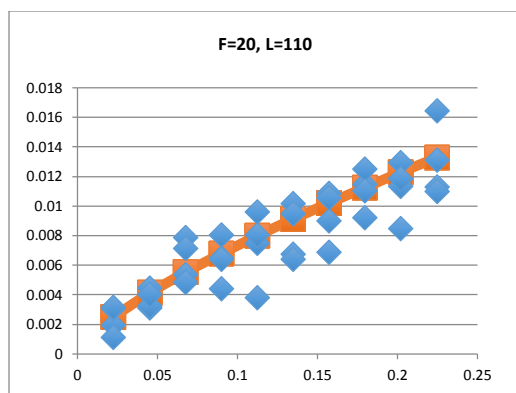


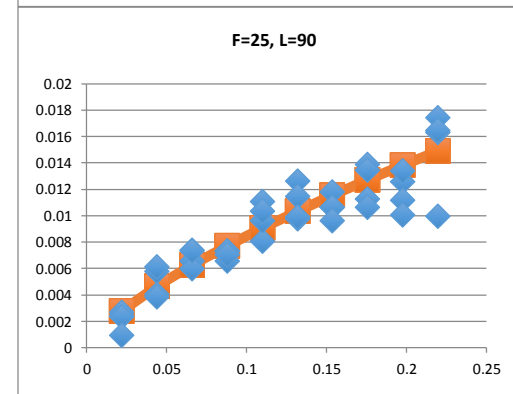
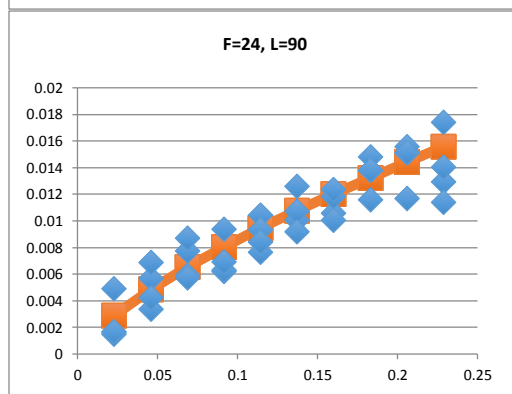
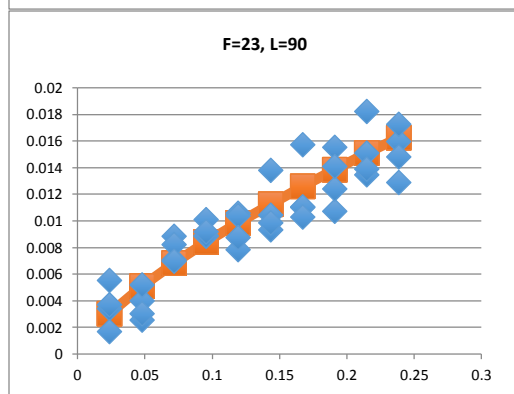
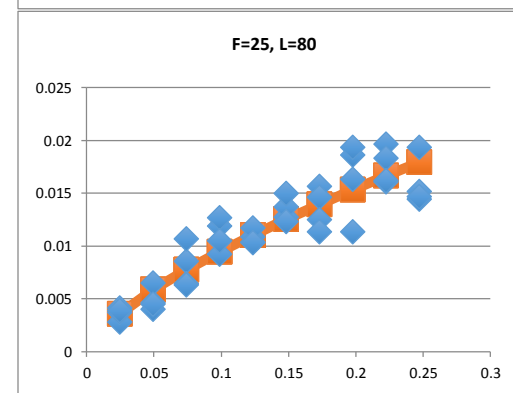
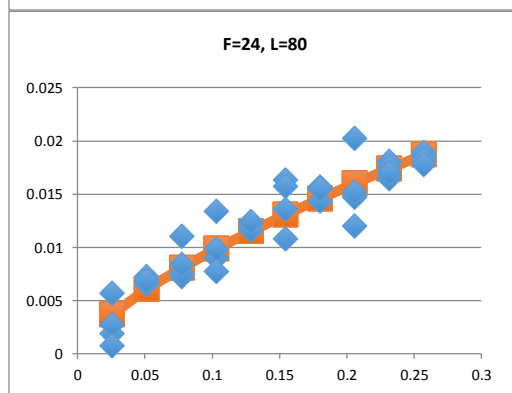
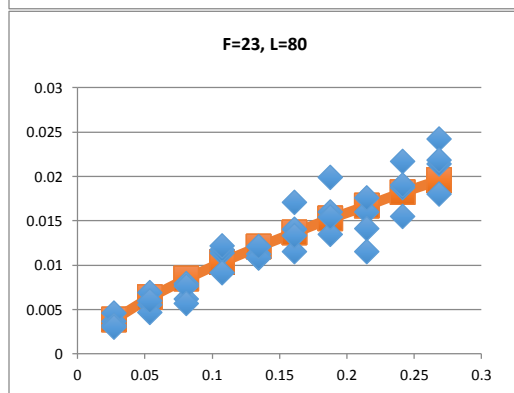
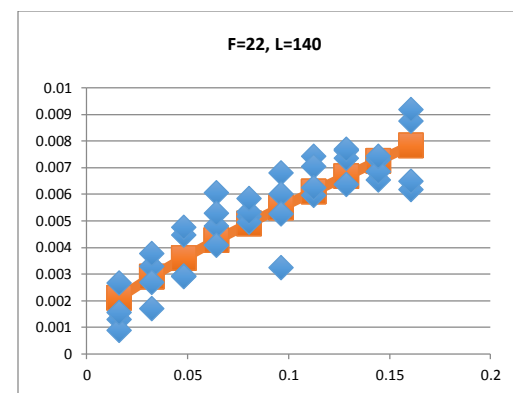
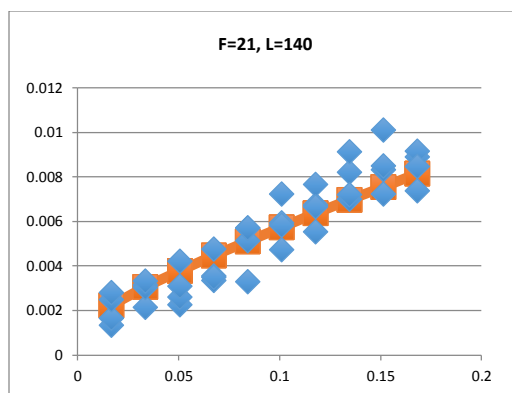
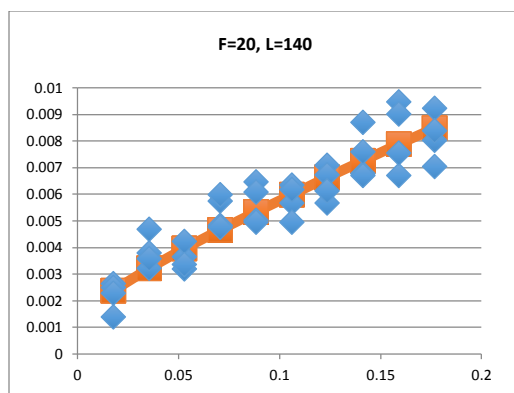


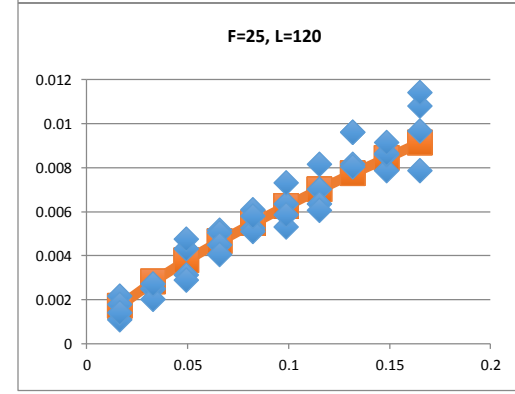
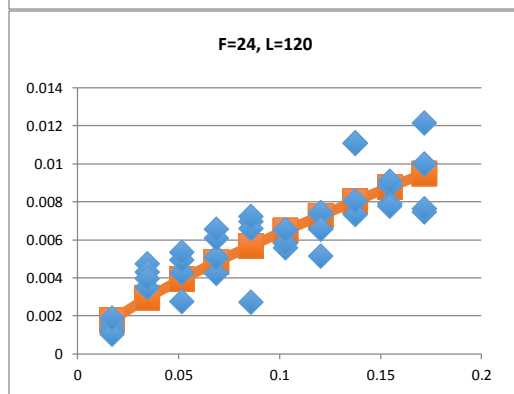
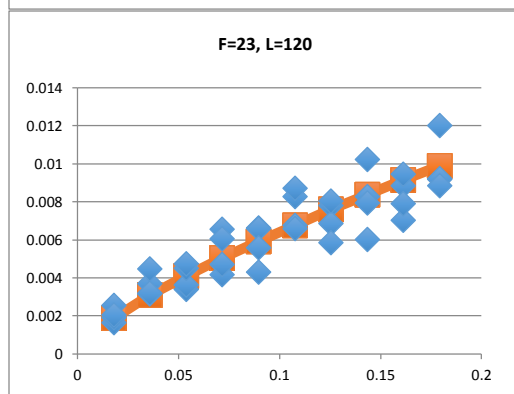
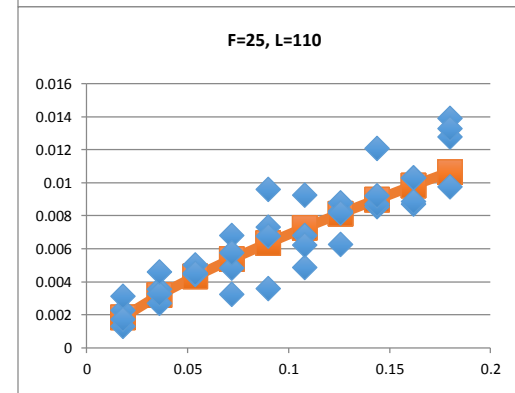
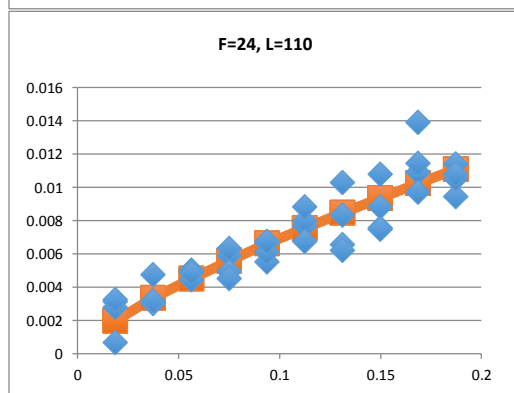
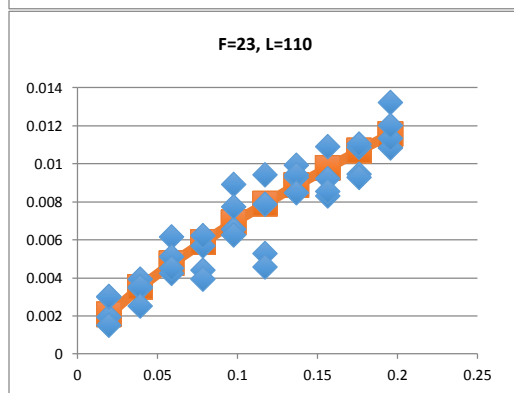
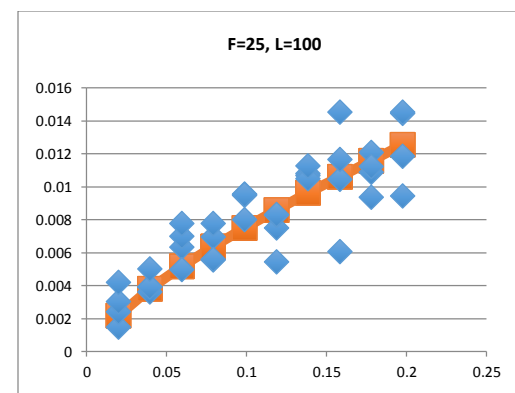
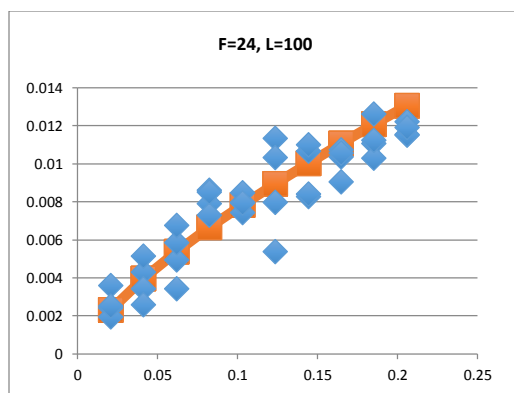
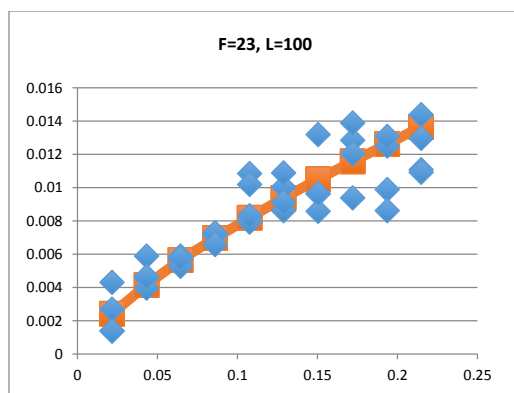


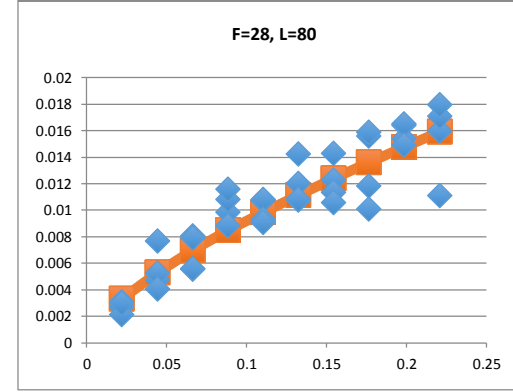
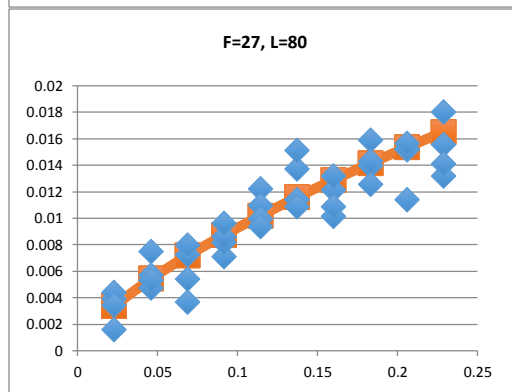
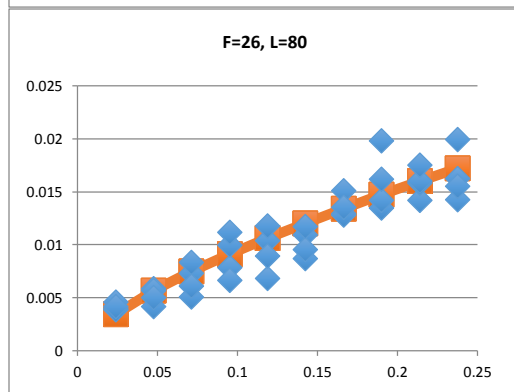
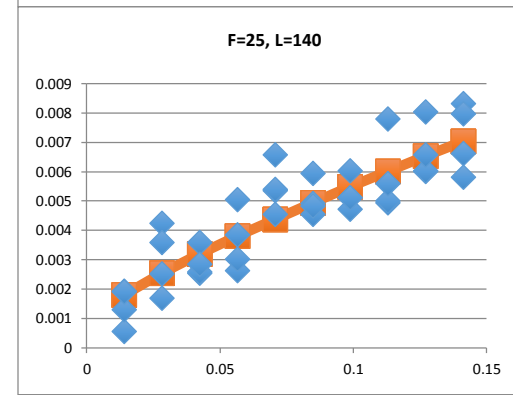
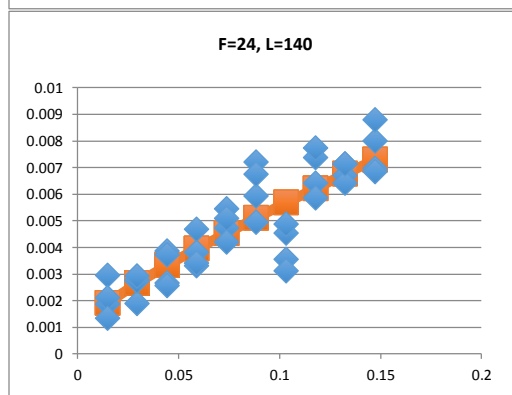
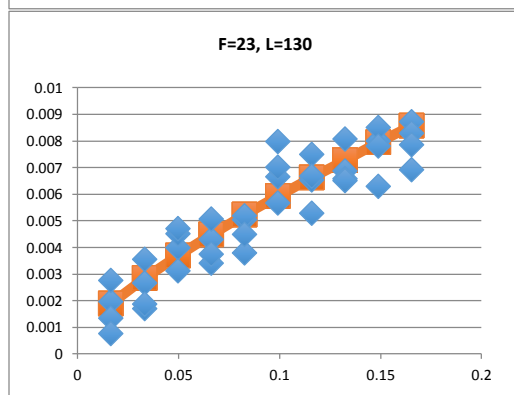
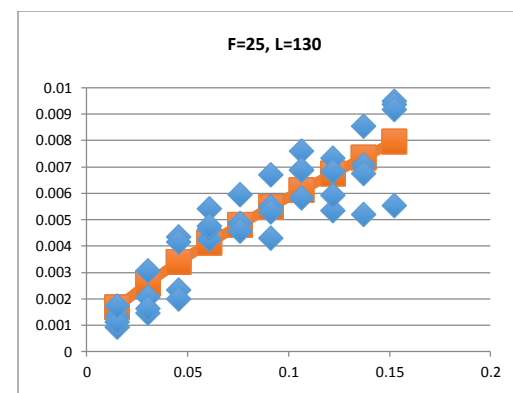
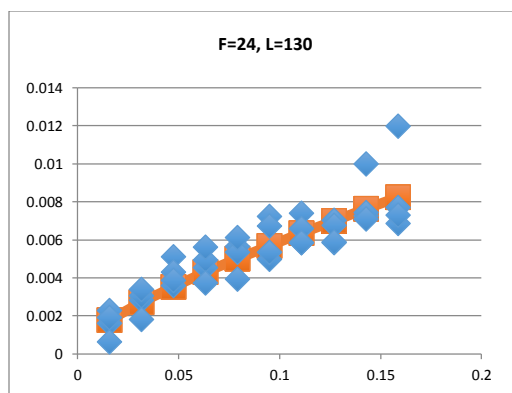
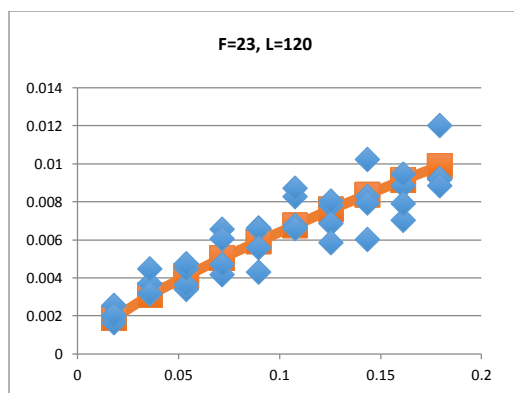
Appendix B – UPM Primary Case Studies with High Order Regression

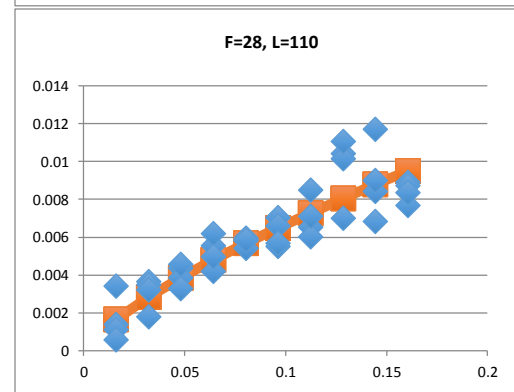
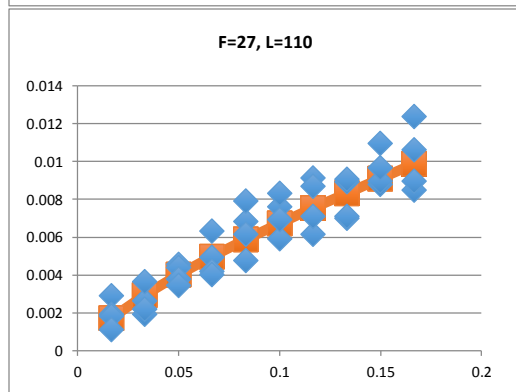
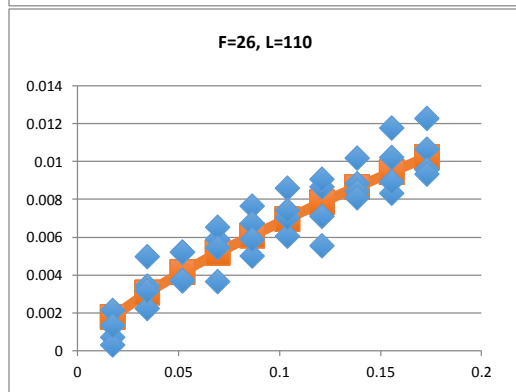
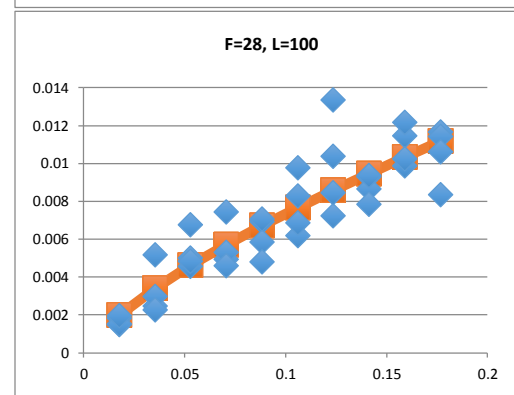
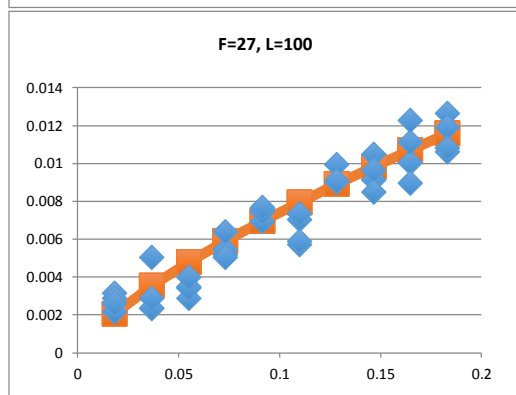
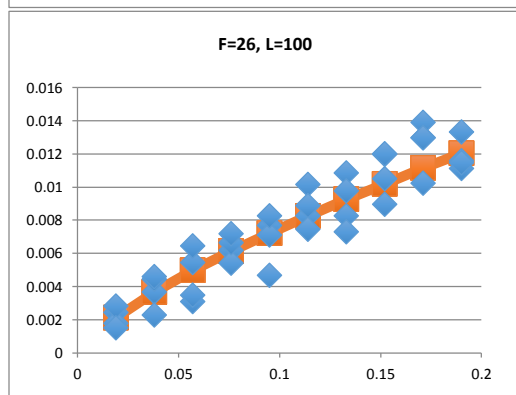
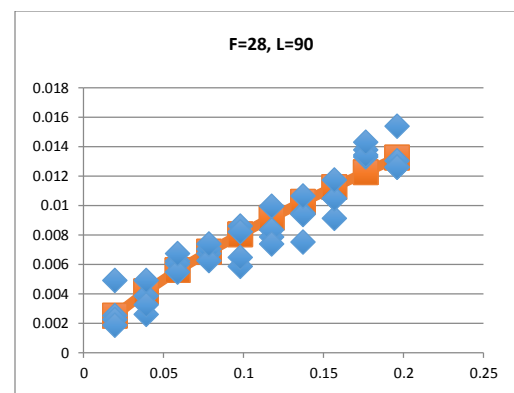
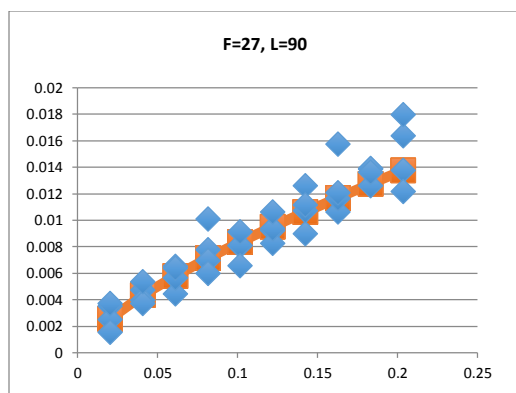
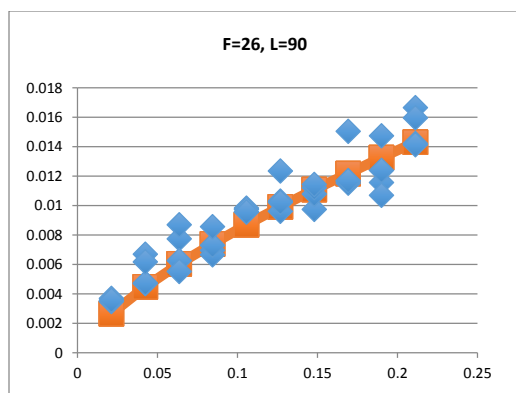


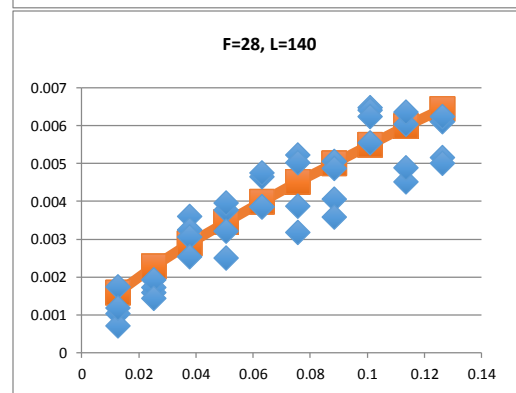
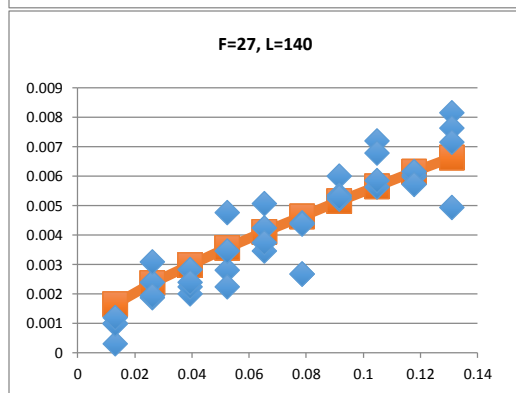
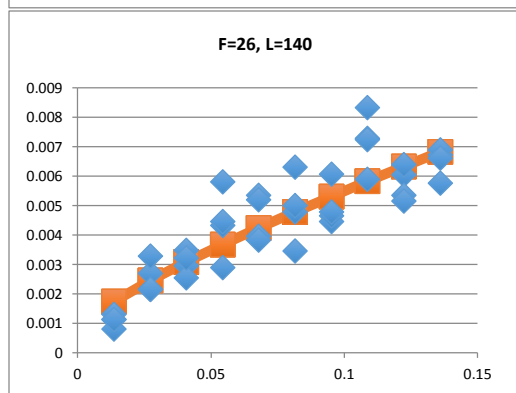
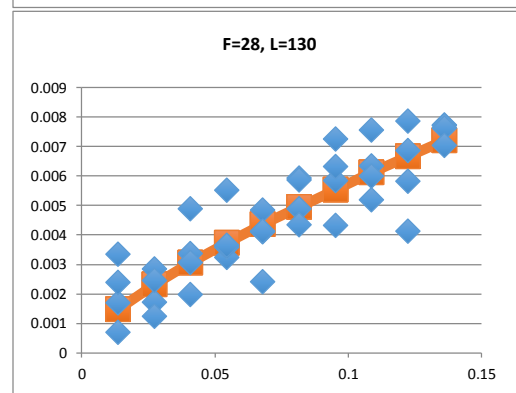
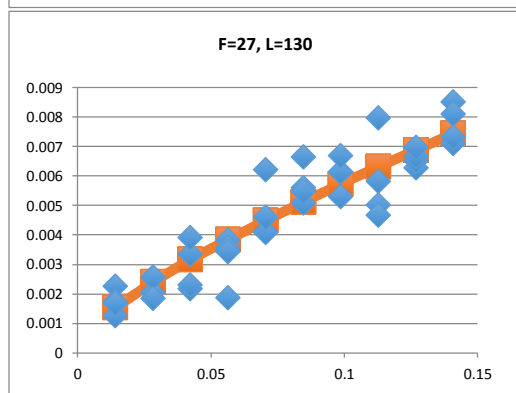
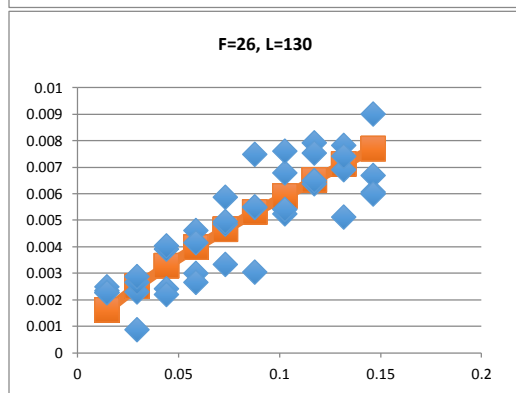
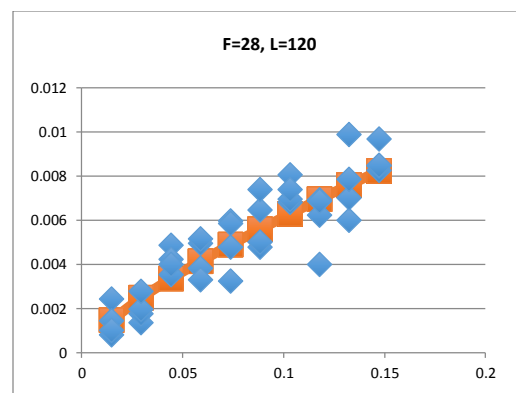
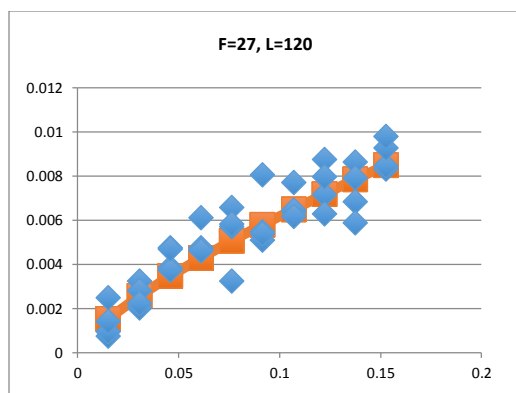
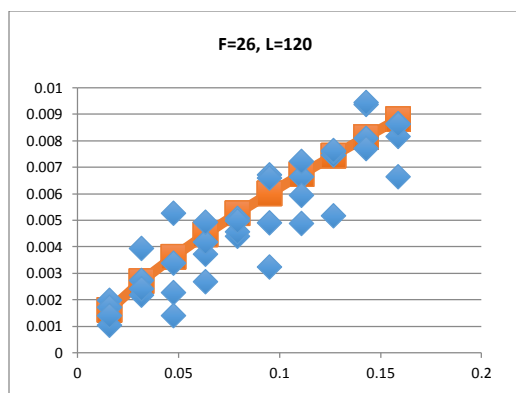


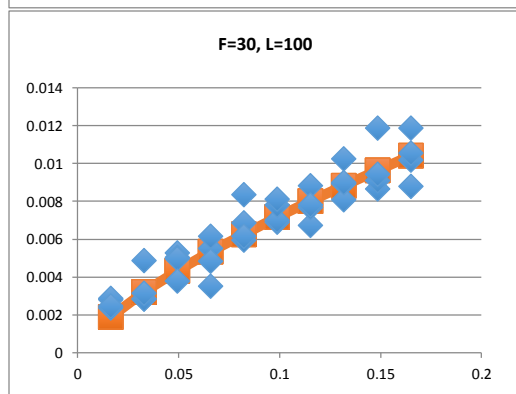
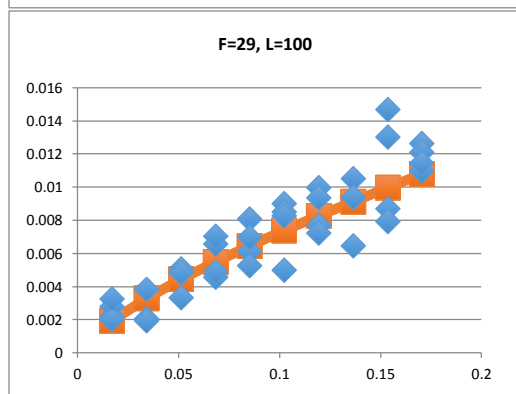
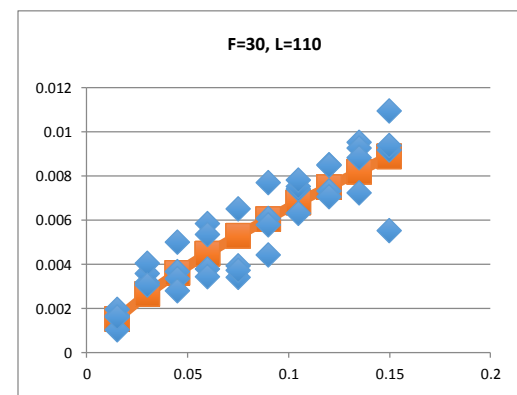
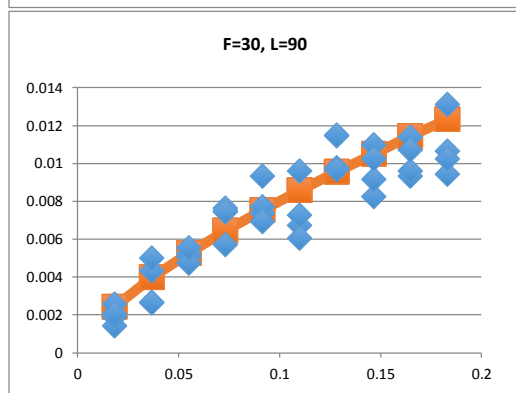
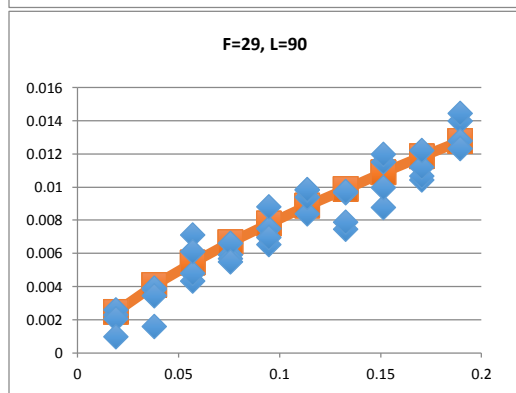
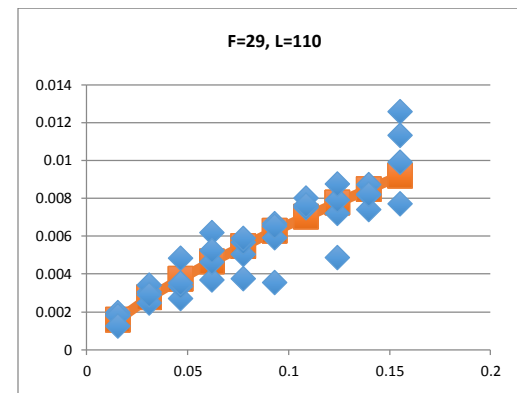
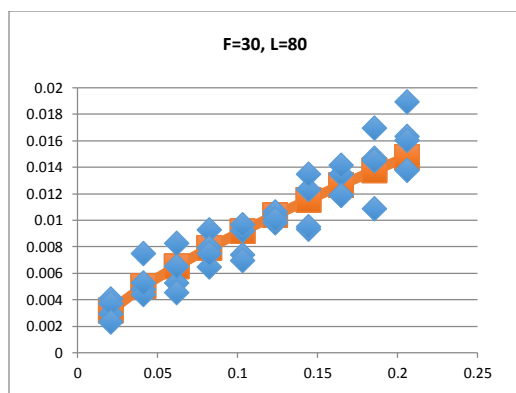
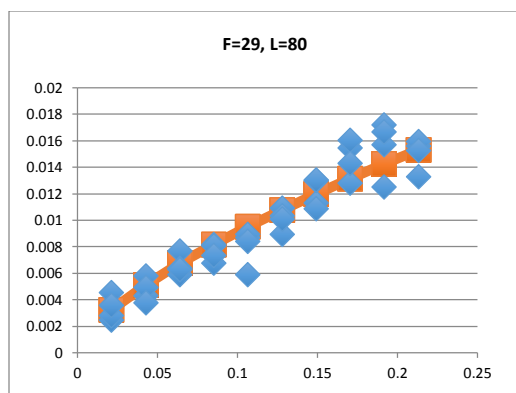


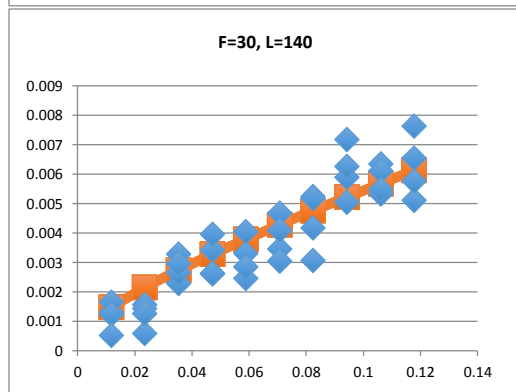
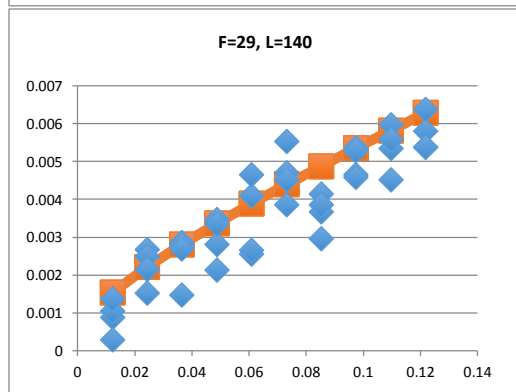
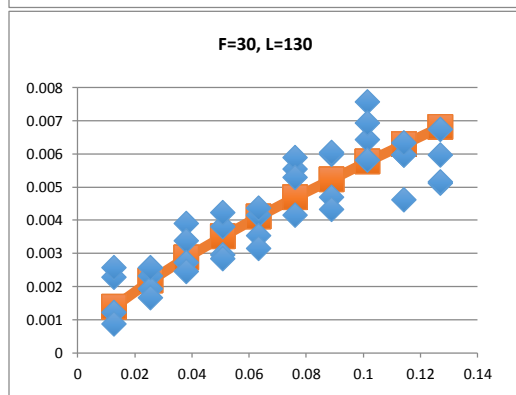
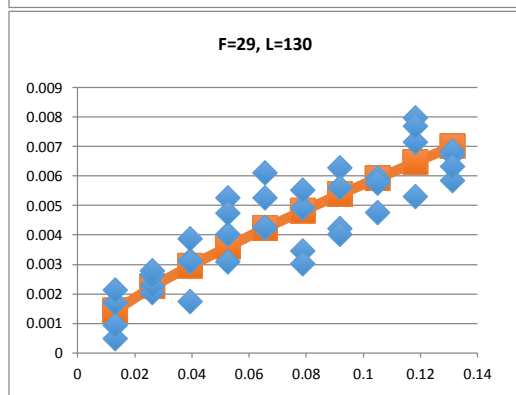
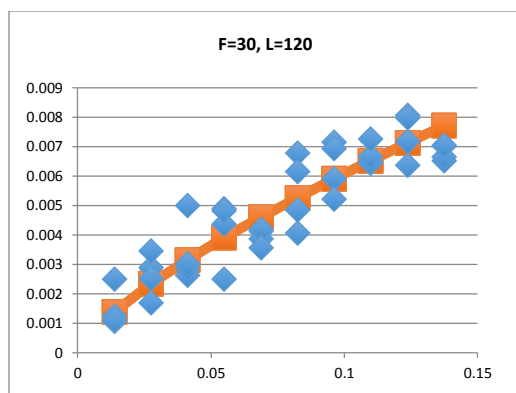
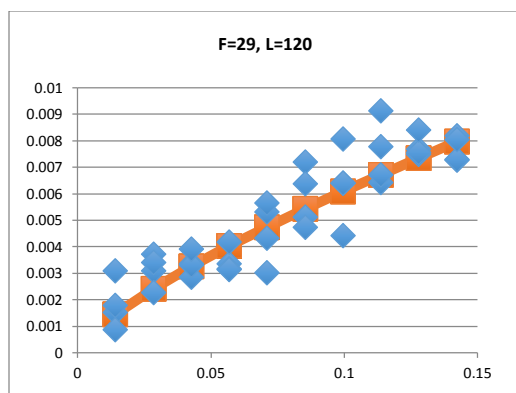


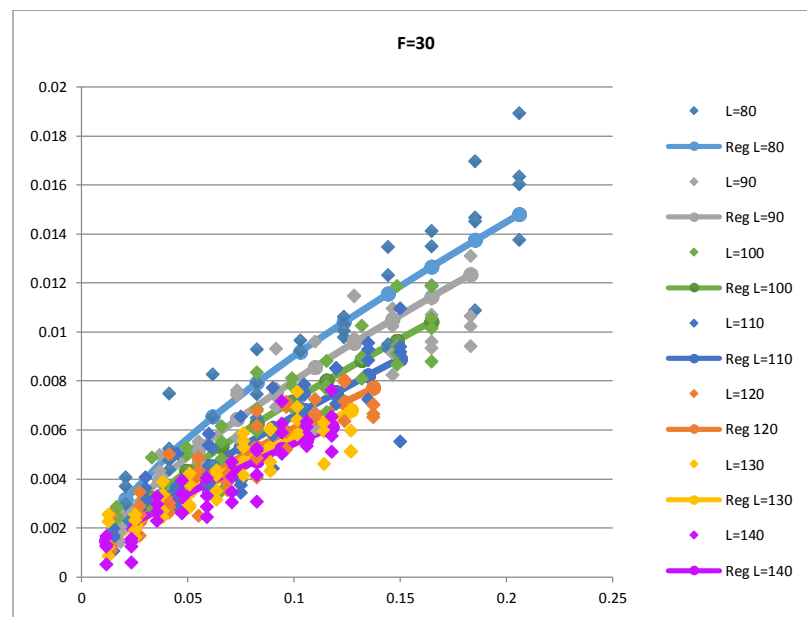
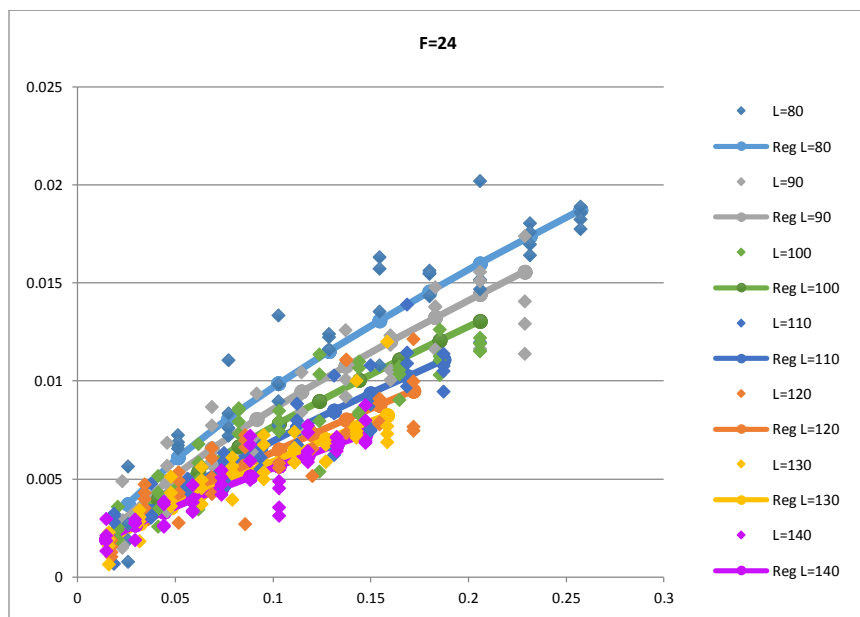
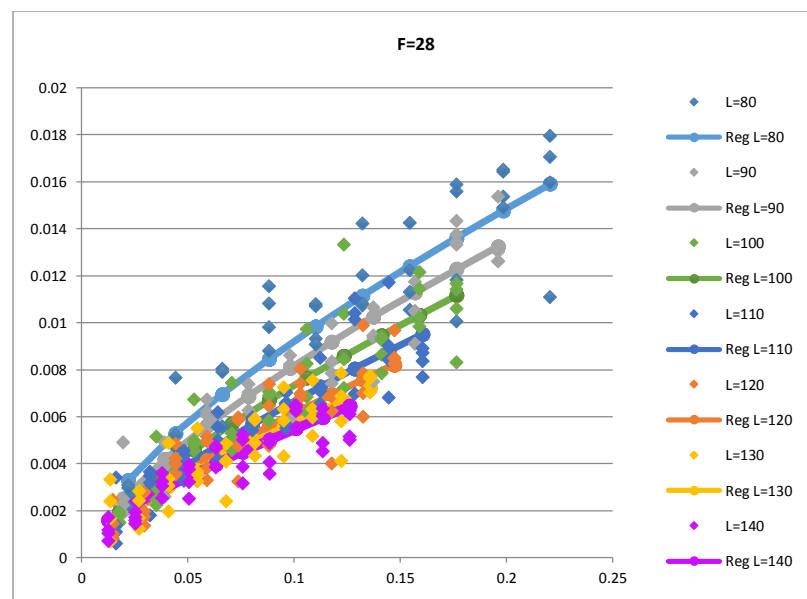
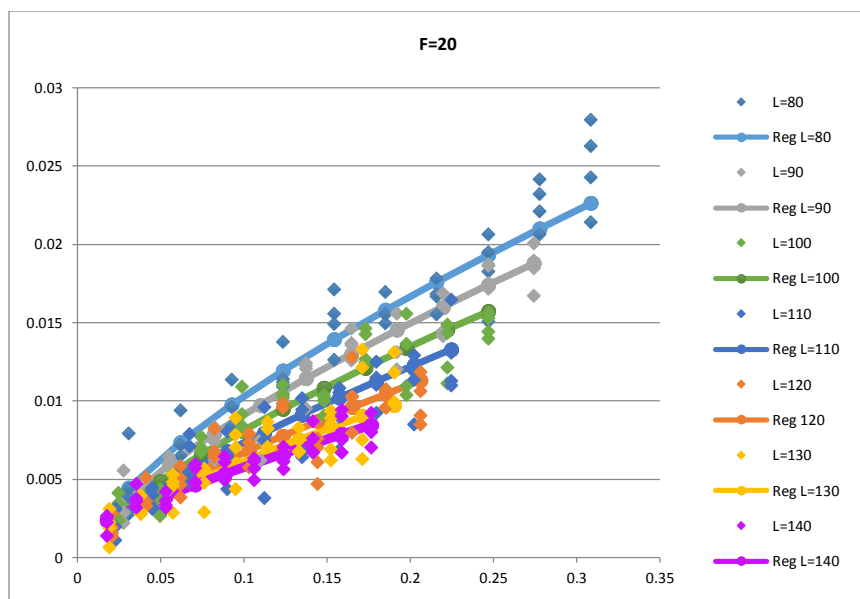


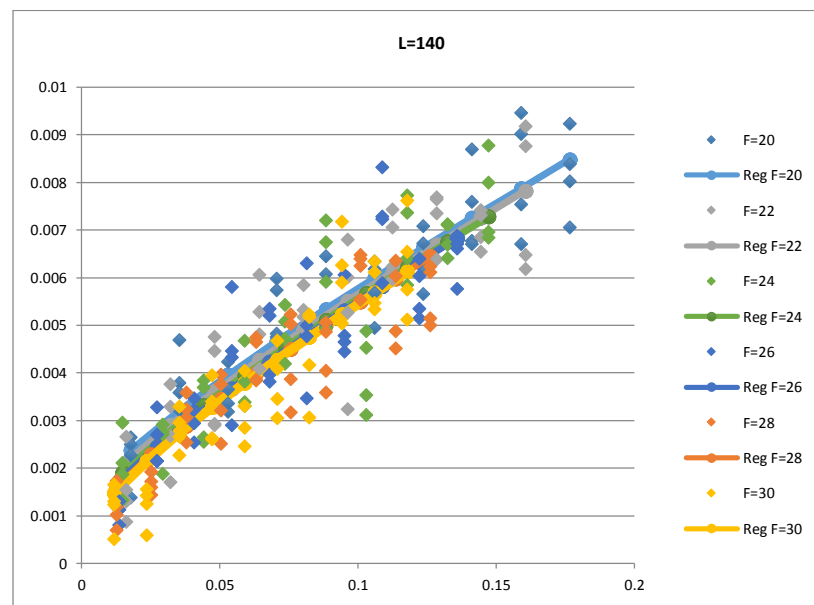
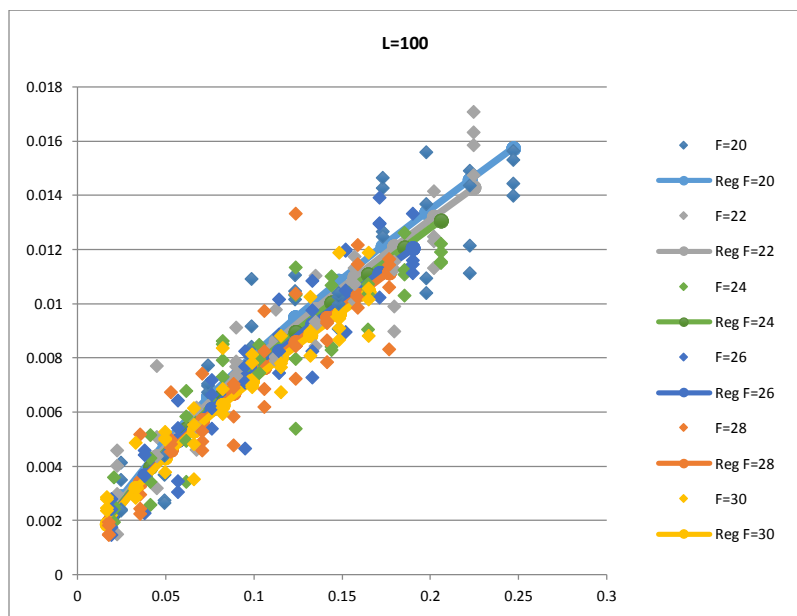
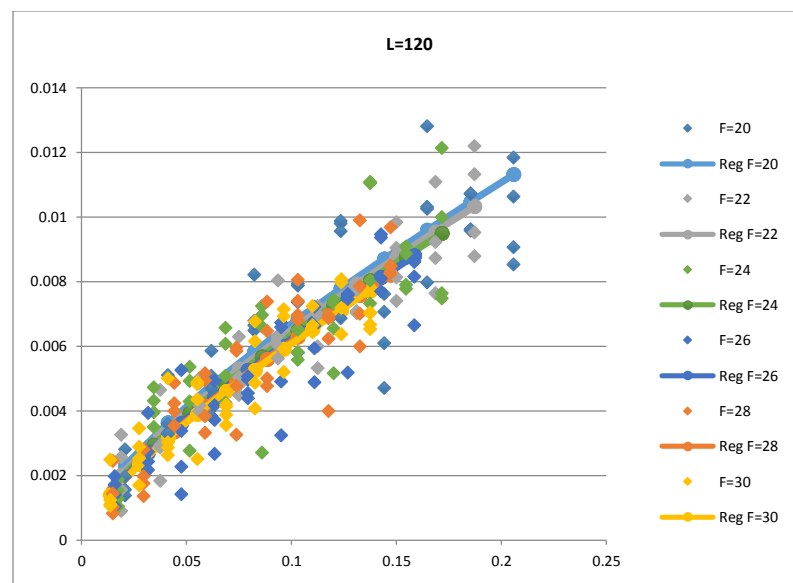
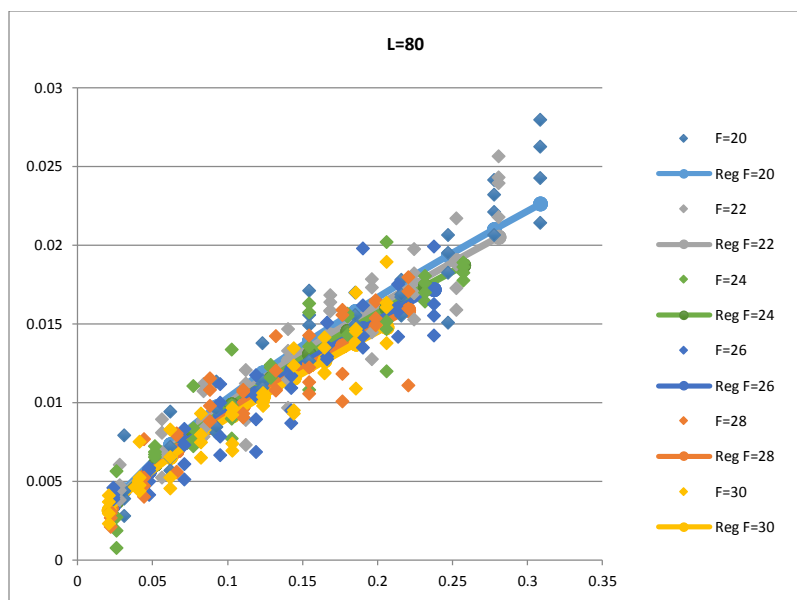




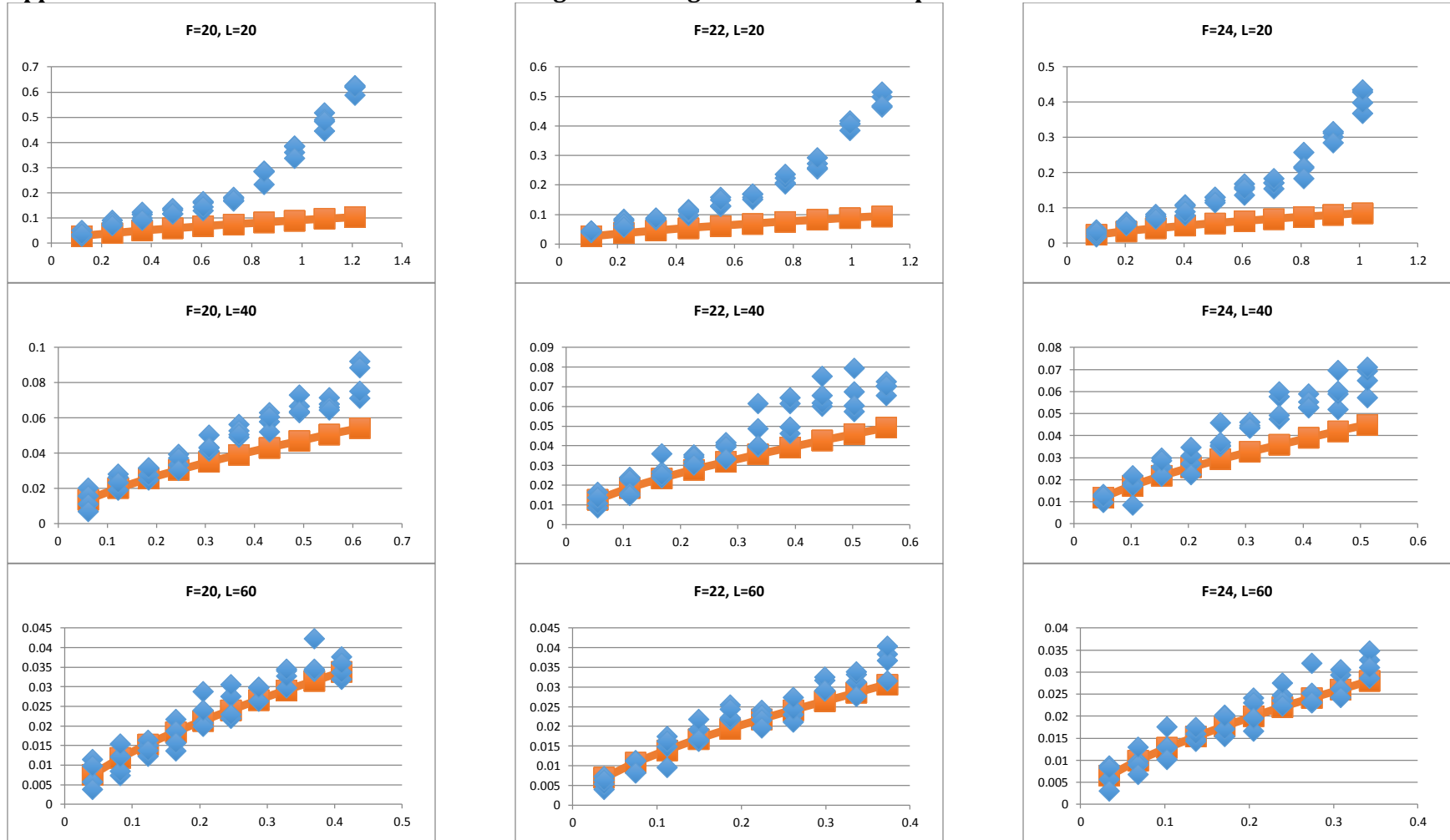


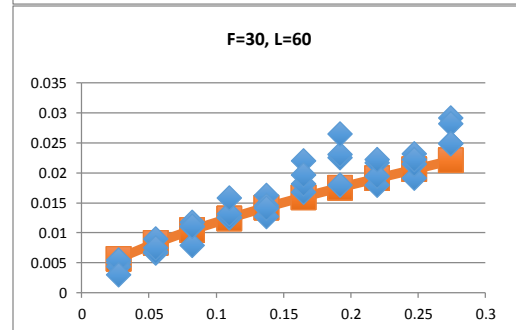
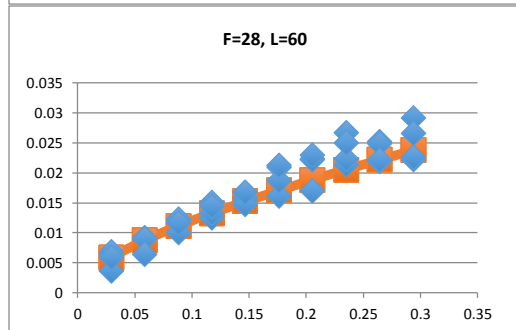
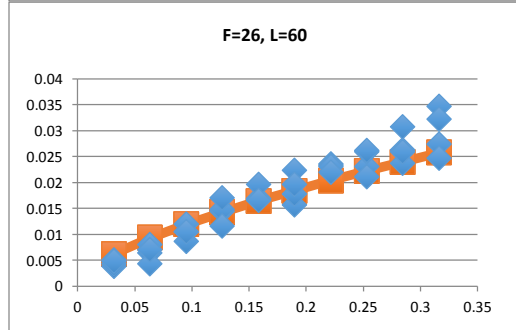
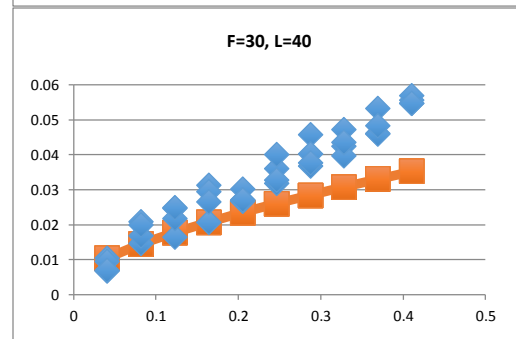
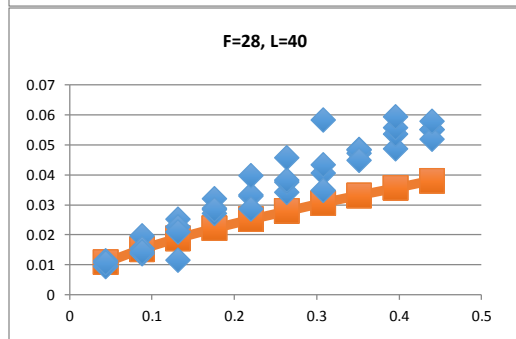
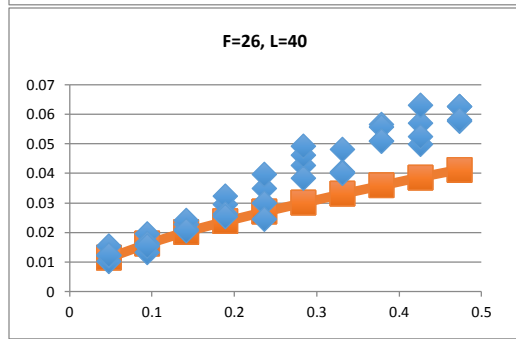
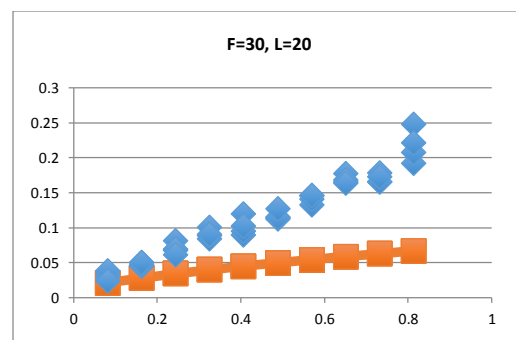
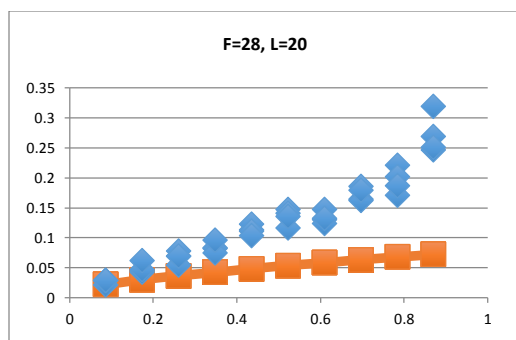
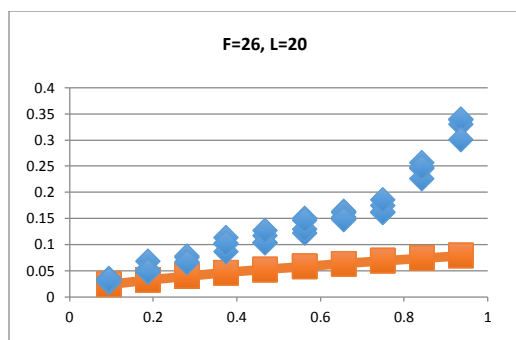




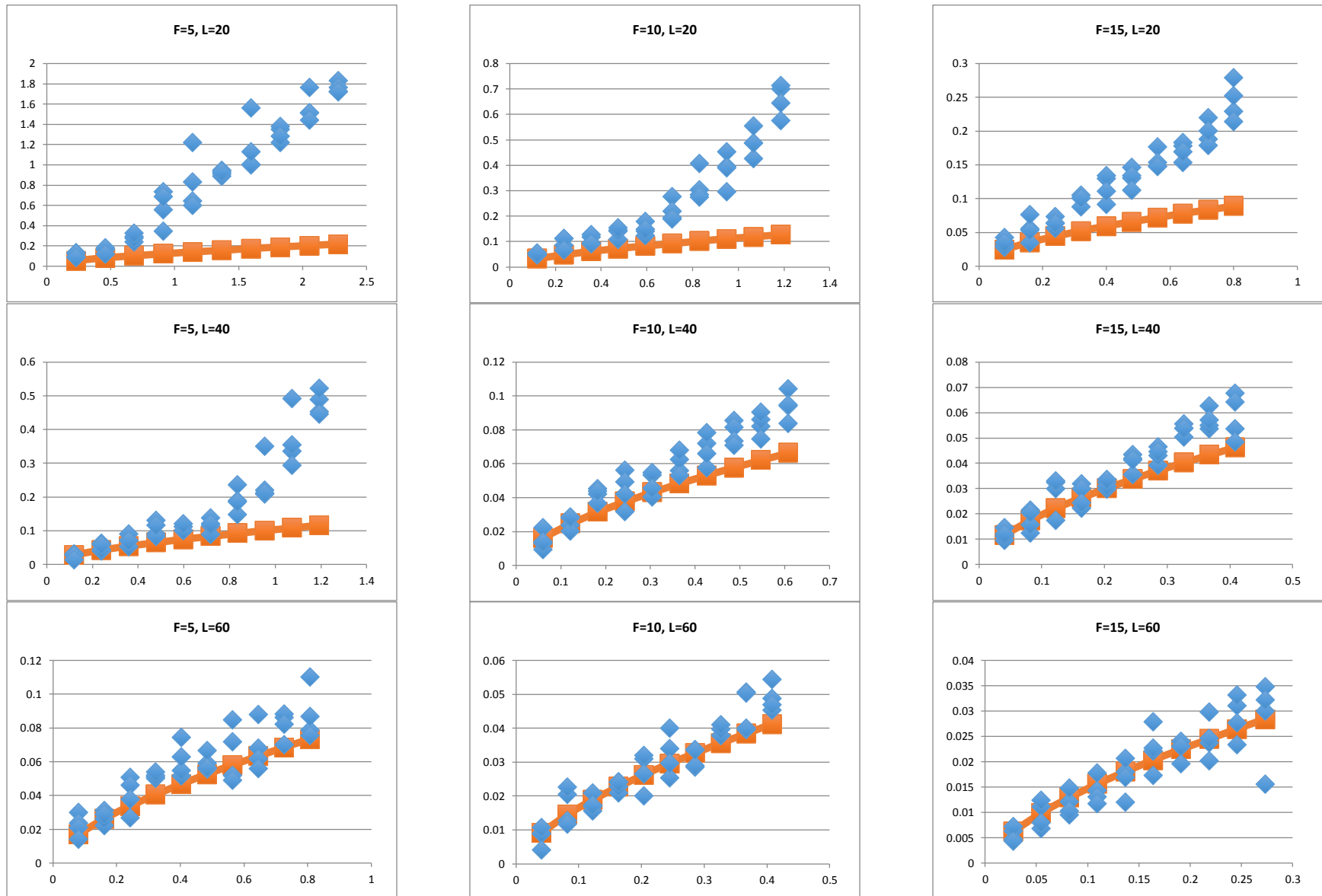


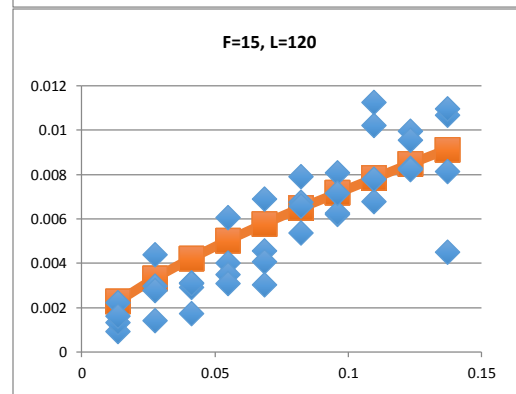
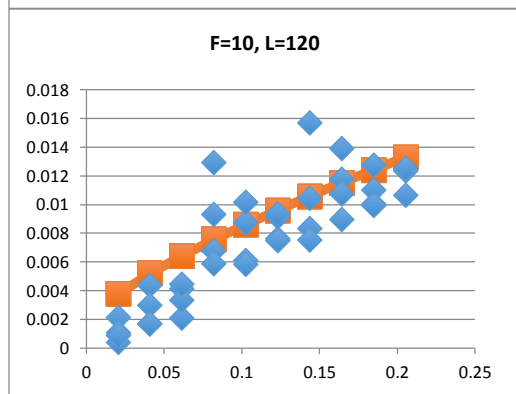
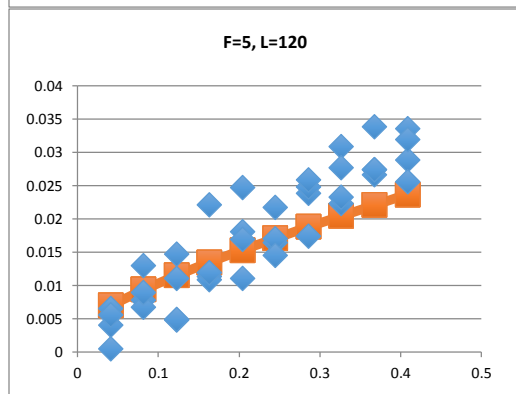
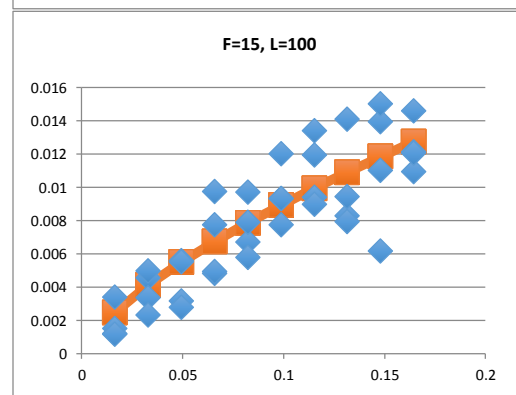
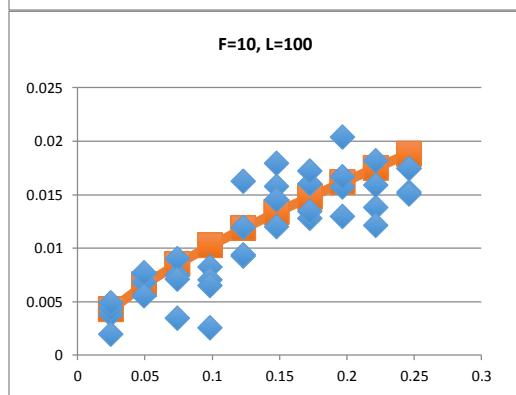
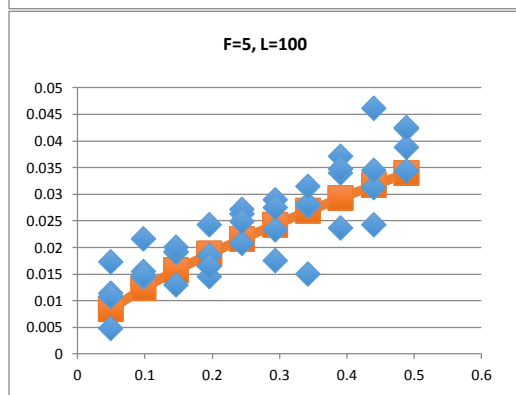
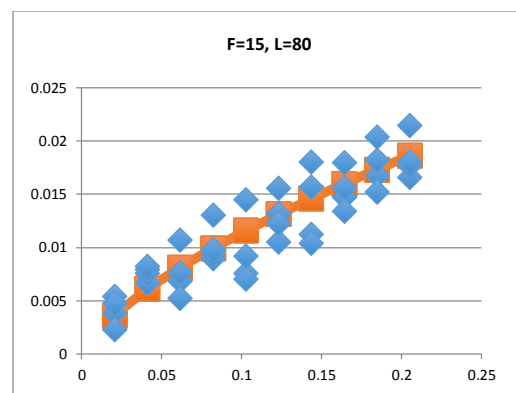
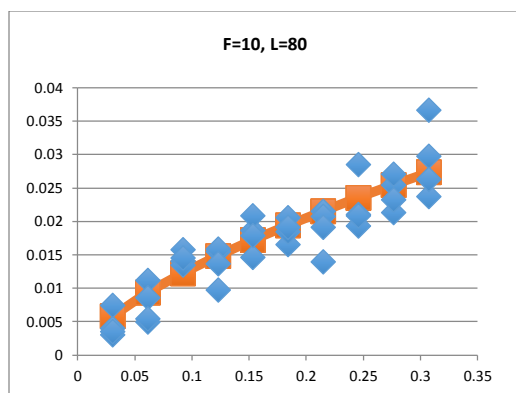
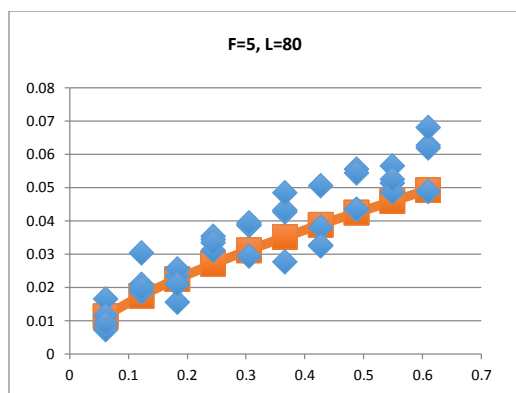
Appendix C - UPM Extended Case Studies with High Order Regression - Low Occupant Loads

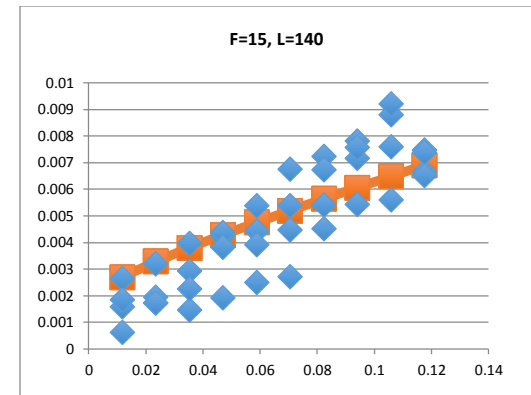
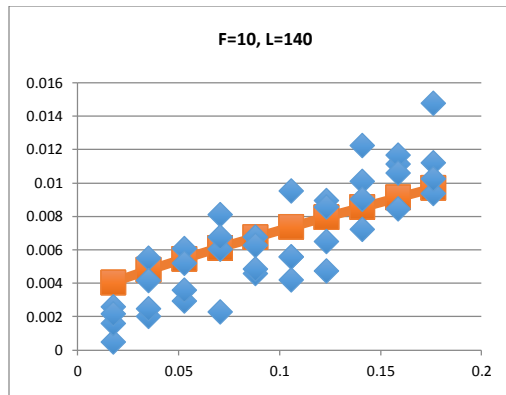
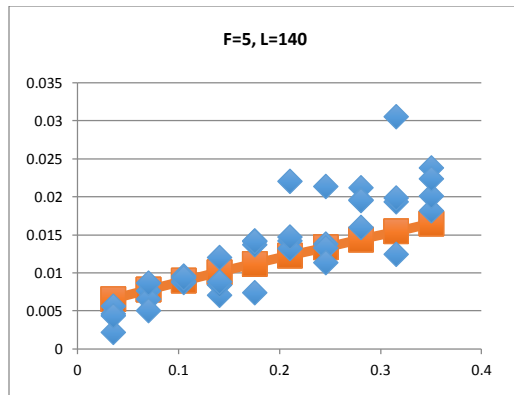




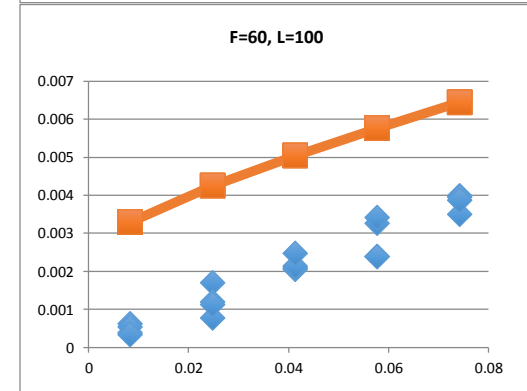
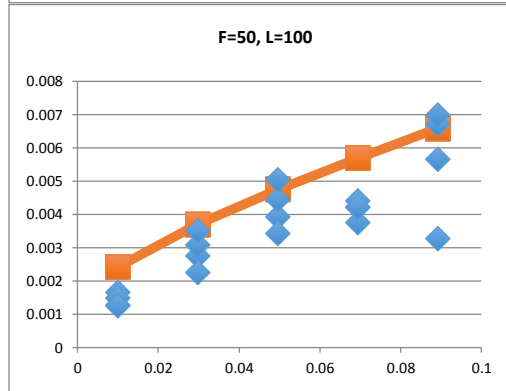
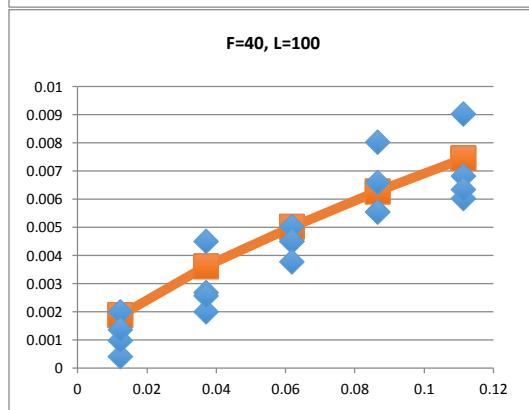
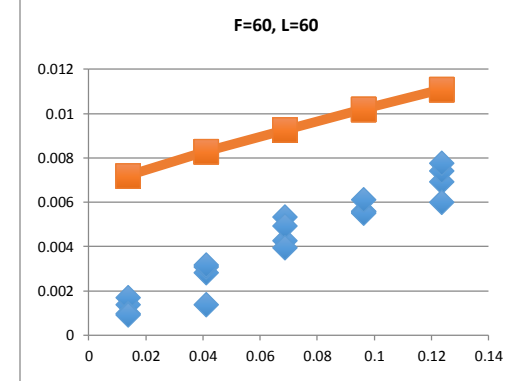
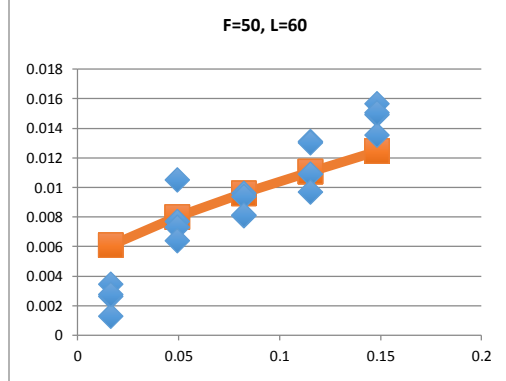
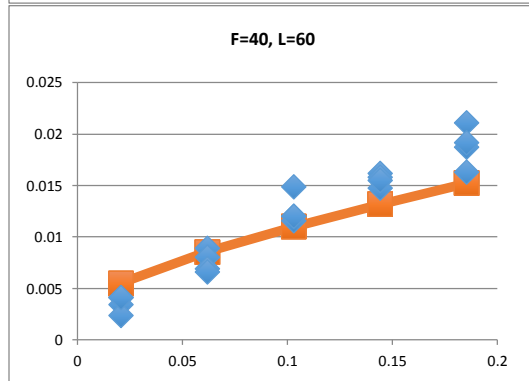
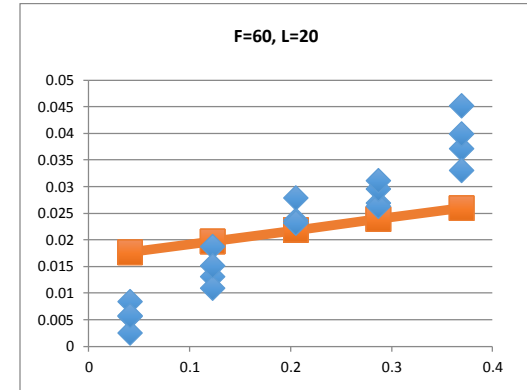
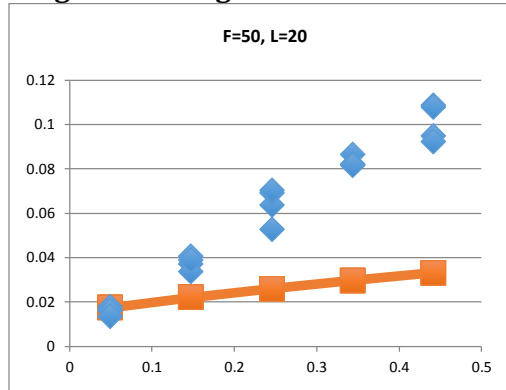
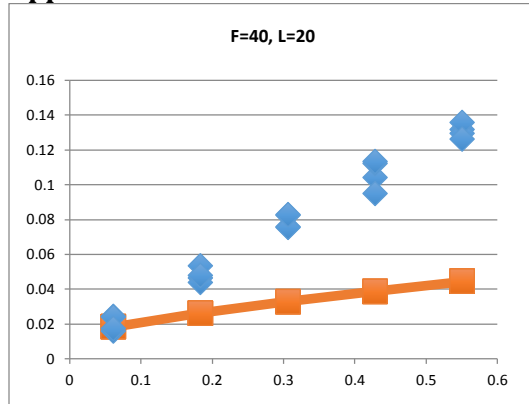
Appendix D – UPM Extended Case Studies with High Order Regression – Short Buildings

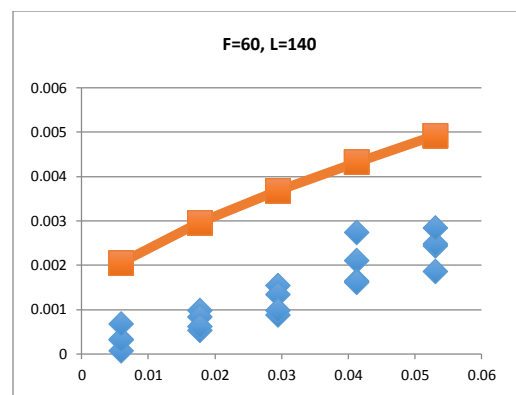
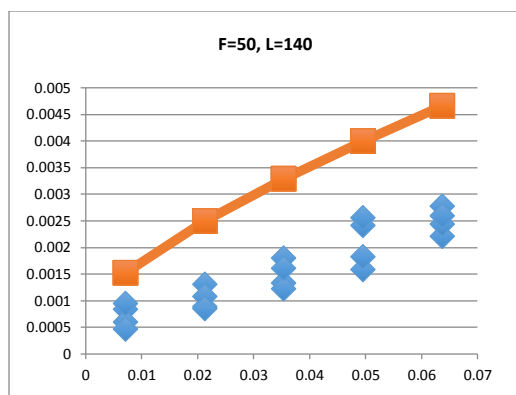
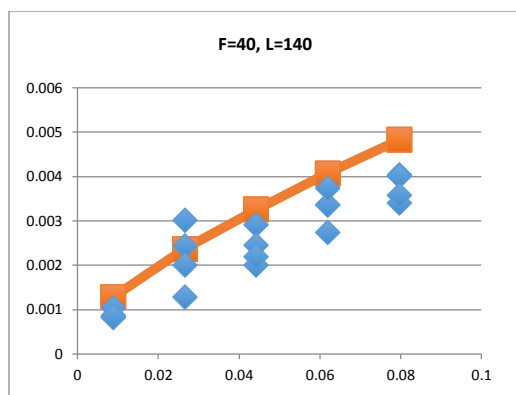




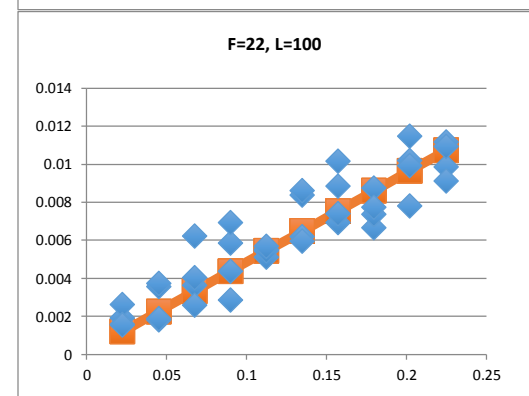
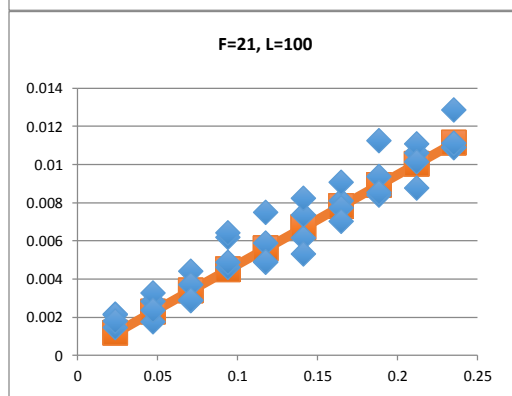
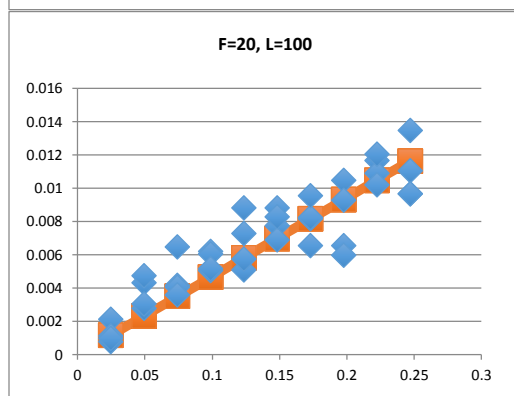
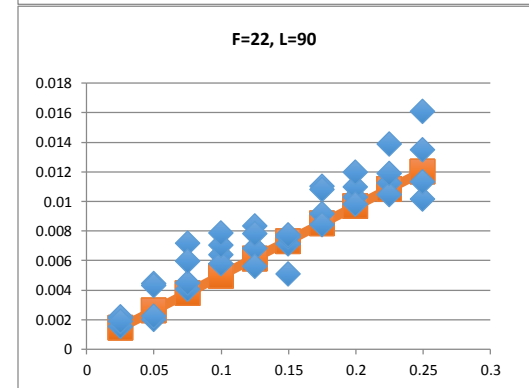
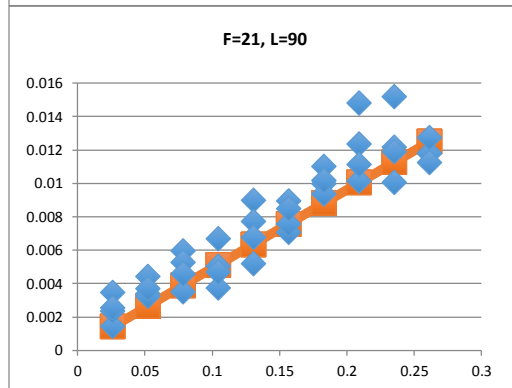
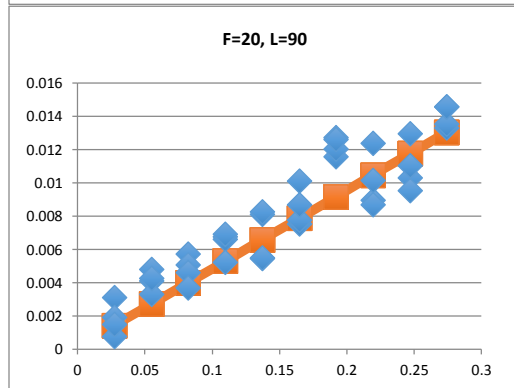
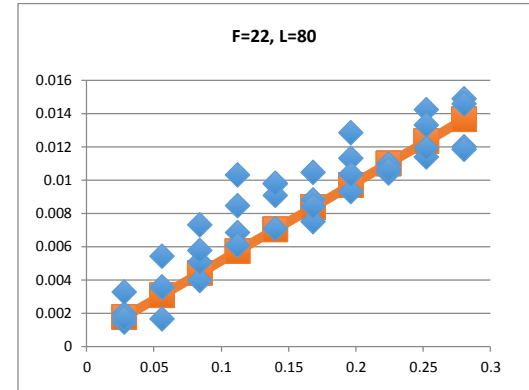
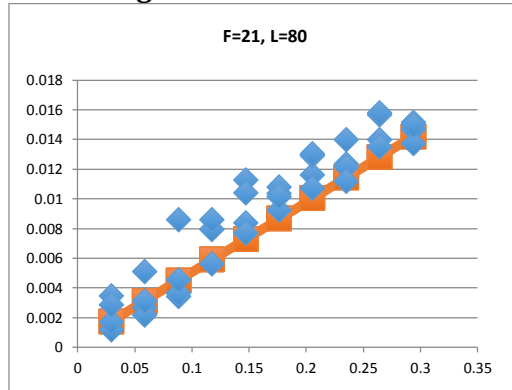
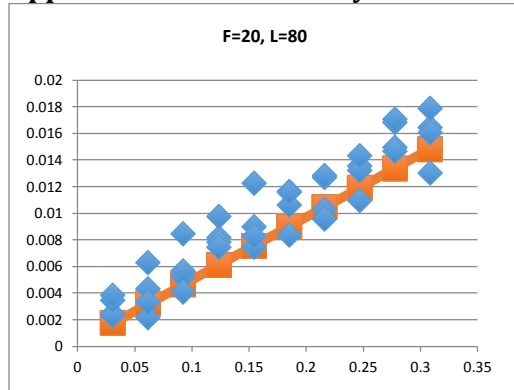


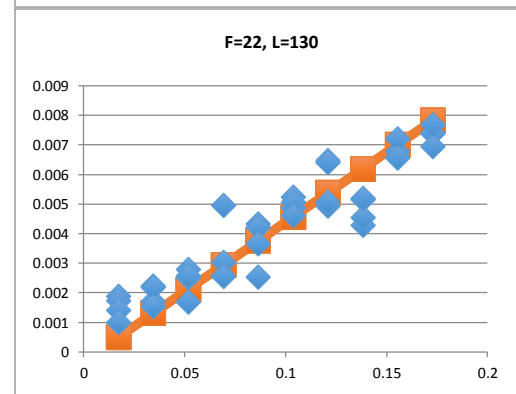
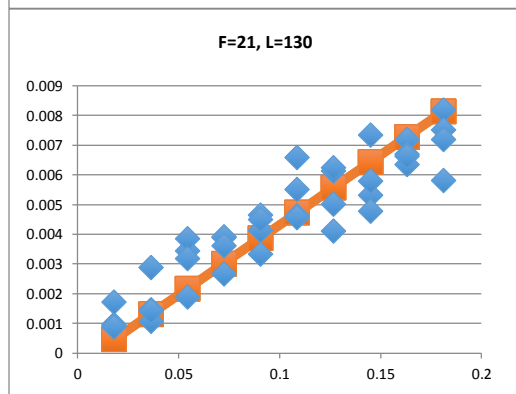
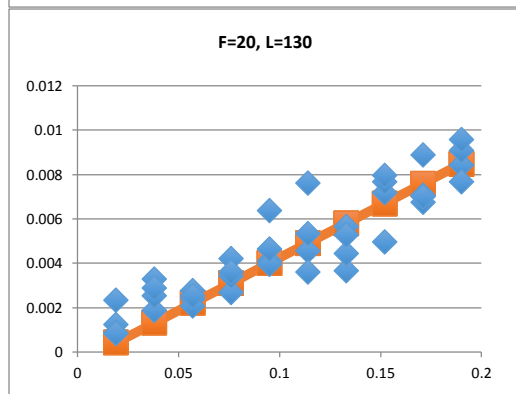
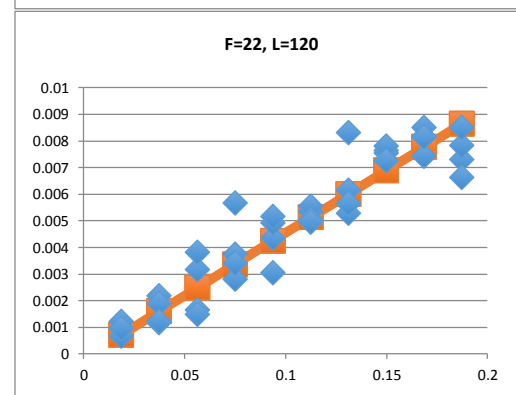
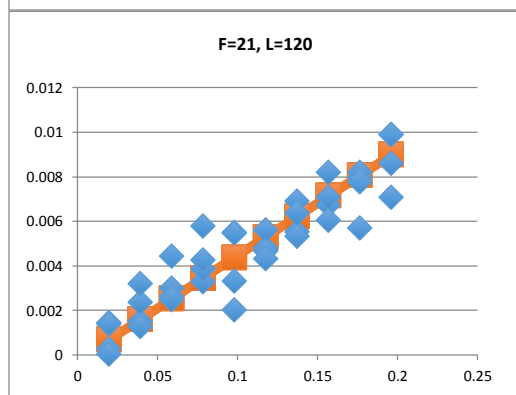
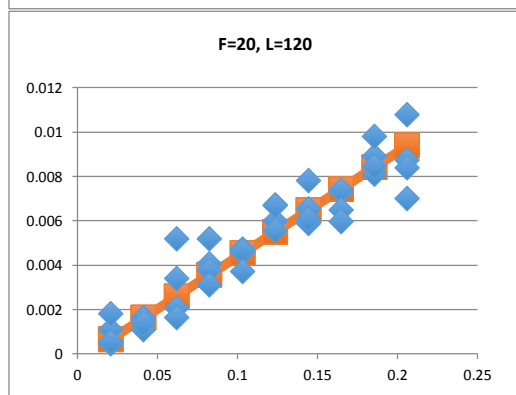
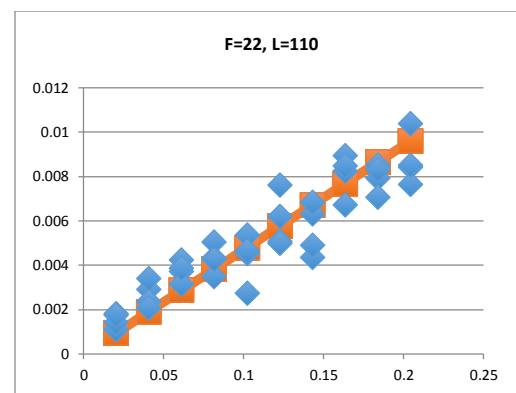
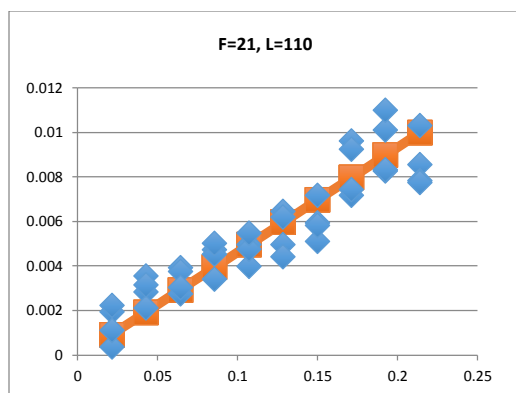
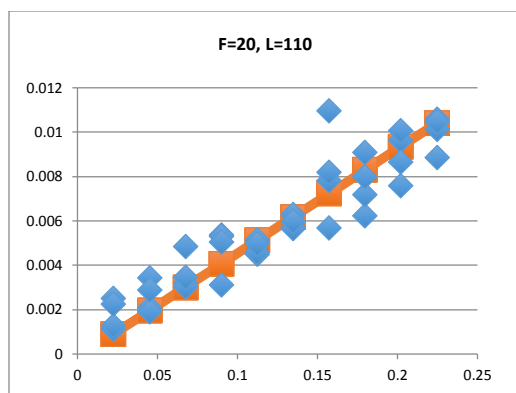
Appendix E - UPM Extended Case Studies with High Order Regression - Tall Buildings

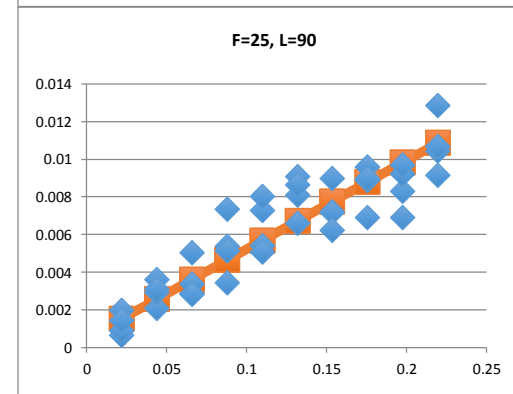
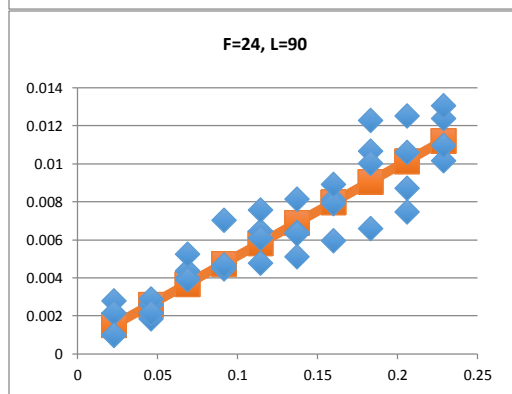
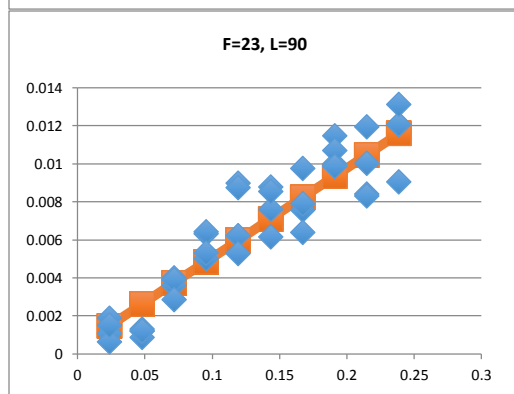
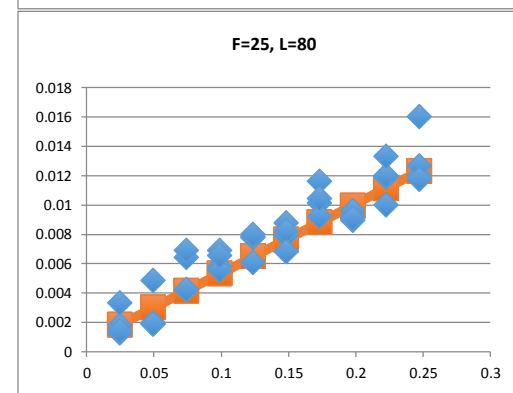
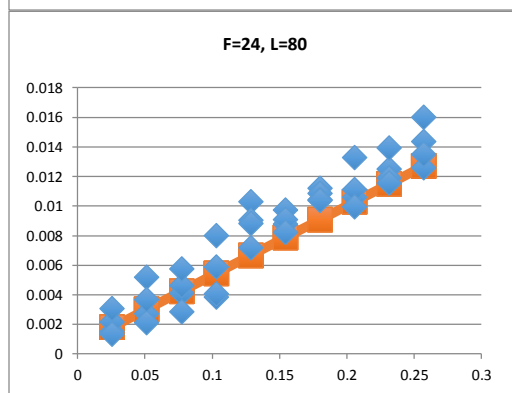
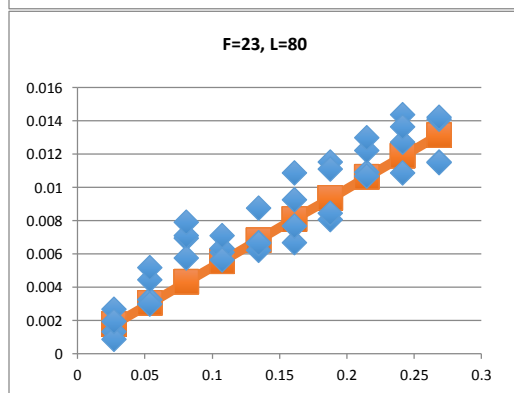
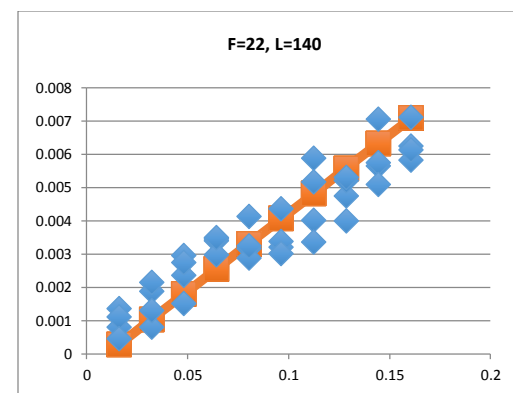
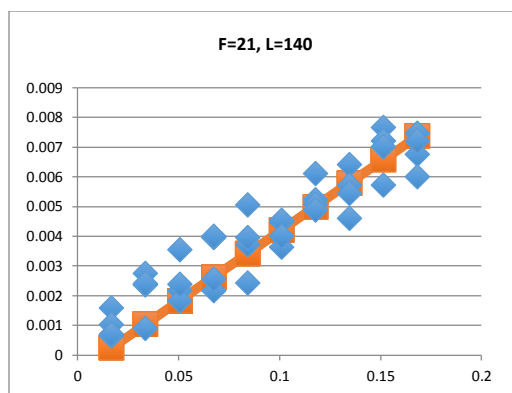
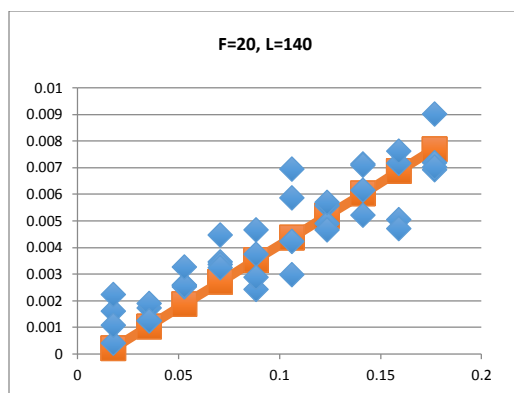


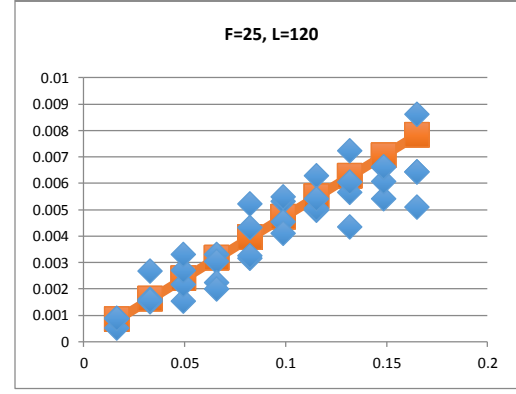
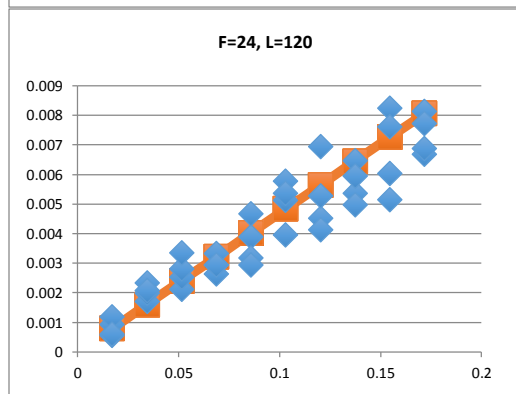
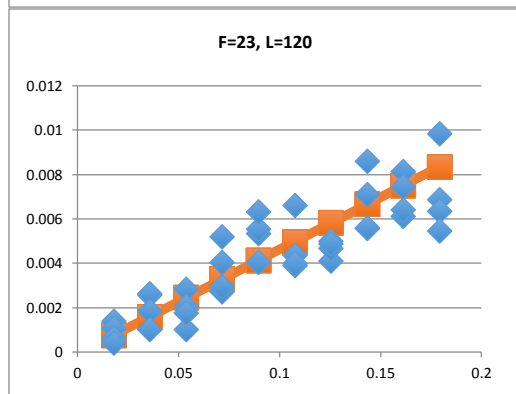
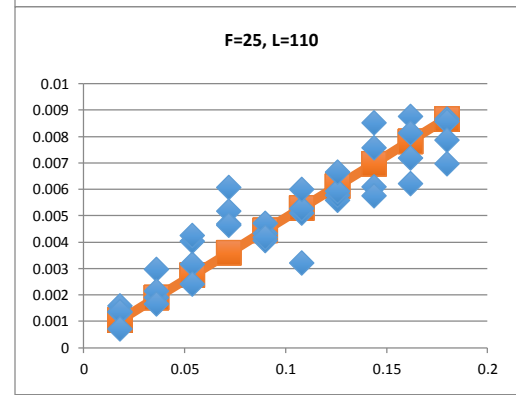
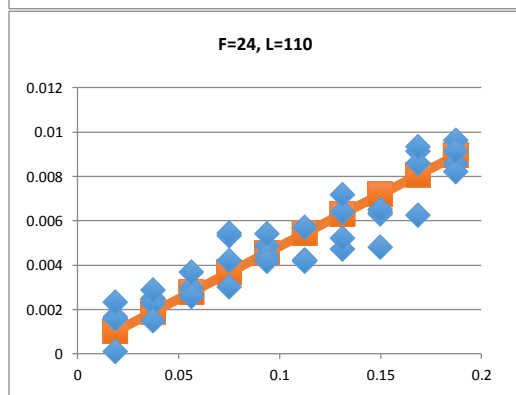
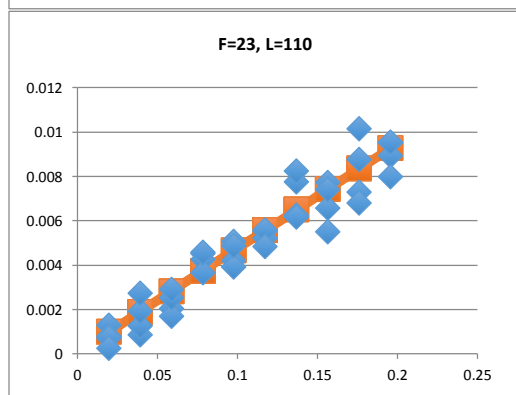
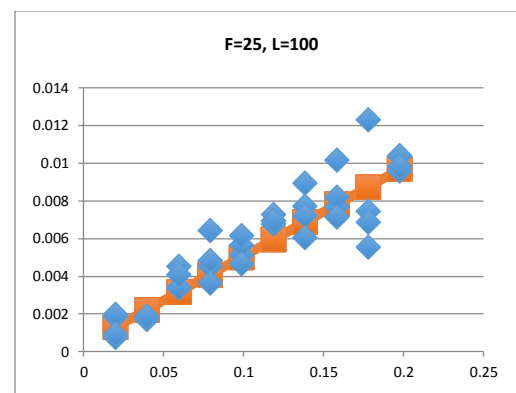
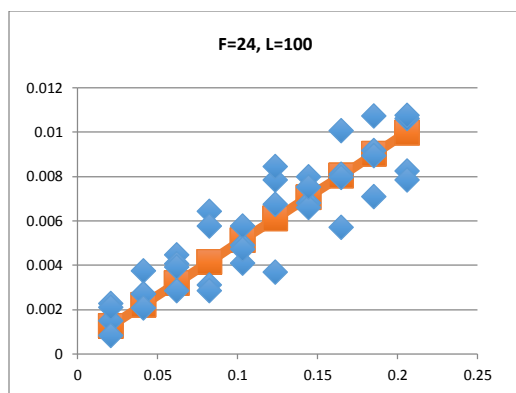
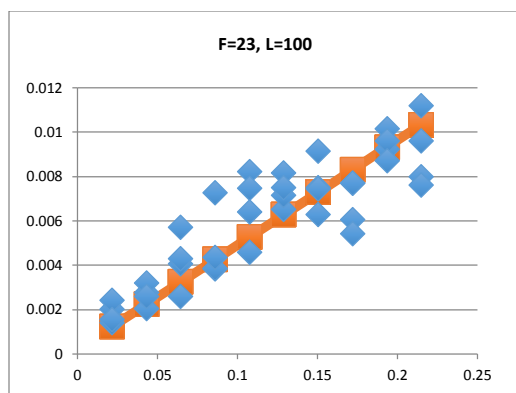


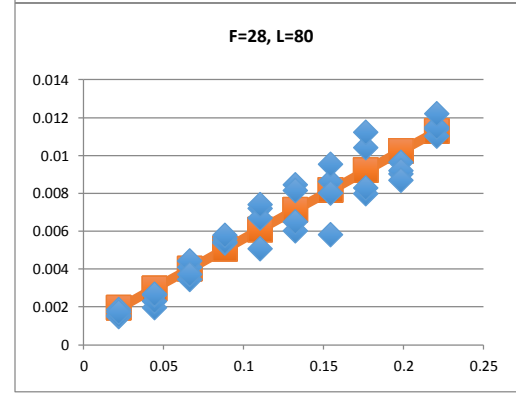
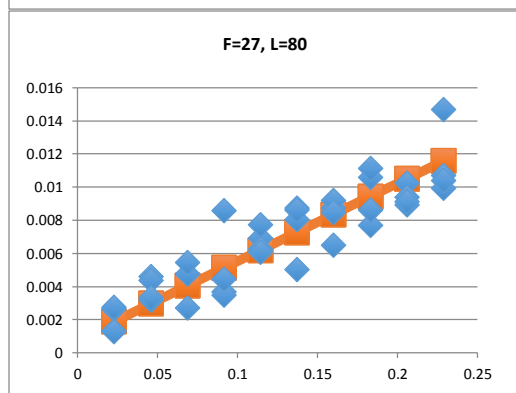
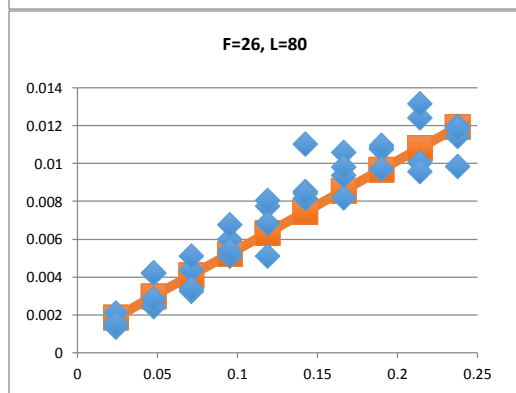
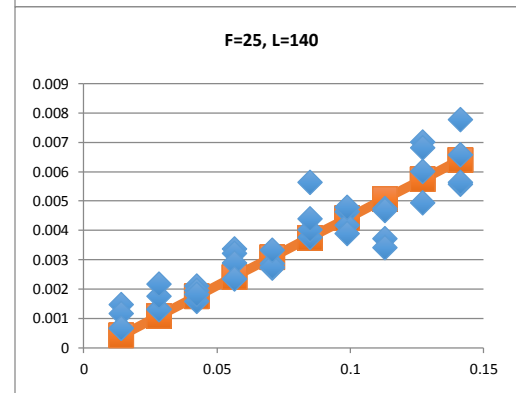
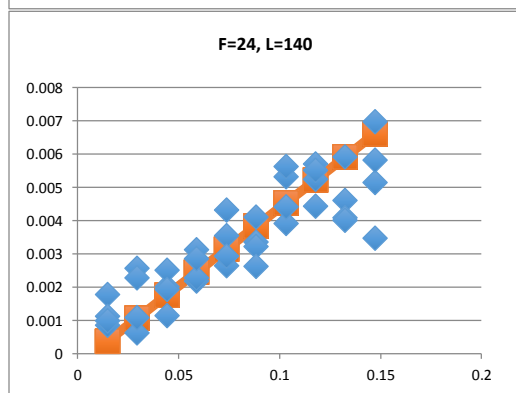
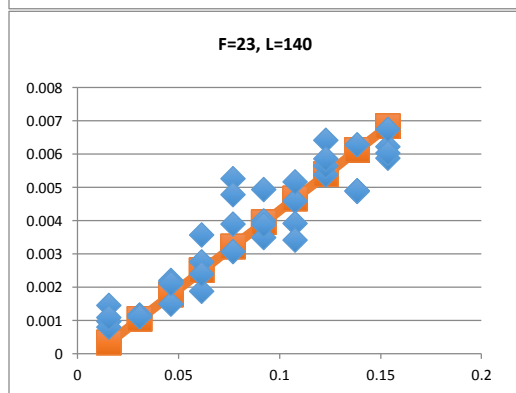
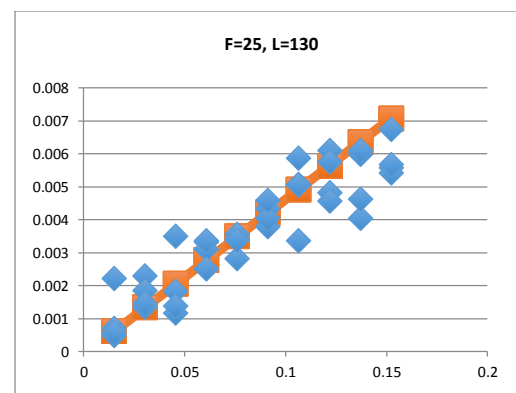
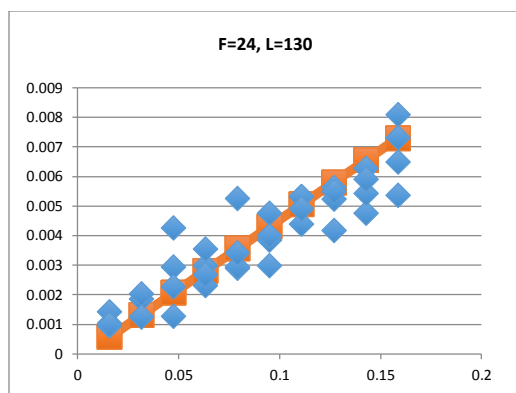
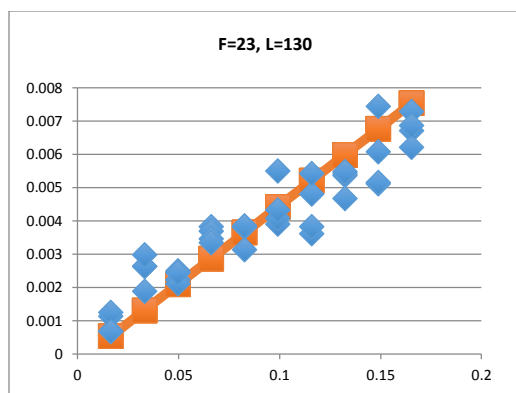
Appendix F – GPM Primary Case Studies with Linear Regression

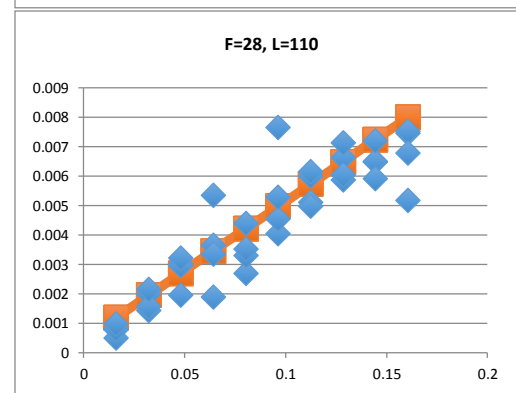
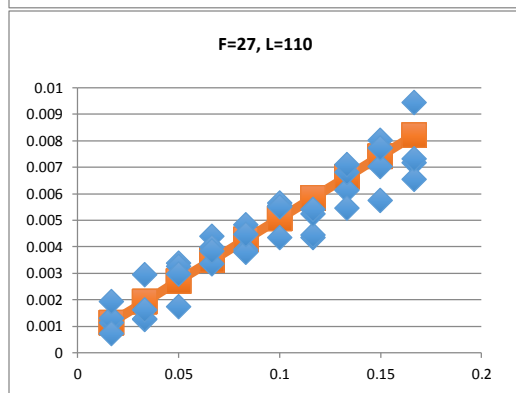
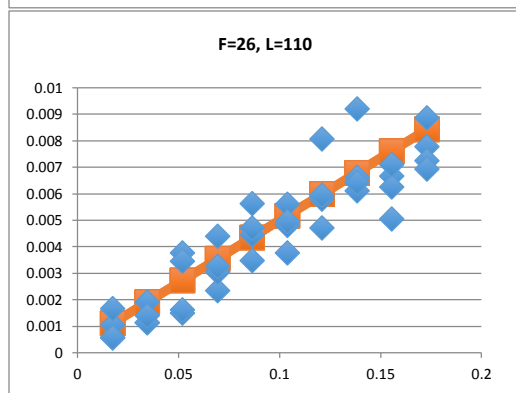
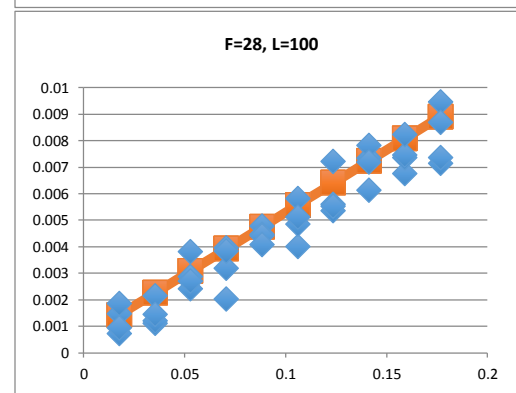
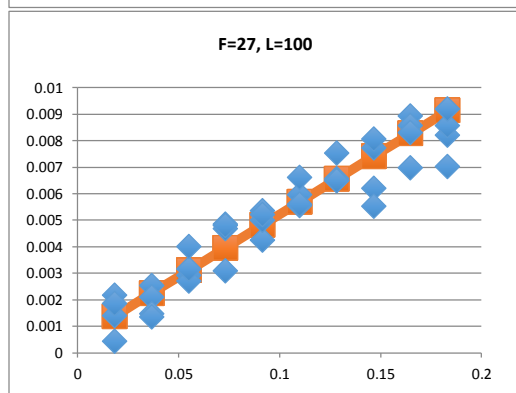
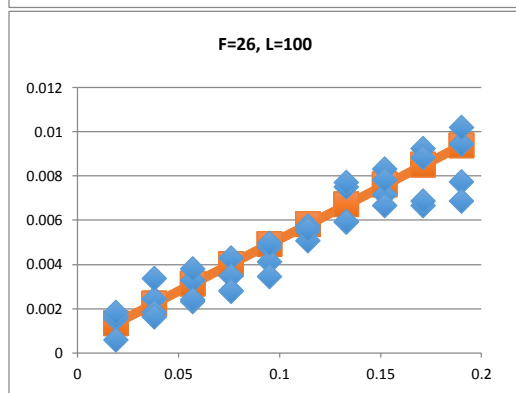
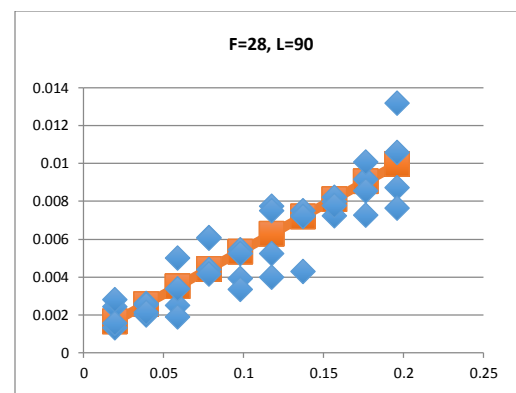
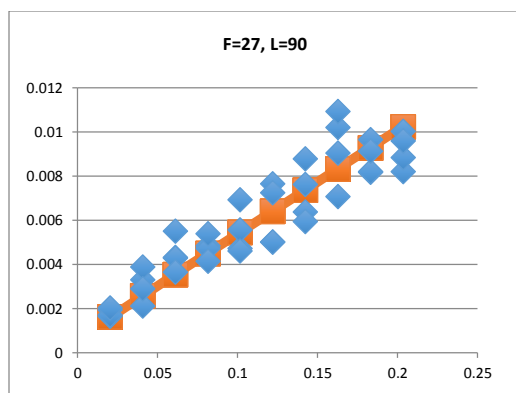
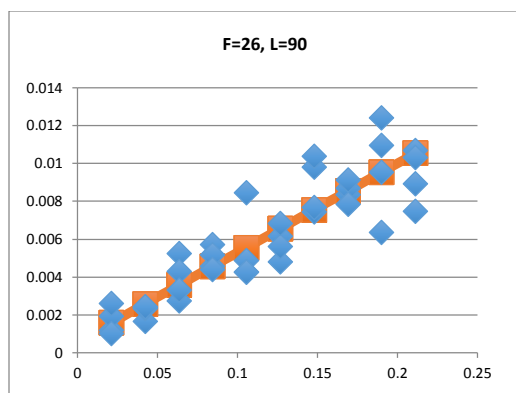


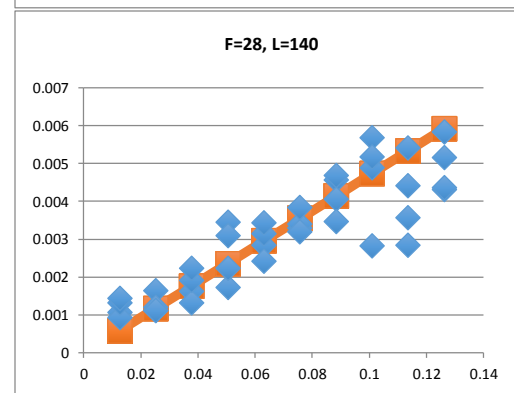
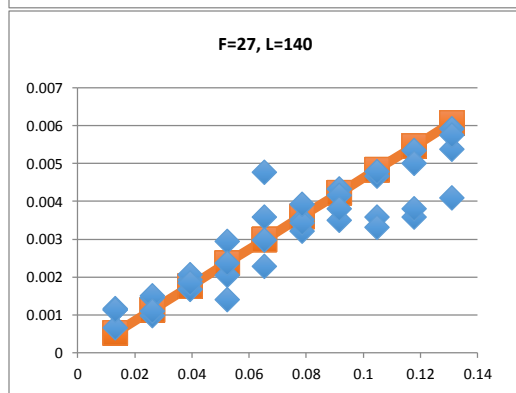
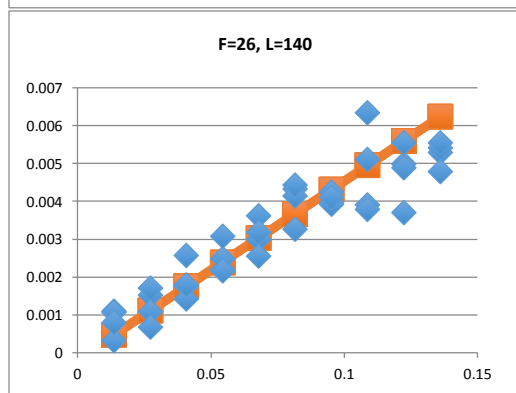
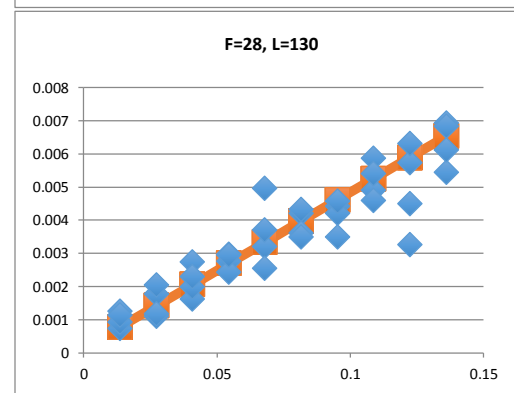
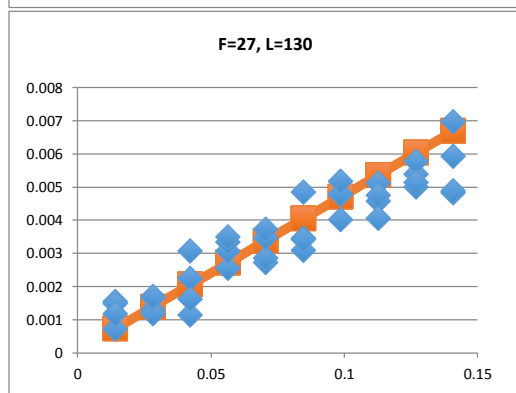
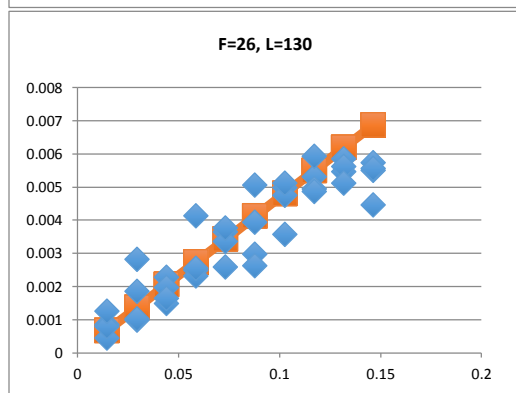
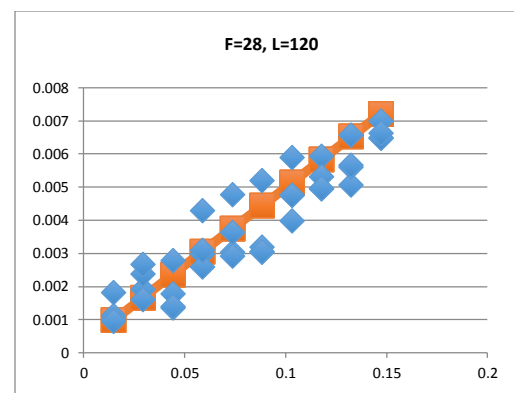
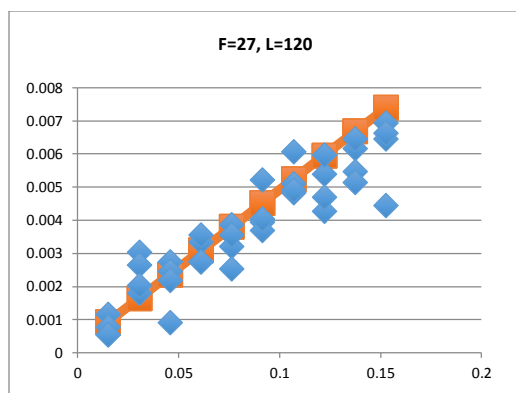
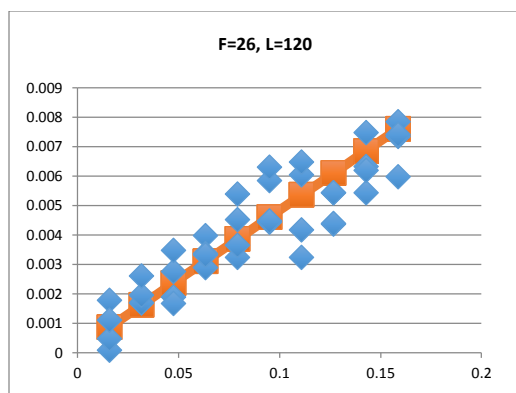


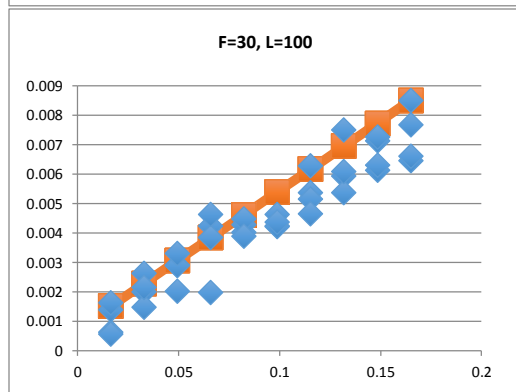
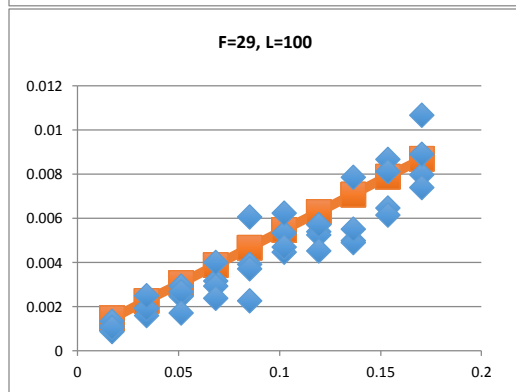
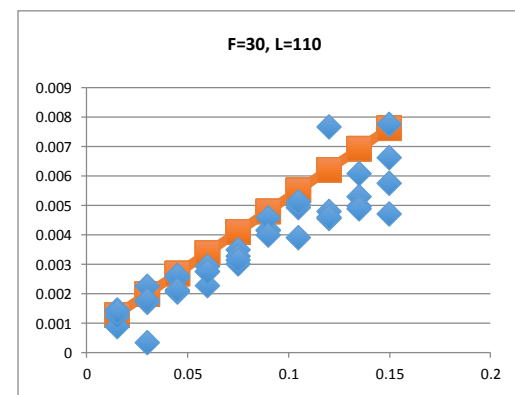
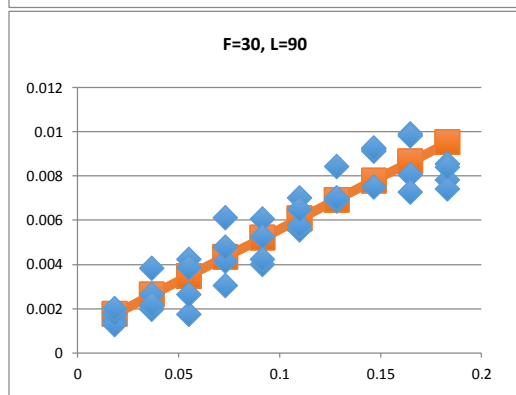
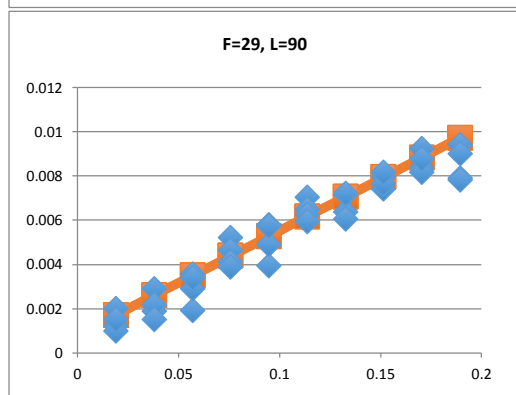
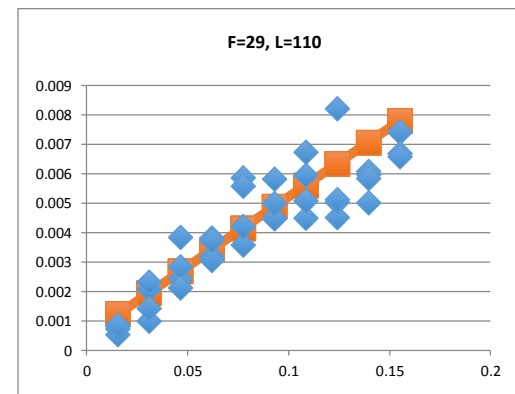
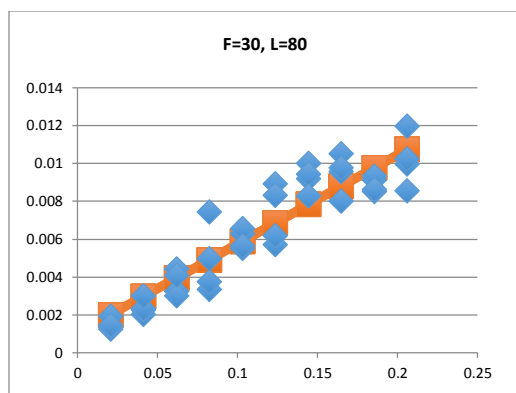
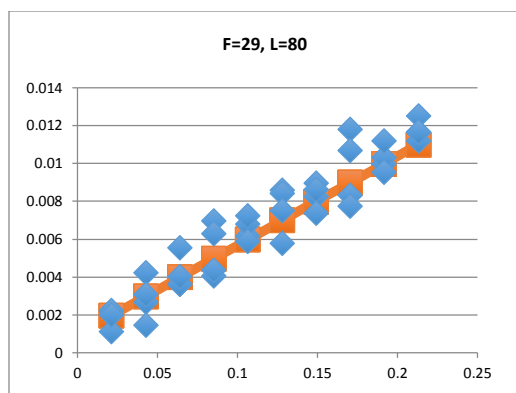


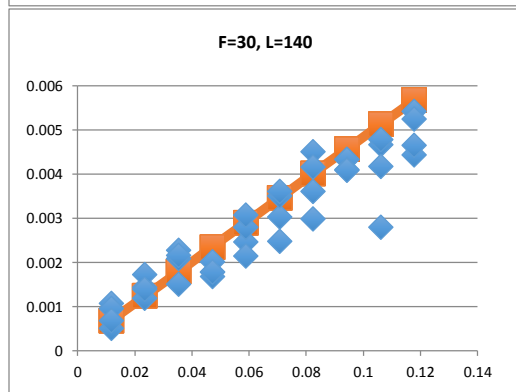
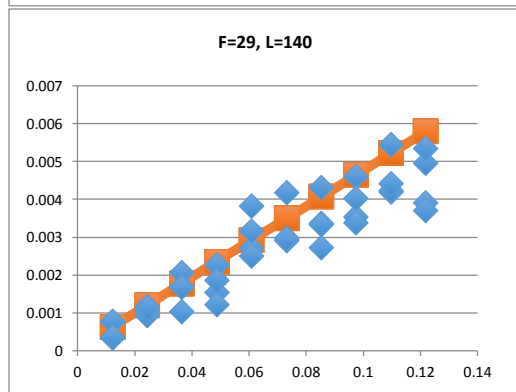
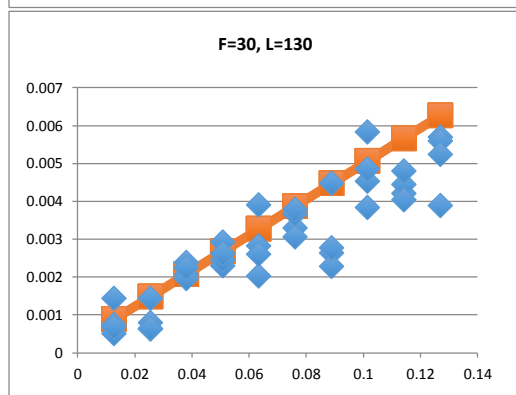
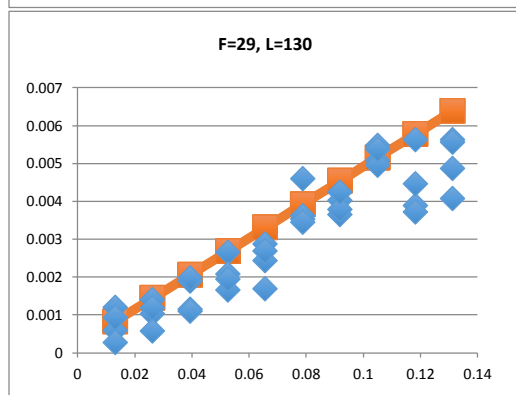
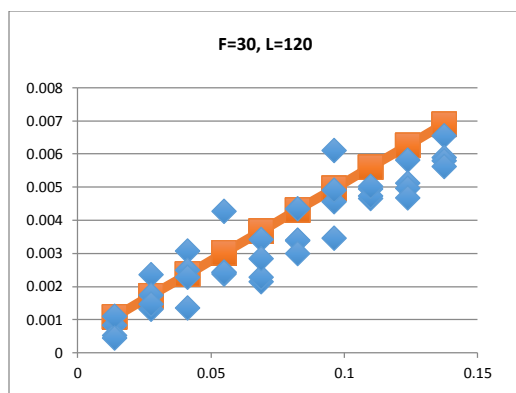
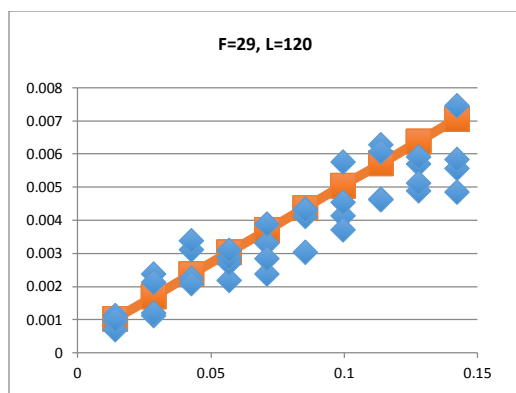


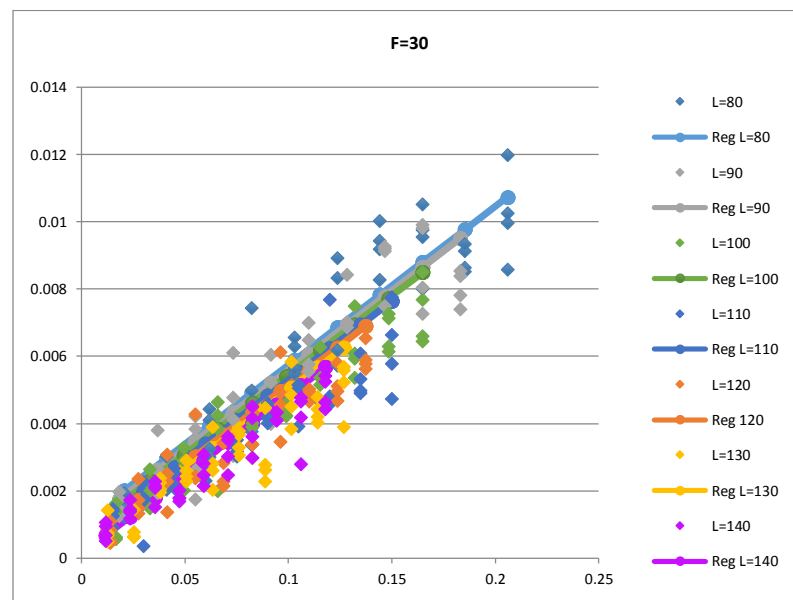
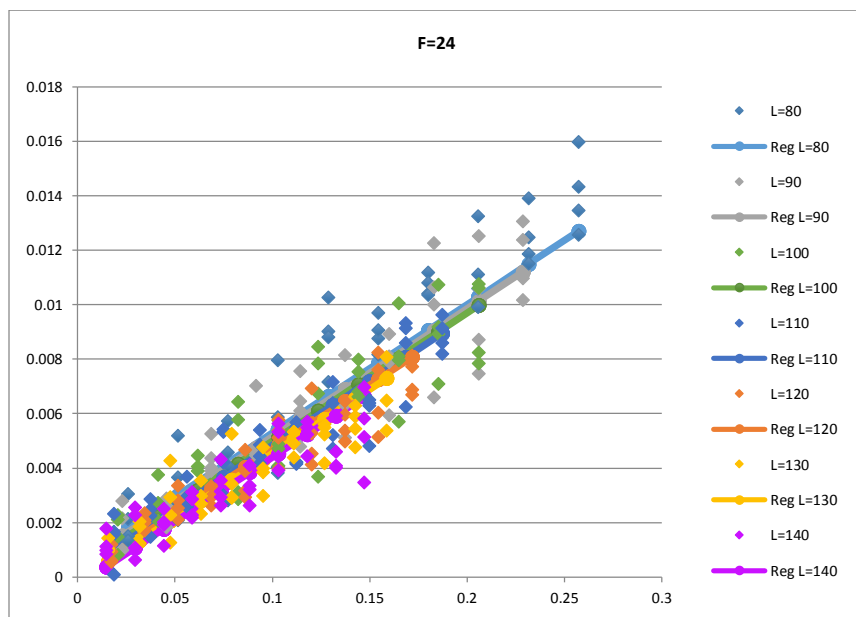
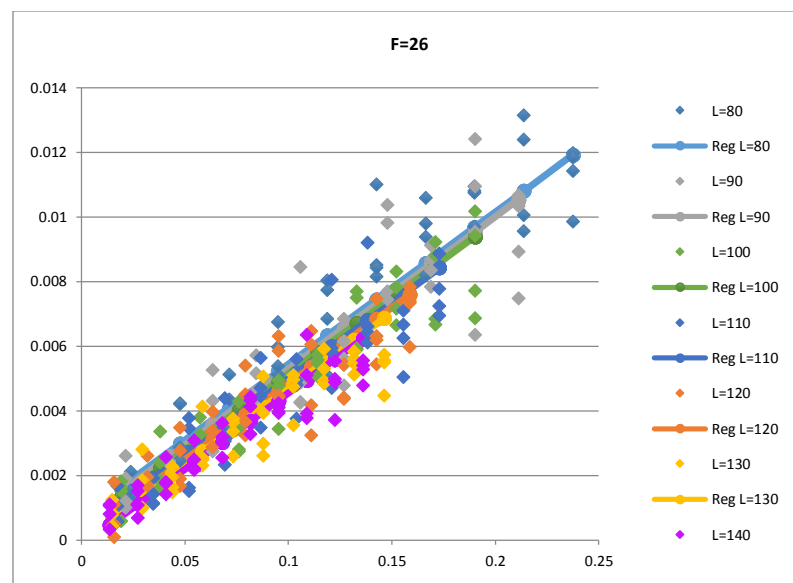
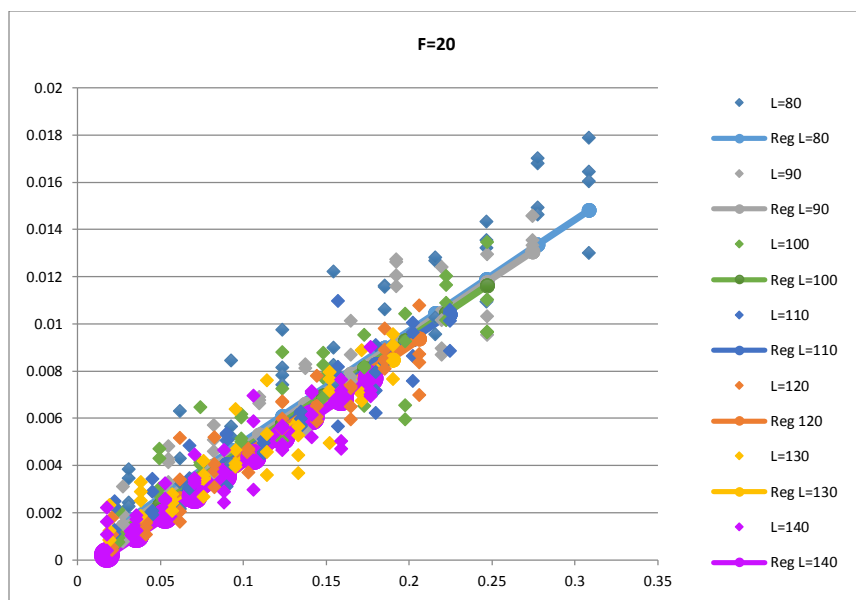


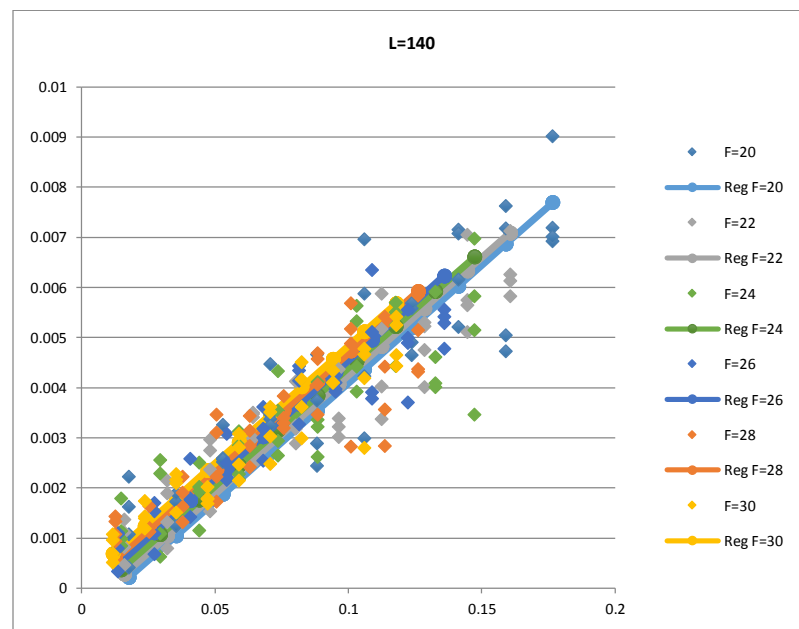
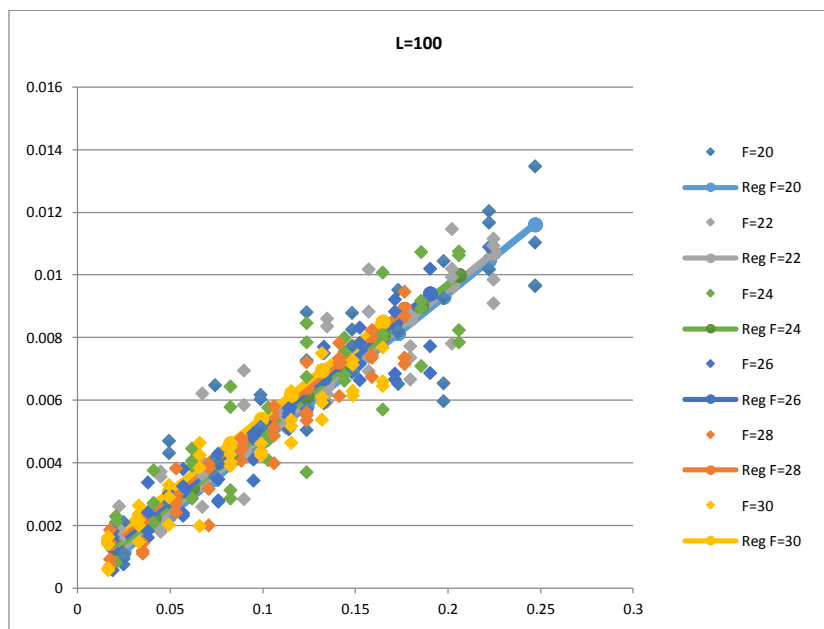
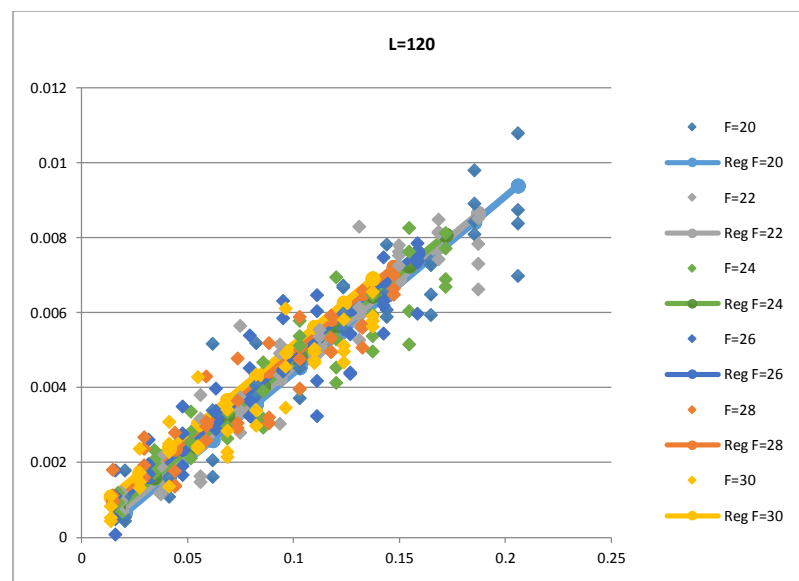
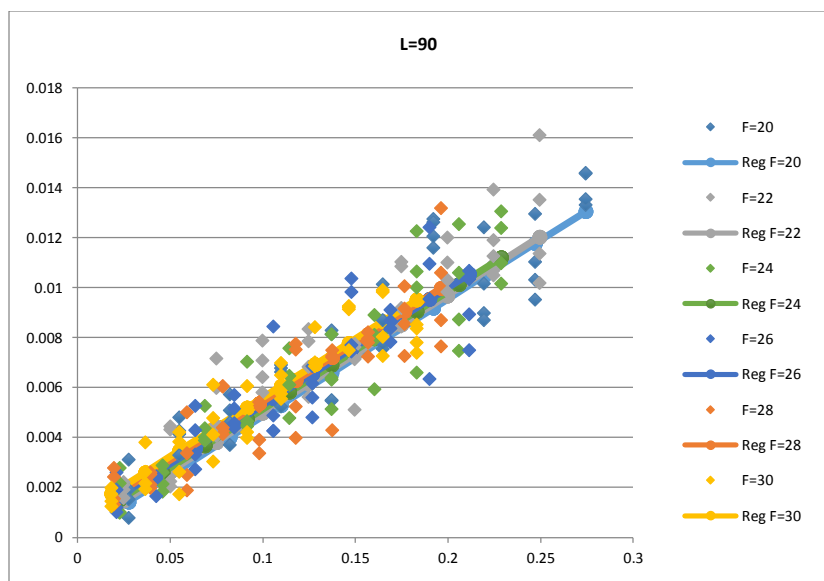




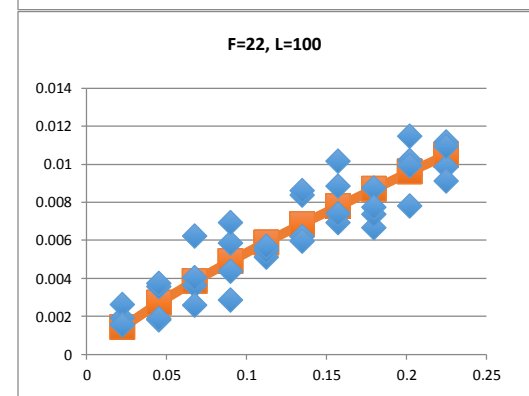
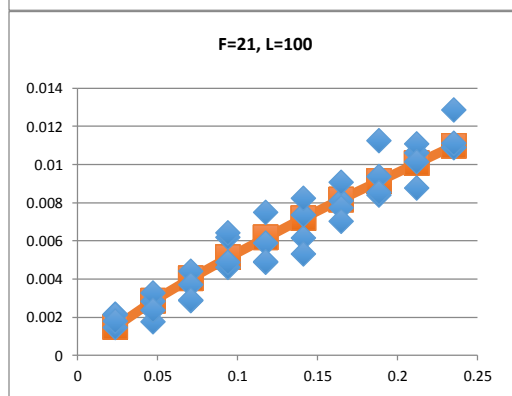
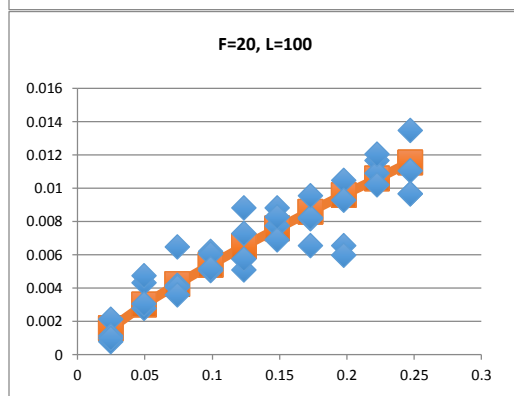
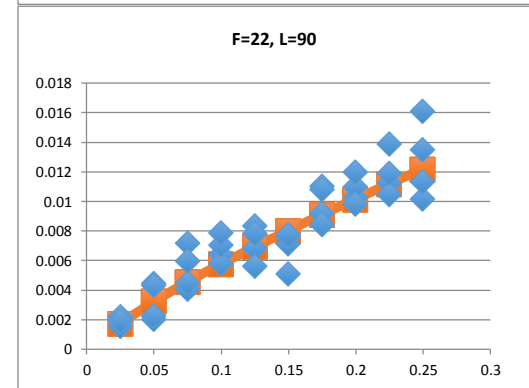
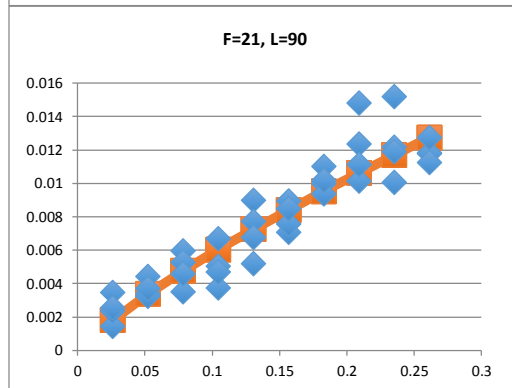
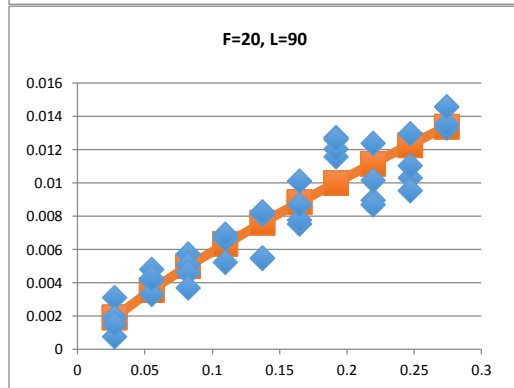
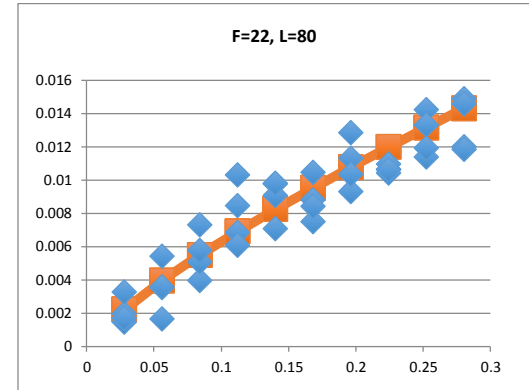
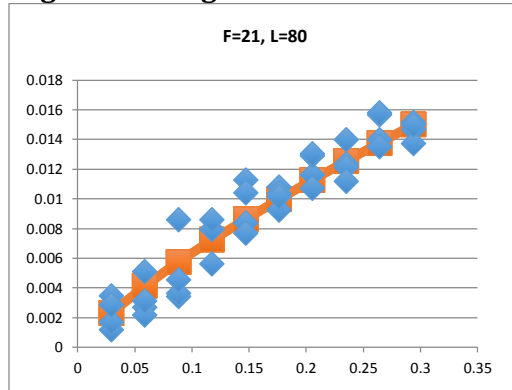
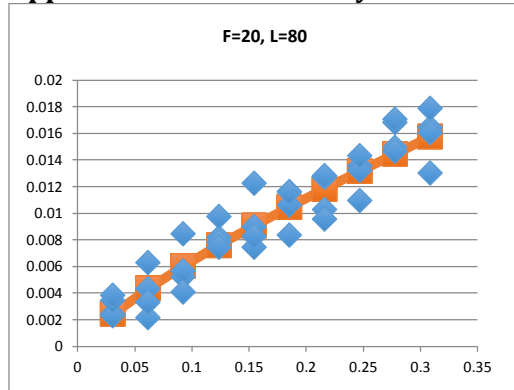


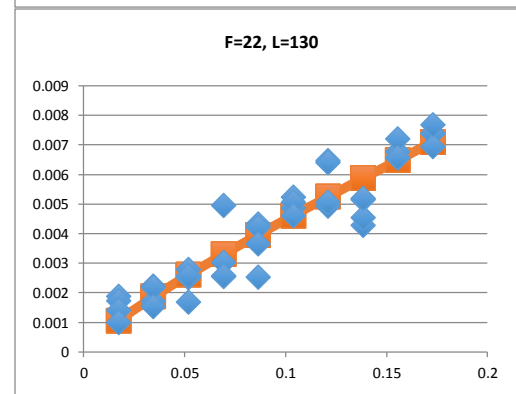
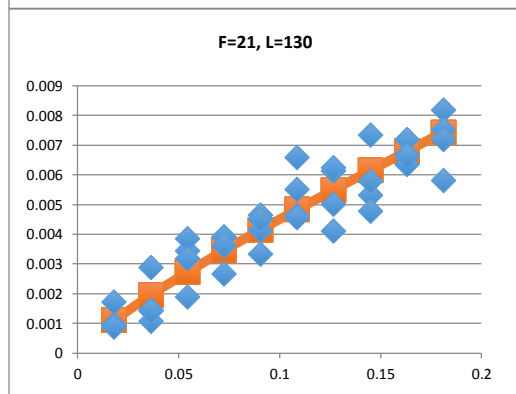
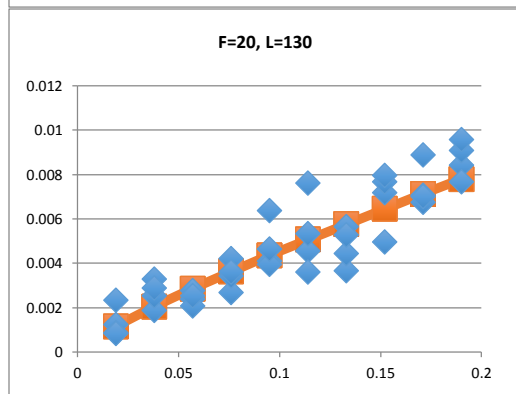
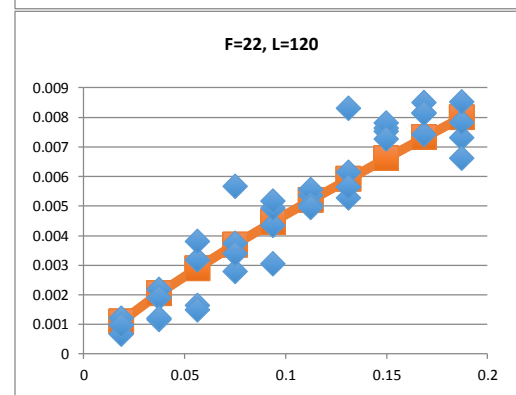
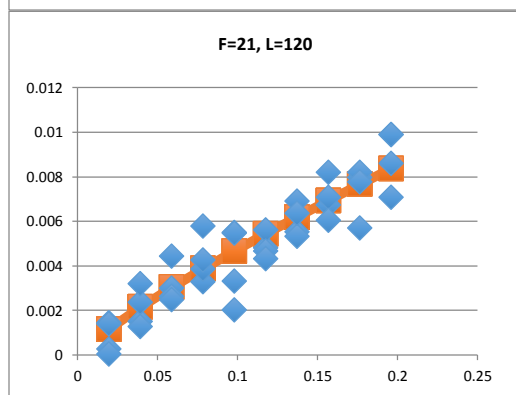
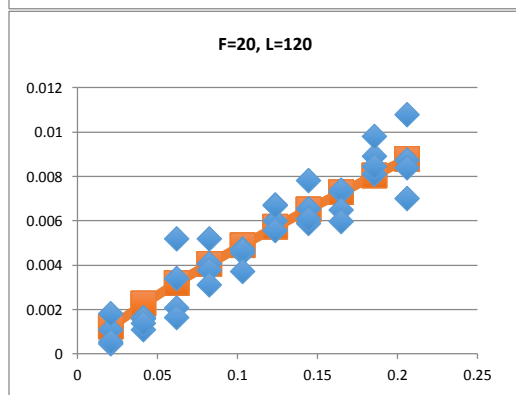
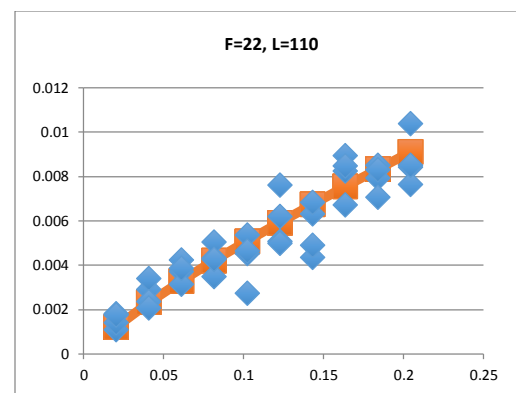
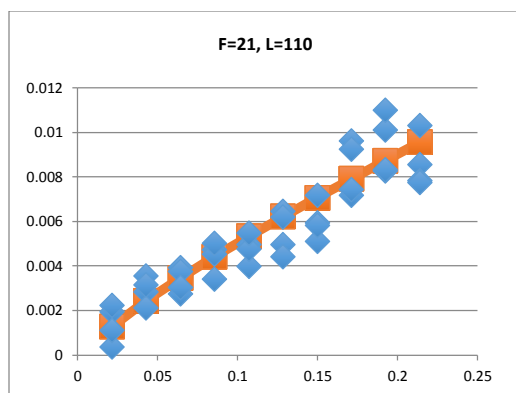
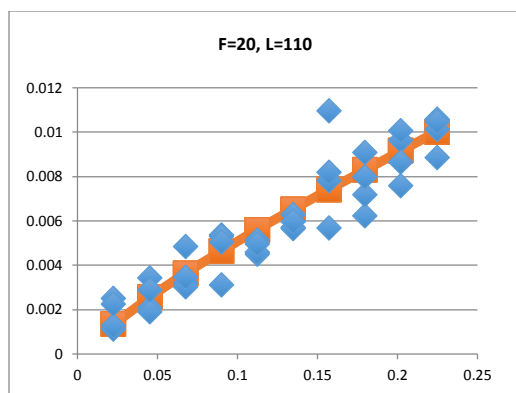


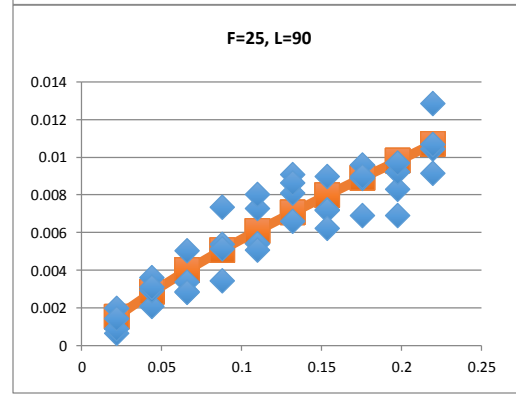
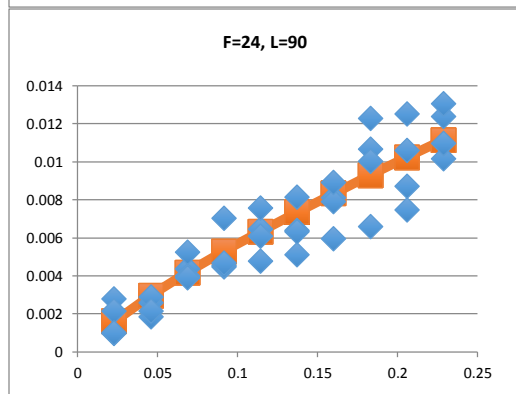
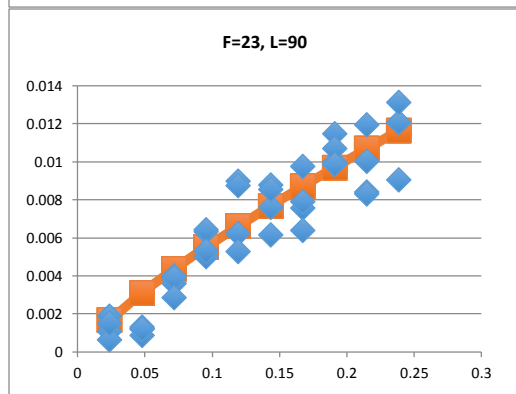
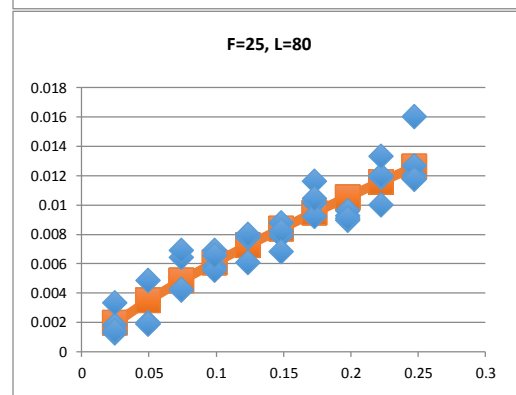
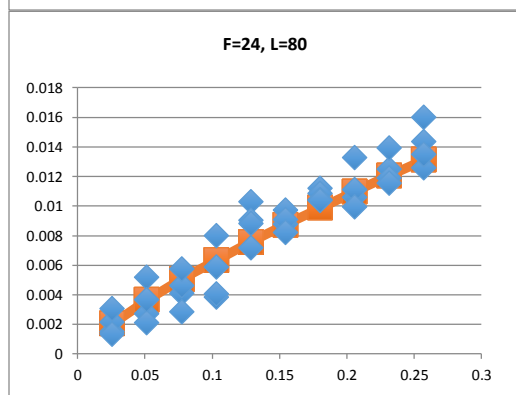
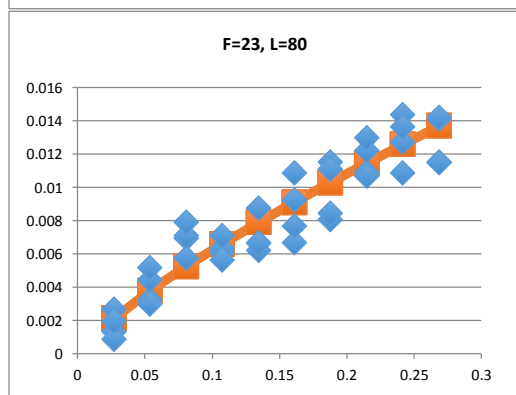
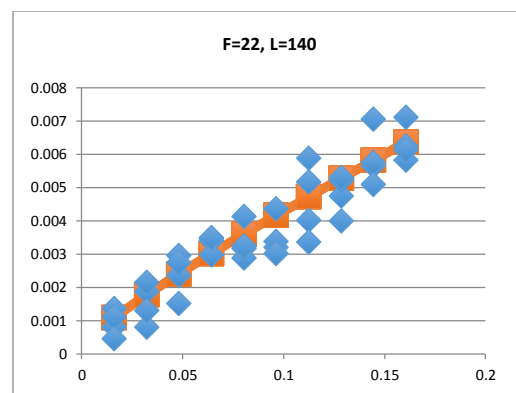
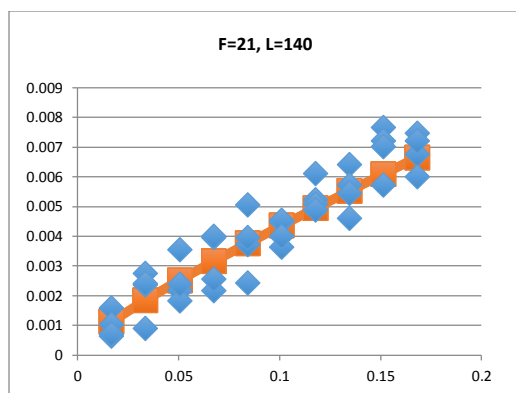
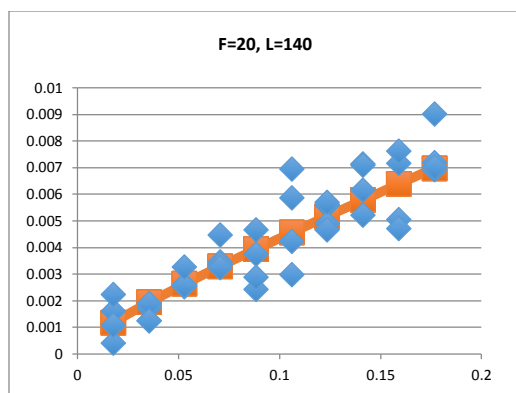


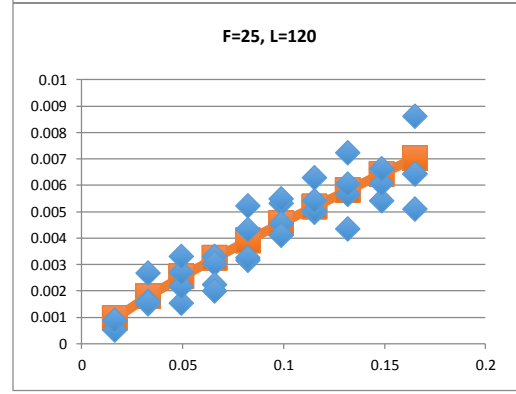
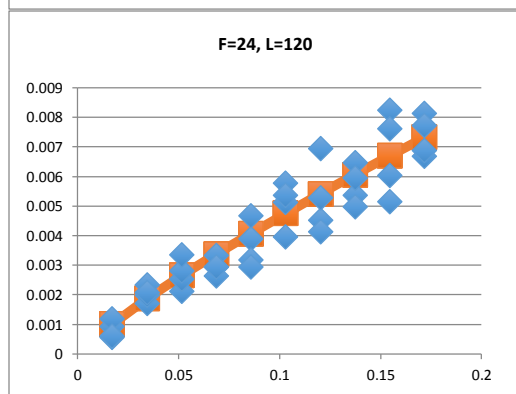
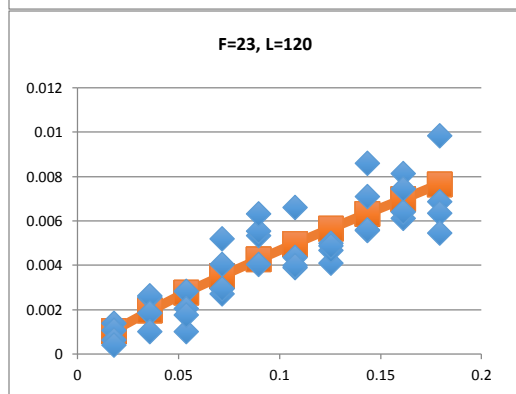
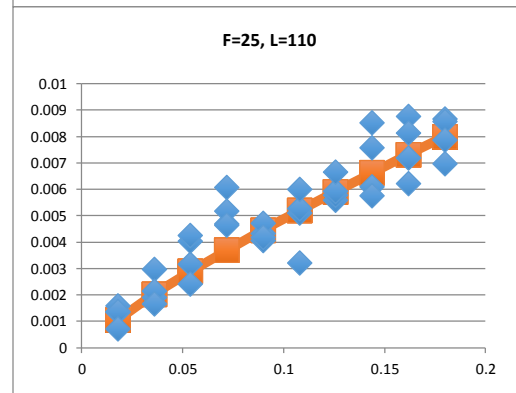
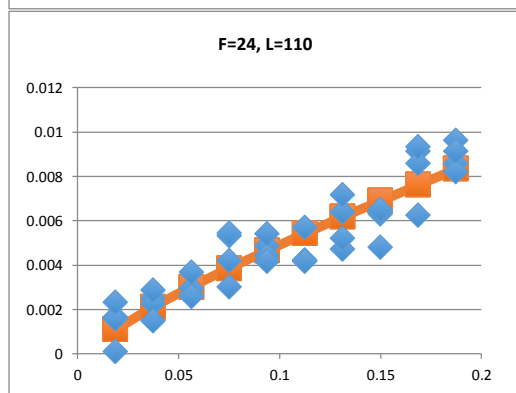
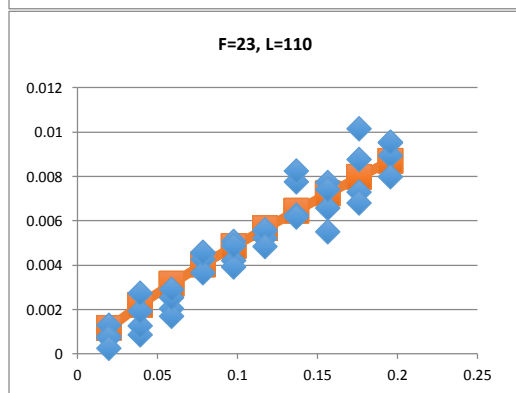
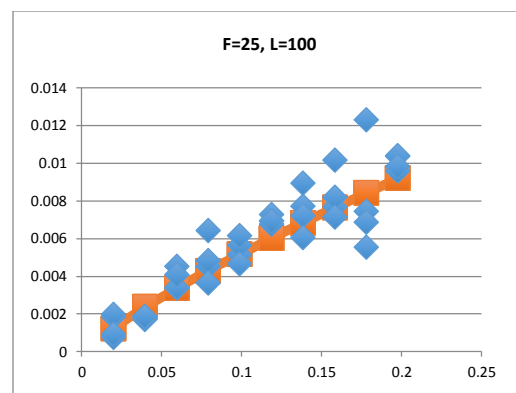
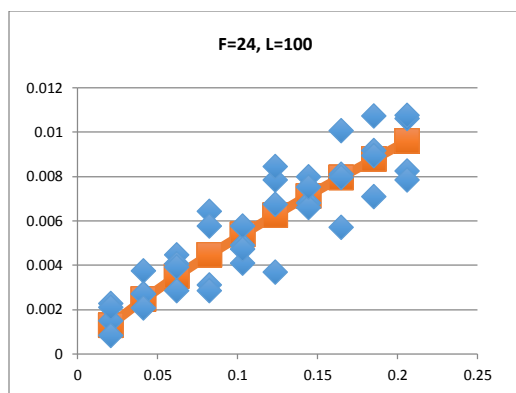
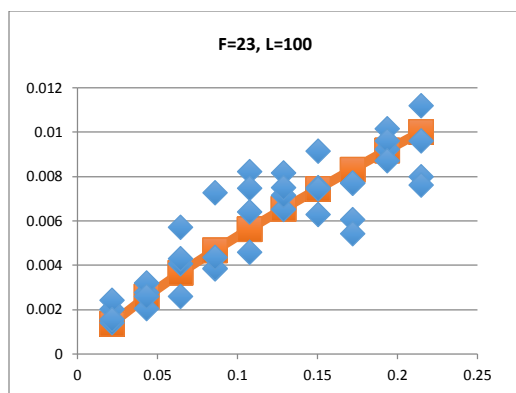


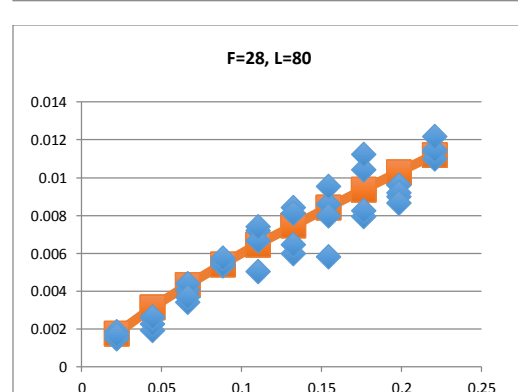
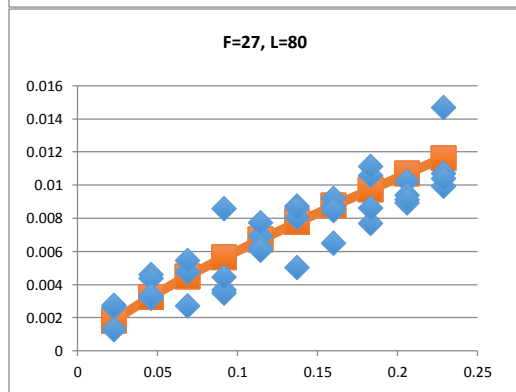
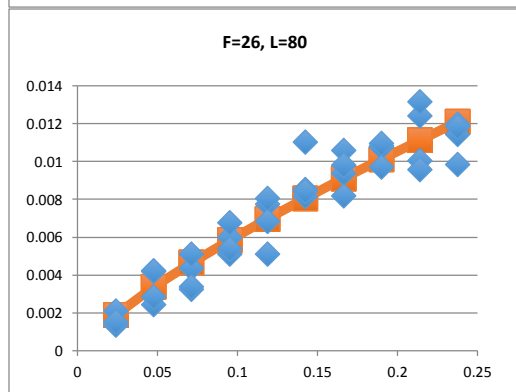
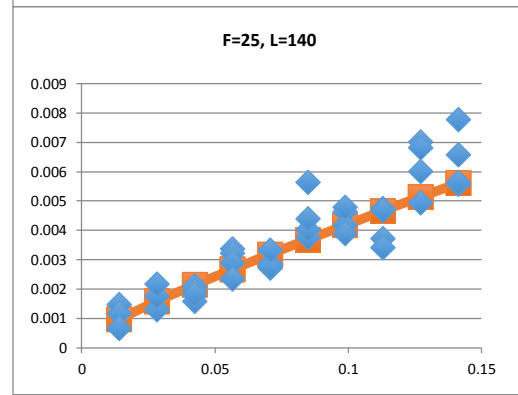
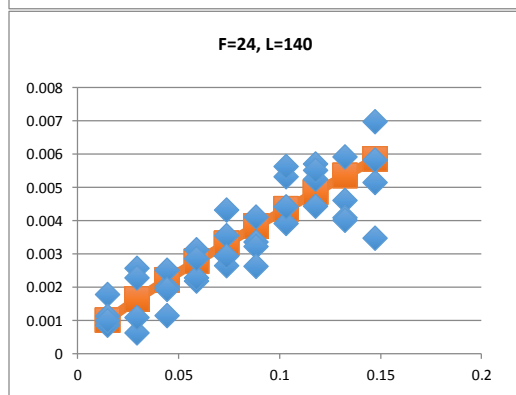
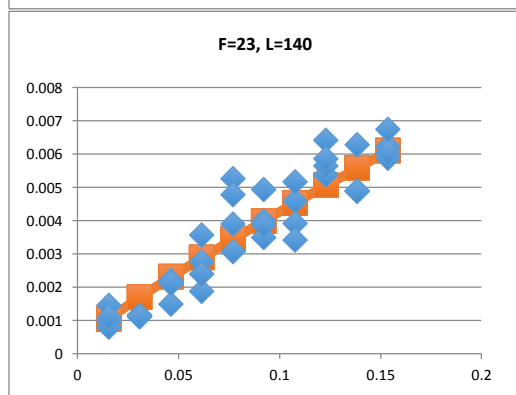
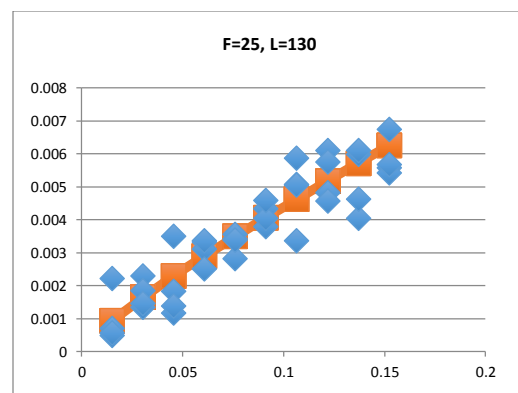
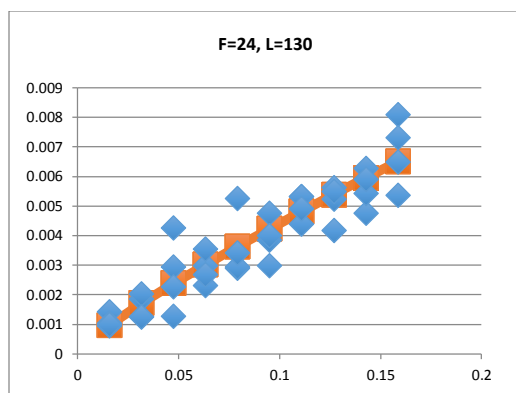
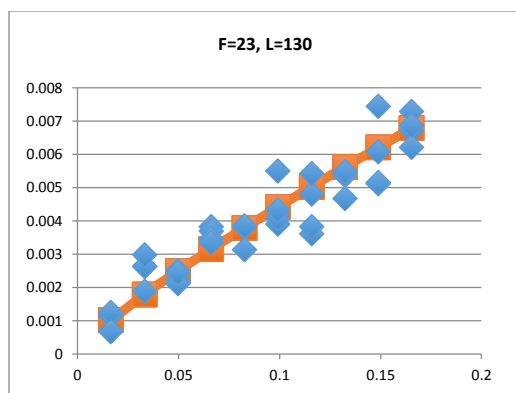
Appendix G – GPM Primary Case Studies with High Order Regression

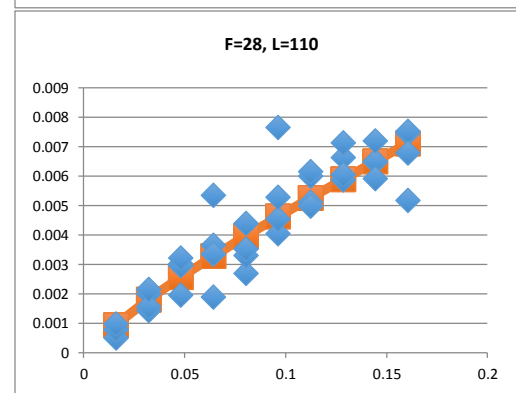
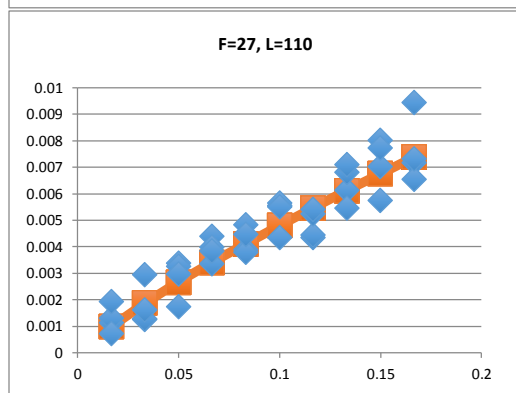
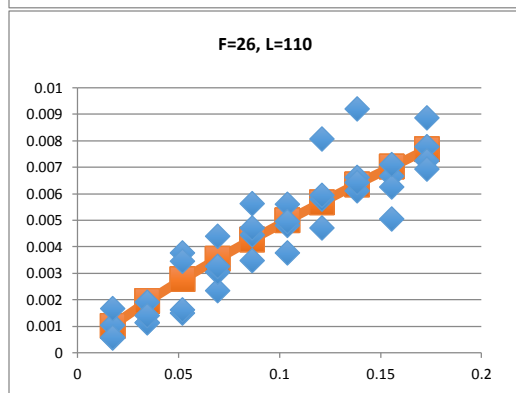
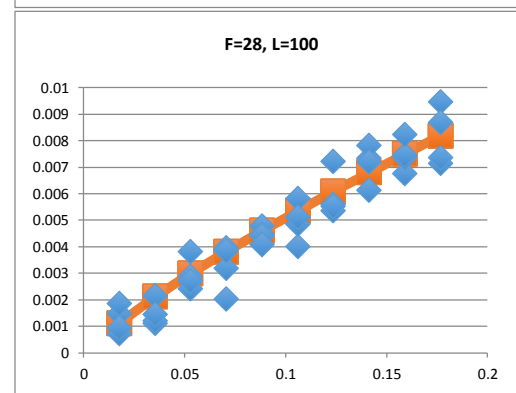
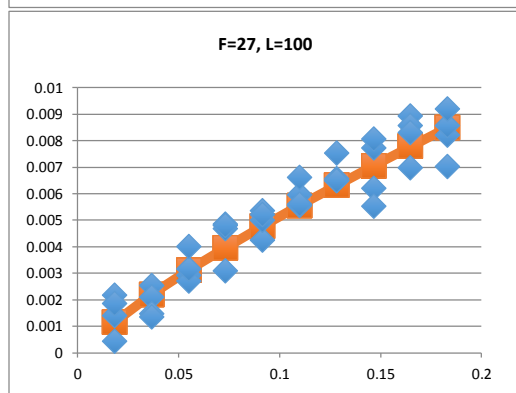
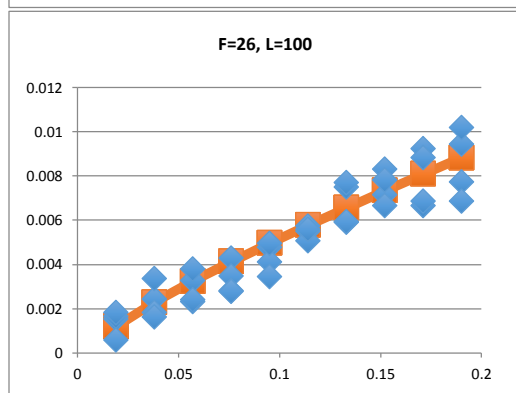
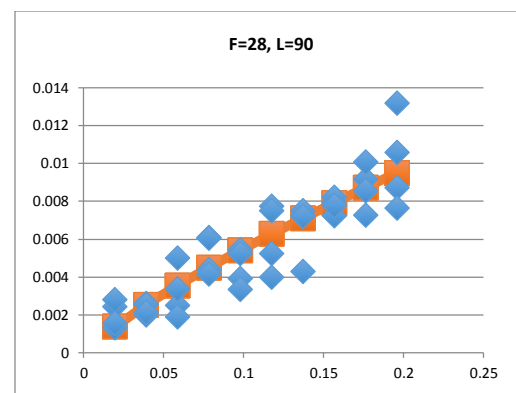
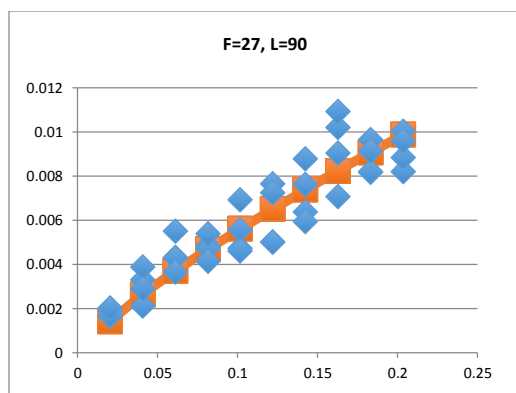
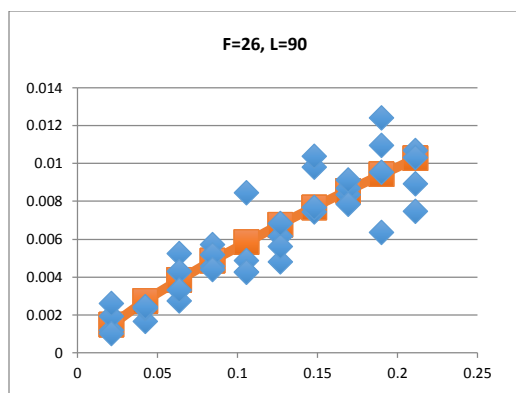


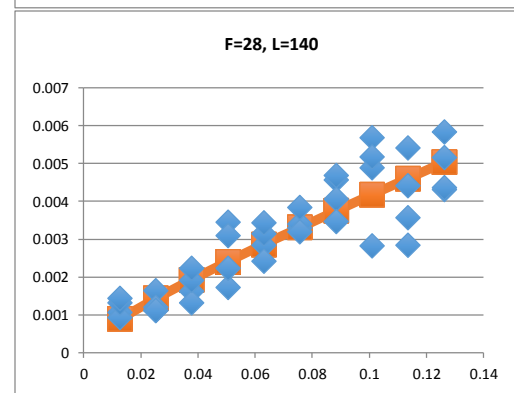
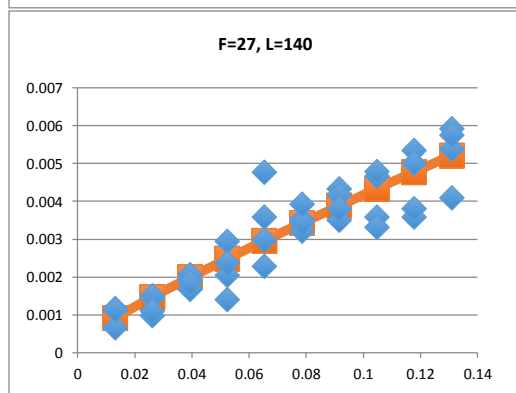
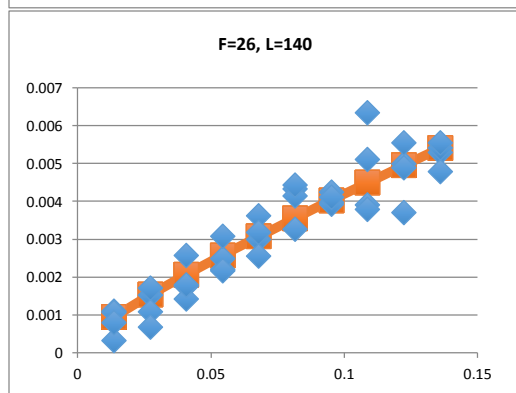
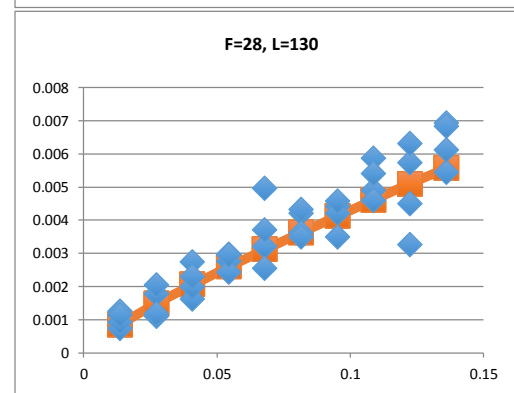
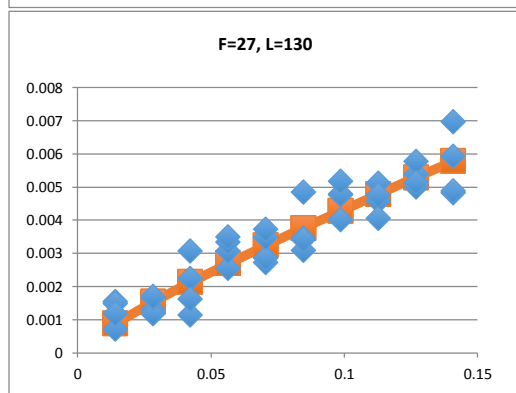
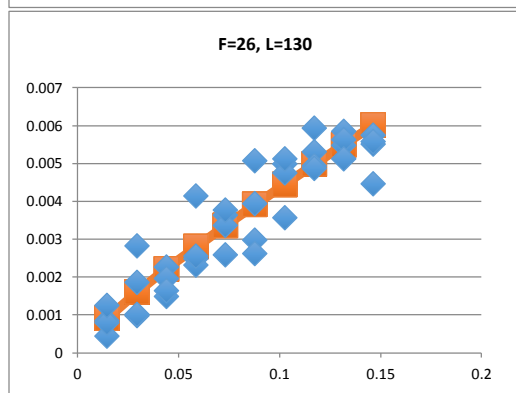
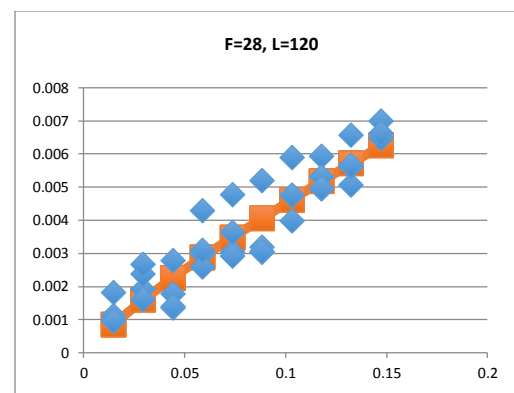
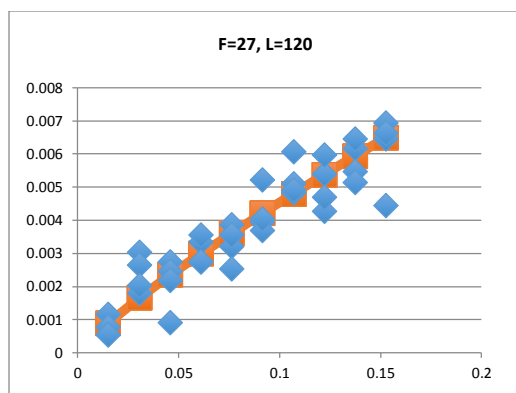
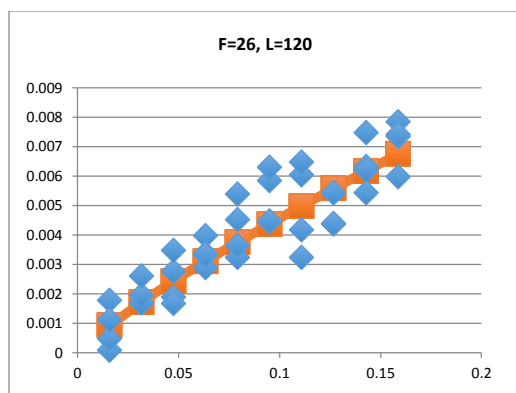


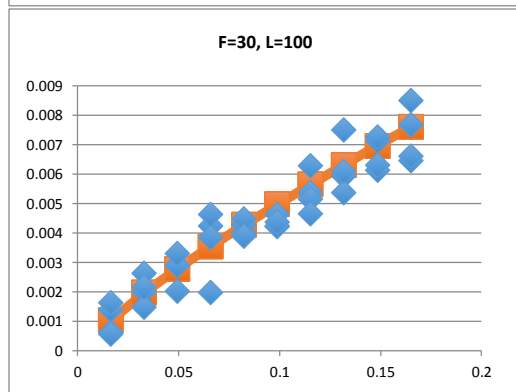
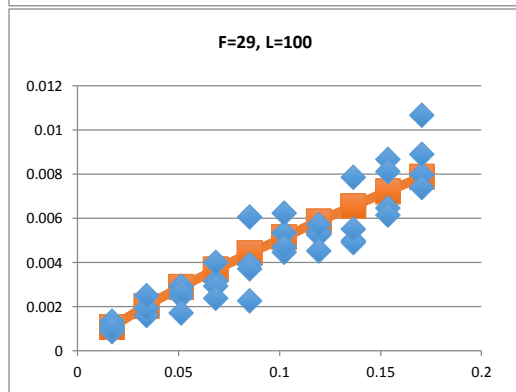
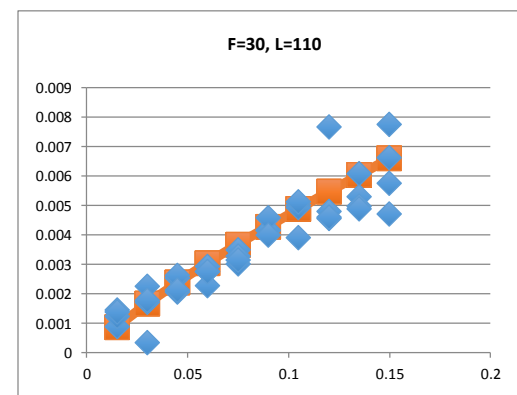
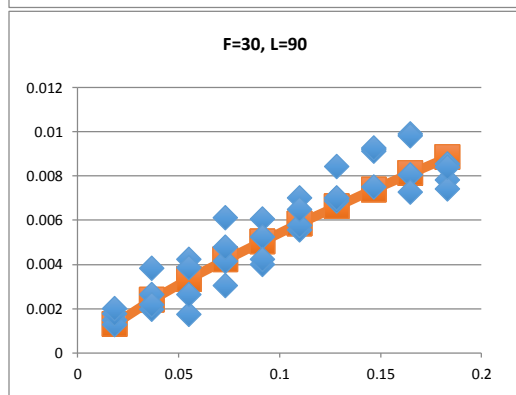
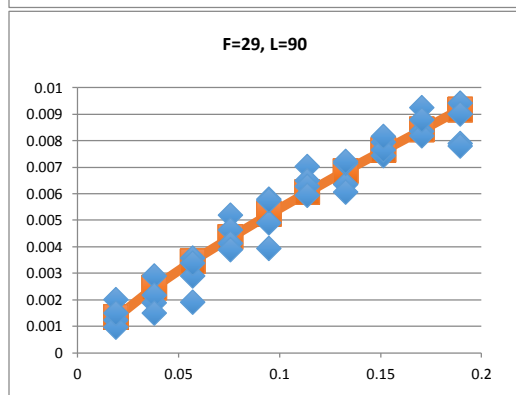
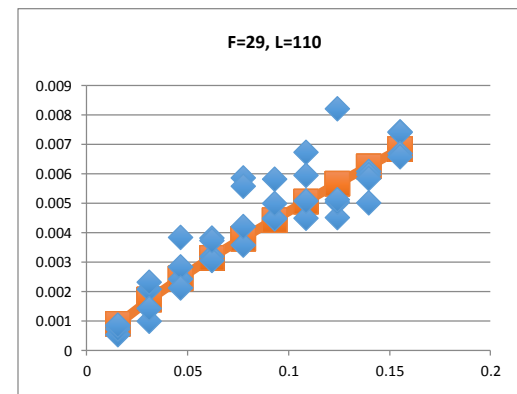
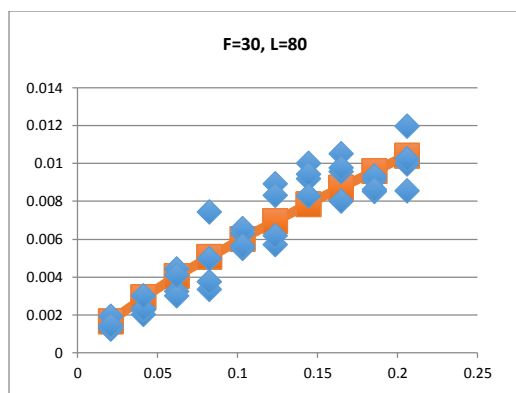
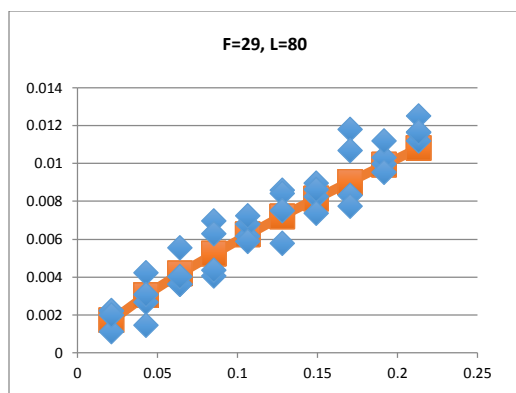


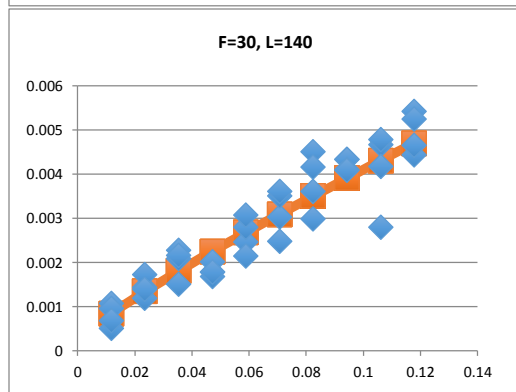
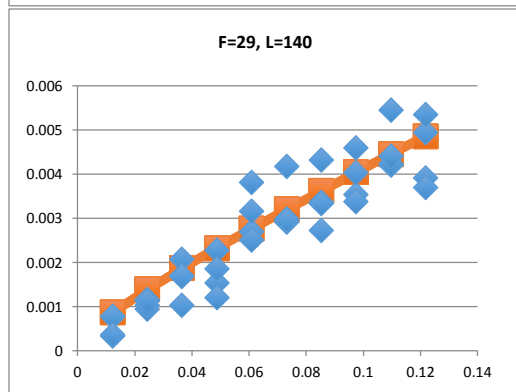
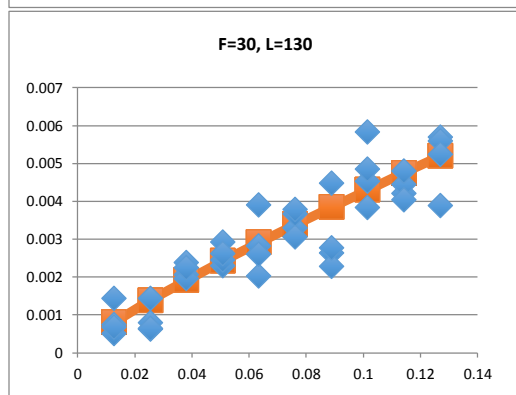
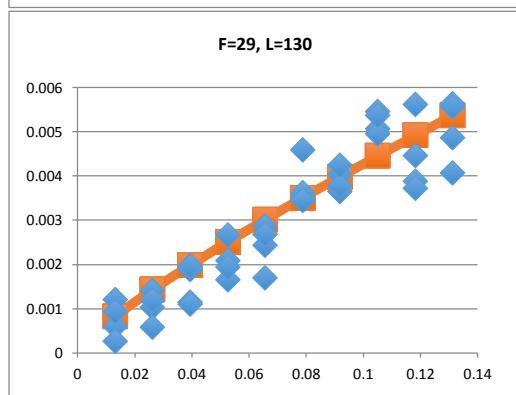
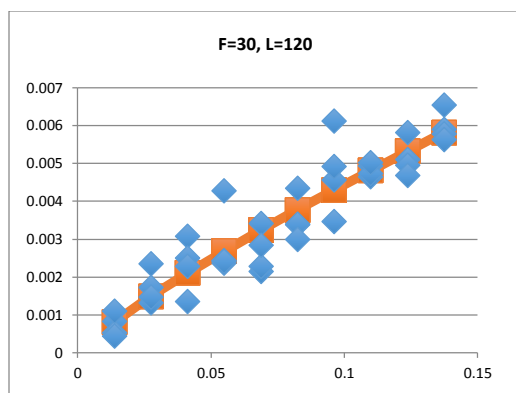
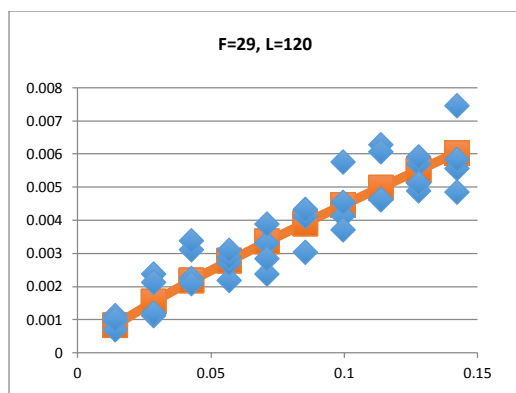


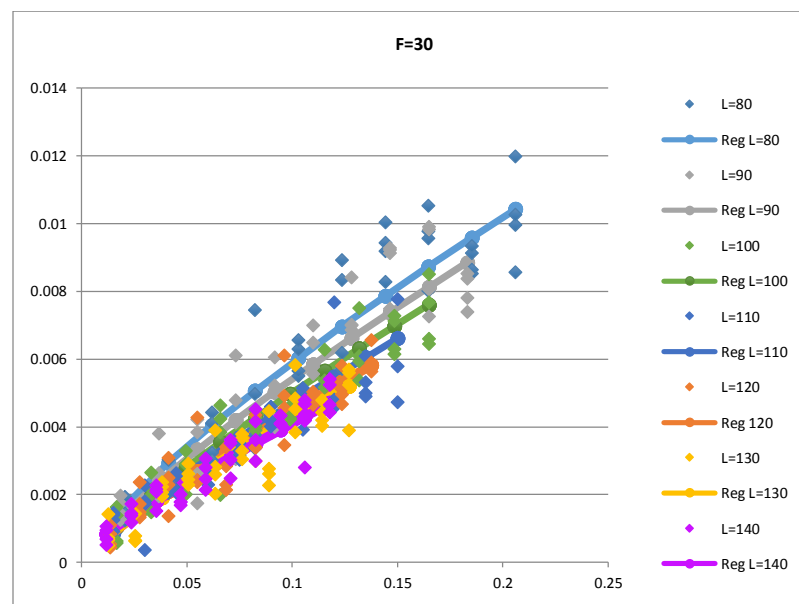
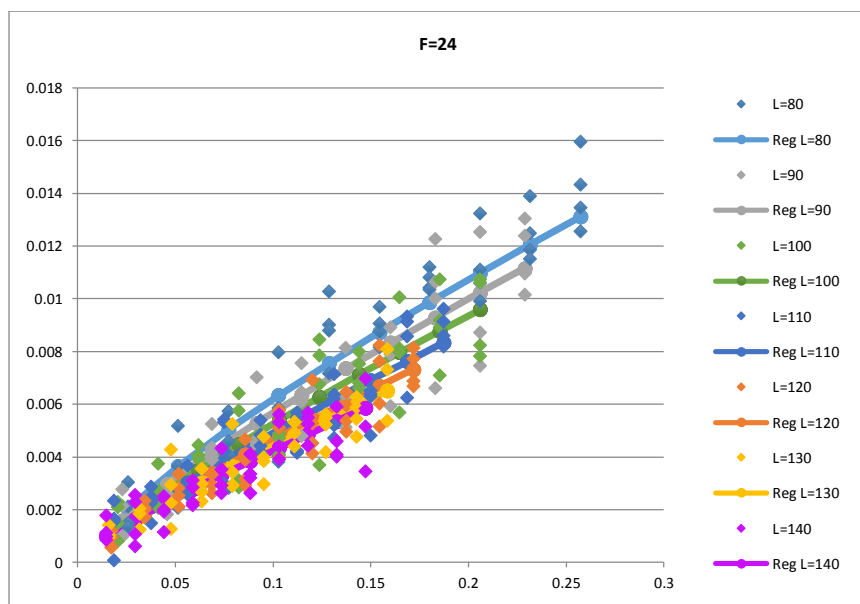
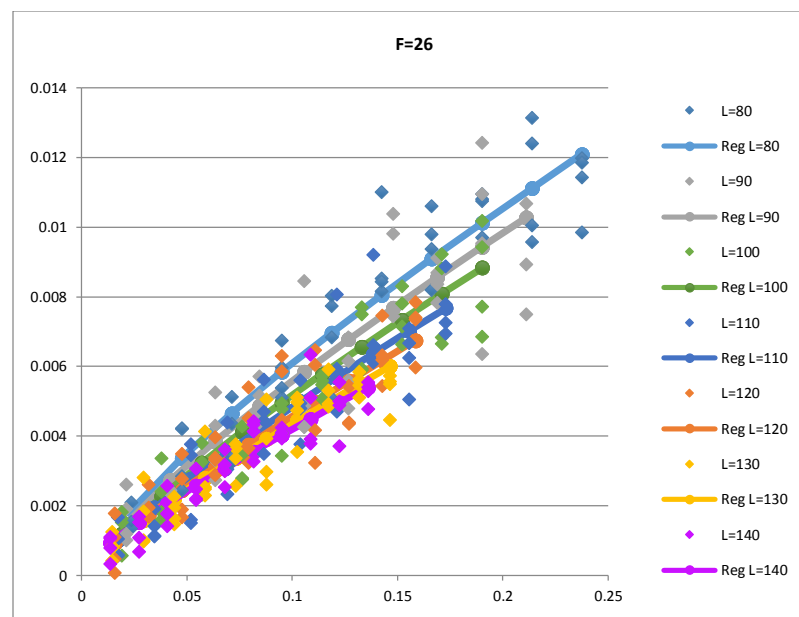
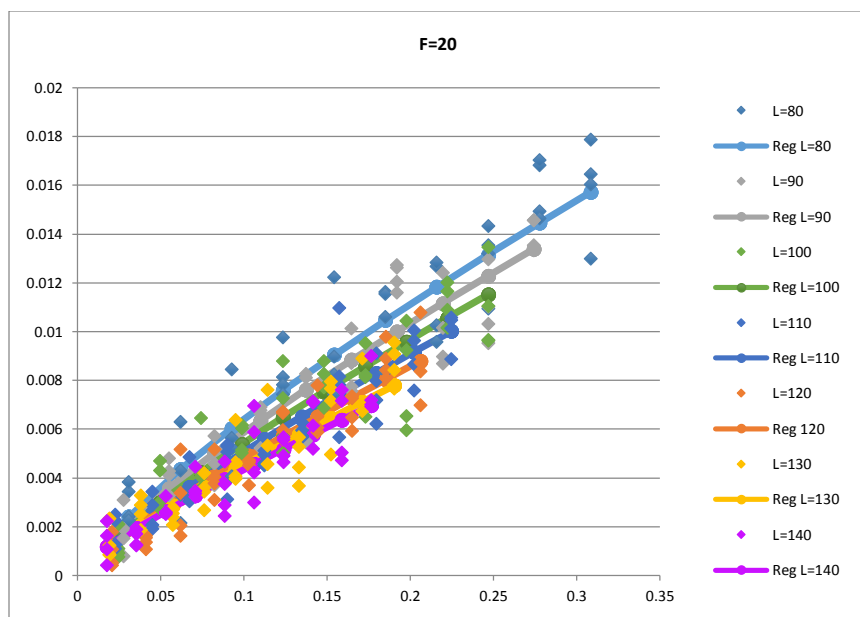


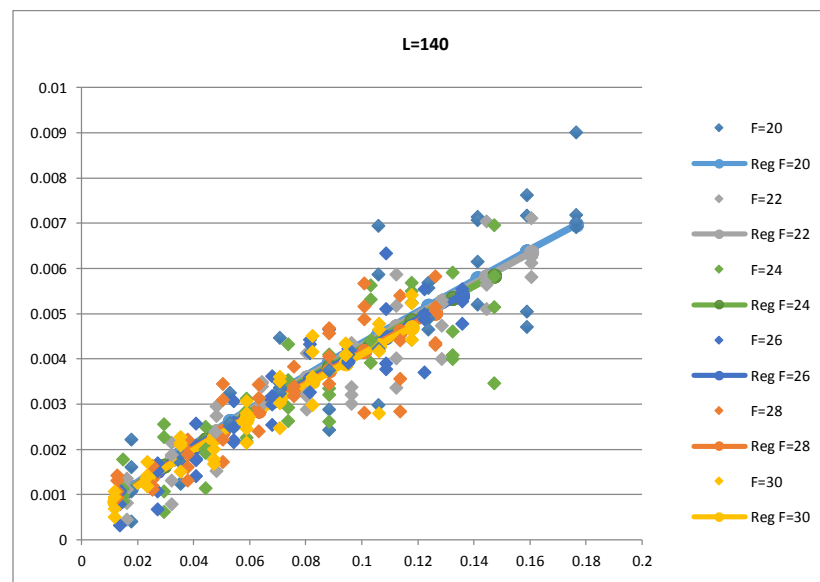
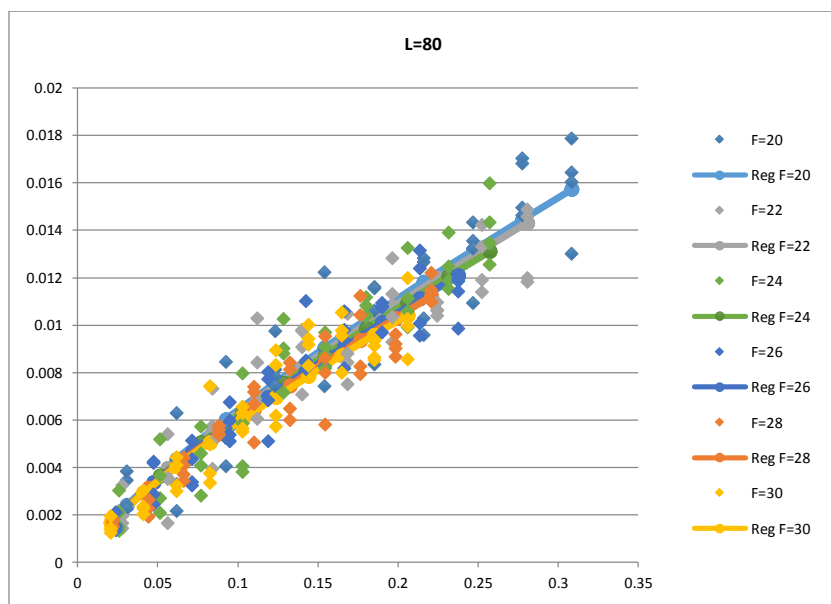
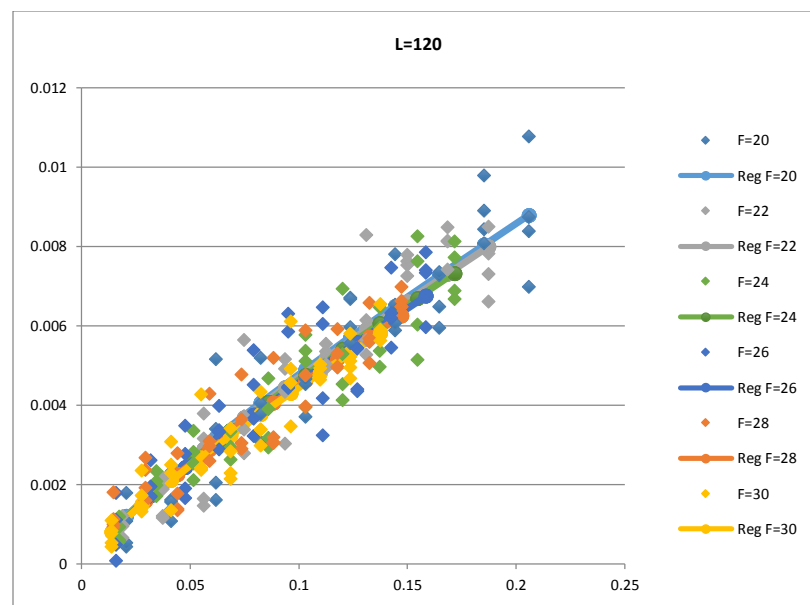
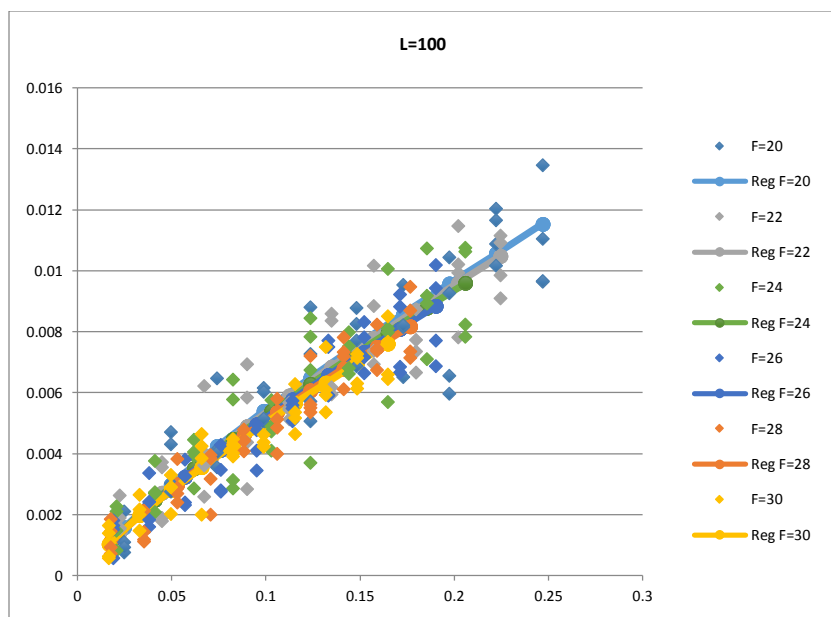




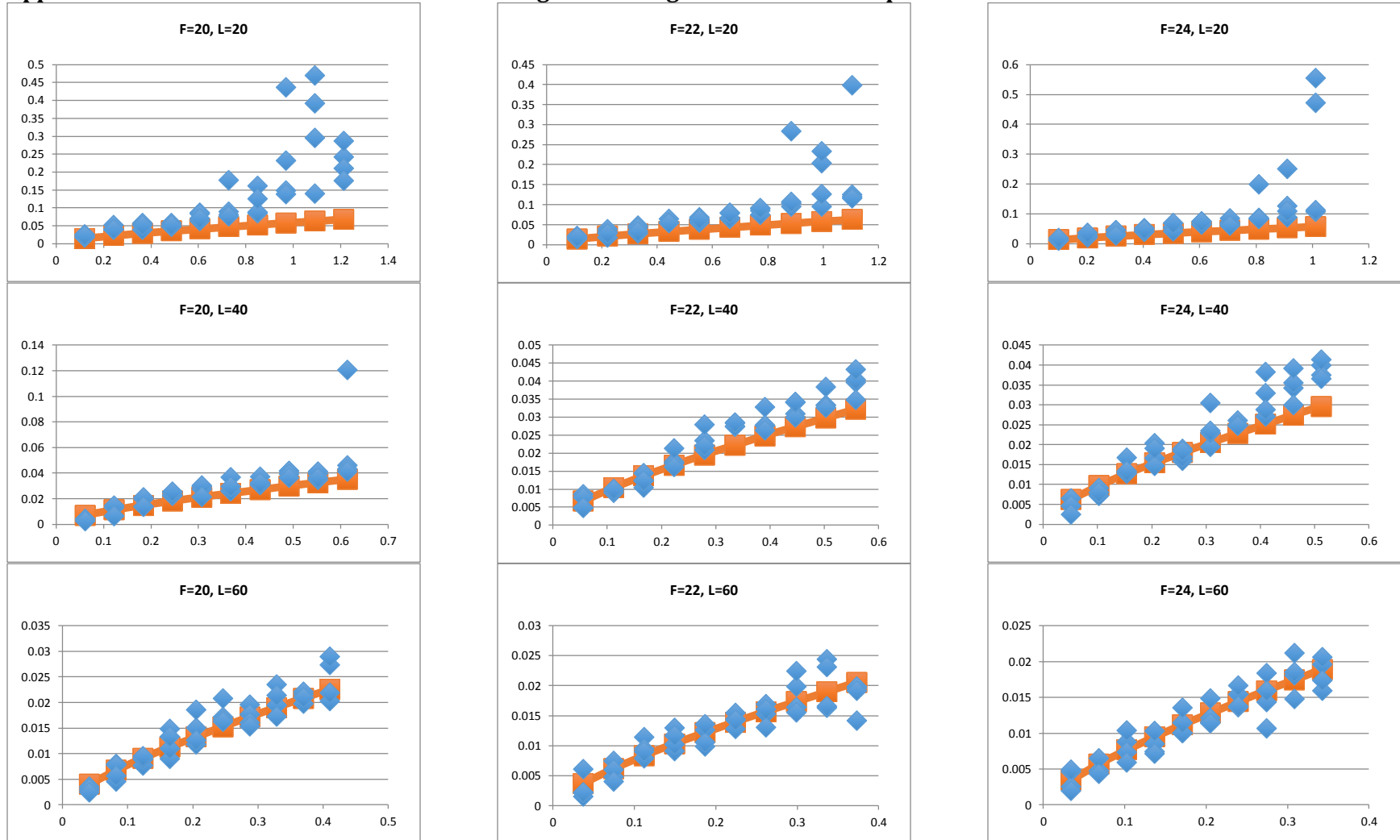


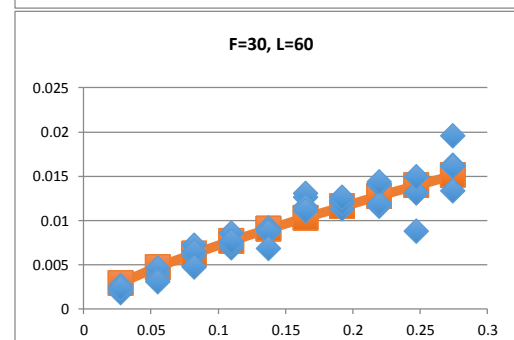
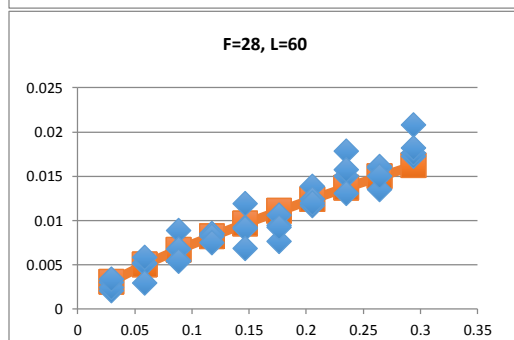
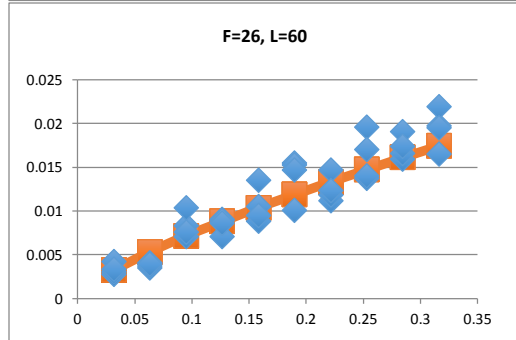
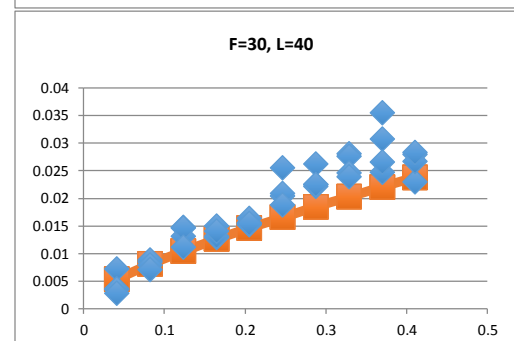
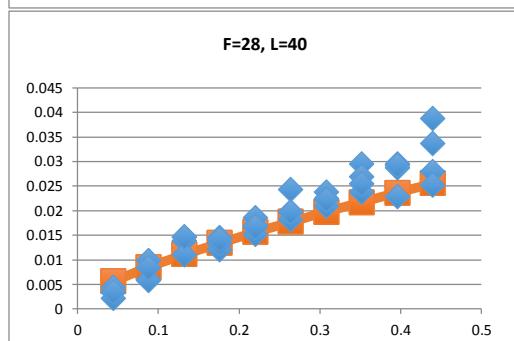
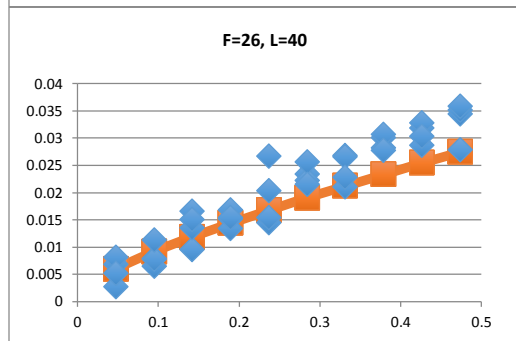
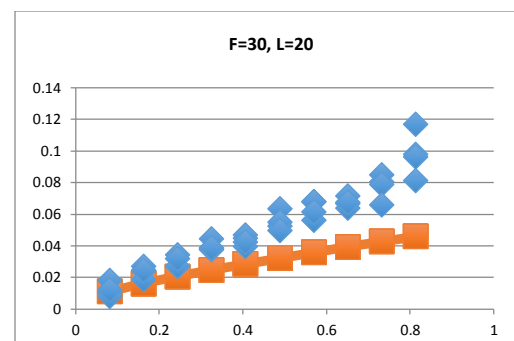
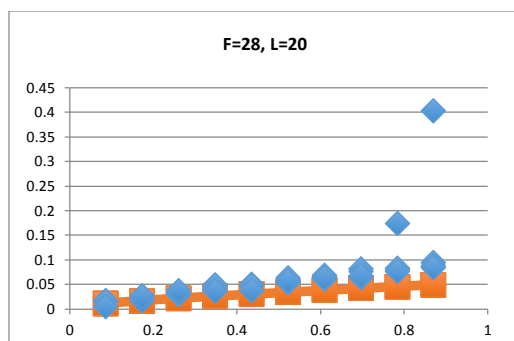
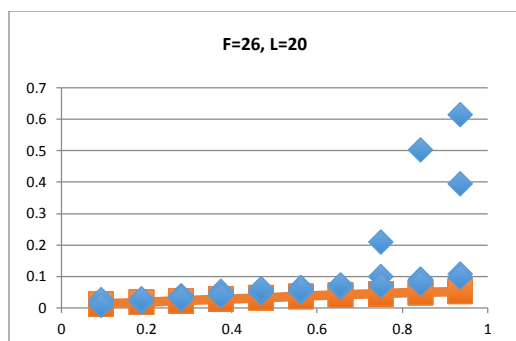




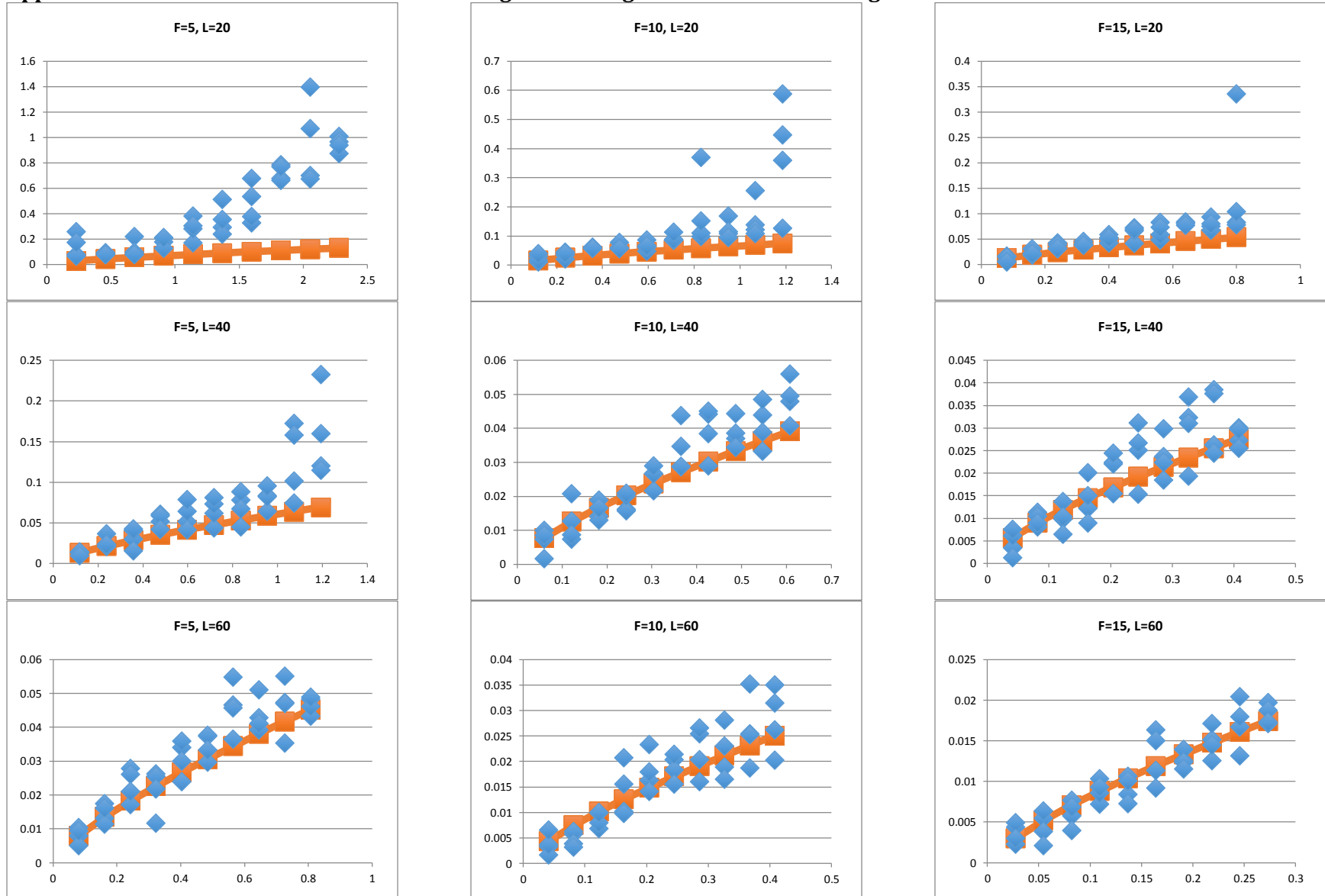


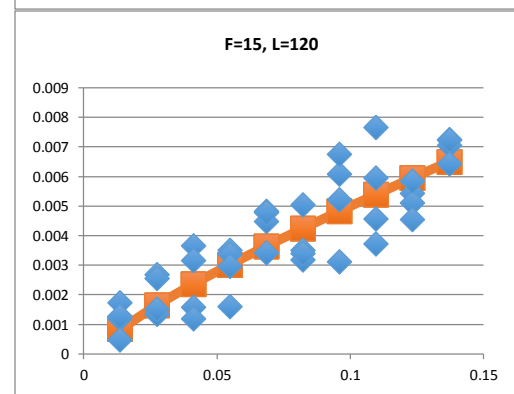
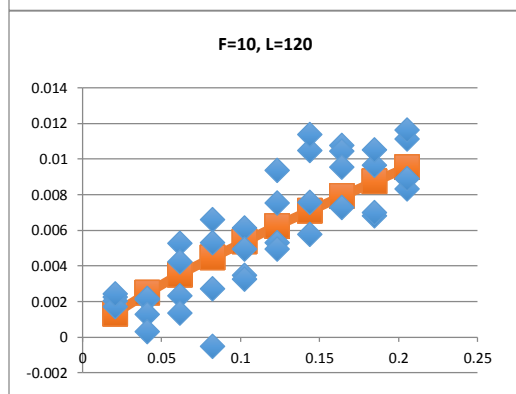
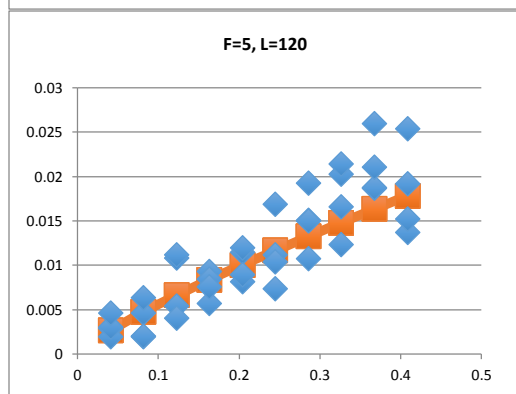
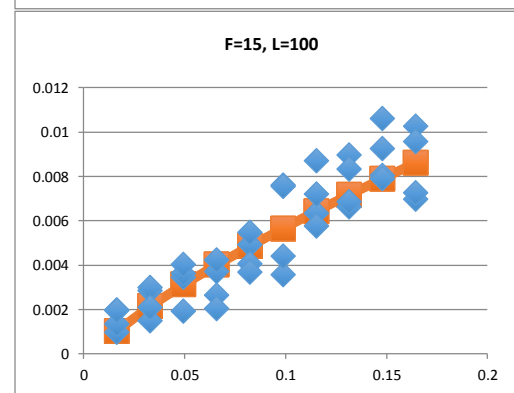
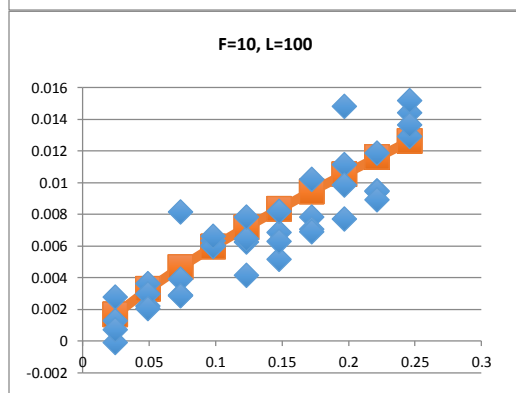
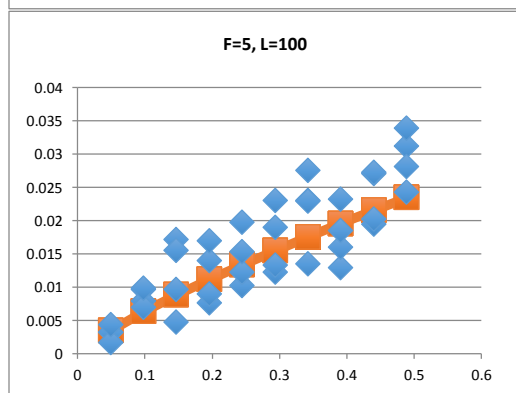
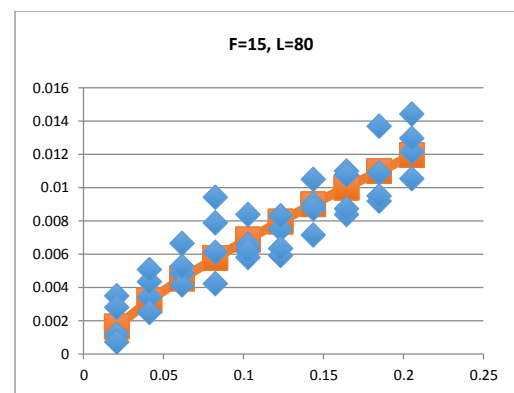
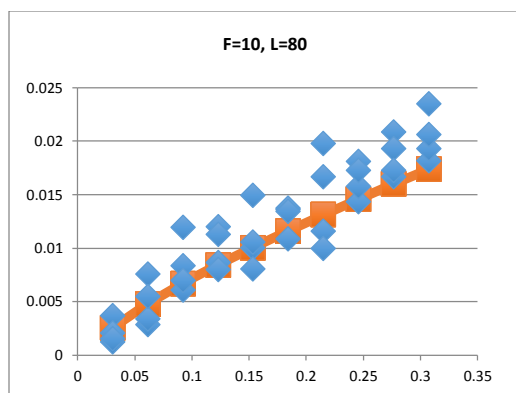
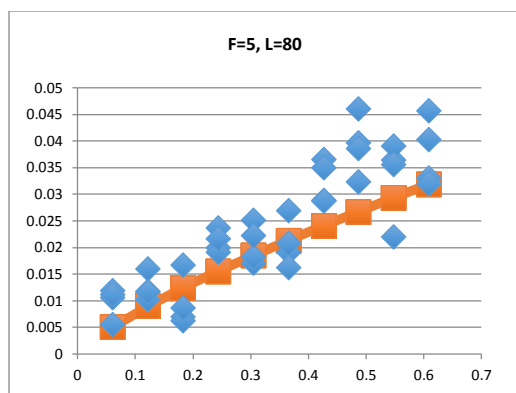
Appendix H - GPM Extended Case Studies with High Order Regression - Low Occupant Loads

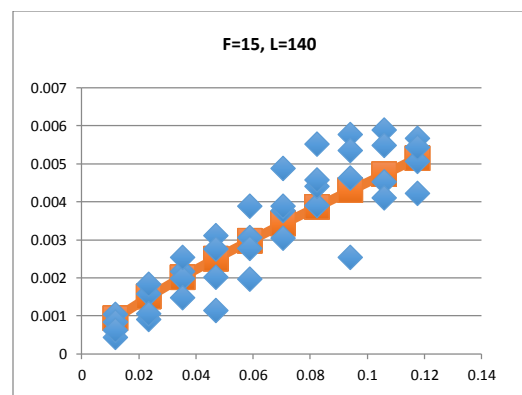
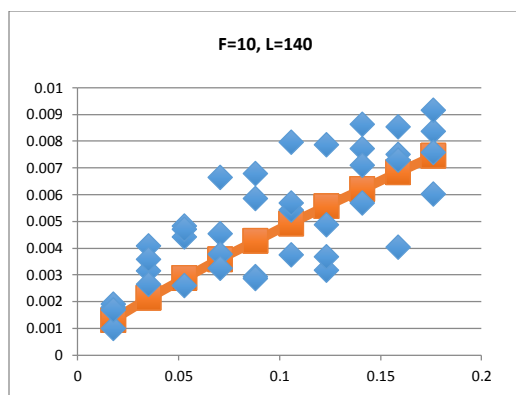
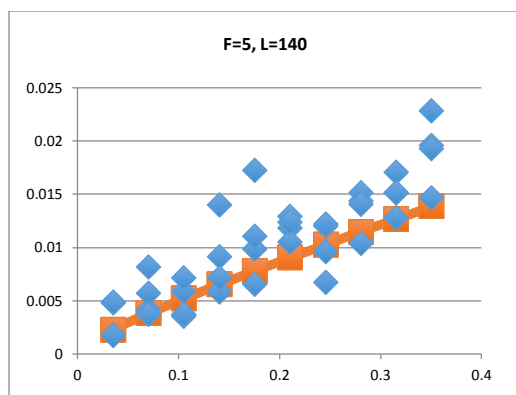




Appendix I – GPM Extended Case Studies with High Order Regression – Short Buildings







Appendix J - GPM Extended Case Studies with High Order Regression - Tall Buildings

